

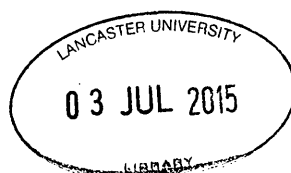
Interplay between Cannabinoids, SOCS3, and Autophagy process in the intestinal epithelium with the use of an established in vitro model system

Luan Ching Koay

**Faculty of Health and Medicine
Lancaster University
Lancaster
LA1 4YQ
UK**

This thesis is submitted for the degree of Doctor of Philosophy.

Submitted June 2014



ProQuest Number: 11003445

All rights reserved

INFORMATION TO ALL USERS

The quality of this reproduction is dependent upon the quality of the copy submitted.

In the unlikely event that the author did not send a complete manuscript and there are missing pages, these will be noted. Also, if material had to be removed, a note will indicate the deletion.



ProQuest 11003445

Published by ProQuest LLC (2018). Copyright of the Dissertation is held by the Author.

All rights reserved.

This work is protected against unauthorized copying under Title 17, United States Code
Microform Edition © ProQuest LLC.

ProQuest LLC.
789 East Eisenhower Parkway
P.O. Box 1346
Ann Arbor, MI 48106 – 1346

CONTENTS

CONTENTS..... I
DECLARATION..... VI
ABSTRACT..... VII
ACKNOWLEDGEMENTS VIII
LIST OF FIGURES IX
LIST OF TABLES XIII
ABBREVIATIONS..... XIV
PUBLICATION XIX

CHAPTER 1. Introduction 1

1.1 The Gastrointestinal tract3
1.1.1 Crosstalk between intestinal epithelium and intestinal microbes4
1.1.2 Inflammatory bowel disease (IBD).....8
1.1.3 Role of intestinal microbes in the pathogenesis of IBD9

1.2 Cannabinoids.....11
1.2.1 The endocannabinoid system (ECS).....12
i. Biosynthesis and hydrolysis of AEA14
ii. Functional consequences of AEA15
iii. The cannabinoid receptors16
1.2.2 Cannabidiol, CBD17
i. CBD in ECS17
ii. Anti-inflammatory action of CBD18
1.2.3 Cannabinoids in IBD18

1.3 Suppressor of Cytokine Signaling (SOCS)21
1.3.1 Structural and functional of SOCS323
1.3.2 SOCS3 in inflammatory regulation24
1.3.3 SOCS3 action in IBD25

1.4 Autophagy26
1.4.1 Overview in autophagy process26
i. Autophagy initiation27
ii. Autophagosome formation29
iii. Autophagy degradation30
1.4.2 Autophagy in the cellular energetic balance30

1.4.3	Autophagy regulation in gastrointestinal tract	31
i.	Autophagy mediated cytokine secretion by macrophages	32
ii.	Autophagy in bacteria handling in dendritic cells	33
iii.	Autophagy in antimicrobial peptide secretion in Paneth cells	33
iv.	Xenophagy induction	34
1.4.4	Autophagy in Crohn's disease	35
1.4.5	Cannabinoid action in autophagy process	37
1.5	Summary	39
 CHAPTER 2. Materials and Methods		41
2.1	Materials	43
2.2	Methods.....	47
2.2.1	Cell culture.....	47
2.2.2	Treatment	49
2.2.3	RNA Extraction	49
2.2.4	Quantitative Real time PCR (qRT-PCR)	50
i.	Primer set and Evaluation	50
ii.	Primer Evaluation	51
iii.	Reliability of real-time PCR detection	52
2.2.5	Western Immunoblot	53
i.	Cell Lysing	53
ii.	Quantifying protein expression	53
iii.	Preparation of SDS-PAGE gel	54
iv.	SDS-PAGE	54
v.	Antibody staining	55
2.2.6	Immunoprecipitation (IP)	56
2.2.7	Cell staining and imaging	56
i.	Dansylcadaverine (MDC) dye	56
ii.	Cyto-ID® autophagy detection kit	57
 CHAPTER 3. System Analysis		59
3.1	Introduction.....	61
3.2	Aims	62
3.3	Cannabinoid receptors in CaCo2 cells	63

3.4 SOCS3 expression in CaCo2 cells66

3.5 CNR1 and SOCS3 expression in cytokine-treated CaCo2 cells:
Proliferate, Confluent, Differentiated67

3.6 Effect of the integration of fetal bovine serum (FBS) in treatments72

 i. CNR1 and SOCS3 mRNA expression72

 ii. mTOR and JAK-STAT signaling pathway76

3.7 Establishing autophagy model system80

3.8 Discussion84

CHAPTER 4.Cannabinoid receptor (CNR)-1 knockdown in CaCo2 cells89

4.1 Introduction.....91

4.2 Aims92

4.3 Generation of CNR1 knockdown CaCo2 cell model93

 4.3.1 Experimental Technique: pRestroSuper(pRS) Retroviral Vector93

 i. Retroviruses93

 ii. OriGene engineered pRS vector94

 4.3.2 Experimental Technique: shRNA Expression Cassette96

 i. ShRNA96

 ii. OriGene shRNA HuSH plasmid (29mer)97

 4.3.3 Puromycin kill curve98

 4.3.4 Experimental Procedures100

4.4 Verifying Transfection Efficiency102

 4.4.1 Immunoblotting102

 4.4.2 [³⁵S]GTPγS binding activity105

 i. Principle of [³⁵S]GTPγS binding activity105

 ii. Preparation of cell samples for [³⁵S]GTPγS binding activity108

 iii. Experimental procedures108

 iv. ACEA-induced functional consequences on GPCR activation in
 CaCo-CNR1KD cell line110

4.5 Discussion113

CHAPTER 5. Cannabinoid action on autophagosome formation117

5.1	Introduction.....	119
5.2	Aims	121
5.3	Cannabinoid action on autophagy induction in intestinal epithelial cells	122
5.4	Mechanism of Action for cannabinoid-induced LC3-II formation.....	127
5.4.1	Canonical autophagy vs Non-canonical autophagy	128
i.	Dose and time course response for 3MA	129
ii.	Cannabinoid differentially impact on canonical pathway	131
iii.	Assess cannabinoid-induced effect via confocal imaging	132
5.4.2	Autophagosome formation vs Autophagosome degradation	134
i.	Time course for Bafilomycin-A1	135
ii.	Cannabinoids inhibit autophagosome degradation	137
5.4.3	Association of Cannabinoid receptor (CNR)-1	138
i.	Assess CNR1 via pharmacologically-induced CNR1 inhibition	139
ii.	Assess CNR1 via CaCo2_CNR1KD cell model	140
5.5	Discussion	141
5.6	Comments on methodologies used	145
5.7	Limitation of the <i>in vitro</i> system	149

CHAPTER 6.

Autophagy mediates cannabinoid induced SOCS3 reduction151

6.1	Introduction.....	153
6.2	Aims	154
6.3	Cannabinoid action on SOCS3 expression in intestinal epithelial cells	155
6.4	Mechanism of action for cannabinoid-induced SOCS3 reduction	160
6.4.1	Involvement of JAK-STAT3 signaling pathway in SOCS3 reduction	162
i.	Cannabinoid-induced p-STAT3 (Ser727) protein expression	163
ii.	Cannabinoid-induced p-STAT3 (Ser727) protein expression in autophagy inhibitor treated cells	165
6.4.2	Involvement of ubiquitin-proteasome proteolytic pathway in SOCS3 protein reduction	167
6.4.3	Involvement of autophagy process in SOCS3 protein reduction	170

6.5 Possible correlation of CNR1 receptor in cannabinoid-induced SOCS3 reduction173

6.6 Discussion175

CHAPTER 7. Conclusion & Future work177

CHAPTER 8. Appendix184

Stock solution recipes186

Product sheet for HuSH shRNA Plasmid, pRS.....187

Quantitative Real time PCR (qRT-PCR) generated DNA melting curves for CNR1 receptor in both CaCo2_CNR1KD and CaCo2_Scrambled cells.188

The use of Dansylcadaverine (MDC) dye in treated cells189

Preliminary data for CBD action in autophagy process under inflammatory setting190

CHAPTER 9. References192

Declaration

I hereby declare that this thesis has been composed by myself, that is has not been accepted in any previous application for a degree, that all the work has been performed by myself and that all the sources used have been specifically acknowledged by way of a reference.

Luan Ching Koay

Abstract

Autophagy is a catabolic process involved in homeostatic and regulated cellular protein recycling and degradation via the lysosomal degradation pathway. Emerging data associates Crohn's Disease (CD) with an impaired ATG16L1 autophagy gene. Increased activity in the endocannabinoid system and up-regulation of suppressor of cytokine signalling (SOCS)-3 protein expression are evident in inflamed intestine. We assessed the impact of phyto-cannabinoid (CBD), synthetic cannabinoid (ACEA) and endocannabinoid (AEA) on autophagosome formation, and investigated the mechanisms involved. Our findings show that all three cannabinoids induce autophagy in a dose-dependent manner in fully differentiated CaCo2 cells. ACEA and AEA induced canonical autophagy, which was cannabinoid receptor (CNR)-1 mediated. In contrast, CBD-induced autophagy is partially non-canonical and not CNR1 receptor mediated. Functionally, all three cannabinoids reduce SOCS3 protein expression. Blocking of autophagy reversed the cannabinoid-induced effect. In conclusion, CBD may have potential therapeutic application in CD where functional CNR1 receptor or autophagy is compromised and the regulatory protein, SOCS3, is itself regulated by the autophagy pathway.

Acknowledgements

I would firstly like to thank both of my supervisors: Dr. Karen Wright and Dr. Rachael Rigby for their invaluable help and guidance throughout the project. Thank you for the encouragement and support throughout the highs and lows in this past 4 years. Especially to Karen, thank you for the patience and understanding over the years.

Thanks to my past and present members of Lab C4: Rowaida Bakri, Imtiyaz Thagia, Air Lertkowitz, Tara Macpherson, Shakil Patel and Dr. Matt Hodges for their advice and help. Thanks are owed in particular to Dr. Jane Andre, for her guidance in the use of confocal microscopy.

I would like to express my gratitude towards Mrs Schachter and BPS for giving me generous amount of funding to support my 4 weeks visit to Professor Ruth Ross's laboratory in University of Aberdeen. Thanks are owed in particular to Professor Ruth Ross for allowing me to work with her group, and to Dr. Gemma L. Baillie, for teaching me the [^{35}S] GTP γ S binding assay.

Special thanks to all my friends across the continent, back in New Zealand and Malaysia, for their support throughout the highs and lows of these past 4 years.

Lastly, I would like to express sincere thank you to my family, who have been financially and emotionally supported me throughout the years. Thank you for giving me this great opportunity to experience this valuable 4 years of PhD and accomplish another great achievement in my life.

List of figures

Figure 1.1	Schematic diagram for small and large intestine	3
Figure 1.2	Common features of Crohn’s disease and Ulcerative Colitis	6
Figure 1.3	Major biosynthesis pathways for endocannabinoid, AEA	13
Figure 1.4	SOCS protein functions	22
Figure 1.5	Molecular event in autophagy	27
Figure 2.1	Schematic diagram for culturing human colonic epithelial cell line, CaCo2	48
Figure 2.2	Mathematical model used in Pfaffl method for qRT-PCR analysis	51
Figure 3.1	Melt curves obtained from qRT-PCR with CNR1, CNR2, RPLPO primers	63
Figure 3.2	Expression of CNR2 at transcriptional level in CaCo2 and immortalized lymphocyte cell line (Jurkats cells)	65
Figure 3.3	Basal SOCS3 mRNA expression level in CaCo2 cells	69
Figure 3.4	Effect of treatments on CNR1 mRNA expression in proliferating CaCo2 cells	69
Figure 3.5	Effect of treatments on SOCS3 mRNA expression in proliferating CaCo2 cell	67
Figure 3.6	Effect of treatments on CNR1 mRNA expression in confluent CaCo2 cells	70
Figure 3.7	Effect of treatments on SOCS3 mRNA expression in confluent CaCo2 cells	70
Figure 3.8	Effect of treatments on SOCS3 MRNA expression in differentiated CaCo2 cells	71
Figure 3.9	Schematic diagram of two experimental protocols: Serum containing and serum staving	72
Figure 3.10	Effect of treatments on CNR1 mRNA expression in serum starved CaCo2 cells	74
Figure 3.11	Effect of treatments on CNR1 MRNA expression in both Serum containing and serum starved CaCo2 cells	74
Figure 3.12	Effect of treatments on SOCS3 mRNA expression in serum starved CaCo2 cells	75
Figure 3.13	Effect of treatments on SOCS3 MRNA expression in both serum containing and serum starved CaCo2 cells	75

Figure 3.14	Effect of fetal bovine serum (FBS) on p-mTOR, p-STAT3 and SOCS3 basal protein expression in fully differentiated CaCo2 cells	78
Figure 3.15	Effect of fetal bovine serum (FBS) on p-mTOR, p-STAT3 and SOCS3 in both serum containing and serum starved CaCo2 cells	79
Figure 3.16	Schematic diagram of experimental protocols applied in the experiment	82
Figure 3.17	Effect of fetal bovine serum (FBS) on basal protein expression of p-mTOR and LC3-II in differentiated CaCo2 cells	83
Figure 3.18	Effect of fetal bovine serum (FBS) on of p-mTOR and LC3-II protein expression in IL-1 β treated CaCo2 cells	83
Figure 4.1	pRS shRNA expression vector	95
Figure 4.2	Structure sequence for OriGene designed gene-specific shRNA	97
Figure 4.3	Viability of CaCo2 cells in response to puromycin treatment	99
Figure 4.4	Immunoblot analysis of the verification analysis of CNR1 protein expression in CNR1 knockdown CaCo2 cells	103
Figure 4.5	Schematic diagram for G-protein mediated signaling cascade	107
Figure 4.6	Schematic diagram for the principle of [35 S]GTP γ S binding assay	107
Figure 4.7	[35 S]GTP γ S binding assay in response to ACEA treatment in CNR1 knockdown CaCo2 cells	110
Figure 5.1	Immunoblot analysis of LC3-II in fully differentiated CaCo2 cells in response to 10 μ M Cannabidiol (CBD) treatment within 24h	123
Figure 5.2	Dose response for CBD on LC3-II formation in CaCo2 cells	124
Figure 5.3	LC3-II formation for 0.1 μ M CBD treated starvation-induced CaCo2 cells	124
Figure 5.4	Dose response for ACEA on LC3-II formation in CaCo2 cells	125
Figure 5.5	Dose response for AEA on LC3-II formation in CaCo2 cells	126
Figure 5.6	Point of inhibition for 3-MA and Baf-A1 on autophagosome formation and degradation	127
Figure 5.7	Alternative routes towards autophagy lysosomal degradation	128
Figure 5.8	Dose response for 3-MA on LC3-II formation in CaCo2 cells	130
Figure 5.9	Effect of cannabinoids treatment on LC3-II formation in the presence of 3-MA	131

Figure 5.10	Confocal images analysis for cannabinoids and/or 3-MA treated CaCo2 cells	132
Figure 5.11	Confocal microscopy projection images of fully differentiated CaCo2 cells stained with Cyto-ID® and Hoechst 33342 dyes following cannabinoids treatments	133
Figure 5.12	Point of inhibition for Baf-A1 in autophagy process	134
Figure 5.13	Immunoblotting showed the effect of Baf-A1 on LC3-II protein expression within 24h time course	136
Figure 5.14	Immunoblotting showed the effect of cannabinoids treatment on LC3-II protein expression in the presence of Baf-A1	137
Figure 5.15	Immunoblotting showed the effect of cannabinoid treatment on LC3-II protein expression in the presence of AM251	139
Figure 5.16	Effects of cannabinoid treatments on LC3-II protein expression in both CaCo2-Scrambled and CaCo2-CNR1KD cell lines	140
Figure 6.1	Immunoblot analysis of SOCS3 in fully differentiated CaCo2 cells in response to 10µM CBD treatment within 24h	156
Figure 6.2	Dose response for CBD in relation to SOCS3 formation	157
Figure 6.3	Dose response for ACEA in relation to SOCS3 formation	158
Figure 6.4	Dose response for AEA in relation to SOCS3 formation	159
Figure 6.5	Possible mechanism of action that is responsible for CBD or Cannabinoids induced SOCS3 reduction	161
Figure 6.6	Schematic diagram shows the JAK-STAT signaling pathway and the negative feedback inhibition of SOCS3	163
Figure 6.7	Cannabinoid induced phospho-STAT3 (Ser727) protein expression	164
Figure 6.8	Cannabinoid induced phosphor-STAT3 (Ser727) protein expression in the presence of Baf-A1	166
Figure 6.9	Ubiquitin-1 interacted with SOCS3 protein in CBD treated CaCo2 cells	168
Figure 6.10	Effect of MG132 treatment on ubiquitin-1 co-precipitated SOCS3 protein in CBD treated CaCo2 cells	169
Figure 6.11	Immunoblotting showed the effect of cannabinoids treatment on SOCS3 protein expression in the presence of 3-MA	171

Figure 6.12	Immunoblotting showed the effect of cannabinoids treatment on SOCS3 protein expression in the presence of Baf-A1	172
Figure 6.13	Immunoblotting showed the effect of cannabinoid treatment on SOCS3 protein expression in the presence of AM251	173
Figure 6.14	Effect of cannabinoid treatments on SOCS3 protein expression In both CaCo2-Scrambled and CaCo2-CNR1KD cell lines	174
Figure 7.1	Cannabinoid action in autophagy process demonstrated in human intestinal epithelial cell model	178
Figure 7.2	Schematic diagram showed the therapeutic potential of CBD for Crohn's disease	180
Figure 8.1	DNA melt curve for CNR1 in wild type CaCo2 cells, CaCo2_Scrambled and CaCo2_CNR1KD cells	188
Figure 8.2	Fluorescence images with the use of dansylcadaverine (MDC) dye in treated cells	189
Figure 8.3	Dose response curve for IL-1 β treatment	190
Figure 8.4	CBD-induced LC3-II protein expression in IL-1 β -induced inflammatory setting	191

List of tables

Table 2.1 Chemical used; supplier and supplier address43

Table 2.2 Chemical used; supplier and supplier address
 (Professor Ruth Ross’s Laboratory, University of Aberdeen).....45

Table 2.3 Drugs used; supplier and supplier address46

Table 2.4 Antibodies used for western blotting; supplier and supplier address46

Table 2.5 CDNA dilution used for testing primer efficiency50

Table 2.6 Primer efficiency and R² value for pre-validated primers for
 CNR1, CNR2, SOCS3, RPLPO and HMBS52

Table 2.7 Recipe for making different percentages of SDS-PAGE gels54

Table 2.8 List of primary antibodies with its associated molecular weight,
 corresponding secondary antibodies and their preference in
 SDS-PAGE gel percentage and blocking solution to be used58

Table 4.1 29-nucleotide sequences for CNR1-specific shRNA constructs97

Table 4.2 Plate set up for [³⁵S]GTPγS binding assay109

Abbreviations

Δ^9 -THC	Δ^9 -Tetrahydrocannabidiol
2-AG	2-arachidonoyl glycerol
2D	2-dimensional
3-MA	3-Methyladenine
AA	Arachidonic acid
Abh4	χ/β -hydrolase
ACEA	Aarachidonyl-2'-chloroethylamide
AEA	Anandamide
AIEC	Adherent-invasive E.coli
AKT	known as Protein Kinase B
AMPK	5' adenosine monophosphate-activated protein kinase
AMT	AEA membrane transporter
ATG	Autophagy-related genes
Baf-A1	Bafilomycin A1
Bcl-2	B-cell lymphoma 2
CBD	Cannabidiol
CD	Crohn's Disease
c-JNK	c-Jun N-terminal kinase
CMA	Chaperon-mediated Autophagy
CNR	Cannabinoid receptor
DC	Dendritic cells
DAMPs	Danger-associated molecular patterns
DNA	Deoxyribonucleic acid

DNBS	Dinitrobenzene sulphonic acid
E.coli	Escherichia coli
ECS	Endocannabinoid System
EDTA	Ethylenediaminetetraacetic acid
ER	Endoplasmic reticulum
ERK	Extracellular signal-regulated kinases
ES cells	Embryonic stem cells
ESS	Extended SH2 subdomain
FAAH	Fatty acid amine hydrolase
FBS	Fetal bovine serum
GEM	Gemcitabine
GDP	Guanosine diphosphate
GI	Gastrointestinal
GPCR	G-protein coupled receptor
GPR55	G protein-coupled receptor 55
GTP	Guanosine-5'-triphosphate
GWAS	Genome-wide association studies
HEPES	Hydroxyethyl piperazineethanesulfonic acid
HMBS	Hydroxymethylbilane synthase
IBD	Inflammatory Bowel Disease
IEC	Intestinal epithelial cells
IL-1	Interleukin-1
IFN	Interferon
IGRM	Immunity-related GTPase family
JAK	Janus kinases

KD	Knockdown
KIR	Kinase inhibitory region
LAMP-2A	Lysosomal-associated membrane protein 2A
LC3	Light chain 3
Lyso-PLD	Lyso-phospholipase
LPS	Lipopolysaccharide
LPR	Leucine-rich repeats
LTR	Long term repeats
MAMP	Microorganism-associated molecular pattern
MAPK	Mitogen-activated protein kinase
MDC	Dansylcadaverine
MDP	Muramyl dipeptide
MEM	Minimum Essential Medium
Met-F-AEA	2-methyl-arachidonyl-2-fluoro-ethylamide
MG132	Carbobenzoxy-Leu-Leu-leucinal
mRNA	messenger Ribonucleic acid
mTOR	mammalian target of Rapamycin
NADA	<i>N</i> -arachidonoyldopamine
NAPE-PLD	<i>N</i> -arachidonylphosphatidyl-ethanolamide phospholipase D
<i>N</i> -ArPE	<i>N</i> -arachidonyl-phosphatidylethanolamine
NAT	<i>trans</i> -N-acyltransferase
NEAA	Non-essential Amino Acid
NDP52	Nuclear dot protein 52KDa
NOD2	Nucleotide-binding oligomerization domain containing-2
PCR	Polymerase Chain Reaction

PE	Phosphatidylethanolamine
PI	Phosphatidylinositol
PI3K	Phosphatidyl inositol-3-kinase
PI3P	Phosphatidyl-inositol triphosphate
PKB	Protein kinase B
PLA ₂	Phospholipase A ₂
PLC	Phospholipase C
PRR	Pattern-recognition receptor
PTPTN22	Protein tyrosine phosphatase 22
qRT-PCR	Quantitative Real Time Polymerase Chain Reaction
RIPK-2	Receptor-interacting serine-threonine-kinase 2
RISC	RNA-induced silencing protein complex
RPLPO	Large ribosomal protein
RNA	Ribonucleic acid
ROS	Reactive oxygen species
rRNA	Ribosomal Ribonucleic acid
SCV	<i>Samonella-containing</i> vacuoles
SDS	Sodium dodecyl sulphate
SOCS	Suppressor of cytokine signalling proteins
SPRR2A	Small proline-rich protein 2A
SH2	Src homology 2
siRNA	Small interfering Ribonucleic acid
shRNA	Short hairpin Ribonucleic acid
STAT	Signal transducer and activator of transcription factor
OPTN	Optineurin

TEMED	<i>N,N,N,N</i> ,-Tetramethylethylenedramine
TBK1	TANK-binding kinase 1
TRIF	TIR-domain-containing-adaptor inducing interferon- β
TLR	Toll-light receptor
TNF- α	Tumor Necrosis Factor-alpha
TRIM	Tripartite motif-containing protein
TRPV1	Transcient Receptor Potential Vanilloid type 1
UC	Ulcerative Colitis
VEGF	Vascular endothelial growth factor
ZO-1	Zona occluden-1

Publication

Koay, L. C., R. J. Rigby, and K. L. Wright, 2011, Cannabinoids differentially modulate leptin signalling in the intestinal epithelial cells under inflammatory condition: Proceedings of the British Pharmacological Society. British Pharmacology Society Winter Meeting 2011. Abstract P054.

Koay, L. C., R. J. Rigby, and K. L. Wright, 2014, Cannabinoid-induced autophagy regulates suppressor of cytokine signaling (SOCS)-3 in intestinal epithelium: American Journal of Physiology. Gastrointestinal Liver Physiology. (Epub ahead of print)

Chapter 1

Introduction

Table of Contents

- 1.1 **The Gastrointestinal tract** **3**
 - 1.1.1 Crosstalk between intestinal epithelium and intestinal microbes 4
 - 1.1.2 Inflammatory bowel disease (IBD)..... 8
 - 1.1.3 Role of intestinal microbes in the pathogenesis of IBD 9

- 1.2 **Cannabinoids**..... **11**
 - 1.2.1 The endocannabinoid system (ECS)..... 12
 - i. Biosynthesis and hydrolysis of AEA 14
 - ii. Functional consequences of AEA 15
 - iii. The cannabinoid receptors 16
 - 1.2.2 Cannabidiol, CBD 17
 - i. CBD in ECS 17
 - ii. Anti-inflammatory action of CBD 18
 - 1.2.3 Cannabinoids in IBD 18

- 1.3 **Suppressor of Cytokine Signaling (SOCS)** **21**
 - 1.3.1 Structural and functional of SOCS3 23
 - 1.3.2 SOCS3 in inflammatory regulation 24
 - 1.3.3 SOCS3 action in IBD 25

- 1.4 **Autophagy** **26**
 - 1.4.1 Overview in autophagy process 26
 - i. Autophagy initiation 27
 - ii. Autophagosome formation 29
 - iii. Autophagy degradation 30
 - 1.4.2 Autophagy in the cellular energetic balance 30
 - 1.4.3 Autophagy regulation in gastrointestinal tract 31
 - i. Autophagy mediated cytokine secretion by macrophages 32
 - ii. Autophagy in bacteria handling in dendritic cells 33
 - iii. Autophagy in antimicrobial peptide secretion in Paneth cells 33
 - iv. Xenophagy induction 34
 - 1.4.4 Autophagy in Crohn’s disease 35
 - 1.4.5 Cannabinoid action in autophagy process 37

- 1.5 **Summary** **39**

1.1 The gastrointestinal (GI) tract

The gastrointestinal (GI) tract is an organ whose major role is nutrient digestion and absorption. A single layer of intestinal epithelial cells line the entire GI tract layer and thus, provide a barrier for microbes in the intestine (Figure 1.1). This barrier exhibits the capability by the formation of intercellular tight junctions on the cell layer. Disruptions of the epithelial layer will lead to activation of inflammatory immune response as the host will be exposed to various pathogens (Kunzelmann and McMorran, 2004).

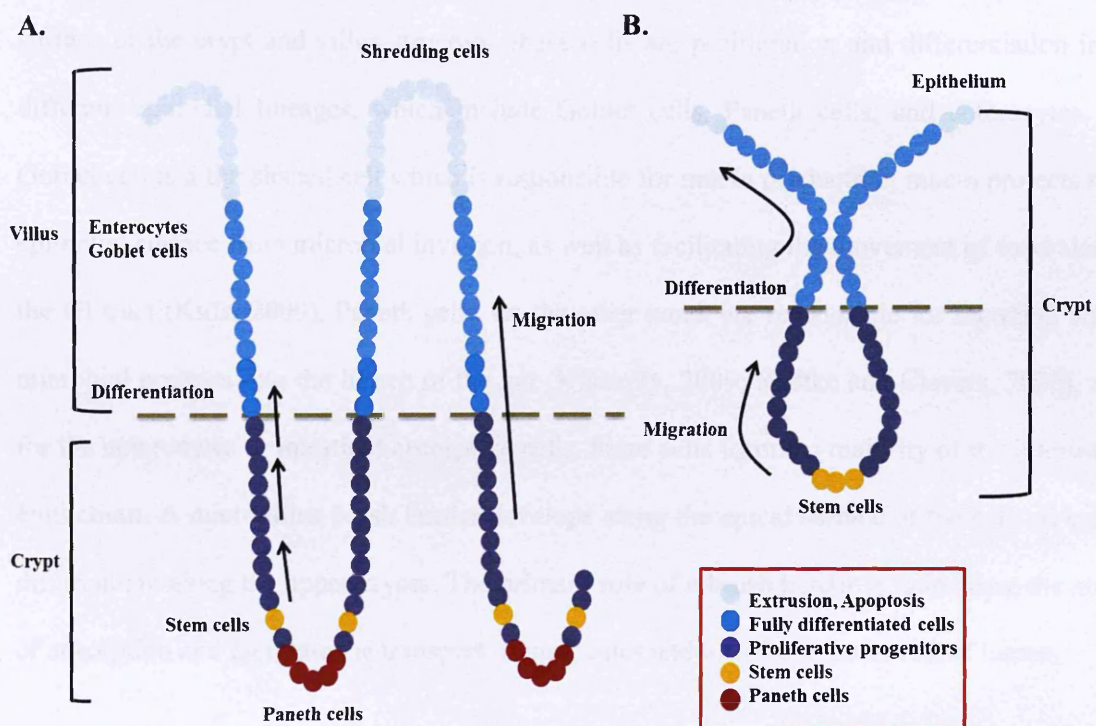


Figure 1.1. Schematic diagram for small and large intestine. (A) Structure of small intestine. Stem cells are located above the Paneth cells. Proliferation occurs and cells migrate towards villus. Progenitors stop proliferating at the villus-crypt junction and start to differentiate. (B) Structure of large intestine. Stem cells are located at the bottom of the crypt. Proliferation occurs at the bottom of the crypt and starts to differentiate when it reaches the top third of the crypt.

The small intestine can be further segregated into duodenum, jejunum and ileum. The small intestine contains villi - finger like structures which project into the lumen of the intestine. This feature is crucial in the small intestine as it increases the surface area of absorption (Wilson, 1962). Conversely, this feature is absent in the large intestine (Figure 1.1). Instead of having the villi structure, large intestine contains only crypts of Lieberkuhn and a flat surface of epithelial cells.

As the undifferentiated multipotent stem cells migrate from the bottom of the crypt to the apical surface of the crypt and villus structure, these cells are proliferation and differentiation into different epithelial lineages, which include Goblet cells, Paneth cells, and enterocytes. A Goblet cell is a flat shaped cell which is responsible for mucin production; mucin protects the epithelial surface from microbial invasion, as well as facilitating the movement of food along the GI tract (Kufe, 2009). Paneth cells, on the other hand, are responsible for secreting anti-microbial proteins into the lumen of the gut (Klionsky, 2009; Radtke and Clevers, 2005). As for the enterocytes or intestinal absorptive cells, these cells form the majority of the intestinal epithelium. A microvillus brush border develops along the apical surface of the cells as cells differentiate along the upper crypts. The primary role of a brush border is to increase the area of adsorption and facilitate the transport of molecules and ions from the intestinal lumen.

1.1.1 Crosstalk between intestinal epithelium and intestinal microbes

The intestinal epithelium forms a physical barrier between the intestinal microbes and the lymphoid tissue (Abraham and Cho, 2009). Under normal physiological conditions, intestinal microbes reside in the gut and contribute towards the regulation of basic physiologic functions, which include the metabolic and immune functions (Blaut and Clavel, 2007; Frazier et al., 2011; Flint, 2012). Microbiota composition may impact on individual differences in immune response towards immunological condition and such

microbiota composition changes in accordance with age and external factors, such as environmental condition and diet (Hooper et al., 2002; Biagi et al., 2012). Research studies proposed that the host is capable of recognizing microbial presence in the intestinal epithelium by identifying the microorganism-associated molecular pattern (MAMPs) through specific pattern-recognition receptors (PRRs) and that this interaction contributes to the crosstalk between intestinal epithelium and intestinal microbes. PRRs are innate immune membrane-bound or cytosolic molecules that recognize bacterial MAMPs; for example, the un-methylated CpG (cytosine-guanine) motif which is well-conserved in bacterial DNA and the lipopolysaccharide (LPS) in gram-negative organisms (Rautava and Walker, 2007). Apart from recognizing bacterial structure, PRRs also identify the presence of protozoan, fungal and the single-stranded RNA characteristic of viral structure (Akira et al., 2006). One of most studied examples of PRRs is human Toll-like receptors (TLRs). TLRs have been shown to express on both intestinal epithelial cells and immune cells such as dendritic cells and macrophages (Didierlaurent et al., 2005; Sirard et al., 2006). Activation of TLRs by microbial ligands will initiate the host's immune response, via the production of cytokines, chemokines or co-stimulatory molecules (Sirard et al., 2006; Rautava and Walker, 2007).

Despite various studies having been performed to investigate the interaction between intestinal epithelium and intestinal microbial, the mechanism which commensal microbes adopt to influence the host physiology and *vice versa* remains largely unknown. This may due to the effect commensal microbes have on host physiology is largely dependent on the microbe-microbe interaction in the GI tract, and such a dynamic ecosystem of commensal microbes is very difficult to recapitulate in the laboratory setting. To date, data relating to the crosstalk between the host and commensal microbes has been derived

mainly from studies with the use of germ-free or gnotobiotic animal models. As such, accumulating evidences has identified the role of commensal microbes in the development of the GI tract. For instance, commensal microbiota has been shown to affect the composition and thickness of the mucosal layer in the GI tract (Sharma et al., 1995; Deplancke and Gaskins, 2001; Petersson et al., 2011). Sharma, et al.'s study revealed that germ-free rats possess fewer goblet cells, a thinner mucus layer and a higher percentage of neutral mucins in the colon as compared to conventionally raised animals. Interestingly, the conventional mucus properties can be re-introduced into the germ-free animal through the stimulation of microbial ligands, such as LPS and peptidoglycan (Petersson et al., 2011), suggesting an indirect role of commensal microflora in inducing defence mechanisms against the invading pathogens via the formation of an intestinal mucosal layer. In addition, commensal microbes are also involved in the modulation of epithelial permeability in the GI tract. This was demonstrated through a study where gram-negative bacterium, *Bacteroides thetaiotaomicron*, increased the resistance of the gut to injury in the germ-free mice through the induction of small amounts of proline-rich protein 2A (SPRR2A), a protein involved in the maintenance of the epithelial junctional complex (Hooper et al., 2001). Such an effect is not limited to commensal microbes, several probiotics, strains such as *Lactobacillus plantarum* 299v and *Lactobacillus reuteri* R2LC, have also been shown to reduce intestinal epithelial permeability in the methotrexate-induced colitis rat model (Mao et al., 1996).

Considering the beneficial functional outcomes contributed by commensal microbes and the fact that the host is tolerant towards indigenous microbes, this suggests that the host may respond to the commensal microbes through a distinct pathway. However, the mechanism utilized by the host to discriminate between indigenous microbes and

pathogens has long been a fascination. The host immune system has to be able to respond adequately to the recognition of pathogens that may act as a potential threat to the tightly regulated host immune response without invoking inflammatory activity, as the failure of such regulation may lead to the onset of chronic intestinal inflammation. An interesting study by Lee et al. (2006) showed that TLR9, a receptor which is expressed on both apical and basolateral surfaces of the intestinal epithelial cells, induces distinct inflammatory response despite both compartments express similar TLR9. In contrast to the basolateral TLR9, apical TLR9 stimulation fails to activate both the nuclear factor kappa-light-chain-enhancer of activated B cells (NF- κ B) and extracellular signal-regulated kinase (ERK) signalling pathways, or the secretion of pro-inflammatory cytokine interleukin (IL)-8. cDNA microarray analysis revealed that both basolateral and apical TLR9 regulates a distinct set of genes and only 40% of the overall induced-targets are shared between the apical and basolateral TLR9 stimulated response, suggesting that, even though TLRs fail to distinguish MAMPs which are present in both commensal microbes and pathogen, TLRs may still be able to act differentially in accordance to the location and induce inflammatory response against pathogens that penetrate through the intestinal epithelial cells barrier.

1.1.2 Inflammatory bowel disease

Inflammatory bowel disease (IBD) comprises two major types of intestinal disorders: Crohn's Disease (CD) and Ulcerative Colitis (UC) (Abraham and Cho, 2009). Both of these diseases are chronic diseases associated with inflammation in the gastrointestinal (GI) tract. According to the Crohn's and Colitis UK, IBD affects about 1 person in every 250 in the UK population. They have shown that the common age for the diagnosis for IBD is between 10 and 40. For UC, between 6000 and 12000 new cases are being diagnosed in each year whereas for CD, the number of new cases is less compared to UC (between 3000 to 6000 new cases per year).

In CD, inflammation can occur anywhere in the digestive system, from mouth to anus. However, it mostly affects the small intestine and colon. CD leads to the growth of ulcers and presence of scars on intestinal wall. In contrast, for UC, inflammation occurs via tiny ulcers in the rectum and colon. The common features for CD include the fat wrapping, thickening of the intestinal wall and the formation of cobble-stoning on the intestinal wall (Figure 1.2). In contrast, the common features for UC include distortion of the crypt structure, the loss of mucosa and haustra and the formation of pseudopolyps on the intestinal wall (Figure 1.2).

The common symptoms associated with both of these diseases include pain, diarrhoea and general tiredness. One of the hallmarks for CD is severe weight loss in CD patients. One fifth of the adults in IBD clinic are 85% under their ideal body weight (Gee et al., 1985). The failure in gaining weight can lead to anorexia and contribute to the increased secretion of several pro-inflammatory cytokines, for instance, tumor necrosis factor-alpha (TNF- α) and IL-1.

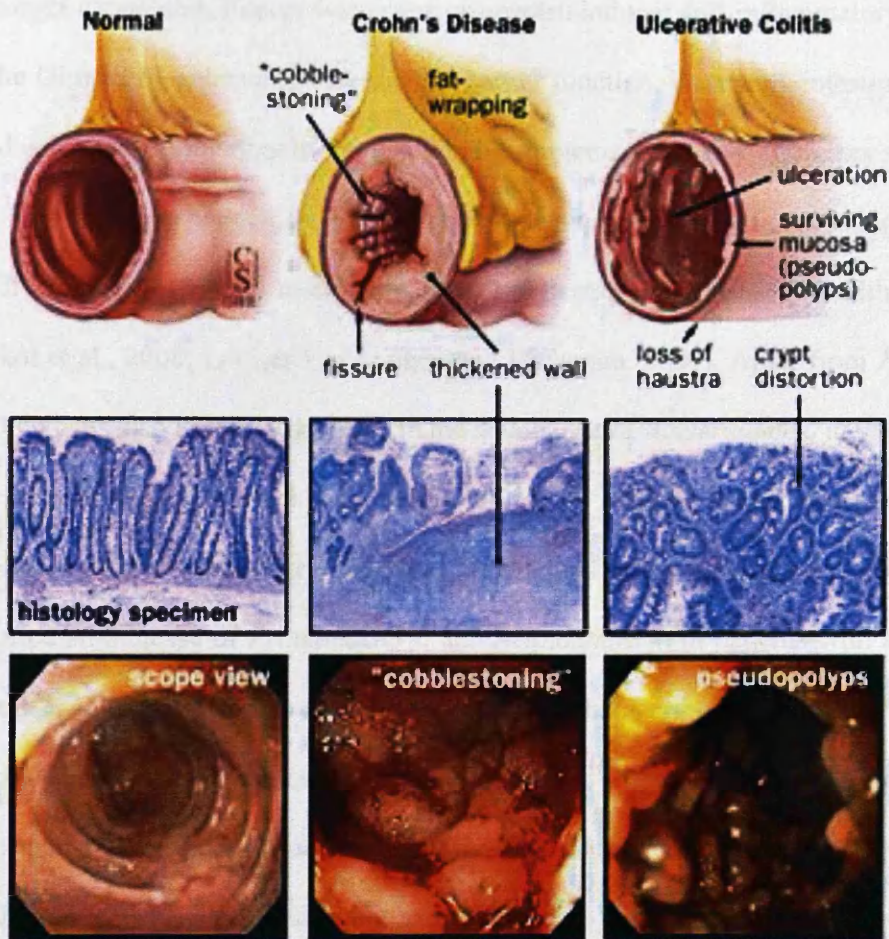


Figure 1.2. Common features of Crohn’s disease and Ulcerative colitis.
Image source: John Hopkins Medicine Gastroenterology & Hepatology.

1.1.3 Role of intestinal microbes in pathogenesis of IBD

To date, accumulating clinical evidences suggest that the dysregulation of the immune response to commensal microflora plays a role in the pathogenesis of intestinal inflammation, such as IBD in the GI tract (Frank et al., 2007; Abraham and Cho, 2009; Knights et al., 2013). Studies showed that the GI tracts of both UC and CD patients suffered from a depletion of commensal microbes, such as *Firmicutes* and *Bacteroidetes*, as compared to the non-IBD controls (Frank et al., 2007).

Amongst *Firmicutes*, *Faecalibacterium prausnitzii* induces anti-inflammatory activities in the GI tract by enhancing the mucosal barrier function, increasing intestinal mucous production and stimulating the production of immunosuppressive cytokines such as IL-10. This microbial population has also been shown to have a significant reduction in the biodiversity of intestinal microbiota in CD patients, as opposed to healthy controls (Sokol et al., 2008; Looijer-van Langen and Dieleman, 2009). Apart from *Firmicutes*, IBD patients also exhibit a decrease in the abundance of *Bacteroidetes*, in particular the *Bacteroides fragilis* (Swidsinski et al., 2005). In contrast to the decrease of both *Firmicutes* and *Bacteroidetes* microbial populations in the inflamed gut, studies have reported an increase of *Proteobacteria* and *Actinobacteria* in patients with active IBD (Frank et al., 2007; Peterson et al., 2008; Chassaing and Darfeuille-Michaud, 2011). For instance, an increased number of mucosa-associated *Escherichia coli* (*E.coli*) has been shown in CD patients. These adherent-invasive *E.coli* (AIEC) invade the intestinal epithelium cell barrier by adhering to the epithelial cells, followed by the replication within these cells. The high prevalence of AIEC in CD patients may be the outcome from the failure of intestinal mucosa to limit microbial invasion, a consequence from the defect in Paneth cell function and the subsequent decreased secretion of antimicrobial peptides in the GI tract (Chassaing and Darfeuille-Michaud, 2011).

Overall, even though there are significant findings suggesting an association of dysbiosis of intestinal microflora to the pathogenesis of IBD, it is still unclear as to whether the dynamic changes in the gut microbiota is a cause or a consequence of chronic intestinal inflammation.

1.2 Cannabinoids

The therapeutic properties of cannabis are first described in Chinese pharmacopoeia dating back to 200A.D, whereas intensive studies with the compound only began in the western world from the 19th century onwards. Since then, research on cannabis has moved progressively from the plant to its components, the associated receptors and the endogenous counterparts in the mammalian system (Di Marzo, 2006). In the 1970s, Hans Kosterlitz and John Hughes, from Marischal College in Aberdeen, started to question the presence of morphine receptors in the mammalian brain and proposed that such receptors should not only be activated via the plant substances, but also via the ligands which are made in association with the receptor within the mammalian system. Given this, together with Howard Morris, from London, they then discovered enkephalins, the endogenous agonist for the uncloned opiate receptors (Hughes et al., 1975). Based on the discoveries of endogenous “morphine-like” compounds, Raphael Mechoulam and his group from Jerusalem strongly believed in the presence of endogenous ligands for the cannabinoid receptor (CNR)-1, a receptor which is highly expressed in mammalian’s brain. In 1992, together with Roger Pertwee from Marischal College, they successfully isolated and chemically identified Anandamide (AEA), the first discovered endogenous cannabinoid (Devane et al., 1992). This was followed in 1995 by the discovery of a second endogenous CNR1 ligand, 2-arachidonoylglycerol (2-AG), by a Japanese team (Sugiura et al., 1995). Later, in 1998, with the discoveries and recognitions of various endogenous ligands for CNR, Vincenzo Di Marzo from Italy proposed the term “endocannabinoids” for all endogenous cannabinoid ligands and from this evolved the so-called “endocannabinoid system” which consists of the cannabinoid receptors, their associated ligands, the enzymes and the proteins which regulate the ligand concentration (Di Marzo, 2006).

1.2.1 *The endocannabinoid system*

The endocannabinoid system (ECS) consists of endogenous cannabinoids, cannabinoid receptors and enzymes that are involved in either synthesizing or degrading endogenous cannabinoids. At first, it was thought that the action of ECS mainly occurred in the centre of the brain, however, it was soon discovered that apart from the brain, GI tract, liver, pancreas, adipose tissue, and skeletal muscle are all involved in the network of the ECS (Cluny et al., 2012).

Endocannabinoids are endogenous lipid signalling molecules. Interestingly, endocannabinoids mimic the pharmacology activity of Δ^9 -THC, an active compound of marijuana, *Cannabis sativa*. Δ^9 -THC, as well as endocannabinoids is shown to be primarily regulated through the cannabinoid G protein coupled receptors: cannabinoid receptor CNR1 and CNR2. The finding of the cannabinoid receptors have led to the discovery of other THC-like compounds: *N*-arachidonylethanolamine, or AEA and 2-AG (Bisogno, 2008; Cluny et al., 2012). Little was known of the endogenous role of the receptors until AEA, 2-AG and other endocannabinoids were identified. Endocannabinoids are formed by amides, esters, and ethers of long-chain polyunsaturated fatty acids. To date, five classes of endocannabinoids have been identified: AEA, 2-AG, Nolethanolamine, virodhamine and lastly *N*-arachidonoyldopamine (NADA) (Bisogno, 2008; Piomelli, 2003). Unlike other modulators that are biosynthesized in advance and stored in intracellular compartments for later use, endocannabinoids are synthesized on demand through the regulation of the intracellular concentration of Ca^{2+} (Cluny et al., 2012).

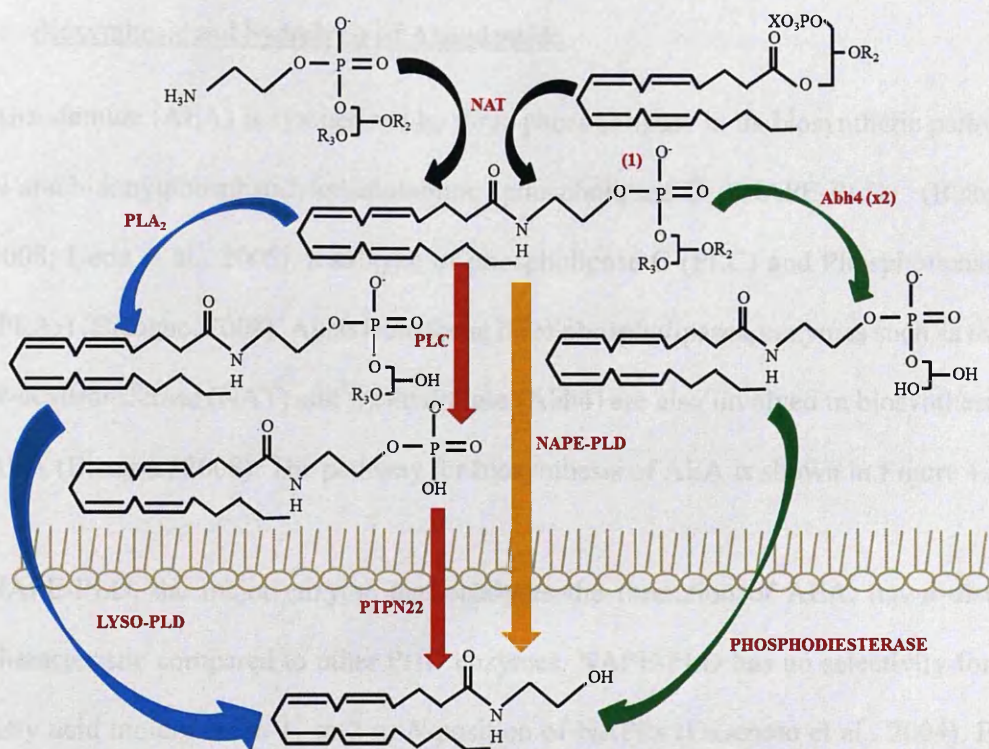


Figure 1.3. Major biosynthesis pathway for endocannabinoid anandamide (AEA). The pathway is divided into two major enzymatic reactions. The first step is the formation of *N*-ArPE where the fatty acid chain from sn-1 position of glycerophospholipids is transferred to the amino group of phosphatidylethanolamine. This step is catalysed by enzyme NAT. Next, there are four major pathways lead to AEA formation. *N*-ArPE can either be catalysed by PLC and PTPN22 via the formation of phospho-AEA or by PLA₂ and lyso-PLD via the formation of 2-lyso-*N*-arachidonoyl-phosphatidylethanolamine, or by Abh4 and phosphodiesterase via formation of glycerol-phospho-AEA or by NAPE-PLD.

**Redrawn from Bisogno, 2008.*

Abbreviation: AEA, anandamide; N-ArPE, N-arachidonyl-phosphatidylethanolamine; NAT, trans-N-acyltransferase; PLC, Phospholipase C; PTPN22, Protein tyrosine phosphatase 22; PLA₂, Phospholipase A₂; lyso-PLD, Lyso-phospholipase; Abh4, χ/β-hydrolase; NAPE-PLD, N-arachidonylphosphatidylethanolamide phospholipase D.

i. Biosynthesis and hydrolysis of Anandamide

Anandamide (AEA) is synthesized by three phospholipase in its biosynthetic pathway: N-arachidonylphosphatidylethanolamine phospholipase-D (NAPE-PLD) (Bisogno, 2008; Ueda et al., 2005), a subtype of phospholipase C (PLC) and Phospholipase A₂ (PLA₂) (Bisogno, 2008). Apart from those three phospholipases, enzymes such as *trans*-N-acyltransferase (NAT) and α/β -hydrolase (Abh4) are also involved in biosynthesis of AEA (Bisogno, 2008). The pathway for biosynthesis of AEA is shown in Figure 1.3.

NAPE-PLD, the major enzyme that catalyses the formation of AEA, has a distinct characteristic compared to other PHD enzymes. NAPE-PLD has no selectivity for the fatty acid moiety on sn-1, sn-2 or *N*-position of NAPEs (Okamoto et al., 2004). Even though NAPE-PLD is named as phospholipase D, its amino acid sequence shows that there is no shared homology between NAPE-PLD and other phospholipase D enzymes (Okamoto et al., 2004). AEA is the ligand for CNR1 and CNR2 receptors which are located in the surface of the target cells. In addition to its endocannabinoid activity, AEA is also an “endovanilloid”, which binds to the intracellular binding site of the Transient Receptor Potential Vanilloid type 1 (TRPV1) receptor (Van Der Stelt and Di Marzo, 2004).

AEA is rapidly hydrolysed and thus removed from the extracellular space by fatty acid amine hydrolase (FAAH). During hydrolysis, FAAH breaks the amide bond of AEA to yield arachidonic acid (AA) and ethanolamide (Ueda et al., 2005). By doing that, FAAH is controlling the cellular uptake of AEA by maintaining or creating the concentration gradient between the intracellular and extracellular space that facilitates diffusion of AEA.

Studies suggest there is a membrane transporter that facilitates the diffusion of AEA from the extracellular milieu into extracellular space, named the AEA membrane transporter (AMT). Accumulation of AEA in FAAH knock-out mice gave the indication of the existence of additional mechanisms involved in the up-taking of AEA (Fegley et al., 2004). Additionally, discovery and development of several compounds such as AM1172 inhibitor, which appeared to have the capability to inhibit cellular uptake of AEA but not the AEA hydrolysis via FAAH, also support the existence of AMT (Fegley et al., 2004). However, this is still under investigation and the existence of AMT will only be certain if further molecular evidences of AMT are found.

ii. Functional consequences of AEA

As for the functional consequences for AEA, this endocannabinoid has been shown to be greatly involved in the modulation of pain, anxiety, as well as the angiogenesis and apoptotic process during tumour progression (Luchicchi and Pistis, 2012; Portella et al., 2003).

The role of AEA in anxiety modulation is demonstrated through the study where enhanced AEA successfully reversed the anxious phenotype in mice which had been exposed to stress and the AEA-induced effect was mediated via the CNR1 receptor. In agreement with that finding, the *in vivo* study also showed that by knocking out the FAAH gene in the system, the anxiety-like behavioural response was significantly reduced in mice and such effect was shown to be CNR1 mediated (Rossi et al., 2010). This implied that the AEA-induced effect on anxiety modulation is mediated through the CNR1 receptor and such outcome may possibly correlate to the inhibition of FAAH.

Apart from the role of AEA in tumour progression, the study showed that administration of endocannabinoid analog 2-methyl-arachidonyl-2-fluoro-ethylamide (Met-F-AEA) to mice with *K-ras* established tumours, dramatically reduced the tumour size, as compared to untreated mice. This effect, however, was significantly inhibited once the treatment was replaced by the CNR1 antagonist SR141716A (Portella et al., 2003). Met-F-AEA is also capable in inhibiting p21^{ras} and subsequently, this can lead to the inhibition of angiogenesis by down-regulation of vascular endothelial growth factor (VEGF) (Portella et al., 2003). This implied that AEA may reduce tumour progression by inhibiting angiogenesis in the tumour cells and such an effect may be CNR1 mediated.

iii. The cannabinoid receptors

CNR1 and CNR2 are two of the well-studied examples of cannabinoid receptors. CNR1 is proficient in coupling and activating G_i/G₀ stages in cell cycle, whilst CNR2 selectivity actuates G₀ (Glass and Northup, 1999). CNR1 was the first to be discovered and studies have shown that the expression level of CNR1 is high in the brain regions that associate with cannabinoids and low in regions where cannabinoids are not normally produced such as the respiratory centres of medulla (Herkenham et al., 1991). The binding of cannabinoids to CNR1 activates many important signalling pathways that control cell fate. These include phosphatidylinositol-3-kinase (PI3K) and its downstream effector protein kinase B (PKB/AKT) signalling pathway, ERKs, c-Jun N-terminal kinase (c-JNK) and the p38 MAP kinase pathway (Guzmán, 2003).

CNR2 was discovered much later than CNR1, as the expression of CNR2 in the cell is lower than that of the CNR1 receptor, resulting in difficulty in creating a highly selective antibody for the CNR2 (Van Sickle et al., 2005). Studies have shown that the CNR2 is

expressed in immune cells, suggesting that CNR2 has a role in the human immune function (Demuth and Molleman, 2006).

1.2.2 Cannabidiol (CBD)

Δ^9 -THC is commonly viewed as the main component that contributes to the cannabis-induced effect but the presence of cannabidiol (CBD), another component which may constitute up to 40% of the cannabis extracts, has often been neglected (Zuardi et al., 2006). CBD was first isolated from marijuana extract in 1940. However, there was a halt in the journey of discovery as no finding was reported for the following 25 years. The next CBD-related finding was published in 1963 by Mechoulam and Shvo where the chemical structure of CBD was revealed. Up to 1975, CBD was reported alongside other cannabis in the publications, but not many studies only concentrated on the action of CBD itself. Only recently (from early 2000's), CBD research started to gain the attention of various research groups, as CBD is a non-psychoactive cannabinoid and exerts positive pharmacological effects in response to inflammation, cancer and even neurodegenerative diseases such as Parkinson's and Alzheimer's diseases (Antonio Waldo, 2008; Capasso et al., 2008; Izzo et al., 2009). To date, CBD has been used in combination with Δ^9 -THC in a 1:1 ratio in Sativex[®] drug for treating multiple sclerosis (Izzo et al., 2009).

i. CBD in Endocannabinoid system (ECS)

CBD, unlike Δ^9 -THC, possesses a low binding affinity for both CNR1 and CNR2 receptors. Apart from the cannabinoid receptors (CNR1, CNR2), CBD also acts as the receptor antagonist for the orphan receptor, GPR55 (Antonio Waldo, 2008). Nonetheless, administration of CBD also stimulates the TRPV1 receptor (Bisogno et al.,

2001), a receptor which also binds to the endocannabinoid, AEA. Furthermore, studies also showed CBD modulated ECS by inhibiting the FAAH-mediated hydrolysis of AEA (Capasso et al., 2008; Watanabe et al., 1996), suggesting that such effect may be mediated through TRPV1 receptor.

ii. Anti-inflammatory action of CBD

Various *in vivo* and *in vitro* studies have demonstrated that the phytocannabinoid, CBD acts as an anti-inflammatory agent by reducing the production of pro-inflammatory cytokines. CBD decreased the production of tumour necrosis factor (TNF)- α in LPS treated mice through an adenosine receptor activation (Izzo et al., 2009). Additionally, CBD has also been shown to reduce croton oil-induced hypermotility in mice and this was shown to be regulated through CNR1 and FAAH (Capasso et al., 2008). This finding implies that CBD may be a potential therapeutic drug to normalise motility in patients with inflammatory bowel disease (IBD).

1.2.3 ***Cannabinoids in IBD***

Various studies have been performed to look into the role of the ECS in gut homeostasis and its relation to the occurrence of IBD. Overall, ECS is shown to be involved in the modulation of inflammation, motility, and permeability of the GI tract (Alhouayek and Muccioli, 2012; Di Marzo and Izzo, 2006; Izzo et al., 2001; Massa et al., 2004; Wright et al., 2005).

During intestinal inflammation, up-regulation of endocannabinoid levels and the increased expression of cannabinoid receptors will enhance the action of endocannabinoid system (Di Marzo and Izzo, 2006). This is shown by the increased CNR1 receptor expression in the colon of the intrarectal dinitrobenzene sulphonic acid

(DNBS) treated mice (Massa et al., 2004). Apart from that, they also highlighted the point that by knocking out the CNR1 gene, it will lower the inflammatory score of the DNBS-treated mice. On the other hand, study showed that in healthy human intestinal epithelium, the CNR2 expression is weak. In IBD patients, there was an increased expression in CNR2 receptor (Wright et al., 2005). However, the actual function and mechanism regarding the increased CNR2 expression on the epithelial cells remains unknown. Most of the findings associated with the CNR2 receptor showed that activation of the CNR2 receptor will lower the secretion of pro-inflammatory cytokines from immune cells. Consequently, this benefits the shift away from inflammation (Klein, 2005).

Next, ECS is also involved in the modulation of gastrointestinal motility. The hypermotility of the intestinal tract is often related to the onset of chronic IBD, which predominantly leads to the consequent effect of diarrhoea due to an increase in secretion and/or a decrease in absorption, with reduced colon contractility (Alhouayek and Muccioli, 2012). Studies showed that cannabinoid receptors are capable of inhibiting inflammation-induced hypermotility. The treatment of CP55940, an agonist for both CNR1 and CNR2 receptors delayed the intestinal motility in inflamed mice. The CP55940 induced effect was inhibited by CNR1 antagonist but not by CNR2 antagonist, suggesting that CNR1 but not CNR2 is involved in the modulation of hypermotility in the GI tract (Izzo et al., 2001). As previously stated, CNR1 is highly expressed during inflammation and with the finding of CNR1's role in inhibiting gastrointestinal hypermotility, this suggests that the increased CNR1 expression may be beneficial to normalize the hypermotility observed in IBD.

Increased intestinal permeability is implicated in IBD pathogenesis, as the presence of a leaky intestinal barrier will promote microbial invasion through the mucosal tissue, which subsequently leads to an increase in pro-inflammatory cytokine production, resulting in chronic inflammation. Study showed that both Δ^9 -THC and CBD are capable of modulating intestinal permeability by increasing the recovery time of EDTA-induced increased permeability in CaCo2 cell and such effect was CNR1-dependent (Alhamoruni et al., 2010). Additionally, the treatment of Δ^9 -THC and CBD also increased the mRNA of tight junction protein zona occluden(ZO)-1 in the cell model, suggesting that both of these cannabinoids may be beneficial for treating abnormally permeable intestinal epithelium (Alhamoruni et al., 2010).

1.3 Suppressor of Cytokine Signalling (SOCS)

Innate immunity is the first defence mechanism induced by the body's immune system in response to pathogen invasion. Activation of such defence mechanism leads to the release of pro-inflammatory cytokines, resulting in the recruitment of immune cells to the site of injury. Therefore, it is essential for the cytokine-mediated signal transduction to be tightly-regulated in the immune system and this is generally regulated by initiating a negative feedback regulatory process via the cytokine-bound-receptor (Dalpke et al., 2008). The importance in SOCS-induced cytokine regulation in the immunity response can be illustrated via a study, which demonstrated an elevated level of interferon (IFN)- γ and IFN- γ production activity, resulting from the loss of SOCS1 gene, could result in an overwhelming inflammatory response, which subsequently led to the development of complex fatal neonatal disease (Alexander et al., 1999).

SOCS protein acts as the negative feedback inhibitor towards the JAK-STAT-induced signal transduction, as the mechanism of action in regulating cytokine production. Binding of cytokines to the associated receptor initiates a conformational change on the receptor itself, resulting in the auto-phosphorylation of the tyrosine residues on Janus kinases (JAK). Consequently, the activated JAK kinases will recruit signal transducer and activator of transcription factors (STAT) via the phosphor-tyrosine-binding Src homology 2 (SH2) domain. In turn, the activated STAT will form STAT dimers with other phosphorylated STAT residue and the accumulation of activated STAT dimers in the cell nucleus will eventually initiate the transcription of SOCS gene (Dalpke et al., 2008; Piessevaux et al., 2008).

There are a total of eight functional proteins in the SOCS family (cytokine-inducible SH2-containing protein (CIS) and SOCS1-7). Among these eight SOCS proteins, SOCS1 and SOCS3 are the well-studied SOCS proteins in the family. They share a similarity in their

structural homology with the presence of SH2 domain and a carboxyl-terminal SOCS box domain. These SOCS proteins are distinguishable via the length of their amino-terminus and the presence of kinase inhibitory region (KIR) domain. SOCS protein utilised its SH2 domain to bind to the phosphorylated tyrosine residue on the JAK kinases, resulting in cytokine inhibition. The action of SOCS protein on cytokine regulation is SOCS protein specific, as each of the SOCS protein members has been shown to act on different cytokine-bound receptors, hence delivering distinct SOCS-induced effects (Dalpke et al., 2008). This can be clearly illustrated through the study which revealed the reciprocal function of SOCS1 and SOCS3 in IL-6 and IFN- γ regulation. Mice with SOCS3 deficiency initiated a prolonged IL-6-induced STAT1 and STAT3 activation but did not deliver an impact towards IFN- γ -induced STAT1 activation. As opposed to that, mice with SOCS1 deficiency developed a prolonged IFN- γ -induced STAT1 activation but showed no impact in response to the IL-6 treatment (Crocker et al., 2003).

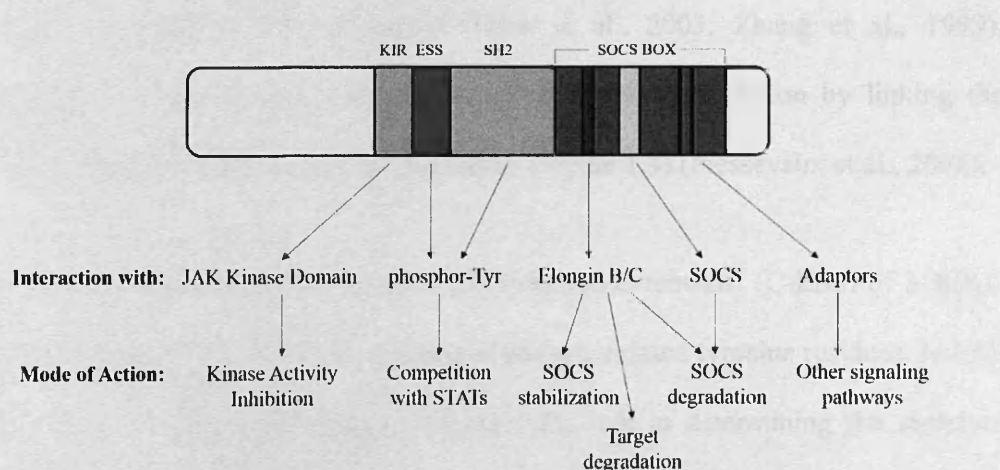


Figure 1.4. SOCS protein functions. Each domain of SOCS protein initiates different interaction and functions. All SOCS proteins share a similar N-terminal domain consists of an extended SH2 subdomain (ESS) and a SOCS box whereas the KIR domain only present at the N-terminal of SOCS1 and SOCS3. The complex of SOCS box interaction provides a diversity of functional consequences, for instance, regulation of SOCS protein stability, the receptor interaction and the elimination of targeted protein.

**Redrawn from Piessevaux, et al., 2008.*

1.3.1 Structural and functional of SOCS

As previously stated, all SOCS proteins share a similar N-terminal domain that consists of an extended SH2 subdomain (ESS) and a SOCS box whereas the KIR domain is only present at the N-terminal of SOCS1 and SOCS3 (Dalpke et al., 2008; Piessevaux et al., 2008).

Protein expression of SOCS protein is regulated through SOCS box, a conserved domain which is located at the C-terminal of SOCS protein (Piessevaux et al., 2008). This region comprises of a total of 40 amino acids which forms three alpha-helices that binds to the E3 ubiquitin ligase complex. Such ligase complex consists of Elongin B/C, a ring-finger protein Rbx1 and a scaffolding protein, Cullin 5 proteins (Crocker et al., 2008). Several studies suggested that Elongin C bound to the SOCS protein, thus provided stabilization to the SOCS protein expression and the disruption of such interaction resulted in proteasome-mediated SOCS destruction (Haan et al., 2003; Zhang et al., 1999). Additionally, the SOCS box is also involved in protein degradation by linking the targeted protein towards proteasomal machinery (Figure 1.4) (Piessevaux et al., 2008).

As for the SH2 domain, both N-terminal (N-ESS) and C-terminal (C-ESS) of SOCS3-SH2 domains are important for the binding of phosphorylated tyrosine residues. N-ESS consists of a 15-residue alpha helix and plays the role in determining the structure orientation of N-ESS bound phosphotyrosine-binding loop (Crocker et al., 2008). Mutation of Val34 and Leu41 which interacted directly with the phosphotyrosine binding loop consequently affected SOCS3 ability to inhibit STAT activation (Sasaki et al., 1999). Hence, this indicated the role of the SH2 domain in completing for the binding site with STAT protein. On the contrary, C-ESS possesses a 35-residue of unstructured PEST motif that is rich in proline, glutamate, serine and threonine (Crocker et al., 2008). The

loss of PEST motif did not impact on the interaction of the SH2 domain with the phosphorylated-tyrosine residue. Interestingly, the removal of the PEST motif induced a greater effect on SOCS3 protein stability, as compared to the loss of the SOCS box. This suggested that the PEST motif also has a role in maintaining SOCS3 protein stability (Babon et al., 2006). Various studies indicated the involvement of PEST motif in SOCS3 degradation. However, there is still a controversy as to whether the PEST motif is modulated through the proteasomal-degradation pathway (Babon et al., 2006; García-Alai et al., 2006; Rechsteiner and Rogers, 1996).

Next, the KIR domain, which is present in both the N-terminal domain of SOCS1 and SOCS3 proteins, is shown to act as the pseudo-substrate to inhibit JAK kinases in the JAK-STAT signalling cascade (Kershaw et al., 2013; Piessevaux et al., 2008; Sasaki et al., 1999). The KIR domain of SOCS3 possesses a higher binding affinity to JAK2, as compared to the KIR domain of SOCS1 (Sasaki et al., 1999).

1.3.2 SOCS3 in inflammatory regulation

SOCS3 is the key regulator for IL-6 and IL-10 cytokines production in response to TLR activation (Yoshimura et al., 2007). TLR is involved in the initiation of innate immune response in response to pathogen invasion. IL-6 is a pro-inflammatory cytokine which is up-regulated in many inflammatory diseases (rheumatoid arthritis, Crohn's disease, ulcerative colitis) (Mudter and Neurath, 2007), whereas IL-10 is an anti-inflammatory cytokine which can inhibit the TLR signalling activation. It is interesting that SOCS3 is induced by both of these cytokines which deliver an absolute opposite effect in response to inflammation. However, interestingly, IL-6 induces an anti-inflammatory response in the absence of SOCS3 and this was demonstrated through the study where both IL-6 and

IL-10 suppressed LPS-induced TNF- α production in SOCS3 deficient macrophages (Yasukawa et al., 2003). Also, despite the fact that SOCS3 is induced by both IL-6 and IL-10, SOCS3 only acts on IL-6 receptor but not on IL-10 receptor and initiates a negative feedback inhibition on IL-6 signaling. With that, this suggests that SOCS3 is the central negative regulator for IL-6 signaling (Yasukawa et al., 2003).

1.3.3 SOCS3 action in IBD

It has been reported that SOCS3 is up-regulated in both animal and human intestinal inflammation (Suzuki et al., 2001). SOCS3 (both mRNA and protein) was shown to be up-regulated in colon samples from UC and CD patients compared with healthy controls. SOCS3 also limits proliferation of epithelial cells in the damaged crypt, but contrary to in vitro investigations, up-regulation of SOCS3 in inflamed intestines, does not appear to sufficiently limit STAT3 and NF-KB inflammatory pathways (Rigby et al., 2007).

1.4 Autophagy

Autophagy is a cellular mechanism utilised to adapt to the cellular environmental changes by promoting proteolytic degradation of the cytosolic compartments at the lysosomes (Chang et al., 2009; Glick et al., 2010; Klionsky and Emr, 2000; Singh and Cuervo, 2011). Autophagy can be characterized into three categories: chaperon-mediated autophagy (CMA), microautophagy, and macroautophagy (Glick et al., 2010; Mizushima, 2007). In CMA, the misfolded proteins are bound to the chaperone proteins and delivered to the lysosome through the lysosomal membrane receptor, the lysosomal-associated membrane protein 2A (LAMP-2A) (Glick et al., 2010). In contrast, for microautophagy, the cytoplasmic cargo is engulfed directly into lysosomes through the lysosomal membrane, whereas in macroautophagy, the cytosolic compartment is degraded via the autophago-lysosomal degradation pathway. The cytosolic compartments are taken up into autophagosome, a double membrane vesicle, which resulted in the fusion with lysosome to form autolysosome where the cytosolic compartment is degraded (Mizushima et al., 2008). Macroautophagy is the major type of autophagy process and it is the main autophagy process investigated in this project, therefore, the term of “autophagy” will be used in the following texts as the synonym for “macroautophagy”.

1.4.1 Overview in autophagy process

Although the autophagy process is well-recognized in the mammalian system, the vast majority of the breakthroughs associated with the understanding of the autophagy process and its regulation are discovered in yeast (*Saccharomyces cerevisiae*) (Glick et al., 2010). To date, 32 autophagy-related genes (ATGs) have been discovered through the genetic screening experiment performed in the yeast model system (Glick et al., 2010; Nakatogawa et al., 2009). The importance of ATG is emphasized as most of the ATG genes are well-conserved in yeast, mammals, flies and even plants (Glick et al., 2010).

The complexity of the autophagy process can be summarized into three key stages: (i) autophagy initiation, (ii) autophagolysosome formation, and lastly, (iii) autophagic degradation (Figure 1.5).

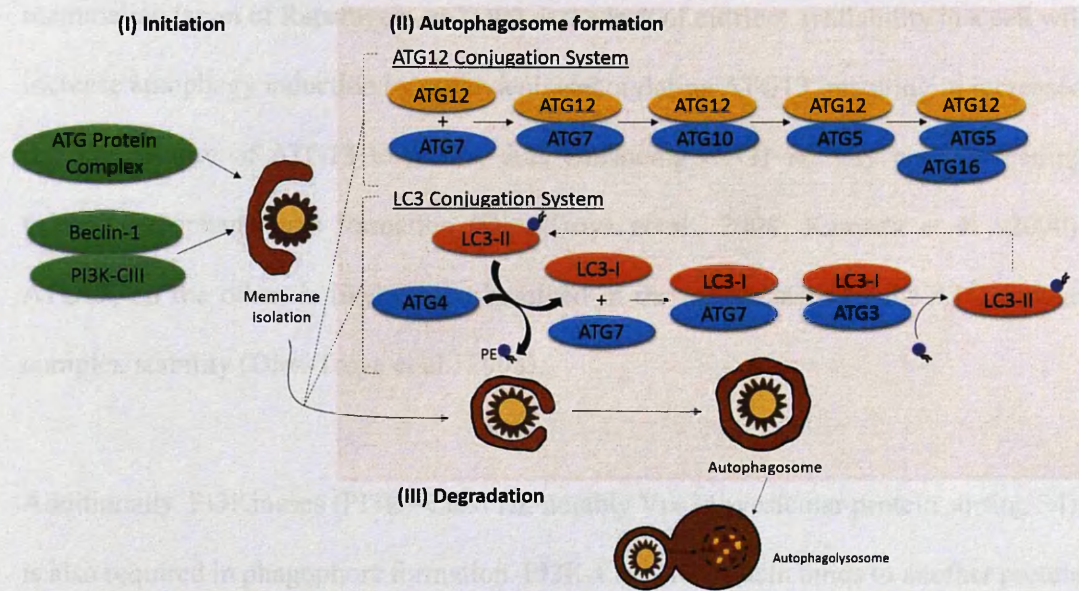


Figure 1.5. Molecular event in autophagy. Autophagy is regulated by a set of autophagy related proteins (ATGs). The complexity of the autophagy process can be categorized into three key stages: (I) autophagy initiation, (II) autophagosome formation, and lastly, (III) autophagic degradation.

**Modified and redrawn from Levine and Deretic, 2007.*

i. Autophagy initiation

The autophagy process begins with phagophore, an isolation membrane (Glick et al., 2010). There is controversy regarding the origin of phagophore. Studies suggest that phagophore may originate from various cellular compartments such as the plasma membrane, endoplasmic reticulum (ER), golgi and mitochondria (Axe et al., 2008; Glick et al., 2010; Moreau and Rubinsztein, 2012; Simonsen and Tooze, 2009). An autophagy protein complex which consists of ATG1-ATG13-ATG17 is required for phagophore

formation and it is thought that ATG9 may facilitate lipid recruitment to expand the phagophore structure. These activities are regulated through the energy-sensing TOR kinase as the TOR kinase will phosphorylate ATG13, hence inhibiting the interaction of ATG13 on ATG1 (Diaz-Troya et al., 2008). Rapamycin-induced inactivation of mammalian target of Rapamycin (mTOR) or the lack of nutrient availability in a cell will increase autophagy induction by rapid dephosphorylating ATG13, resulting in increased binding affinity of ATG13 to ATG1, thus enhancing ATG1 activity and proceeding towards autophagosome formation (Diaz-Troya et al., 2008; Kamada et al., 2000). ATG17, on the other, is likely to be involved in the maintenance of the ATG protein complex stability (Diaz-Troya et al., 2008).

Additionally, PI3Kinases (PI3K)-Class III, notably Vps34 (vesicular protein sorting 34), is also required in phagophore formation. PI3K-Class III protein binds to another protein complex that consists of ATG6-Beclin1 (Figure 1.5) (Levine and Deretic, 2007). PI3K-Class III uses phosphatidylinositol (PI) as its substrate to produce phosphatidyl inositol triphosphate (PI3P), which is required for phagophore elongation and recruitment of the ATG6-Beclin1 protein complex to the phagophore (Glick et al., 2010). The beclin-1 activity in autophagy induction on the other hand, is regulated through the apoptosis regulator, B-cell lymphoma 2 (Bcl-2). Interaction of bcl-2 to beclin-1 disturbs the interaction between PI3K-Class III and beclin-1 (Pattingre et al., 2005). During starvation, bcl-2 inhibits beclin-1 associated autophagy activity by binding to the BH3 domain on beclin-1, resulting in the disruption of bcl-2 apoptotic action and the activation of the autophagy process in response to starvation (Glick et al., 2010; Pattingre et al., 2005).

ii. Autophagosome formation

Two ubiquitin-like systems are required for autophagosome formation: the conjugation of ATG12 and ATG5 and the processing of the microtubule-associated protein light chain 3 (LC3B) (Figure 1.5).

Once the membrane is isolated by ATG6-Beclin1 protein complex, ATG7, the E1-like ubiquitin-activating enzyme, binds to the carboxy-terminal glycine residue of ATG12 and activates the enzyme activity of ATG12. This subsequently leads to the transferring of ATG12 to ATG10, where ATG10 acts as an E2-like ubiquitin carrier protein to facilitate the interaction of ATG12 to the lysine 130 residue on ATG5 (Glick et al., 2010; Klionsky and Emr, 2000). This is then followed by the association of ATG16L to the conjugated ATG5-ATG12 protein complex, resulting in the formation of a multimeric protein complex (Glick et al., 2010). Initiation of ATG5-ATG12 conjugation is not dependent on the activation of autophagy (Barth et al., 2010) but the conjugation of ATG12-ATG5 is crucial for the elongation of the phagophore membrane as the study showed that the loss of the ATG5 gene led to a defect in autophagosome formation in the mouse embryonic stem (ES) cells (Mizushima et al., 2001; Yoshimori, 2004). ATG5 protein complex binds to the back of the isolation membrane and only dissociates from the phagophore membrane prior to the closure of the membrane, resulting in autophagosome formation (Yoshimori, 2004). In addition to the role of ATG5-ATG12-ATG16L1 protein complex in facilitating isolation membrane elongation, such protein complex also appears to be required for targeting LC3 to the isolation membrane as the study showed that the loss of ATG5 gene in mouse ES cells consequently disrupted the recruitment of LC3 to autophagic membrane (Mizushima et al., 2001).

The newly synthesized LC3 (22 amino acid) is cleaved at its c-terminal by ATG4 protease to form LC3-I. This subsequently leads to a series of ubiquitin-like reactions with the involvement of ATG7 and ATG3, resulting in the conversion of LC3-I (18KDa) to LC3-II (16KDa). Upon the conversion, LC3-I is distributed in the cytoplasm whereas LC3-II is bound to the autophagosome (Glick et al., 2010; Mizushima, 2007; Patel and Stappenbeck, 2013; Yoshimori, 2004). A phosphatidylethanolamine (PE) group is attached to the LC3-II where this protein promotes the integration of LC3-II into the lipid membrane of autophagosome (Barth et al., 2010; Patel and Stappenbeck, 2013). It is worth noted that LC3-II is the only discovered protein that is specifically localised to the autophagic structure (starting from phagophore membrane to lysosomal degradation) and the amount of LC3-II correlates well to the number of autophagosome (Yoshimori, 2004). Taken together, this has made LC3-II a hallmark feature in studying the autophagic process.

iii. Autophagic degradation

In the final stage, the autophagosome maturation stage, the completed autophagosome will fuse with lysosome to form autophagolysosome for degradation (Glick et al., 2010; Klionsky and Emr, 2000; Patel and Stappenbeck, 2013).

1.4.2 Autophagy in the cellular energetic balance

The autophagic process can be triggered by various occasions and one of the best characterized stimuli is starvation. The removal of nutrient source such as nitrogen and carbon and the lack of amino acid are the contributors towards autophagy induction (Deretic and Levine, 2009; Kuma and Mizushima, 2010; Mizushima, 2007; Singh and Cuervo, 2011). The autophagic activity in response to nutrient status is regulated by the

mTOR (Diaz-Troya et al., 2008; Singh and Cuervo, 2011). Under normal nutritional status, mTOR phosphorylates ATG13 and inhibits its interaction with ATG1, which subsequently prevents the formation autophagosome. In contrast, during starvation, the activation of a second cellular energy sensor protein, 5' adenosine monophosphate-activated protein kinase (AMPK) will inhibit mTOR activity by phosphorylating ATG1, which promotes the release of ATG1 from mTOR, resulting in the autophagy induction (Singh and Cuervo, 2011).

In addition to the role of autophagy in response to nutritional status, the autophagic process is also involved in protein aggregates turnover or degradation (Komatsu et al., 2005; Singh and Cuervo, 2011). This role of autophagy is clearly demonstrated in the liver where autophagy is responsible for breaking down 1.5% to 5% of the total proteome per hour, under normal nutritional condition or starvation, respectively (Deter et al., 1967). Amino acids which result from protein breakdown may be used to maintain protein synthesis, as well as for the replenishment of the intracellular pool of amino acid (Onodera and Ohsumi, 2005; Singh and Cuervo, 2011). However, the mechanism involved in the regulation of the intracellular pool of amino acid and autophagy process is still unclear. Despite that, it is certain that defect in autophagy often relates to the formation of protein aggregates and study suggested that this may contribute to the developing of protein conformation diseases such as Alzheimer's disease (Komatsu et al., 2006; Singh and Cuervo, 2011).

1.4.3 Autophagy regulation in gastrointestinal (GI) tract

The GI tract is composed from a single layer of intestinal epithelial cells. This cellular structure is responsible for facilitating the GI tract in nutrient absorption and digestion.

Nonetheless, it also serves as the intestinal barrier against microbial invasion, as well as antigens passing through the intestinal lumen (Patel and Stappenbeck, 2013). In addition to hosting innate and adaptive defence mechanisms, various autophagy proteins are shown to be required for the cellular intestinal function in response to inflammatory threat. Autophagy proteins were demonstrated to be involved in: (i) cytokine secretion by monocyte-derived cells, (ii) bacteria handling in dendritic cells, (iii) antimicrobial peptide secretion by Paneth cells, and lastly, (iv) xenophagy induction.

i. Autophagy mediated cytokine secretion by macrophages

Autophagy suppresses intestinal inflammation by mediating macrophage-induced cytokine secretion. A study showed that LPS-treated ATG16L1-deficient macrophages induced a high level of pro-inflammatory cytokines, IL-1 β and IL-18 (Saitoh et al., 2008). The loss of the ATG16L1 gene in mice impacts on the recruitment of ATG12-ATG5 conjugate to the isolation membrane, which subsequently affects autophagosome formation, as well as degradation of lone-lived proteins (Saitoh et al., 2008). Additionally, another study revealed that the LPS-induced effect in ATG16L1-deficient macrophages was mediated through the TRIF (TIR-domain-containing-adaptor inducing interferon- β), the key adaptor protein for TLR3 and TLR4 signalling (Hardy et al., 2004). This was concluded based on the finding where ATG16L1-deficient macrophages did not respond to both TLR2 and TLR5 ligand but induced an increase in IL-1 β production in response to LPS treatment, a TLR4 ligand (Saitoh et al., 2008). As the production and secretion of IL-1 β and IL-18 are both mediated via the activation of inflammasome (Petrilli et al., 2005), this suggests that ATG16L1 is responsible for regulating endotoxin-mediated inflammasome activation via a TRIF-dependent manner.

ii. Autophagy in bacteria handling in dendritic cells

Activation of the autophagy process is also required for bacteria-handling in dendritic cells (DCs) (Cooney et al., 2010; Patel and Stappenbeck, 2013). These cells have been implicated to protect the intestine from microbial invasion by sampling luminal bacteria through the formation of tight junction-like structure with intestinal epithelial cells (IEC), allowing the projection of dendritics into the lumen to capture the invasive bacteria (Coombes and Powrie, 2008). Study showed that nucleotide-binding oligomerization domain-containing-2 (NOD2), the bacteria sensor in DC, induces autophagy activation in response to bacteria ligand treatment (Cooney et al., 2010). Such effect is mediated by autophagy proteins ATG5, ATG7, as well as ATG16L1 and receptor-interacting serine-threonine kinase-2 (RIPK-2) protein. The NOD2-mediated autophagy process is crucial in bacteria-handling and the importance of the role of NOD2 in IEC is further emphasized in CD where mutation in the NOD2 gene disrupts autophagy induction, as well as bacteria-trafficking in IEC (Cooney et al., 2010).

iii. Autophagy in antimicrobial peptide secretion in Paneth cells

Paneth cells are located at the base of the intestinal crypt villus structure. These cells are responsible for secreting anti-microbial proteins which are present in the lumen of the gut (Klionsky, 2009; Radtke and Clevers, 2005). Interestingly, studies showed that there seems to be a cross-talk between Paneth cells and the intestinal bacteria. Paneth cells alter the composition of microbes in the gut lumen and the microbes influence the gene expression and function of Paneth cells (Cadwell et al., 2008; Stappenbeck, 2010).

Autophagy is shown to be actively involved in Paneth cells as the loss of function for the ATG16L1 gene leads to the disruption of the secretory function of Paneth cells

(Stappenbeck, 2010). Moreover, the complete loss of autophagy function in Paneth cells impacts on the packaging of antimicrobial proteins into granules and thus disrupts the exportation of these anti-inflammatory components into gut lumen (Cadwell et al., 2008). Taken together, this emphasizes the importance of autophagy in Paneth cells in targeting antimicrobial proteins to limit the expression of inflammatory cytokines in the intestinal epithelium.

iv. Xenophagy induction

Xenophagy is the term for the process where autophagy is used as a tool to destroy intracellular bacterial pathogens in a selective manner (Patel and Stappenbeck, 2013). Intracellular bacteria pathogens are generally engulfed by autophagosome and killed in the acidic environment through the lysosomal degradation pathway. However, some of the invasive pathogens are capable of avoiding the conventional autophagy degradation pathway by possessing a phagosome-like structure. Upon infection, *Salmonella*, for instance, evades the destructive pathway through its *Salmonella*-containing vacuoles (SCV) and some of these invasive pathogens will escape from SCV to proliferate in the cytosol. To stop further pathogen invasion, these pathogens will be rapidly ubiquitinated, resulting in the recruitment of autophagy adaptor proteins, p62 and several autophagic receptors such as NDP52, TANK-binding kinase 1 (TBK1), and optineurin (OPTN) (Galluzzi et al., 2011). NDP52 binds to the ubiquitin-coated pathogen, as well as LC3 and delivers the targeted pathogen into autophagosome. Cells with NDP52 deficiency will fail to restrict pathogen proliferation and invasion (von Muhlinen et al., 2010). TBK1, on the other hand, responds to LPS activated TLR4 by binding to NDP52 receptor. This indirectly limits the replication of cytosolic *Salmonella* (Galluzzi et al., 2011). As for the OPTN autophagy receptor, the study showed that the OPTN-contained LIR domain

regulates the interaction between OPTN and LC3 via its N-terminal, which subsequently leads the ubiquitylated-pathogen to nascent autophagosome, hence initiating xenophagy clearance (Galluzzi et al., 2011).

1.4.4 Autophagy in Crohn's Disease (CD)

As previously stated, not only is autophagy responsible for maintaining cellular and energetic balance, such a process is also crucial in regulating the immunity and cellular defence mechanism in intestinal epithelium (Kirkegaard et al., 2004; Levine et al., 2011; Mihalache and Simon, 2012; Patel and Stappenbeck, 2013). Thus, it is not surprising to discover that a number of autophagy-associated genes, such as ATG16L1 and NOD2, are linked to the pathogenesis of CD (Henderson and Stevens, 2012; Patel and Stappenbeck, 2013).

A single nucleotide polymorphism (T300A) in the ATG16L1 is often associated with pathogenesis of CD in the Caucasian population (Henderson and Stevens, 2012). As previously stated in *section 4.1*, ATG16L1 forms a multimeric protein complex with ATG5 and ATG12, and this protein complex is involved in LC3 lipidation during autophagosome formation (Mizushima et al., 2001). Henderson and Stevens (2012) revealed that it is vital to correctly localise ATG16L1 to sites of LC3 lipidation, as correct localization of the gene is required for appropriate autophagosome formation. Low expressing ATG16L1 in hypomorphic mice demonstrated that the autophagy inducer, rapamycin, could no longer induce p62 and LC3-II degradation, and such effects could be reversed by restoring ATG16L1 into the system (Cadwell et al., 2008). Furthermore, ATG16L1 is also involved in Paneth cells regulation, as these hypomorphic mice developed abnormalities in the morphology of these cells in response to a reduced

ATG16L1 gene in the model system (Cadwell et al., 2008). In agreement with these findings, ileocolic resection specimens obtained from CD patients carrying ATG16L1 risk allele also exhibited morphology changes in Paneth cells (Henderson and Stevens, 2012), which further demonstrates the role of ATG16L1 in autophagy, as well as Paneth cell regulation.

In addition to ATG16L1, NOD2 is also one of the susceptible genes for CD. NOD2 was first discovered through the fine mapping of IBD1 locus on chromosome 16, where it was discovered that the leucine-rich repeats (LRR) at the C-terminal of NOD2 are susceptible to CD (Hugot et al., 2001). As previously stated in *section 4.3*, NOD2-mediated autophagy is crucial in bacteria-handling and mutation in the NOD2 gene disrupts autophagy induction, as well as bacteria-trafficking in the intestinal epithelium (Cooney et al., 2010). Kersse et al. (2011) also proposed that NOD2 may be involved in the recognition of danger-associated molecular patterns (DAMPs), a signal which is released in response to the cellular membrane damage and the presence of pathogenic infection. Taken together with a recent study by Philpott, et al. (2013) which demonstrated the localisation of NOD2 on the plasma membrane, these data suggest that NOD2 may engage directly with the pathogens, resulting in the activation of inflammatory and antimicrobial response during microbial invasion.

Possible action of both ATG16L1 and NOD2 in pathogen recognition is further assessed in a study where both NOD2 and ATG16L1 were found to surround the invading pathogens at the entry foci, an activity not observed with mutant NOD2 proteins. Additionally, in the same study, muramyl dipeptide (MDP), a NOD2 ligand, was shown to activate autophagy process, resulting in an increase of *Salmonella* eradication in the

IEC, such events were facilitated by CD-associated NOD2 mutation (Homer et al., 2010). An abnormal capture of internalised *Salmonella* has also been observed in the autophagosome of epithelial cells which carry the polymorphism T300A in ATG16L1 (Kuballa et al., 2008). Again, these findings demonstrate the functional consequences of autophagy-associated genes in CD and the importance of autophagy as a pathogenic mechanism in CD.

1.4.5 Cannabinoid action in autophagy process

To date, cannabinoids (Δ^9 -THC or CBD) have been shown to exhibit therapeutic potential in inducing autophagy process in breast cancer cell lines, as well as human glioma cell (Donadelli et al., 2011; Shrivastava et al., 2011). CBD induced autophagy-mediated cell-death in human breast cancer cell lines and this effect was not mediated through the cannabinoid receptors (CNR1 and CNR2) or vallinoid receptor (TRPV1). This study suggested that CBD-mediated autophagy cell-death by inducing endoplasmic reticulum (ER) stress, which subsequently inhibits both AKT and mTOR signalling pathways (Shrivastava et al., 2011). The action of cannabinoid-mediated autophagy via the activation of ER stress was also demonstrated in Δ^9 -THC-mediated autophagy cell death in human glioma cell. Also, unlike the CBD action on breast cancer cells, the Δ^9 -THC-induced effect may be mediated through CNR1 receptor (Salazar et al., 2009).

In addition to CBD and Δ^9 -THC action in breast cancer cells and human glioma cells, a recent study demonstrated the use of cannabinoid ligands (ACPA, synthetic agonist of CNR1; SR141716, CNR1 antagonist; GW405833, CNR2 agonist) in combination with the chemotherapy drug Gemcitabine (GEM) on pancreatic adenocarcinoma cells (Donadelli et al., 2011). GEM is currently used to treat advanced pancreatic

adenocarcinoma but this drug only delivers a response rate of <20%, therefore the study was conducted with the purpose of improving the drug efficiency by having the cannabinoid ligands as the combination treatment. The study showed that combined treatment of cannabinoids and GEM successfully inhibited pancreatic adenocarcinoma cell growth through ROS-dependent autophagic cell-death (Donadelli et al., 2011), suggesting that the combined treatment of GEM and cannabinoids may be a new therapeutic strategy in treating pancreatic cancer.

1.5. Summary

As previously stated, the autophagy process not only responsible for the maintenance of cellular energetic balance, this is also crucial in the regulation of the immunity and cellular defence mechanisms in the intestinal epithelium. The polymorphism of autophagy-associated genes (ATG16L1, NOD2) has been correlated to the pathogenesis of CD (Hugot et al., 2001; Henderson and Stevens, 2012), emphasizing the importance of this cellular mechanism in disease regulation.

Both ECS and SOCS3 are thought to have a role in IBD, as the production of both endocannabinoids and SOCS3 are evident in inflamed intestines (Izzo et al., 2001; Suzuki et al., 2001; Di Marzo and Izzo, 2006). CBD is an attractive therapeutic entity due to its non-psychoactive effect and its beneficial pharmacological effects in various diseases. To date, both Δ^9 -THC and CBD-mediated autophagy cell-death have only been demonstrated in cancer cell models (breast cancer, glioma cells, pancreatic adenocarcinoma), but not in any non-cancer cell model system (Donadelli et al., 2011; Shrivastava et al., 2011). The autophagy process is a particularly valuable therapeutic target in CD, as this cellular mechanism is involved in pathogen clearance, along with the polymorphism of autophagy genes, which contributes to the pathogenesis of CD (Henderson and Stevens, 2012), suggesting that the autophagic process is disrupted in CD, thereby promoting the penetration of pathogens across the epithelial barrier and exploiting the mucosal host defence.

CBD, but not Δ^9 -THC, was shown to reduce NF- κ B activity, up-regulate the activation of STAT3 and decrease the mRNA expression level of SOCS3 (Kozela et al., 2010b). Both mRNA and protein expression of SOCS3 was up-regulated in colon samples obtained from CD patients, as compared to healthy controls (Suzuki et al., 2001). Furthermore, *in vivo* SOCS3

limits proliferation of the inflammatory epithelial cells in damage crypts, which leads to the reduction of TNF- α mediated NF- κ B activation (Rigby et al., 2007). However, it is noted that cellular SOCS3 expression level is constantly oscillating, and there are no current data that identify how cyclic SOCS3 is regulated beyond the transcriptional level (Yoshiura et al., 2007; Li et al., 2012).

Based on the emerging data, the onset of intestinal inflammation is associated with an impaired autophagy, increased activity in the ECS and up-regulation of SOCS3 protein expression. In this project, I explored the impact of cannabinoids administration (synthetic, endo-, and phyto-cannabinoid) on the autophagy process in the intestinal epithelial cell model. I hypothesized that cannabinoid administration would increase autophagic activity in my intestinal epithelial CaCo2 cell model. Furthermore, I also explored whether these actions were responsible for cyclic SOCS3 protein levels. This project may possibly offer a new functional role of cannabinoid in intestinal regulation, as well as a possible role of autophagy as a homeostatic regulator for cyclic proteins, such as SOCS3.

Chapter 2

Materials and Methods

Table of Contents

- 2.1 Materials43
- 2.2 Methods.....47
 - 2.2.1 Cell culture.....47
 - 2.2.2 Treatment49
 - 2.2.3 RNA Extraction49
 - 2.2.4 Quantitative Real time PCR (qRT-PCR)50
 - i. Primer set and Evaluation50
 - ii. Primer Evaluation51
 - iii. Reliability of real-time PCR detection52
 - 2.2.5 Western Immunoblot53
 - i. Cell Lysing53
 - ii. Quantifying protein expression53
 - iii. Preparation of SDS-PAGE gel54
 - iv. SDS-PAGE54
 - v. Antibody staining55
 - 2.2.6 Immunoprecipitation (IP)56
 - 2.2.7 Cell staining and imaging56
 - i. Dansylcadaverine (MDC) dye56
 - ii. Cyto-ID® autophagy detection kit57

2.1. MATERIALS

Table 2.1 Chemicals used; supplier and supplier address.

*These chemicals were used in all experiment except for the [³⁵S]GTPγS binding assay.

Chemical	Supplier	Supplier address
1-bromo-3-chloro-propane	Sigma-Aldrich	Poole, UK
2-Mercapoethanol	Sigma-Aldrich	Poole, UK
2-Propanol	Sigma-Aldrich	Poole, UK
2% Bis Solution	BioRad Laboratories	Herts, UK
40% Acrylamide Solution	BioRad Laboratories	Herts, UK
Albumin, from bovine serum	Sigma-Aldrich	Poole, UK
Agarose powder	Sigma-Aldrich	Poole, UK
Ammonium Persulfate	Sigma-Aldrich	Poole, UK
Bradford Reagent	Sigma-Aldrich	Poole, UK
Cannabinoid-receptor 1 primer	Qiagen	Manchester, UK
Cannabinoid-receptor 2 primer	Qiagen	Manchester, UK
Clarity Western ECL Substrate	BioRad Laboratories	Herts, UK
Cyto-ID® autophagy detection kit	Enzo Life Science	Exeter, UK
Dansylcadaverine (MDC)	Sigma-Aldrich	Poole, UK
Dried Skimmed milk	Marvel	-
Dulbecco's Phosphate Buffered saline	Sigma-Aldrich	Poole, UK
Dulbecco's Phosphate Buffered saline, Gibco	Life Technologies	Paisley, UK
Dyna Beads Protein G	Life Technologies	Paisley, UK
Ethanol	Thermo Fisher Scientific	Loughborough, UK
Fetal Bovine Serum (FBS) Lot No: 07F4314K	Life Technologies	Paisley, UK
Glycine	Sigma-Aldrich	Poole, UK
HMBS pre-validated primer	Qiagen	Manchester, UK

Chemical	Supplier	Supplier address
HuSH 29mer shRNA Construct_Human Cannabinoid receptor 1 specific	Cambridge Bioscience Ltd.	Cambridge, UK
Hydrochloric Acid (36.5-38%)	Sigma-Aldrich	Poole, UK
iBlot® Gel Transfer Stacks, Nitrocellulose	Life Technologies	Paisley, UK
iScript One-Step RT-PCR kit with Syber Green	BioRad Laboratories	Herts, UK
IGEPAL CA-630	Sigma-Aldrich	Poole, UK
Laemmli sample buffer	BioRad Laboratories	Herts, UK
Minimum Essential Medium (MEM), Gibco	Life Technologies	Paisley, UK
N,N,N,N,- Tetramethylethylenedramine	Sigma-Aldrich	Poole, UK
Non-Essential Amino Acid (NEAA)	Life Technologies	Paisley, UK
NuPAGE, LDS Sample buffer (4X)	Life Technologies	Paisley, UK
O ₂ /CO ₂ gas	BOC Gases	-
Paraformaldehyde powder	BDH	Poole, UK
Phosphatase Inhibitor Cocktail 2	Sigma-Aldrich	Poole, UK
Precision Plus Protein Dual Colour Standard	BioRad Laboratories	Herts, UK
PrestoBlue® Cell Viability Reagent	Life Technologies	Paisley, UK
Protease Inhibitor Cocktail	Sigma-Aldrich	Poole, UK
RPLPO Pre-validated primer	Qiagen	Manchester, UK
SOCS3 pre-validated primer	Qiagen	Manchester, UK
Sodium dodecyl sulphate (SDS), 10%	Sigma-Aldrich	Poole, UK
Sodium deoxycholate	Sigma-Aldrich	Poole, UK
Sodium chloride	Melford	Ipswich, Suffolk, UK
SuperBlock blocking buffer	Thermo Fisher Scientific	Loughborough, UK
Tris(hydroxymethylaminomethane)	Melford	Ipswich, Suffolk, UK
TRI reagent®	Sigma-Aldrich	Poole, UK
Tween-20	Sigma-Aldrich	Poole, UK

As the work for [³⁵S]GTPγS binding assay was performed in Professor Ruth Ross’s laboratory in University of Aberdeen (UK), an additional list of chemicals used for [³⁵S]GTPγS binding assay was shown in Table 2.2.

Table 2.2 Chemicals used; supplier and supplier address.

Chemical	Supplier	Supplier address
[³⁵ S]GTPγS	Perkin Elmer	Massachusetts, USA
BioRad Dc Protein Assay	BioRad Laboratories	Herts, UK
Dithiothreitol	Sigma-Aldrich	Poole, UK
EDTA	BDH	Poole, UK
Fatty acid free BSA	Thermo Fisher Scientific	Loughborough, UK
GDP	Sigma-Aldrich	Poole, UK
GF/B filters	Semat	Hertfordshire, UK
HEPES	Sigma-Aldrich	Poole, UK
Magnesium chloride	Sigma-Aldrich	Poole, UK
Sodium chloride	Melford	Ipswich, Suffolk, UK
Trizma base	Sigma-Aldrich	Poole, UK
Trizma hydrochloride acid	Sigma-Aldrich	Poole, UK
Ultima Gold scintillation fluid	Perkin Elmer	Massachusetts, USA

Table 2.3. Drugs used; supplier and supplier address.

Drugs	Supplier	Supplier address
(-)-Cannabidiol	R&D System Europe Ltd.	Abingdon, UK
3-Methyladenine	R&D System Europe Ltd.	Abingdon, UK
ACEA	R&D System Europe Ltd.	Abingdon, UK
AEA	R&D System Europe Ltd.	Abingdon, UK
AM251	PeproTech EC Ltd	London, UK
Bafilomycin A1	R&D System Europe Ltd.	Abingdon, UK
IFN- γ	PeproTech EC Ltd	London, UK
IL-1 β	PeproTech EC Ltd	London, UK
Leptin	PeproTech EC Ltd	London, UK
LPS	PeproTech EC Ltd	London, UK
MG132	PeproTech EC Ltd	London, UK
TNF- α	PeproTech EC Ltd	London, UK

Table 2.4. Antibodies used for western blotting; supplier and supplier address.

Primary Antibodies	Supplier	Supplier address
β -actin	New England Biolab	Herts, UK
Cannabinoid receptor 1 (Caymen Bioscience)	Cambridge BioScience	Cambridge, UK
phospho-mTOR	New England Biolab	Herts, UK
phospho-STAT3 (Tyr705)	New England Biolab	Herts, UK
phospho-STAT3 (Ser727)	Insight Biotechnology Ltd.	Middlesex, UK
SOCS3 (Anti-rabbit)	New England Biolab	Herts, UK
SOCS3 (Anti-mouse)	abcam [®]	Cambridge, UK
Total-STAT3	New England Biolab	Herts, UK
Ubiquitin-1 (used for IP)	abcam [®]	Cambridge, UK

2.2. METHODS

2.2.1 Cell Culture

Human colonic epithelial cell line, CaCo2, is extensively used in studies associated with drug permeability, transport mechanism, and gene regulation of transporters and enzymes (Sun et al., 2008). To date, CaCo2 cells are currently the best characterised gut epithelial monolayer system available for *in vitro* study. CaCo2 cells exhibit similar characteristics as enterocytes residing in the human small intestinal epithelium. These cells differentiate to reach confluency where a monolayer of polarised cells that functionally and structurally resembled the small intestinal epithelial are formed (Bailey et al., 1996). Fully differentiated CaCo2 address the intact intestinal epithelial cell barrier where both luminal and basolateral compartments are present in the model system (Hidalgo et al., 1989; Hilgers et al., 1990). Interestingly, there were reviews stating differences in the finding with the use of CaCo2 cells in different laboratories and they have suggested this may due to several reasons, for instance, the source of the cells, the culturing conditions and maintenance and the associated passage numbers (Bailey et al., 1996). Taken that, CaCo2 cell differentiation from day 0 to day 21 was monitored via cell staining for a brush border enzyme alkaline phosphatase (ALP). This set of experiment was performed by Tara Macpherson (Karen Wright's PhD student). ALP is a common marker of enterocyte differentiation and it has been shown to be highly expressed in differentiated CaCo2 cells (Ferruzza et al., 2012; Matsumoto et al., 1990). In agreement with previous findings, Tara's result showed that ALP is highly expressed in the CaCo2 cells when they were grown for 14 to 21 days, as compared to the third day of culturing, confirming that the CaCo2 cells exhibit differentiated phenotype from day 14 onwards.

In this study, CaCo2 was cultured routinely in T75 culture flasks with roughly 12mL of Minimum Essential Medium-MEM. Media were supplemented with 8% (vol/vol) fetal bovine serum (FBS) and 1% of MEM Non-Essential Amino Acid (NEAA). This would be referred as “complete medium”. The cells were cultured in the humidified incubator that was maintained at 37°C in the 5% CO₂ atmospheric condition. The culture medium was changed in every 2 to 3 days. When the growing cells reached 70% confluency, they would either be passaged into new T75 culture flask for further culture or into Petri dishes or 6/12-well plates for experimental use (Figure 2.1).

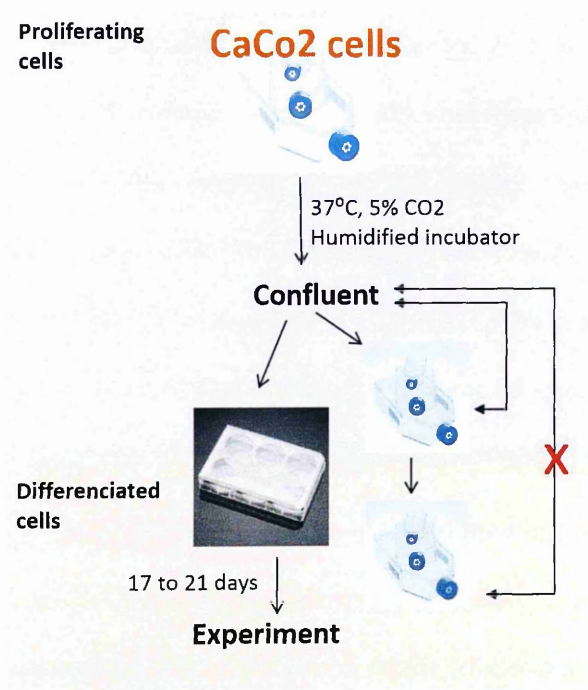


Figure 2.1. Schematic diagram for culturing human colonic epithelial cell line, CaCo2. CaCo2 cells were cultured in a humidified 37°C, 5% CO₂ incubator. Growing cells reached with ~70% confluency would either be passaged into new T75 culture flask or onto culture dishes for experimental use. Only CaCO2 cells that were actively proliferating would continue the passaging process as these cells display changed phenotypes from proliferating to post-confluent stage. Differentiated post-confluence CaCo2 cells that were developed into a polarized monolayer of cells would be used in this project.

2.2.2. *Treatments*

Unsynchronized differentiated CaCo2 cells were used for all experiments, unless otherwise stated. 1 hour prior to treatment induction, culturing medium for the treated cells would change from MEM medium with 8% serum into MEM medium with 1% serum. The rationale for this additional step was to ensure the treated cells were in stress-free condition before treatments were added.

2.2.3. *RNA Extraction*

RNAs from the treated CaCo2 cells were extracted by using TRI reagent[®]. To minimize genomic DNA contamination during tissue preparation, 1-bromo-3-chloro-propane was added to each of the RNA sample. Samples were centrifuged at 10,000rpm, 15min at 4°C. Total RNA from the aqueous phase was further purified via isopropanol precipitation, washed twice with 75% (v/v) ethanol and resuspended in 20µL to 30µL of RNase-free water. The final concentration of total RNA for each sample was between 1.5-4.5µg/µL. Purity of RNA was accessed by a ratio of absorbance at 260nm and 280nm through NanoDrop 2000c Spectrophotometer (Thermo Scientific). A ratio of ~2.0 is accepted as “pure” for RNA. Lastly, to verify the integrity of total RNA, RNA samples were run on a 2% denaturing agarose gel and stained with ethidium bromide. Two sharp, non-smearing 28S and 18S rRNA bands would indicate the non-degrading condition of the RNA samples. Extracted RNA was then stored at -80°C for later use.

2.2.4 *Quantitative Real Time PCR (qRT-PCR)*

i. Primer set and Evaluation

Validated primer sets for cannabinoid receptor (CNR)-1, suppressor of cytokine signaling (SOCS)-3, human large ribosomal protein (RPLPO), hydroxymethylbilane synthase (HMBS) were purchased from Qiagen. RPLPO and HMBS were used as the reference genes in the PCR reaction. Prior to the analysis of cytokines or drug-treated CaCo2 samples, each primer set was evaluated. In order to generate standard curve, each validated primer set was used to amplify from different dilution of cDNA (Table 2.5). Ct values obtained were plotted against log₂ of the dilution factor against the Ct value for these five reactions to generate standard curve for each set of primers. Equation of linear regression line along with the R² value could be used to evaluate optimization of the qRT-PCR assay. Only primer set with R² value ≥ 0.90 would be used for further QRT-PCR analysis on the treated CaCo2 cell samples. Efficiency obtained from the equation was incorporated into the final calculation using the Pfaffl method (Pfaffl, 2001).

Table 2.5. CDNA dilution used for testing primer efficiency.

cDNA Dilution	Log₂ of the dilution factor
No dilution	0
1:2 dilution	-1
1:4 dilution	-2
1:8 dilution	-3
1:16 dilution	-4

ii. Primer Evaluation

Validated primer designed for cannabinoid receptor (CNR)-1 and suppressor of cytokine signalling (SOCS)-3 were used for qRT-PCR analysis. qRT-PCR data were analysed using Pfaffl Method. The relative mRNA expression ratio or the fold changes were analysed based on the efficiency of the associated primers and the ΔC_T deviation of the test sample versus a control. Results were standardised by comparison to the expression of reference genes (Figure. 2.2). RPLPO and HMBS were integrated in the qRT-PCR analysis.

$$\text{Ratio} = \frac{(E_{\text{target}})^{\Delta C_T(\text{test}) (\text{control-sample})}}{(E_{\text{reference}})^{\Delta C_T(\text{ref}) (\text{control-sample})}}$$

Figure 2.2. Mathematical model used in Pfaffl method for qRT-PCR analysis (Pfaffl, 2001).

iii. Reliability of real-time PCR detection

Overall, due to the fact that these purchased primers were pre-validated primers from Qiagen, reliability for these primers should not be an issue in this context. However, the calculations of the efficiency for each primer were performed, as results were required to integrate into the qRT-PCR analysis that been shown in Table 2.6. Primer efficiency was determined as the correlation coefficient from standard curve where ΔC_T values for cDNA dilution were plotted against the concentration for each primer.

Table 2.6. Primer efficiency and R^2 value of the pre-validated primers for Cannabinoid receptor (CNR)-1, CNR2, Suppressor of cytokine signalling (SOCS)-3, Human Large Ribosomal protein (RPLPO) and hydroxymethylbilane synthase (HMBS).

Gene	Product Code	Primer Efficiency (%)	R^2 value
CNR1	QT00203287	95.5	0.9996
CNR2	QT00012376	94	0.9632
SOCS3	QT00244580	87	0.9521
RPLPO	QT00075012	82.93	0.7207
HMBS	QT01002176	82	0.9474

Primer efficiency was the correlation coefficient from the standard curve where ΔC_T values for cNDA dilution were plotted against the concentration of each primer. For 100% efficiency, there would be a doubling of the amount of cNDA at each cycle and as a result, the factor was 2.0 for each cycle. R^2 value was also obtained from the standard curve.

**Pre-validated primers were purchased from Qiagen*

2.2.5. *Western Immunoblot*

i. Cell Lysing

Treated cells were washed with cold PBS and lysed in cold RIPA buffer supplemented with phosphatase inhibitor cocktail 2 and protease inhibitor cocktail. Lysing procedure required to be performed on ice to avoid degradation of the protein samples. Insoluble cell debris was removed by centrifugation at 12,000 rpm for 3min. Lysed protein was then stored at -20°C for later use.

ii. Quantifying protein concentration

Protein concentrations across samples were quantified with the use of Bradford Reagent. Performing a Bradford assay is to ensure equivalent protein loading in the SDS-PAGE gel, which will be performed in later stage. Such assay involves the formation of a complex between the dye, Brilliant Blue G, and the proteins in solution. Absorption of the dye towards the present proteins can be detected by measuring the dye absorbance at 595nm; a microplate reader was used for further analyse.

To determine protein samples with unknown concentration, a standard curve was prepared by using protein standards which were made up from BSA with known concentration ranging from 0 to 20µg/mL. 450µL of Bradford Reagent was added into 50µL of the protein standards. Samples were incubated at room temperature for 5-10 minutes. Absorbance for the protein standards were measured at 595nm. Absorbance readings obtained were plotted against protein standard concentration to generate a standard curve. After obtaining the standard curve, the whole procedure was repeated with protein samples obtained from treated cells. Protein concentrations for treated samples were determined by comparing the absorbance values against the generated standard curve.

iii. Preparation of SDS-PAGE gel

Molecular weight of the protein of interest determined the percentage of the SDS-PAGE gel to be used (Table 2.7). *N,N,N,N*,-Tetramethylethylenedramine (TEMED) was the last reagent to be added into the mixed solution as the use of TEMED leads to the polymerization of the gel matrix.

Table 2.7. Recipe for making different percentages of SDS-PAGE gels.

	Stacking gel 4%	Resolving gel		
		10%	12%	14%
Range of molecular weight (kD)		16-70	14-60	12-45
40% Acrylamide	480 µL	2.43 mL	2.92 mL	3.40 mL
2% Bis	260 µL	1.34 mL	1.61 mL	1.88 mL
0.5M of Tris HCL pH6.8	1.26 mL	-	-	-
1.5M of Tris HCL pH8.8	-	2.5 mL	2.5 mL	2.5 mL
10% SDS	50 µL	100 µL	100 µL	100 µL
10% Ammonium persulfate	25 µL	75 µL	75 µL	75 µL
TEMED	10 µL	10 µL	10 µL	10 µL
Water	2.92 mL	3.58 mL	2.83L	2.03L

iv. SDS-Page

Prepared protein samples were mixed with 4X NuPAGE LDS sample buffer supplemented with 5% of 2-mercapoethanol, boiled at 95°C for 2min. 20–30µg aliquots resolved on SDS PAGE gels. 5-7µL of BioRad precision plus protein standards were loaded along with the protein samples for molecular weight referencing. The precision plus protein standards are a mixture of ten recombinant proteins which have the molecular weight ranging from 10-250kD. The gel was run at 50-60V for 10min to ensure all protein samples were evenly stacked through the stacking gel

before increasing the running voltage to 160V. Proteins from the gel were transferred onto a nitrocellulose membrane by using a Trans-Blot Turbo Transfer System (BioRad). The electrophoretic transfer of proteins was performed at 1.3A, 25V for 7 min.

v. Antibody Staining

To prevent non-specific bindings between the nitrocellulose membrane and the primary antibody used for detecting the target protein, the nitrocellulose membrane was incubated with blocking solution for a minimum of 2 hour. After the blocking step, membrane was incubated with primary antibody which has been diluted with SuperBlock Blocking buffer. Incubation was performed overnight in a cold room. Followed by the incubation, membrane was washed with 1X TBS supplemented with 0.1% (vol/vol) Tween-20 for 3 times, 10min each. This was followed by incubation with the appropriate anti-mouse monoclonal antibody (1:10,000) or anti-rabbit monoclonal antibody (1:10,000) for 1 hour in room temperature. Washing steps were repeated after the incubation, followed by blot developing with Clarity western ECL. Image was taken via BioRad ChemiDox™ XRS+ System. Densitometry was performed via Image Lab™ software to quantify the expression of the protein of interest.

**Primary antibodies used to detect the protein of interest with their corresponding secondary antibodies and their preference in SDS-PAGE gel percentage and the type of blocking solution to be used were listed in Table 2.8.*

2.2.6. Immunoprecipitation (IP)

Protein concentrations were normalized across the samples tested. 1 µg of anti-SOCS3 antibody was added into a total of 1 mL protein lysate, followed by 1 h incubation on ice. After the incubation, 50 µL of DynaBeads Protein G suspension with the concentration of 1.5 mg was added into each sample, followed by 1 h incubation in cold temperature. During incubation, samples were constantly mixed by placing on a rotating machine. After incubation, samples were placed in the Magnet DynaMag rack (Life Technologies, Paisley, UK) to separate out the magnetic bound SOCS3 protein, supernatant was removed and the magnetic bound SOCS3 proteins were rinsed by PBS. The rinsing procedure was repeated three times. The magnetic bound protein samples were resuspended with 15 µL of PBS and 15 µL of 1x NuPAGE sample buffer. Samples were boiled at 95°C for 2 min. The total of 30 µL of protein samples would be loaded into the SDS-PAGE gel. The SOCS3 protein would then be analysed by immunoblotting with ubiquitin-1 specific antibody.

2.2.7 Cell staining and imaging

10⁶ cells/well of CaCo2 cells were seeded on sterilised cover slips that were inserted into a 12-well culturing plate. Cells were grown until a cell monolayer was formed before proceeding to experimental use. Two different autophagic dyes (MDC and Cyto-ID[®] autophagy Green Detection reagent) were optimized and used in this project.

i. Dansylcadaverine (MDC) dye

Treated cells were stained with MDC dye at the concentration of 0.05 mM for 10 min, at 37°C in MEM medium. After the incubation, cells were carefully rinsed with PBS and fixed with 2% paraformaldehyde for 10 min at room temperature. Images were

captured with Delta Vision microscopy with the excitation wavelength of 360nm and emission wavelength of 525nm.

ii. Cyto-ID® autophagy detection kit

Treated cells were stained with Cyto-ID® autophagy detection kit. The kit consists of Cyto-ID® Green Detection reagent, Hoechst 33342 nuclear stain reagent, and associated 10X assay buffer. Microscopy Dual Detection Reagent was prepared by diluting 2µL of Cyto-ID® Green Detection reagent and 1µL of Hoechst 33342 nuclear stain reagent into 1mL of 1X Assay Buffer (Enzo Life Science, Exeter, UK) supplemented with 1% FBS. Treated cells were carefully rinsed with 1X Assay Buffer to remove any dead cells in the well, followed by incubating treated cells with 300µL of Microscopy Dual Detection Reagent per well for 30min at 37°C. After the incubation, cells were carefully rinsed with 1X Assay Buffer and fixed with freshly made 4% paraformaldehyde for 20 min at room temperature. Paraformaldehyde was rinsed off by Assay Buffer before imaging with confocal microscopy. Images were captured with a Zeiss confocal microscope by using FITCS and DAPI filter sets and analysed with LSM Image software.

Table 2.8. List of primary antibodies with its associated molecular weights, corresponding secondary antibodies and their preference in SDS-PAGE gel percentage and blocking solution to be used.

Primary Antibody (Company, Product code)	Molecular Weight (kDa)	Gel Percentage	Blocking solution	Secondary Antibody
CNR1 (Cayman BioScience; #10006590)	60	10%	5% Milk	Anti-rabbit
Phospho-mTOR, S2448 (Cell Signaling; #2971)	289	*Any kD™	5% BSA	Anti-rabbit
Phospho-STAT3, Tyr705 (Santa-Cruz; #9145)	86 & 91	10% or 12%	2% BSA	Anti-rabbit
Phospho-STAT3, Ser727-R (Cell Signaling; #sc8001-R)	86 & 91	10% or 12%	2% BSA	Anti-rabbit
LC3 (Sigma-Aldrich; #L8918)	14 & 16	14%	5% Milk	Anti-rabbit
SOCS3, L210 (Cell Signaling; #2932)	27	12%	2% BSA	Anti-rabbit
Total STAT3 (Cell Signaling; #9139)	79	10% or 12%	2% BSA	Anti-mouse
Ubiquitin-1 (Abcam® ; #ab7254)	8.5	*Any kD™	5% Milk	Anti-mouse
β-Actin (Cell Signaling; #4967)	45	Any	Any	Anti-rabbit

*Criterion™ Precast gradient gels were purchased from BioRad Laboratories (product code: #456-9033)
Any kD™ is a unique single-percentage formulation from BioRad that provides a broad separation range and short running time.

Chapter 3

System Analysis

Table of Contents

- 3.1 Introduction..... 61
- 3.2 Aims 62
- 3.3 Cannabinoid receptors in CaCo2 cells 63
- 3.4 SOCS3 expression in CaCo2 cells 66
- 3.5 CNR1 and SOCS3 expression in cytokine-treated CaCo2 cells:
Proliferate, Confluent, Differentiated 67
- 3.6 Effect of the integration of fetal bovine serum (FBS) in treatments 72
 - i. CNR1 and SOCS3 mRNA expression 72
 - ii mTOR and JAK-STAT signaling pathway 76
- 3.7 Establishing autophagy model system 80
- 3.8 Discussion 84

3.1 Introduction

This chapter comprises a series of experiments performed for the understanding of the CaCo2 cell model system and the generation of the optimized CaCo2-autophagy model system to be used to investigate the correlation between autophagy, SOCS3 and ECS in human intestinal epithelium. Although CaCo2 cell line is the best characterised gut epithelial monolayer system available for *in vitro* study, there is an inconsistency among the results generated with its use in different laboratories. For example, Ligresti, et al. (2003) reported that CNR2 was absent in their CaCo2 cell model system, whereas Wright, et al. (2005) showed the presence of both functional CNR1 and CNR2 receptors in their CaCo2 cell line. Such controversy makes it vital for us to understand my CaCo2 cell line by clarifying the presence of the genes of interest (CNR1, CNR2) in my model system and exploring the differences of my CaCo2 cell model system as compared to the CaCo2 cell lines from other laboratories.

Additionally, CaCo2 cells display different characteristic of intestinal epithelium during different stages of cell growth, as they lose their tumorigenic phenotype and display characteristics of mature enterocytes upon differentiation (Stierum et al., 2003; Sambuy et al., 2005). A recent proteomics study revealed that such phenotypic change of CaCo2 is associated with the change in the expression of tumorigenesis-associated proteins, as well as a variety of distinct biochemical pathways which are involved in protein folding, cytoskeleton formation and maintenance and nucleotide metabolism (Stierum et al., 2003). SOCS3 has previously been shown to act as an anti-proliferative agent in several cancer cell lines, and this includes the CaCo2 cell line (Rigby et al., 2007; Barclay et al., 2009). However, given the distinct characteristic of the CaCo2 cell line, it is essential to determine the basal expression of SOCS3 in each of these growth stages and its regulatory pattern across the 21 days of culture period.

Furthermore, both proliferating and confluence CaCo2 cells have commonly been utilised in various studies as the autophagy model system to investigate the cellular autophagy activity in human colorectal cancer (Comes et al., 2007; Kuballa et al., 2008; Xie et al., 2011), but, to date, no study has demonstrated the use of differentiated CaCo2 cells to study cellular autophagy activity in human intestinal epithelium systems. Considering that autophagy is a cellular mechanism utilised to adapt to the cellular environment changes (Klionsky and Emr, 2000), it is necessary to maintain cellular stress at a minimal level in order to avoid false positive findings resulting from cannabinoid treatment. Thus, the generation of the optimised CaCo2-autophagy model system is reviewed in this chapter.

3.2 Aim



Determine presence of the gene of interests (CNR1 and CNR2) in CaCo2 cell model



Explore changes of basal expression of CNR1 and SOCS3 in three growth stages of CaCo2 cells: Proliferating, Confluent and Differentiated



Establish an ideal experimental model that was closer to the cell system in the GI tract to study autophagosome formation

3.3 Cannabinoid receptors in CaCo2 cells

To determine whether transcript for CNR1 and CNR2 were present in CaCo2 cells, one step quantitative real time PCR (qRT-PCR) was performed with pre-validated primers for CNR1 (Qiagen, QT00203287), CNR2 (Qiagen, QT00012376) and RPLPO (human large ribosomal protein; Qiagen, QT00075012) on RNAs obtained from pooled cytokines-treated CaCo2 samples. RPLPO, a house keeping gene, was selected as the positive control in this study.

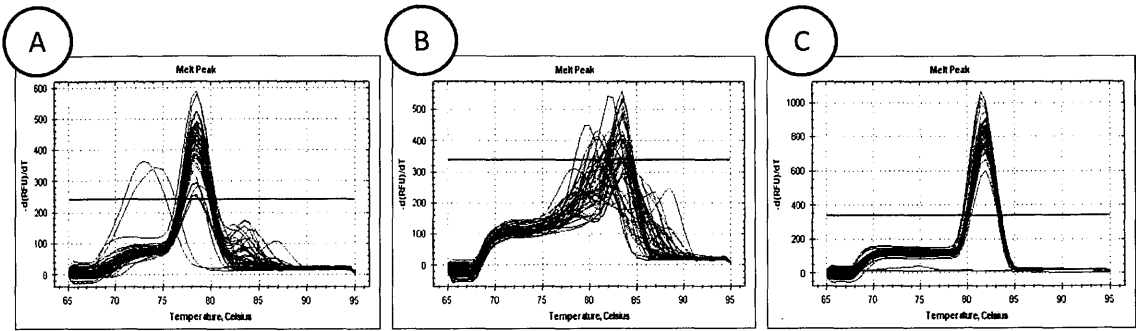


Figure 3.1 Melt curves obtained from quantitative real time PCR (qRT-PCR) with (A) CNR1, (B) CNR2 and (C) RPLPO primers. 10ng/μl of pooled RNAs from cytokines-treated differentiated CaCo2 cells were used as the templates. Non-template control was integrated as the negative control for this study. qRT-PCR performed with the use of one-step QuantiTect Qiagen primer assay kit.

DNA melt curve indicates the total number of products generated from the amplification of the gene of interest (Pfaffl, 2001). Following qRT-PCR, only sample amplification against CNR2 primer showed more than one DNA melting curve (Figure 3.1B). The outliers presented in both CNR1 (Figure 3.1A) and RPLPO (human large ribosomal protein) (Figure 3.1C) were the gene amplification obtained from the negative control sample (negative control sample = presence of associated primers for the gene of interest without RNA template).

The experiment was repeated twice to ensure that the multiple melting curves obtained were not related to the degradation of RNA samples or the degradation of CNR2 receptor primer, as well as the insensitivity of *QuantiTect* primer assay kit used. Considering that experiments were performed by using the same RNA template with the same primer assay kit, this leave us to question the quality of CNR2 primer used in this study. Furthermore, I also speculate that the number of copy for CNR2 gene is too low in my CaCo2 cell line, resulting in the difficulty for qRT-PCR to detect the presence of the gene.

Therefore, to further verify the status of CNR2 in this cell line, I performed Polymerase Chain Reaction (PCR) with the CNR2 primer on cDNA generated from the same cytokines-treated CaCo2 samples used in previous qRT-PCR experiment. Experiment was conducted by using CaCo2 cell, as well as the immortalized T lymphocyte (Jurkats) cell line. The use of Jurkats cells in this study provided us with a positive control for my experiments, as the expression of CNR2 has previously been reported in this cell line (Ghosh et al., 2006). DNA for both CNR2 and RPLPO were amplified with pre-validated CNR2 and RPLPO primers. RPLPO is the house keeping gene and used as the second positive control in this study.

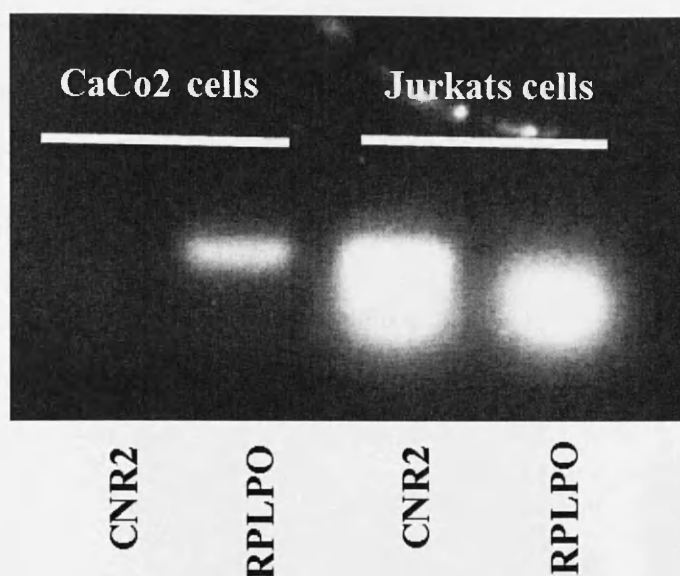


Figure 3.2. Expressions of cannabinoid receptor (CNR)-2 at transcriptional level in CaCo2 and immortalized T lymphocyte cell line (Jurkats cells). Polyacrylamide gel electrophoresis (PAGE) was performed on RNAs obtained from cytokines-treated CaCo2 and Jurkats cells. RNAs (2µg) were amplified against CNR2 and human large ribosomal protein (RPLPO) pre-validated primers with the annealing temperature of 53°C. RPLPO with 141base pair (bp) was observed in both CaCo2 and Jurkats cell lines whereas CNR2 receptor with 116bp only present in Jurkats cell line.

Result showed that RPLPO band with 141base pair (bp) was observed in both CaCo2 and Jurkats cell lines whereas CNR2 band with 116bp only present in Jurkats cell line (Figure 3.2), indicating the absence of CNR2 receptor in my CaCo2 cell model. There has been a controversy regarding to the presence of functional CNR1 and CNR2 receptors in CaCo2 cells (Ligresti et al., 2003; Wright et al., 2005). In agreement to my finding, Ligresti and group also reported that CNR2 was absence in their CaCo2 cell model system (Ligresti et al., 2003). The absence of CNR2 simplifies the cell model system and provides us with the advantage in experiment setting as I can entirely rule out the possible involvement of CNR2 in response to cannabinoid treatment and only concentrate on CNR1 action in the system.

3.4 SOCS3 expression in CaCo2 cells

Due to the cancerous nature of CaCo2 cells, qRT-PCR was performed to determine the changes of basal SOCS3 mRNA expression level throughout the growth of CaCo2 cells and determine whether this cell line is an appropriate model.

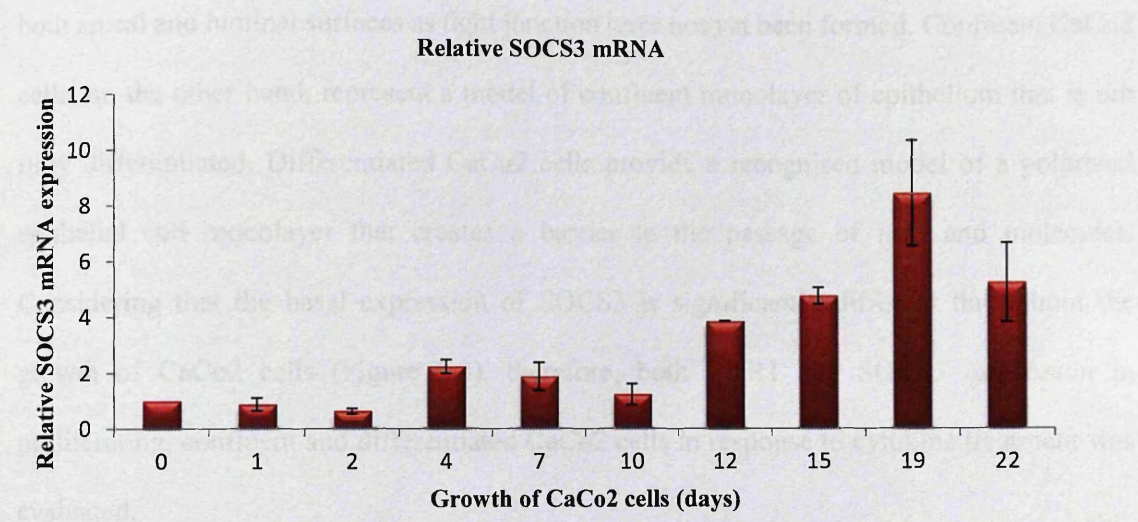


Figure 3.3. Basal SOCS3 mRNA expression in CaCo2 cells. 10⁶ cells/dish of CaCo2 cells were seeded in petri dishes. RNAs of the seeded cells was extracted and collected from day 1 where cells are proliferating to day 22 where cells are fully differentiated. All data were analysed in relative fold change against day 0 (the day cells were seeded). Data were given as fold change with error bars representing standard error of the mean (n≤2).

Level of SOCS3 mRNA expression was shown to be gradually increasing from day 1 to day 22 (Figure 3.3). CaCo2 cells reached its confluency around day 7 and achieved fully differentiated cell monolayer around day 14 (Sambuy et al., 2005). Quantitative RT-PCR detected relatively low SOCS3 expression in proliferating cells and high SOCS3 expression in fully differentiated cells (Figure 3.3). SOCS3 has previously been shown to exert a modest anti-proliferative effect in CaCo2 cells and this may explain the absence of SOCS3 mRNA expression in proliferating CaCo2 cells (Rigby et al., 2007).

3.5 CNR1 and SOCS3 expression in cytokine-treated CaCo2 cells: Proliferate, Confluent, Differentiated

Different growth stages of CaCo2 ostensibly reflect different characteristic of intestinal epithelium (Sambuy et al., 2005). Proliferating CaCo2 cells were exposed to treatments from both apical and luminal surfaces as tight junction have not yet been formed. Confluent CaCo2 cells, on the other hand, represent a model of confluent monolayer of epithelium that is not fully differentiated. Differentiated CaCo2 cells provide a recognised model of a polarized epithelial cell monolayer that creates a barrier to the passage of ions and molecules. Considering that the basal expression of SOCS3 is significantly different throughout the growth of CaCo2 cells (Figure 3.3), therefore, both CNR1 and SOCS3 expression in proliferating, confluent and differentiated CaCo2 cells in response to cytokine treatment was evaluated.

Proliferating, confluent, and differentiated CaCo2 cells were cultured for 2 days, 7 days and 17 days, respectively. Treated CaCo2 cells had not been starved overnight. TNF- α , IFN- γ , CBD, Leptin and LPS were the main five treatments applied in the experiments. Leptin, TNF- α and IFN- γ were selected to be the main factors/treatments because studies have illustrated their role as the pro-inflammatory cytokines and these cytokines are highly involved in IBD. LPS, on the other hand, is a cell wall component of Gram-negative bacteria and this TLR4 ligand has been shown to contribute to the occurrence of inflammation in GI tract. Lastly, CBD was selected because it was one of the main cannabinoid of interest in this project.

Result showed that in proliferating CaCo2 cells, CNR1 mRNA expression was up-regulated in response to LPS treatment (Figure 3.4). Both IFN- γ and CBD treatments significantly reduced CNR1 mRNA expression, as compared with no treatment control (Figure 3.4).

Interestingly, as the same experiment was repeated on confluent CaCo2 cells, result showed that CNR1 mRNA expression did not respond to any of the treatments, compared to no treatment control (Figure 3.6).

Conversely, SOCS3 mRNA expression was up-regulated in response to IFN- γ and LPS treatments in proliferating CaCo2 cells, as compared with no treatment control (Figure 3.5). TNF- α treatment increased SOCS3 mRNA expression in confluent CaCo2 cells and this was the only treatment induced a response in confluent cells (Figure 3.7). Again, as the same experiment was repeated on differentiated CaCo2 cells, result showed that SOCS3 mRNA expression did not respond to any of the treatments compared with non-differentiated CaCo2 (Figure 3.8).

i. Proliferating CaCo2 cells

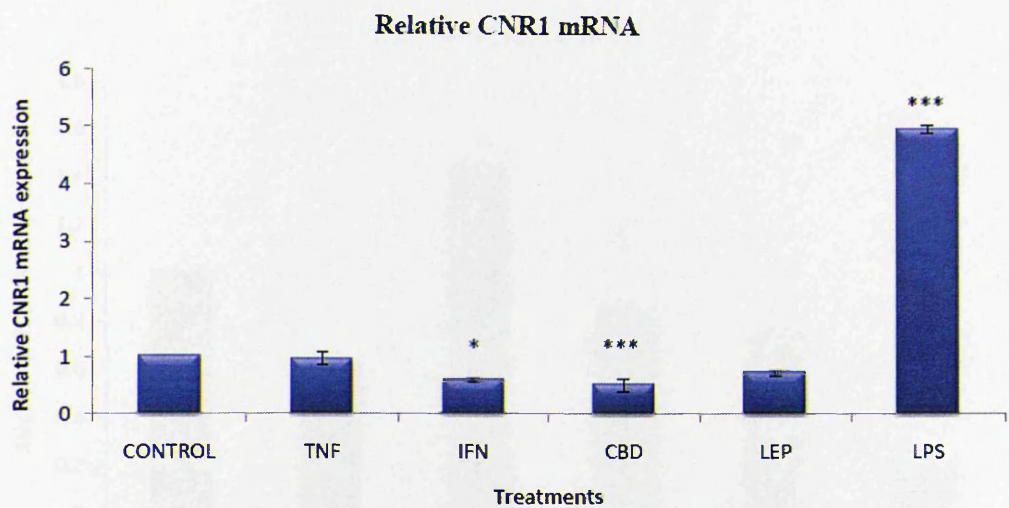


Figure 3.4. Effect of treatments on CNR1 mRNA expression in proliferating CaCo2 cells. Cells were treated for 4 hour. Data were given as fold change with error bars representing standard error of the mean ($n=3$, $*P<0.05$, $***P<0.001$, compared to no treatment control, ANOVA).

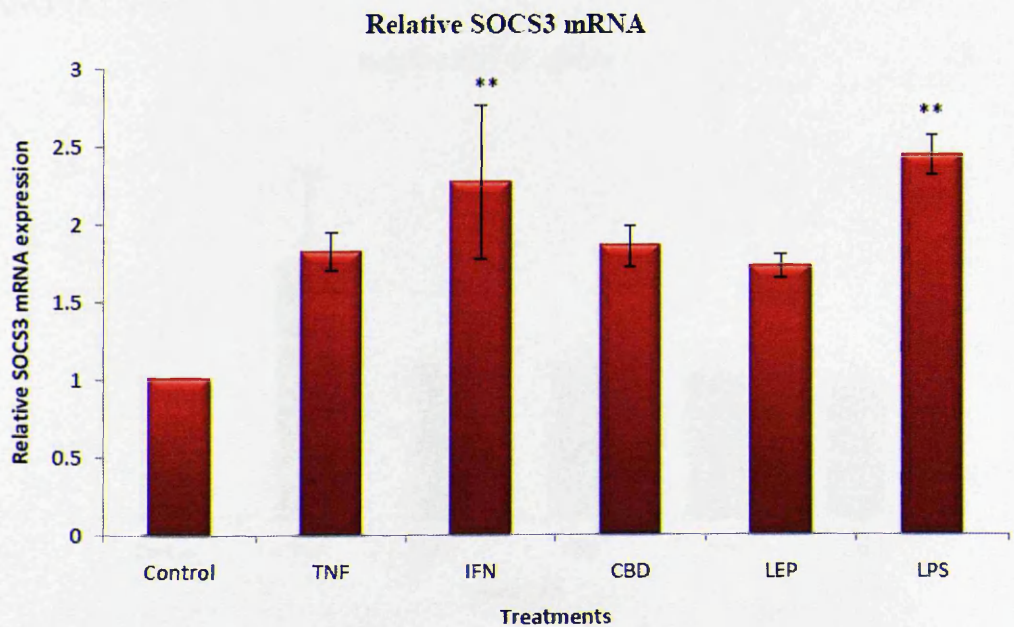


Figure 3.5. Effect of treatments on SOCS3 mRNA expression in proliferating CaCo2 cells. Cells were treated for 4 hour. Data are given as fold change with error bars representing standard error of the mean ($n=3$, $**P<0.01$, compared to control with no treatment, ANOVA).

ii. Confluent CaCo2 cells

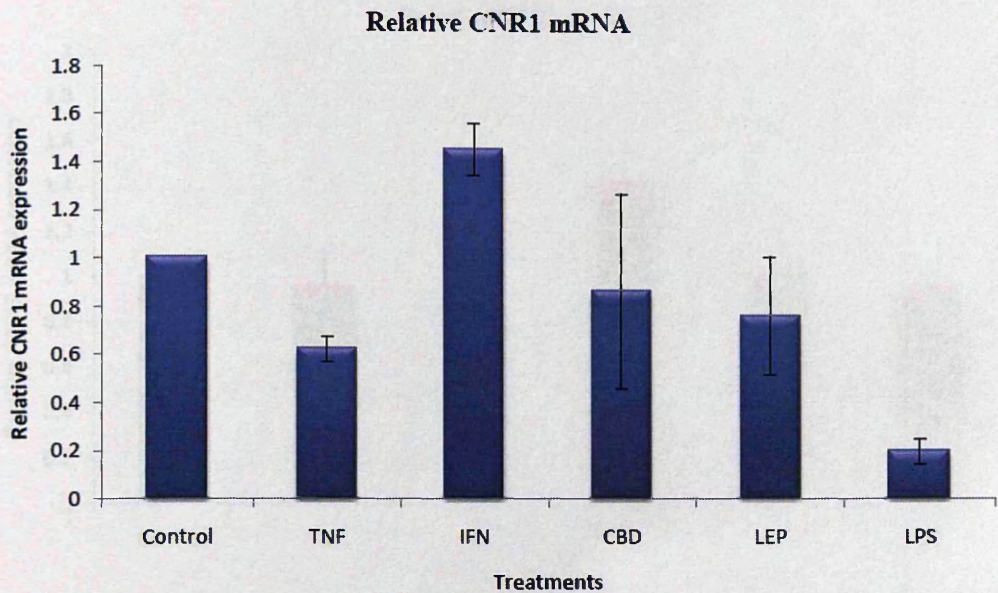


Figure 3.6. Effect of treatments on CNR1 mRNA expression in confluent CaCo2 cells. Cells were treated for 4 hour. Data are given as fold change with error bars representing standard error of the mean ($n=3$, data were analysed versus no treatment control, ANOVA).

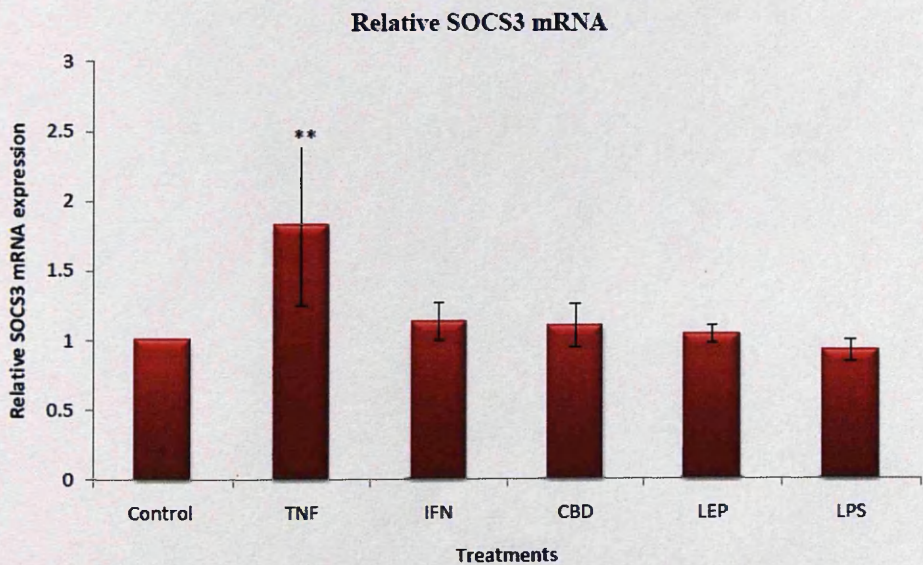


Figure 3.7. Effect of treatments on SOCS3 mRNA expression in confluent CaCo2 cells. Cells were treated for 4 hour. Data are given as fold change with error bars representing standard error of the mean ($n=3$, ** $P<0.01$, compared to no treatment control, ANOVA).

iii. Differentiated CaCo2 cells

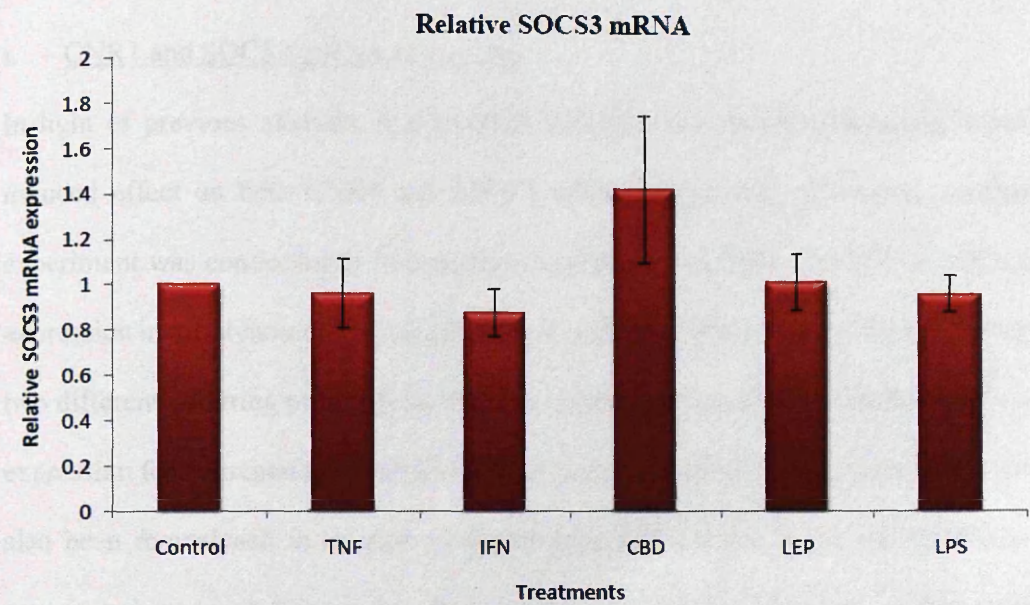


Figure 3.8. Effect of treatments on SOCS3 mRNA expression in differentiated CaCo2 cells. Cells were treated for 4 hour. Data are given as fold change with error bars representing standard error of the mean ($n=3$, data were analysed versus no treatment control, ANOVA).

3.6 Effect of the integration of fetal bovine serum (FBS) in treatments

i. CNR1 and SOCS3 mRNA expression

In light of previous analysis, it is possible that FBS may interfere with treatment-induced effect on both CNR1 and SOCS3 mRNA expression. Therefore, another experiment was conducted to investigate serum effect on CNR1 and SOCS3 mRNA expression in differentiated CaCo2 cells. The experiment was performed by comparing two different culturing protocols as stated in Figure 3.9. Considering that the baseline expression for no treatment control in both of the experiments were different, data has also been re-analysed in relation to the no treatment control based on the ‘serum containing’ protocol (Figure 3.9, Protocol A). Significance of the results was obtained through Dunnett statistical test with 95% confident interval.

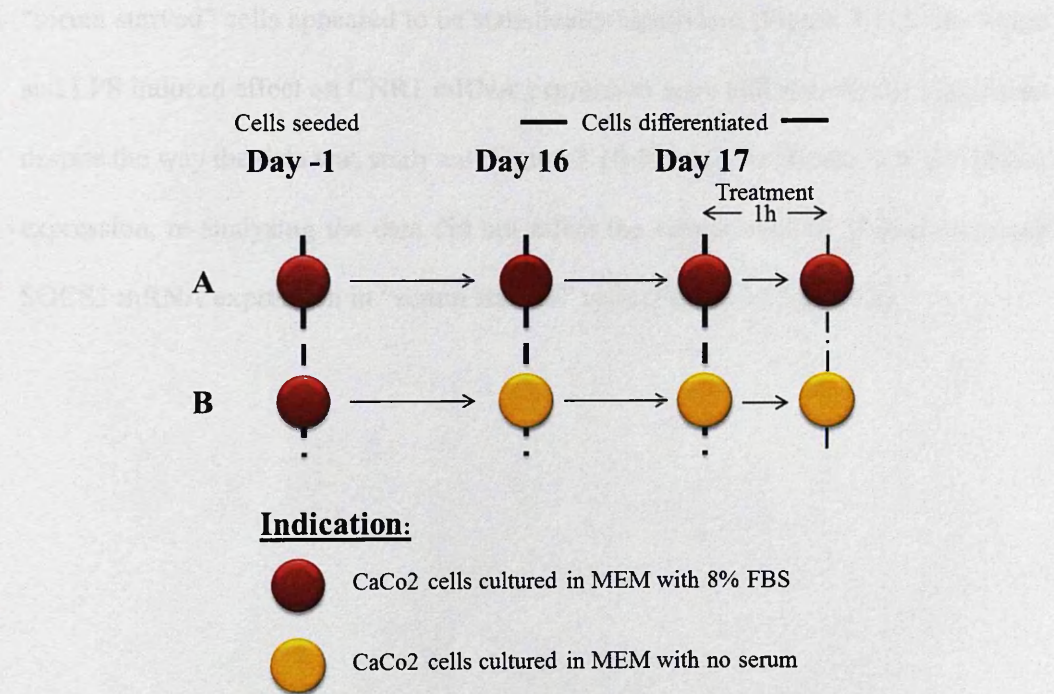


Figure 3.9. Schematic diagram of two experimental protocols: ‘serum containing’/Protocol A and ‘serum starved’/Protocol B. Colour variation indicated the type culture medium used during culturing process.

Following 1 hour treatment, CNR1 mRNA expression was up-regulated with both leptin and LPS treatments (Figure 3.10). On the contrary, CNR1 mRNA expression was reduced in IFN- γ treated cells (Figure 3.10). SOCS3, on the other hand, its mRNA expression was significantly up-regulated in response to TNF- α treatment in differentiated CaCo2 cells.

As stated previously, considering that the baseline expression for no treatment control in both of the experiments were different, data were re-analysed in relation to the no treatment control from “serum containing” protocol. Based on that analysis, previously found IFN- γ -induced CNR1 mRNA reduction was no longer statistically significant (Figure 3.11). Interestingly, increased CNR1 mRNA in response to CBD-treated “serum starved” cells appeared to be statistically significant (Figure 3.11). The leptin and LPS induced effect on CNR1 mRNA expression were still statistically significant despite the way the data was analysed (Figure 3.10 & 3.11). As for the SOCS3 mRNA expression, re-analysing the data did not affect the significance of TNF- α increased SOCS3 mRNA expression in “serum starved” cells (Figure 3.12 & 3.13).

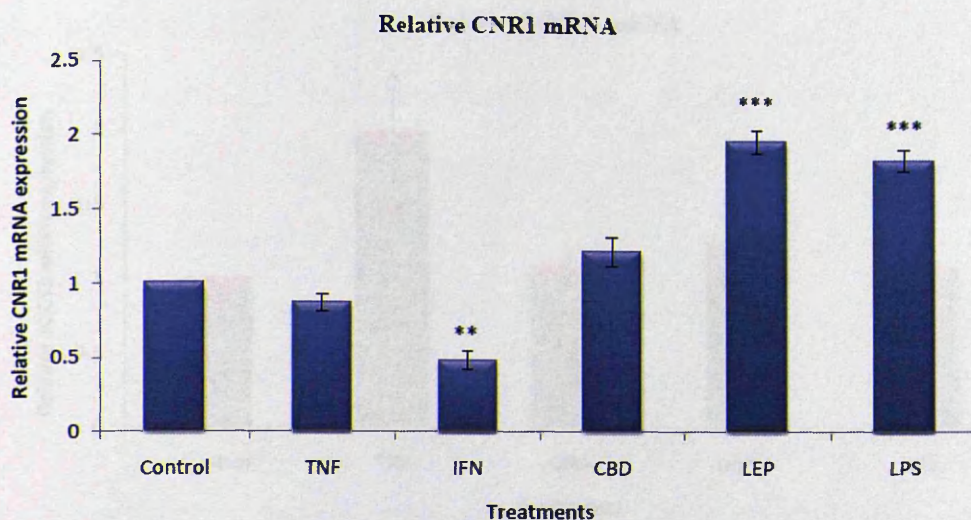


Figure 3.10. Effect of treatments on CNR1 mRNA expression in serum starved CaCo2 cells. Treatments were applied for 1 hour. Data are given as fold change with error bars representing standard error of the mean (n=3, ** P <0.01, *** P <0.001, compared to no treatment control, ANOVA).

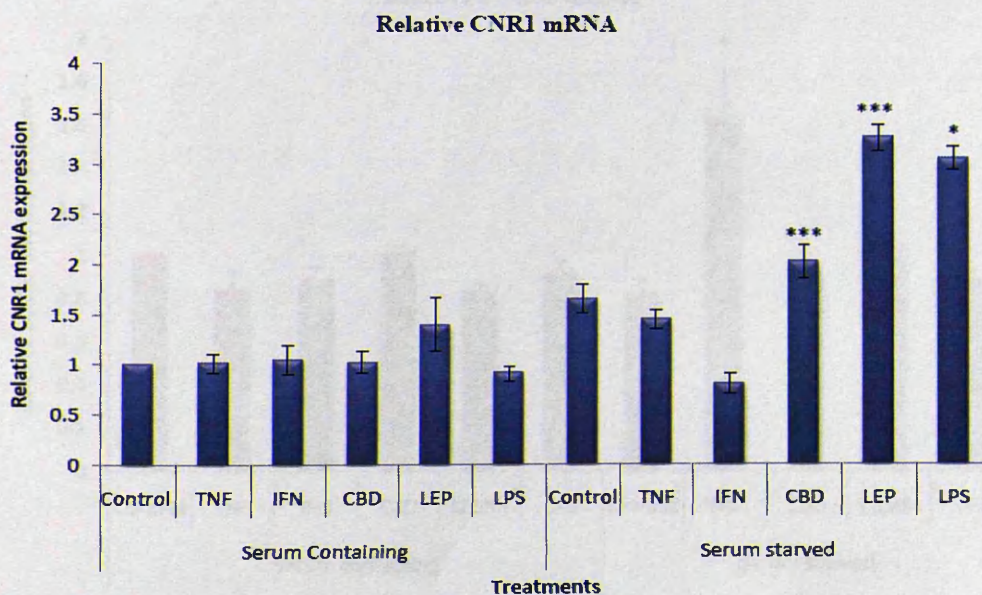


Figure 3.11. Effect of treatments on CNR1 mRNA expression in both serum containing and serum starved CaCo2 cells. Treatments were applied for 1 hour. Data are given as fold change with error bars representing standard error of the mean (n=3, * P <0.05, *** P <0.001, compared to no treatment control from 'serum containing' protocol, ANOVA).

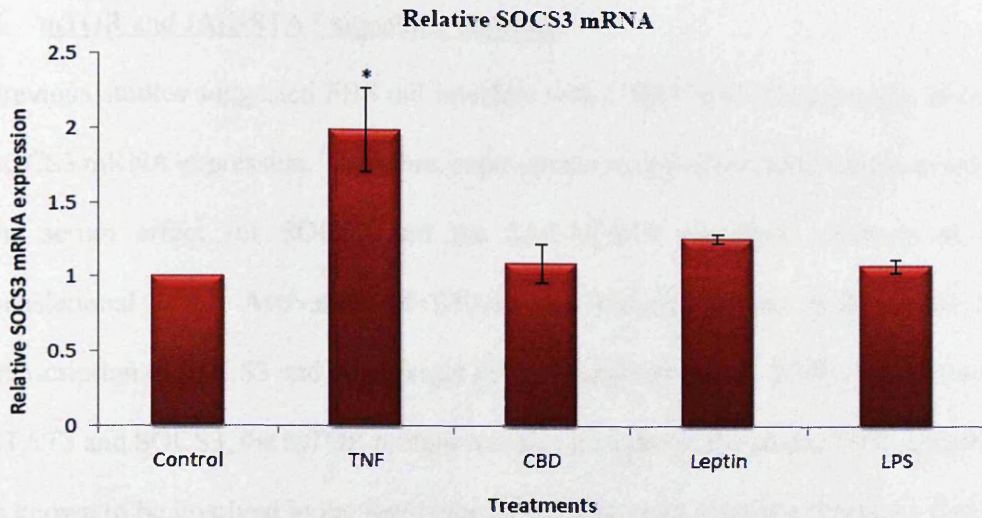


Figure 3.12. Effect of treatments on SOCS3 mRNA expression in serum starved CaCo2 cells. Treatments were applied for 1 hour. Data are given as fold change with error bars representing standard error of the mean (n=3, * $P<0.05$, *** $P<0.001$, compared to no treatment control, ANOVA).

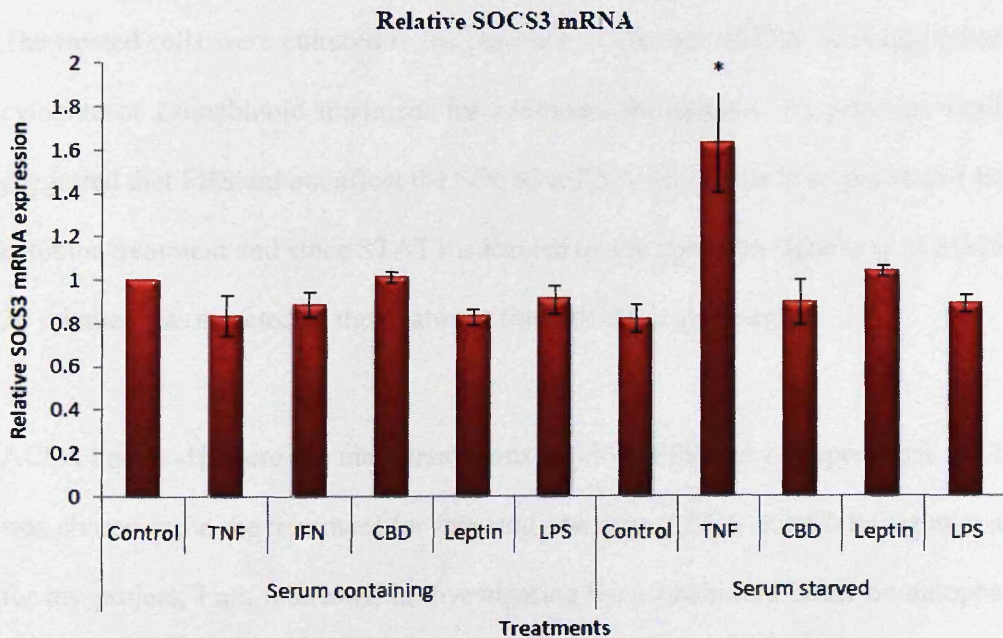


Figure 3.13. Effect of treatments on SOCS3 mRNA expression in both serum containing and serum starved CaCo2 cells. Treatments were applied for 1 hour. Data are given as fold change with error bars representing standard error of the mean (n=3, * $P<0.05$, compared to no treatment control from ‘serum containing’ protocol, ANOVA).

ii. mTOR and JAK-STAT signalling pathway

Previous studies suggested FBS did interfere with CNR1 mRNA expression but not SOCS3 mRNA expression. Therefore, experiments were performed to further evaluate the serum effect for SOCS3 and the JAK-STAT3 signalling pathway at the translational level. Activation of STAT3 via phosphorylation will initiate the transcription of SOCS3 and other target genes (Piessevaux et al., 2008). In addition to STAT3 and SOCS3, the mTOR protein was also included in the study. TOR signalling is known to be involved in the regulation of cellular stress response. Previous finding showed that TOR signalling was inhibited in response to starvation-induced stress in *Drosophila* fat body (Scott et al., 2004), therefore the activation of mTOR protein was selected as a positive control for this study.

The treated cells were cultured in the presence or absence of FBS overnight prior to cytokine or cannabinoid treatment for additional 30 minutes. As previous finding suggested that FBS did not affect the SOCS3 mRNA expression in response to 1 hour cytokine treatment and since STAT3 is located on the upstream signalling of SOCS3, 30 minutes was selected as the treatment time for this experiment.

ACEA and IL-1 β were the main treatments applied in this set of experiment. ACEA was chosen to be the treatment for this study because ACEA is a CNR1 agonist and for my project, I am interested in investigating the cannabinoid effect on autophagy process, therefore it was crucial to determine whether serum status has an impact on cannabinoid-induced effect on both p-MTOR and JAK-STAT signalling pathways in my model system. As for IL-1 β , studies showed an increase of IL-1 β production in inflamed gut mucosa in IBD patients (Reimund et al., 1996; Reinecker et al., 1993).

IL-1 β , a pro-inflammatory cytokines, is released by immune cells to the site of injury during inflammation (Harris et al., 2011). Taken together, it was interesting to explore whether serum status has an impact on IL-1 β induced effects in this context. Overall, this data would offer us further understanding of my model system and the importance of serum availability to both cannabinoid-induced effects, as well as the IL-1 β induced inflammatory setting.

Result showed that the basal protein expression for p- mTOR was up-regulated in the presence of FBS (Figure 3.14). ACEA-induced effect was not affected in p-mTOR protein expression, albeit the serum status. However, IL-1 β -induced effect on p-mTOR protein expression was dependent on the serum status in the treated cells (Figure 3.15).

In agreement to my previous finding (Figure 3.13), the presence of FBS did not impact on the basal expression of SOCS3 (Figure 3.14). Consistent with the SOCS3 respond, the basal protein expression of p-STAT3 was not affected by the addition of FBS (Figure 3.14). Interestingly, both IL-1 β and ACEA reduced SOCS3 protein expression in “serum-starved” cells but such effects were not observed in “serum containing” cells (Figure 3.15). As for p-STAT3, both IL-1 β and ACEA did not affect p-STAT3 protein expression, albeit the serum status (Figure 3.15).

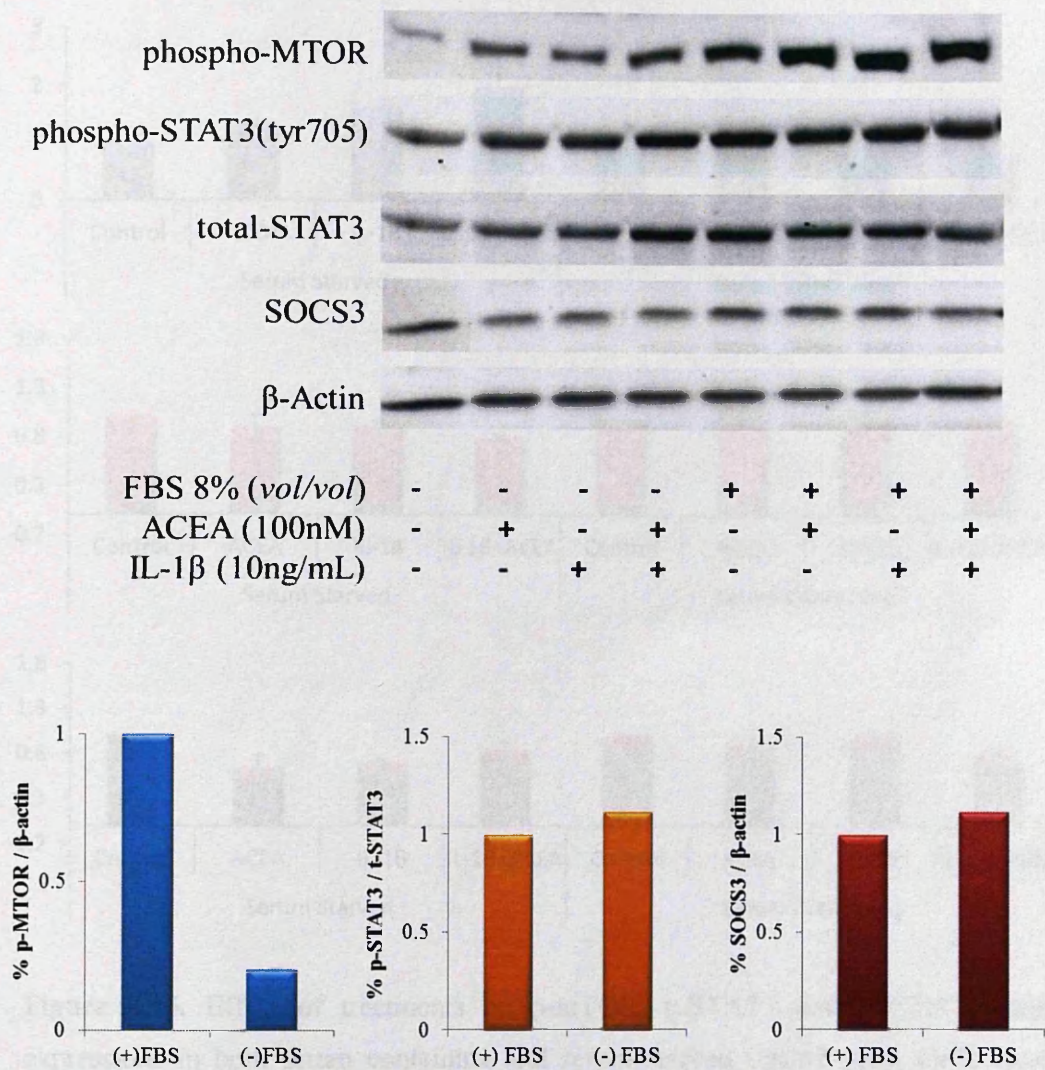


Figure 3.14. Effect of Fetal Bovine Serum (FBS) on p-mTOR, p-STAT3 and SOCS3 basal protein expressions in fully differentiated CaCo2 cells. Data are given as fold change compared to cells that were pre-starved overnight prior to protein lysing for western blotting; n=1.

(Molecular weight for p-MTOR:289KDa; p-STAT3:91KDa; t-STAT3:79KDa; SOCS3:27KDa; β -Actin:45KDa)

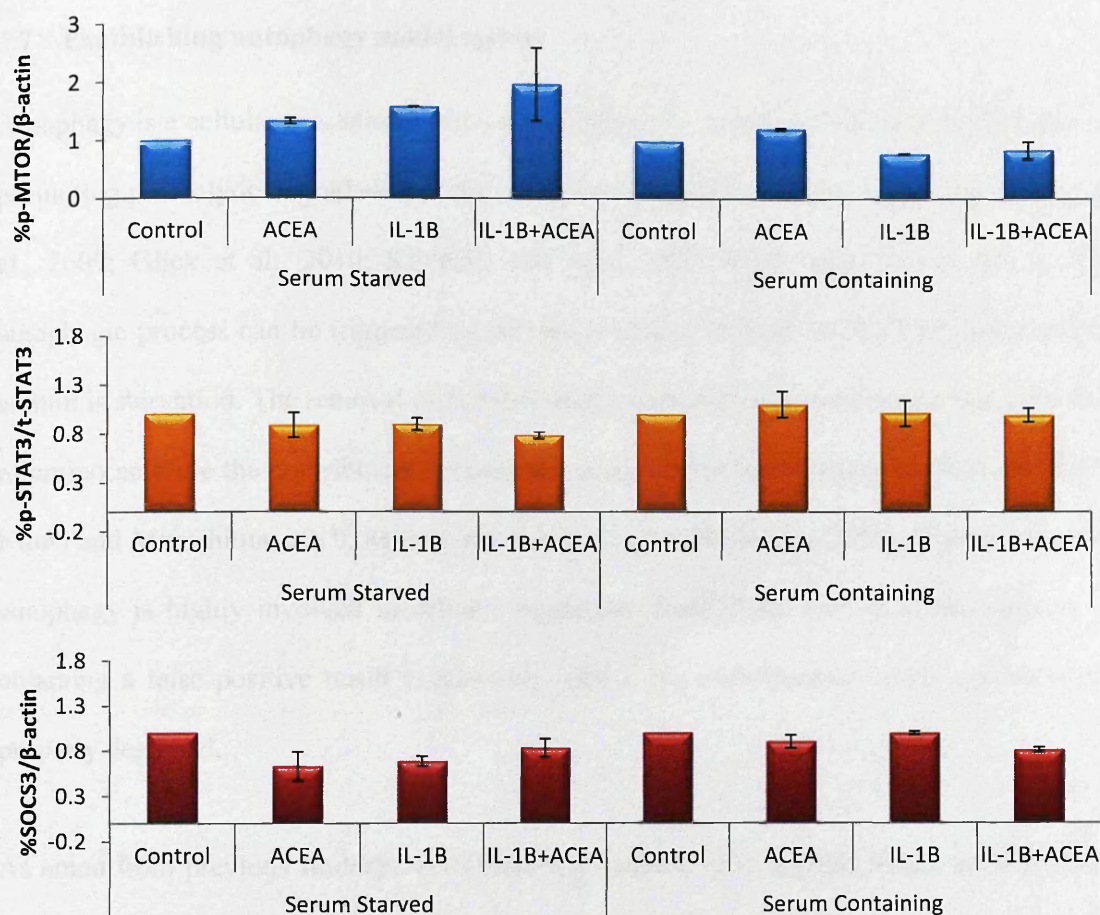


Figure 3.15. Effect of treatments on p-mTOR, p-STAT3 and SOCS3 protein expressions in both serum containing and serum starved CaCo2 cells. Cells were starved overnight prior to treatment application for additional 30minute. Data are given as fold change with error bars representing standard deviation ($n \geq 2$), compared to their corresponded no treatment control.

3.7 Establishing autophagy model system

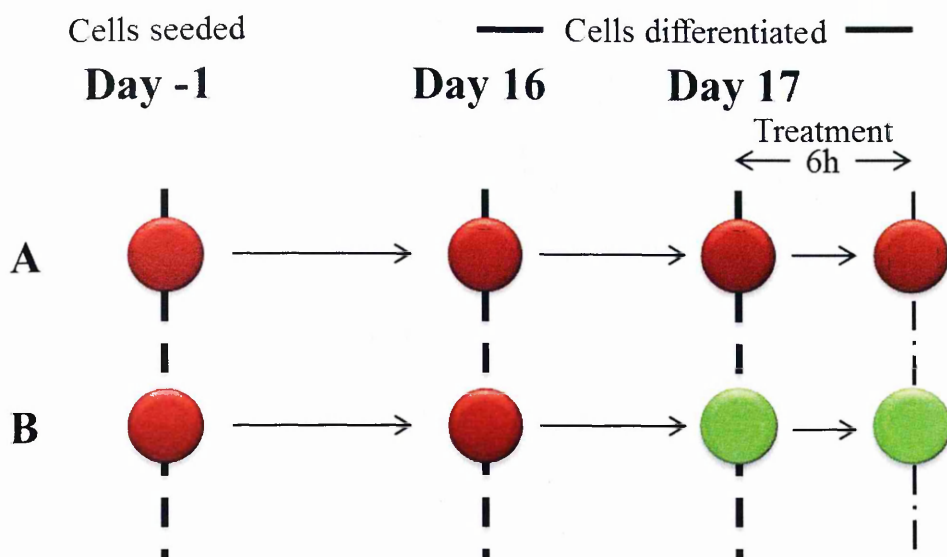
Autophagy is a cellular mechanism utilised to adapt to the cellular environmental changes by promoting proteolytic degradation of the cytosolic compartments at the lysosomes (Chang et al., 2009; Glick et al., 2010; Klionsky and Emr, 2000; Singh and Cuervo, 2011). The autophagic process can be triggered by various occasions and one of the best characterized stimuli is starvation. The removal of nutrient source such as nitrogen and carbon and the lack of amino acid are the contributors towards autophagy induction (Deretic and Levine, 2009; Kuma and Mizushima, 2010; Mizushima, 2007; Singh and Cuervo, 2011). Considering that autophagy is highly involved in cellular regulation of catabolic processes, the chances of obtaining a false positive result is relatively high if the experimental model system is not properly designed.

As noted from previous findings, cells were less responsive to applied treatment when they were treated with 8% FBS. Equally, a complete absence of serum in culture media may not be physiologically relevant as well as it will be unrealistic for nutrients to be inaccessible to epithelial cells in GI. Taken together, a new experimental protocol was designed to compromise both settings by reducing the serum concentration from 8% to 1%. Therefore, in this section, experiments were performed to evaluate the impact of FBS concentration (8% or 1% FBS) on p-mTOR and LC3-II protein expression. LC3-II is the hallmark feature in autophagy process. The formation of autophagosome was monitored through the conversion of LC3 from LC3-I to LC3-II (Kabeya et al., 2000).

Experiments were performed only in “serum containing” differentiated CaCo2 cells. Based on previous experiments, the rational for pre-starving treated cells was to synchronize cells into G₀ position in cell cycle. However, a recent study by Mehran and group demonstrated that CaCo2 cells that were cultured for 20 days were mostly in the G₁ phase of the cell cycle.

Around 18% of the cells were found in the proliferating state which included the S, G₂ and M phase of the cell cycle (Mehran et al., 1995), suggesting that by synchronizing the cell cycles back to G₀ position may interfere with the physiological setting as not all the epithelial cells in GI tract were in the G₀ position. Furthermore, in light of previous finding, phosphorylation of mTOR protein was greatly reduced in pre-starved cells (Figure 3.14), suggesting that the cells may experience starvation-induced cellular stress, which may subsequently impact on treatment-induced LC3-II expression in later stage. Therefore, taken together, the pre-starved protocol was aborted and experiments were proceeded only with “serum-containing” cells.

Result showed that the basal p-mTOR and LC3-II protein expression were unaffected by changes of serum concentration in treated cells (Figure 3.17). As mTOR signalling is known to be involved in the regulation of cellular stress response (Jung et al., 2010), the result suggested that the reduction of serum from 8% to 1% did not induce unnecessary cellular stress in treated cells. Furthermore, the result showed that IL-1 β increased p-mTOR protein expression only in 1% serum-treated cells (Figure 3.18). This finding was consistent with previous finding which suggested that IL-1 β -induced effects on p-mTOR protein expression were serum dependent. In contrast, IL-1 β increased LC3-II protein expression in 1% serum treated cells but not in 8% serum treated cells (Figure 3.18), suggesting that similar to the mTOR expression, the IL-1 β -induced effect on LC3-II protein expression was also serum dependent. This finding is in agreement with previous study which showed that the IL-1 β -induced autophagy effect in rat annulus fibrosis cells was serum dependent (Shen et al., 2011).



Indication:



CaCo2 cells cultured in MEM with 8% FBS



CaCo2 cells cultured in MEM with 1% FBS

Figure 3.16. Schematic diagram of two different experimental protocols applied in the experiment. Colour variation indicated the differences of serum concentration in the culture medium.

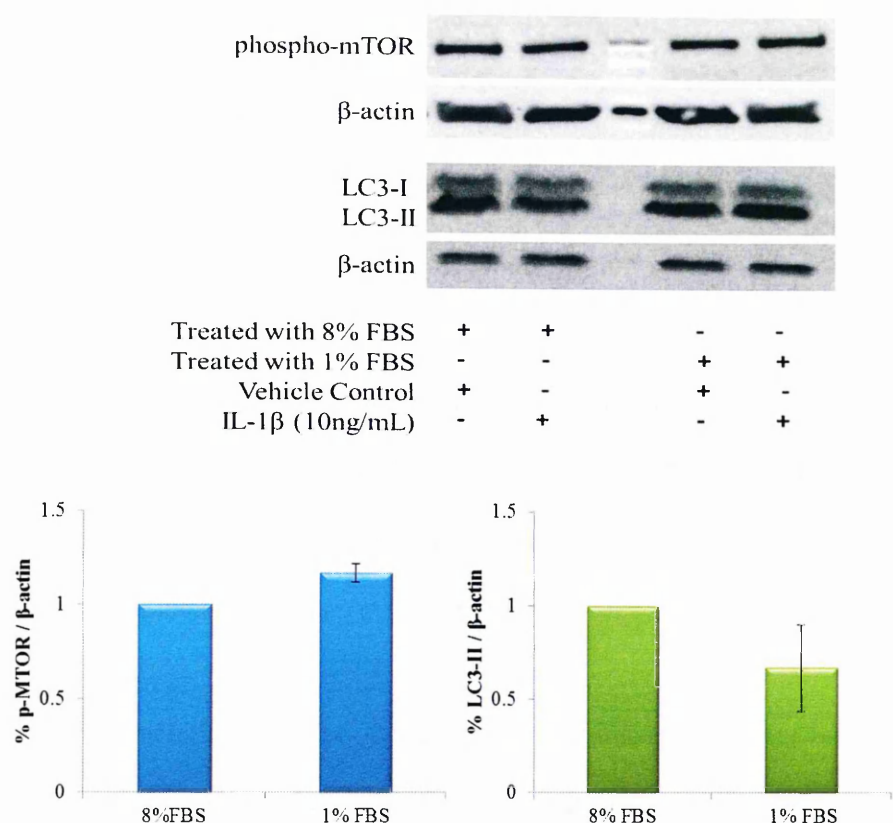


Figure 3.17. Effect of fetal bovine serum (FBS) on basal protein expression of p-mTOR and LC3-II in differentiated CaCo2 cells. Data are given the as fold change normalised to 8% FBS-treated cells with error bars representing standard deviation; n=2. Further detail for the experimental set up was presented on the schematic diagram on Figure 3.16.

(Molecular weight for p-MTOR:289KDa; LC3-I & II: 14&16KDa; β -Actin:45KDa)

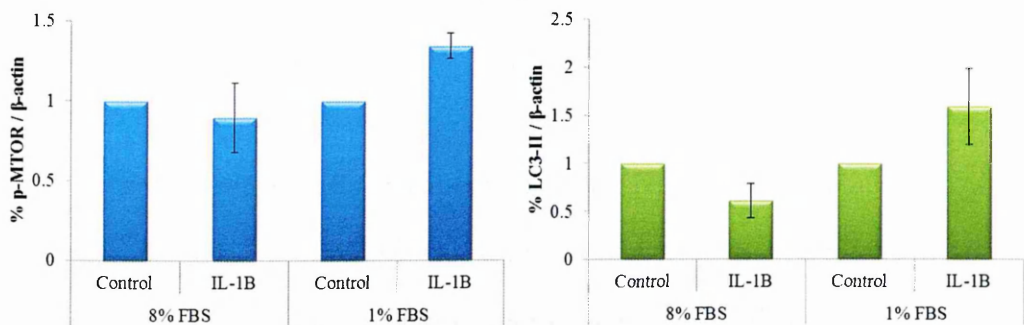


Figure 3.18. Effect of fetal bovine serum (FBS) on p-mTOR and LC3-II protein expression in IL-1 β -treated CaCo2 cells. Data are given as fold change associated untreated control within the same experimental protocol with error bars representing standard deviation; n=2. Further detail for the experimental set up was presented on the schematic diagram on Figure 3.16.

3.8 Discussion

CaCo2 cells are derived from the human epithelial colorectal adenocarcinoma cells. This cell line was chosen as the inflammatory cell model system based on their ability to mimic primary intestinal epithelium after differentiation in culture (Bailey et al., 1996). The inter-laboratory variation in the morphology and permeability of CaCo2 cells has been addressed in previous publications (Hayeshi et al., 2008; Sambuy et al., 2005). Despite of the variation in CaCo2 cells, this cell model is still the best characterised gut epithelial monolayer system available for *in vitro* study. CaCo2 cells mimic the characteristics of enterocytes residing in human small intestinal epithelium (Bailey et al., 1996).

Due to the characteristic of CaCo2 cells as stated above, there has been a controversy regarding the presence of functional CNR1 and CNR2 receptors in CaCo2 cells (Ligresti et al., 2003; Wright et al., 2005). Therefore, experiments were performed to verify the presence of CNR1 and CNR2 in my model system. Interestingly, in my CaCo2 cell model system, only CNR1 is being expressed in the cells. With that, the absence of CNR2 can be beneficial to my cell model system as it not only simplifies the cellular regulatory system but also provides us with the advantage of excluding possible involvement of CNR2 in response to cannabinoid treatment in the regulatory system.

Even though characteristic of CaCo2 had been previously reported, it is essential that the cell culture system employed is carefully characterized and thus experimentally controlled. Therefore, the CNR1 and SOCS3 mRNA were explored in proliferating, confluent and differentiated CaCo2 cells. In general, treatments-induced CNR1 and SOCS3 expressions were less significant as the cells started to form confluent, differentiated monolayer. Decline responses of CaCo2 cells to exogenous stimulation upon reaching confluency may be the consequence results from the formation of tight junctions in the cells. Presence of tight

junctions will limit the absorption of treatments applied to the cells as treatments will only be exposed to the apical or luminal surface on the cell monolayer whereas the treatments approach the proliferating cells on both the basal and apical cell surfaces. Apart from a possible consequences from the tight junction formation, stationary growth stage of the cells' progress may also contribute to the decline response of both confluent and differentiated CaCo2 cells to exogenous stimulation. During the phase of stationary growth, cells will stop proliferating (Watanabe and Okada, 1967) and considering that these cells were well-maintained with sufficient growth nutrients in culture dishes, the rate of response for these cells may slowly decline, hence explains the decline responses of CaCo2 cells to exogenous stimulation upon reaching confluency.

Proliferating CaCo2 cells showed a significant increase of CNR1 mRNA expression in response to LPS treatment (Figure 3.4). This may indicate the involvement of TLR4 signalling pathway on CNR1 expression. TLR4 signalling pathway is required for pathogen recognition activation of innate immunity and so, presence of bacteria ligands will stimulate the activation of TLR4 receptor (Fukata et al., 2005). Interestingly, in proliferating CaCo2 cells, SOCS3 mRNA illustrated an increase expression in response to LPS and IFN- γ treatments as well (Figure 3.5). This phenomenon only occurred in proliferating cells and not in confluent and differentiated cells. This is a new observation as it has not been shown in previous studies. Based on this result, I suggest that the increase of SOCS3 mRNA may be due to the initiation of the negative feedback loop of SOCS3 in reducing inflammatory cytokines induced activities. In contrast to proliferating CaCo2 cells, result showed that in confluence cells, SOCS3 expression was increased in response to TNF- α treatment, but not LPS and IFN- γ treatments (Figure 3.7). Again, this may due to stationary growth stage of the cells' progress, as well as the formation of tight junctions in confluent cells and the tight junctions act as a barrier to penetration of inflammatory treatments.

On the whole, I have a better understanding of the implication of using cells at different growth stages in my model system based on the results I have obtained. Even though differentiated CaCo2 cells were less responsive to applied treatments, these cells were most likely to be the closest model system to the physiological setting in intestinal epithelium. Therefore, I have decided to perform all the following experiments in differentiated CaCo2 cells.

Next, experiments were performed to explore the serum effect on CNR1 and SOCS3 expression in both serum containing and serum starved differentiated CaCo2 cells. The rationale of pre-starving the treated cells prior to cytokine treatment was to normalize the cell cycle by returning all the cells to G₀ position. As a result, this should provide more significant fold changes for both CNR1 and SOCS3 expression in the treated CaCo2 cells. My result showed that FBS may interfere with CNR1 mRNA expression and this was demonstrated through the CBD treatment. This finding was in agreement with previous findings from Jacobsson and groups where they demonstrated that FBS did affect CBD expression in human glioblastoma cells. However, the mechanism behind this finding is still unknown (Jacobsson et al., 2000). Additionally, considering that leptin is involved in nutrient sensing regulatory pathway (Wang et al., 1998), it was interesting to notice that leptin increased CNR1 mRNA expression regardless of the serum availability in the treated cells.

In contrast to serum-induced effect on CNR1 mRNA expression, SOCS3 was not affected by the presence of serum at both transcriptional and translational level. Consistent with the SOCS3 finding, FBS did not cause an impact on p-STAT3 protein expression level, suggesting that the JAK-STAT3-SOCS3 signalling pathway was unaffected by the change of nutritional status in the model system. Interestingly, both ACEA and IL-1 β induced SOCS3 protein expressions were serum dependent, as opposed to their induced effect on p-STAT3

expression. This implied that even though the basal expression of SOCS3 was unaffected regardless of the serum status in treated cells, cytokine or cannabinoid treatment may act differently according to the serum availability in the treated cells, hence indirectly impact on the SOCS3 expression.

In my model system, the basal p-mTOR protein expression was reduced in pre-starved cells, as compared to cells treated with full serum (8%), suggesting that the starvation step may deliver unnecessary cellular stress into the cellular system. Additionally, the starvation step may also interfere with the physiological setting as not all the epithelial cells in the GI tract were in G₀ position. Taken together, the “serum starving” protocol was later being excluded from the experimental setting. It has been reported that starvation-induced stress may inhibit TOR activation in *Drosophila* fat body (Scott et al., 2004). Inhibition of p-mTOR may act as a rescue mechanism for the cell to initiate autophagy activation, a cellular process that maintains the cellular energetic homeostasis in the cells (Diaz-Troya et al., 2008). Considering that autophagy pathway was the main readout for this project and autophagy pathway is tightly regulated by the nutritional status in the model system, the exclusion of this additional starvation protocol may also reduce the probability of attaining false positive result for cytokine or cannabinoid-induced effect on autophagy process in treated cells.

Apart from the impact of starvation-induced onto the treated cells, I also noticed that the differentiated CaCo2 cells were less responsive to applied treatments in the presence of 8% serum, suggesting that the use of 8% serum may dominate over cytokines or cannabinoids treatments in the cells and a higher concentration of cytokines/cannabinoids may be required to obtain a significant induced-response in this experimental set up. Consequently, increased dosage of the cytokines and cannabinoids treatment may increase the cytotoxicity in the

treated cells, subsequently affect the experimental outcome. Therefore, experiments were performed to explore the use of reduced serum concentration (1% serum) in the experimental protocol. My results showed that the changes of serum concentration from 8% to 1% did not affect the basal p-mTOR protein expression, suggesting that the cellular homeostasis in treated cells was not disturbed by the serum reduction. Taken together, this finding implied that 1% serum culturing protocol may be more appropriate to study autophagy induction in my cell model.

Overall, differentiated CaCo2 cells were selected as my *in vitro* model system to study cannabinoid-induced effect on autophagy process in the intestinal epithelial cells. Treated CaCo2 cells would not be pre-starved and treatment would be applied along with MEM supplemented with 1% serum.

Chapter 4

Cannabinoid receptor (CNR)-1 knockdown CaCo2 cell model

Table of Contents

- 4.1 Introduction..... 91
- 4.2 Aims 92
- 4.3 Generation of CNR1 knockdown CaCo2 cell model 93
 - 4.3.1 Experimental Technique: pRestroSuper(pRS) Retroviral Vector 93
 - i. Retroviruses 93
 - ii. OriGene engineered pRS vector 94
 - 4.3.2 Experimental Technique: shRNA Expression Cassette 96
 - i. ShRNA 96
 - ii. OriGene shRNA HuSH plasmid (29mer) 97
 - 4.3.3 Puromycin kill curve 98
 - 4.3.4 Experimental Procedures 100
- 4.4 Verifying Transfection Efficiency 102
 - 4.4.1 Immunoblotting 102
 - 4.4.2 [³⁵S]GTPγS binding activity 105
 - i. Principle of [³⁵S]GTPγS binding activity 105
 - ii. Preparation of cell samples for [³⁵S]GTPγS binding activity 108
 - iii. Experimental procedures 108
 - iv. ACEA-induced functional consequences on GPCR activation in CaCo-CNR1KD cell line 110
- 4.5 Discussion 113

4.1 Introduction

Cannabinoid receptor (CNR)-1 is one of the most well studied examples of cannabinoid receptors. CNR1 was the first to be discovered and studies have shown that the expression level of CNR1 is high in brain regions that associate with cannabinoids and low in regions where cannabinoids are not normally produced such as the respiratory center of medulla (Herkenham et al., 1991). CNR1 is classified under G-coupled protein receptor (GPCR) superfamily, where CNR1 couples and activates the G_i/G_o subunits in G-proteins (Glass and Northup, 1999).

To date, studies have reported several beneficial effects of cannabinoid administration to the gut (Izzo and Sharkey, 2010; Wright et al., 2005). Association of CNR1 to cannabinoid treatments have previously been reported and studies have suggested that the role of CNR1 in cannabinoid-induced effect is functionally dependent. For instance, administration of CBD, a non-psychoactive phytocannabinoid, induced a concentration-dependent inhibition of the migration of glioma cells and this effect was not mediated by CNR1 (Vaccani et al., 2005). Interestingly, in other study, CBD was shown to inhibit inflammatory hypermotility and such effect was mediated by CNR1 despite the fact that CBD does not bind to cannabinoid receptors with high affinity (Capasso et al., 2008). However, the association of CNR1 in cannabinoid-induced autophagosome formation was unknown. The use of antagonists to the CNR1 receptor has been an important tool in the dissection of receptor-mediated signalling and function, but a novel way to study the functional consequence of CNR1 loss is through reduced gene expression in the cell system, thus by shRNA-induced knockdown of CNR1 gene, a new cell model was generated. The methods applied in developing this new cell model system are reviewed in this chapter.

4.2 Aims



To generate cannabinoid receptor (CNR)-1 knockdown CaCo2 cell model (CaCo2_CNR1KD).



To determine the optimal puromycin concentration to be used as a selectable marker for in CaCo2_CNR1KD cells.



To verify the percentage of knockdown for CNR1 gene in CaCo2_CNR1KD cell model.

4.3 Generation of CNR1 knockdown CaCo2 cell model

In this project, CNR1 gene knockdown CaCo2 cell model (CaCo2-CNR1KD) was generated by introducing CNR1-specific HuSH short-hairpin RNA (shRNA) (CNR1 Gene ID = 1268) into the wild type CaCo2 cells through direct transfection. Introduction of shRNA allows the generation of stable and long-term knockdown of CNR1 gene in CaCo2 cell model. During transfection, pRetroSuper (pRS) retroviral vector was selected by OriGene to deliver the inserted CNR1- shRNA expression cassettes into the CaCo2 cell. pRS vectors with CNR1 shRNA inserts were purchased from OriGene (product code, TR316500).

4.3.1 *pRetroSuper (pRS) retroviral vector*

i. Retroviruses

Retroviruses are enveloped viruses which consist of a linear, single-stranded RNA as the genome (Zhang and Godbey, 2006). Retroviruses integrate into the host genome by initiating fusion between the viral envelopes and the host cell membranes, resulting in the release of viral components into the cell cytoplasm. The viral RNA will be utilised as a template by the viral reverse transcriptase to generate a double stranded cDNA and incorporate into the host genome. With the use of the host machinery, cDNA will be transcribed into mRNA and subsequently translated into a viral protein (Zhang and Godbey, 2006). Such replication system employed by the retroviruses was targeted and engineered into retroviral vector, which has become a valuable approach in introducing a foreign gene of interest into a target cell.

ii. OriGene engineered pRetroSuper (pRS) vector

A pRS retroviral vector contains the retroviral long terminal repeats (LTRs) from the murine moloney leukemia virus, a puromycin resistance gene, an ampicillin resistance gene, a SV40 promoter and a U6 small nuclear RNA gene promoter (Figure 4.1). LTRs are the main gene expression regulator for the retrovirus by ensuring the integration between the pRS vector and the host cell. The U6 promoter, which is designated straight upstream from the shRNA construct, drives the expression of the inserted shRNA expression cassettes. The presence of the selectable markers is crucial in determine the efficacy of transformation/transfection. The bacterial selection maker for this pRS vector is ampicillin whereas the mammalian selection marker is puromycin. The first is expressed by the LTR promoter whereas the latter is expressed by SV40, an internal and heterologous promoter (Figure 4.1). Based on the selection system, cells that were successfully transfected with CNR1-shRNA contained pRS vector, which would have the puromycin resistance gene integrated into the genome. Consequently, the puromycin antibiotic treatment would have no impact on the transfected cells, and *vice versa*.

Features for pRS vector:

Start	End	Description
1	6	EcoRI
75	331	U6 promoter
335	340	BamHI
379	385	HindIII
386	391	Sall
413	681	SV40 promoter
743	1342	Puromycin-N-acetyl transferase sequence
1441	2034	3' LTR
2391	3010	pBR322 ORI
3172	4032	Beta-lactamase for ampicillin resistance
4168	4639	5' LTR

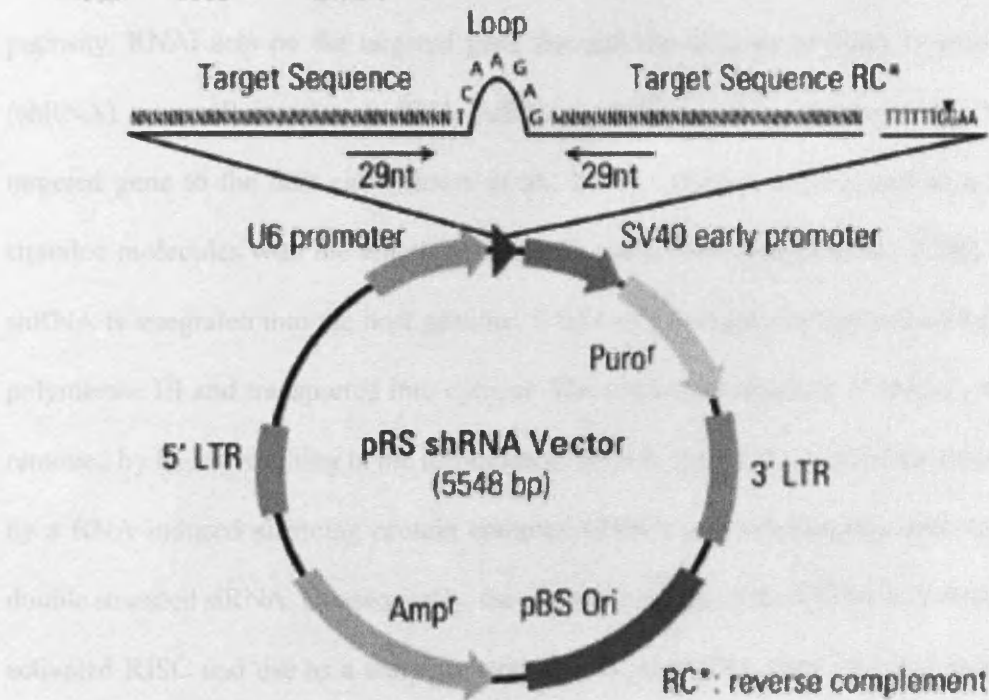


Figure 4.1. pRS shRNA expression vector. Please see appendix for the complete DNA sequence of the pRS vector without shRNA expression cassette.

Figure adapted from OriGene HUSH shRNA plasmids (29-mer) application guide.

4.3.2 *Short hairpin RNA (shRNA) expression cassette*

i. shRNA

RNA interference (RNAi) is a post-transcriptional cellular machinery which involves in the sequence-specific gene silencing process (Sandy et al., 2005). RNAi has become a powerful research tool, both *in vivo* and *in vitro* (Hausmann et al., 2011; Ikonomou et al., 2012; Szymanska, 2007). Such technique is broadly used to study gene regulation in disease states and subsequently, their associated proteins function in the interactive pathway. RNAi acts on the targeted gene through the delivery of short hairpin RNA (shRNA) or small interfering RNA (siRNA) with sequence complementary to the targeted gene to the host cell (Moore et al., 2010). shRNA is produced as a single stranded molecules with the length of 50 to 70 nucleotides (Sandy et al., 2005). Once shRNA is integrated into the host genome, it will be constitutively transcribed by RNA polymerase III and transported into cytosol. The stem-loop structure of shRNA will be removed by Dicer, resulting in the formation of siRNA. Such siRNA will be encountered by a RNA-induced silencing protein complex (RISC) and subsequently unwound the double stranded siRNA. Consequently, the antisense strand of the siRNA will bind to the activated RISC and use as a template strand to target mRNA with identical sequence. This results in the degradation of the targeted mRNA in the cell, hence impacts on the expression of the targeted gene in the cells (Sliva and Schnierle, 2010).

ii. OriGene HuSH shRNA plasmid (29-MER)

HuSH-29 hairpin shRNA construct consists of a longer nucleotide sequence compared to the conventional 19-21mer shRNA construct. The increase length in shRNA sequences results in an increase in the efficacy of the shRNA in inhibiting the targeted gene (Siolas et al., 2005). The gene-specific shRNA construct was inserted downstream of U6 promoter in the pRS expression vector (Figure 4.1.). Each shRNA constructs was designed based on the structure sequence as stated in Figure 4.2. In this project, four different CNR1-specific shRNA constructs were directly transfected into the wild type CaCo2 proliferating cells, resulting in four versions of CaCo2_CNR1KD cells. The sequences for each of the shRNA constructs were stated in Table 4.1.

U6 promoter – **GATCG** -- 29 nt sense –TCAAGAG – 29 nt reverse complement --TTTTTT (termination) - **GAAGCT**

Figure 4.2. Structure sequence for OriGene designed gene-specific short-hairpin RNA (shRNA). The nucleotide sequences highlighted in bold were the BamHI/Hind III cloning sites to be found in the pRS expressing vector. “29 nt sense” represented 29 nucleotide gene-specific sequences inserted in plus (+) orientation; the nucleotide sequences for TCAAGAG formed a 7 nucleotide loop in the shRNA.

Table 4.1. 29-nucleotides sequences for CNR1-specific short hairpin RNA (shRNA) constructs. *Nucleotide sequences were listed in plus (+) orientation.*

shRNA ID	Lot number	shRNA nucleotides sequences
TI363209	0312	GAAGTCGATCCTAGATGGCCTTGCAGATA
TI363210		TGGAGAACCTCCTGGTGCTGTGCGTCATC
TI363211		TACTGCTTCTGTTCATCGTGTATGCGTAC
TI363212		GTGTCCACAGACACGTCTGCCGAGGCTCT

4.3.3 Puromycin kill curve

To determine the optimal concentration of puromycin to be used as the selectable marker for eliminating the non-transfected cells, a puromycin kill curve was performed by using wild type proliferating CaCo2 cells. Proliferating CaCo2 cells were seeded at the cell density of 50,000 cells per well in a 96 well plate. Puromycin with the concentration ranging from 0.05µg/mL to 100µg/mL was applied to the cells and incubated for 72hours. A cell viability assay was performed to evaluate the viability of treated cells in response to puromycin treatment. 20µL of PrestoBlue™ Cell Viability Reagent was added to a total of 180µL culture media with treated puromycin CaCo2 cells, followed by 10 minutes incubation at 37°C. Such reagent acts as a cell viability indicator by using the reducing environment maintained by the living cells to quantitatively measure the proliferation of cells. Addition of such reagent to the cells induces a fluorescent colour change from blue to red, which can then be detected via fluorescence measurement. Fluorescence readouts were obtained at the excitation wavelength of 535nm and emission wavelength of 615nm. A graph was plotted with the percentage of cell viability against the puromycin concentration applied to the CaCo2 cells (Figure 4.3).

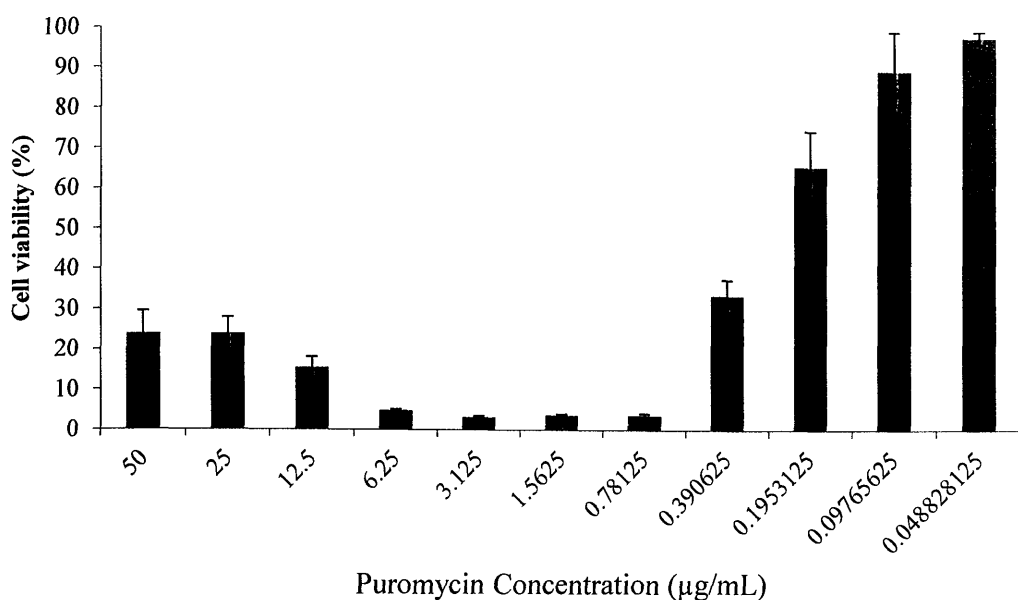


Figure 4.3. Viability of CaCo2 cells in response to puromycin treatment. Proliferating CaCo2 cells were treated with puromycin concentration ranging from 0.05µg/mL to 50µg/mL. Cell viability assay was performed by using PrestoBlue™ Cell Viability Reagent. Readings were obtained at the excitation wavelength of 535nm and emission wavelength of 615nm (n=3).

As fluorescence readouts reflect the metabolic activity in the cells, result suggested that the treatment of puromycin concentration ranging from roughly 0.5µg/mL to 5µg/mL was lethal to the proliferating CaCo2 cells. Such response was consequence from the puromycin-induced inhibition in the translational process during protein synthesis (Azzam and Algranati, 1973). Taken that, puromycin at 0.6µg/mL was chosen to apply as the selectable marker for the knockdown cells. Cells which have been successfully transfected with shRNA-expressed vector will be resistant to puromycin treatment, or *vice versa*. Treatment with puromycin at the concentration of 0.6µg/mL will therefore allow cells to differentiate and eliminate the non-transfected CaCo2 cells, hence maintaining the culture under selection process.

4.3.4 Experimental Procedures

TurboFectin 8.0, as recommended by OriGene, was chosen as the transfection reagent to achieve optimal delivery of nucleic acid into the CaCo2 cells. Overall, CaCo2 cells were transfected with four different CNR1-specific shRNA cassettes, resulting in four different CaCo2-CNR1KD cell lines. An additional OriGene provided shRNA construct which consisted of pRS vector with non-effective (scrambled) shRNA cassette has also been transfected into the CaCo2 cells. The CaCo2 cells that have been transfected with scrambled shRNA cassette (CaCo2-Scrambled) were treated as the specific negative control for gene down regulation in this procedure.

Wild type CaCo2 cells were seeded at a cell density of 2×10^5 cells per well in a 6 well culture plate a day before the transfection. A mixture of different reagents was required to be freshly prepared before proceeding towards transfection. The order of reagent to be added into the mixture was crucial in order to achieve an optimal transfection. First, 100 μ L of serum free-MEM culture medium were prepared in a sterile plastic tube. 3 μ L of TurboFectin 8.0 was added directly into the prepared MEM culture medium and mixed thoroughly with gentle pipetting, followed by incubation at room temperature for 5minutes. Next, 1 μ g of shRNA cassette was added into the TurboFectin-containing media and mixed thoroughly with gentle pipetting. The mixture was incubated at room temperature for 30minutes. After the incubation, the mixture was carefully added and evenly distributed onto the seeded CaCo2 cells and incubated for additional 48hours. During the incubation period, cells were observed by light microscopy to ensure the cells did not overgrown.

After 48h incubation, transfected cells were passaged in complete medium supplemented with 0.6µg/mL of puromycin antibiotic reagent. These transfected cells were evenly distributed into a 96 well plate for selection process. A large number of cells were killed under the puromycin treatment as a result of the lack of puromycin resistance gene in the cells. After 4-7 days, some treated cells started to show sign of recovery from the selection pressure, indicating that HuSH shRNA cassette has been successfully integrated into the CaCo2 cell genome. 3 to 4 clonal populations of cells were selected, passaged and transferred into a 6-wells culture plates and gradually into T75 culture flask to promote further cell growth. Cells were maintained in complete medium with the selection pressure of puromycin.

4.4 Verifying transfection efficiency

Two experimental methods have been used to verify the transfection efficiencies in each of the CaCo2-CNR1KD cell lines: immunoblotting and [³⁵S]GTPγS binding assay. Immunoblotting was chosen as the method to study CNR1 protein expression in the knockdown cells. In contrast, [³⁵S]GTPγS binding assay, a functional ligand binding assay, was employed to study the functional consequences resulting from the binding activity of CNR1 agonist on GPCR, hence revealed the status of functional CNR1 in the CNR1 knockdown CaCo2 cells.

4.4.1 Immunoblotting

Protein samples for different clones of CNR1knockdown CaCo2 cells were run on two separate SDS-PAGE gels (Figure 4.4). Protein samples prepared for CNR1 immunoblotting were heated at 65°C for 2 minutes before loading into the gel. The modification of boiling temperature from 95°C to 65°C was based on the immunoblotting protocol described by Grimsey *et.al.* study (Grimsey et al., 2008).

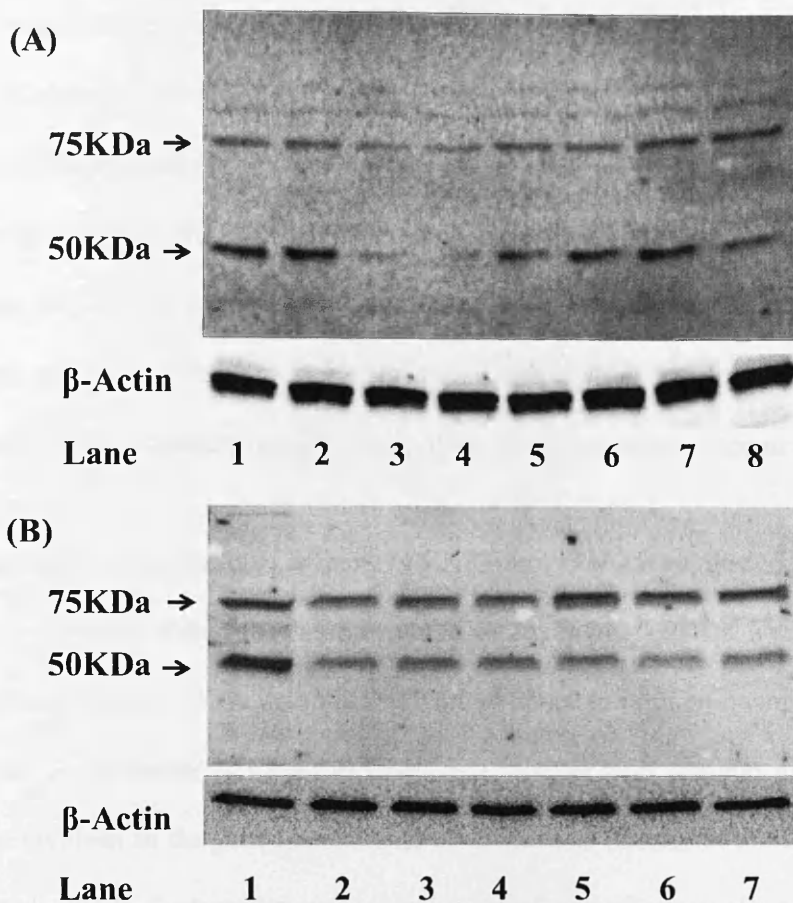


Figure 4.4. Immunoblot analysis of the verification of cannabinoid receptor (CNR)-1 protein expression in CNR1 knockdown CaCo2 cells (CaCo2_CNR1KD). In total, 4 different CNR1 shRNA -expressed cassettes were used for the transfection with 2 to 3 clones selected from each shRNA cassettes. Both non-transfected CaCo2 cells and cells transfected with shRNA cassette with non-effective (scrambled) sequence insert (CaCo2-Scrambled) were treated as the negative controls for the experiment. Samples in Gel A were run in a 12% SDS-PAGE gel whereas the samples in gel B was run in a 10% SDS-PAGE gel. Samples loading order for gel A: (1-2) Non-transfected CaCo2; (3-4) CaCo2_CNR1KD with shRNA cassette ID: TI363209; (5-6) CaCo2_Scrambled; (7-8) CaCo2_CNR1KD with shRNA cassette ID: TI363210. Sample loading order for Gel B: (1) Non-transfected CaCo2; (2-4) CaCo2_CNR1KD with shRNA cassette ID: TI363211; (5-7) CaCo2_CNR1KD with shRNA cassette ID: TI363212.

CNR1 immunoblots showed that out of all four CNR1-specific shRNA cassettes used, only CaCo2 cells that have been transfected with shRNA cassette with the sequence ID of TI363209 successfully knockdown the CNR1 gene in CaCo2 cell line. As for the remaining CaCo2_CNR1KD cell line, the concentration and purity of the shRNA construct may be the factor which influences the successful transfection. Additionally, this may also due to experimental error during transfection as every small procedures performed during transfection can greatly affect the transfection outcome.

Despite that the manufacture company of CNR1 antibody has suggested a single CNR1 band to be detected at the molecular weight of approximately 60KDa, a minimum of two clear protein bands (75KDa and 50KDa) were obtained in both immunoblots. This may due to the characteristic of CNR1 as CNR1 is a receptor with complex architecture and actively involves in the post-translational modifications (Bosier et al., 2010; Console-Bram et al., 2012). Such modifications can have profound effects on the protein structure and consequently affect the molecular weight of the associate protein (Beck-sickinger and Mörl, 2006). Apart from that, additional protein bands may also due to the lack of specificity in CNR1 antibody. Specificity of the commercially available CNR1 antibody has been addressed in a recent study by Grimsey, *et al.* (2008). In agreement to my finding, they have encountered similar problem of obtaining multiple protein bands with the use of CNR1 antibody via western blotting. Interestingly, there was a significant inconsistency in the range of bands detected with the use of different CNR1 antibodies purchased from different manufacture companies (Grimsey et al., 2008). Considering the difficulty in the use of CNR1 antibody to access CNR1 protein expression, [³⁵S]GTPγS binding assay was employed to verify the knockdown efficiency by studying the functional consequence of receptor activation followed by the binding of CNR1 agonist.

4.4.2 [³⁵S] GTPγS Binding Assay

[³⁵S]GTPγS binding assay was the second technique used to determine the CNR1 knockdown efficiency in CaCo2 cell model. CNR1 is classified under G-coupled protein receptor (GPCR) superfamily, where CNR1 couples and activates the G_i/G_o subunits in G-proteins (Glass and Northup, 1999). The rationale for performing such assay was to further evaluate the transfection efficacy as results obtained from western immunoblotting were unable to deliver a clear picture for the protein expression of CNR1 in the cell model system. Difficulty in assessing CNR1 protein expression has been addressed previously and this is mainly due to the lack of good commercially available antibody for the receptor (Grimsey et al., 2008). Therefore, [³⁵S] GTPγS binding assay was a better strategy in verifying CNR1 knockdown efficiency in the cell model system as this assay relies on direct CNR1 binding data rather than the reliability of antibody specificity.

i. Principle of [³⁵S] GTPγS Binding Assay

The [³⁵S]GTPγS binding assay measures the level of G-protein activation following agonist occupation of the GPCR (Harrison and Traynor, 2003). This functional assay is a popular tool to study ligand binding for GPCR as it measures the functional consequences resulting from GPCR occupancy. Binding of an agonist to the receptor will mediate a guanine nucleotide exchange event on the G-protein Gα subunit. Such nucleotide exchange is the first event to be mediated by GPCR activation in the signalling cascade (Harrison and Traynor, 2003). This assay provides an accurate measure of the ligand binding activity on GPCR by excluding the likelihood of receptor modulation in response to other events that may occur further down the signalling cascade.

GPCR consists of an extracellular N terminus, seven transmembrane spanning domains and an intracellular C terminus. The heterotrimeric protein, which couples to the C terminus of GPCR, comprises a $G\alpha$ subunit and a dimer of $G\beta$ and $G\gamma$ subunits. $G\beta\gamma$ subunit plays an important role in maintaining the protein structure as it is required for the binding of $G\alpha$ subunit to the receptor and acting as a scaffolding protein to connect the G-protein to the cell membrane (Harrison and Traynor, 2003). An inactive G-protein has a GDP bound to the $G\alpha$ and $G\beta\gamma$ subunits, presented as $G\alpha(\text{GDP})\beta\gamma$. Binding of an agonist to the receptor will initiate a conformation change in the receptor, resulting in the exchange of GDP to GTP and the release of $G\beta\gamma$ subunit. Such event activates the G-protein and leads to the initiation of the downstream effectors. Intrinsic GTPase activity on the $G\alpha$ subunit hydrolyses the bound GTP, resulting in the re-association of G-protein into its heterotrimeric protein structure (Figure 4.5) (Harrison and Traynor, 2003).

In contrast, in the [^{35}S]GTP γ S binding assay, [^{35}S]GTP γ S replaces the endogenous GTP and binds to the $G\alpha$ subunit, forming $G\alpha$ -[^{35}S]GTP γ S. The γ -thiophosphate in [^{35}S]GTP γ S is resistant to hydrolysis by the GTPase of $G\alpha$ subunit, hence inhibiting the reformation of $G\alpha$ -[^{35}S]GTP γ S back to $G\alpha(\text{GDP})\beta\gamma$. Consequently, this results in an accumulation of $G\alpha$ subunit labelled with [^{35}S]GTP γ S (Figure 4.6). Taken that, the level of GPCR activation in response to ligand binding can then be measured by quantifying the amount of [^{35}S]-labelled GTP γ S in the sample (Harrison and Traynor, 2003).

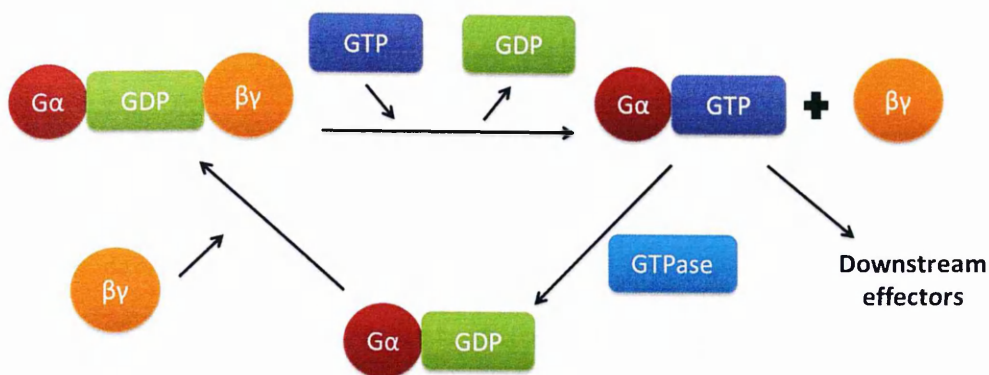


Figure 4.5. Schematic diagram for G-protein mediated signalling cascade. The binding of agonist to the receptor initiates the exchange of GDP to GTP in the G-protein Gα subunit. Gα-GTP and Gβγ subunits will initiate downstream cellular effectors. However, Gα-GTP subunit can be re-formed back into Gα(GDP)βγ by GTPase activity and return the G-protein into an inactive state. *Figure adapted from (Harrison and Traynor, 2003).*

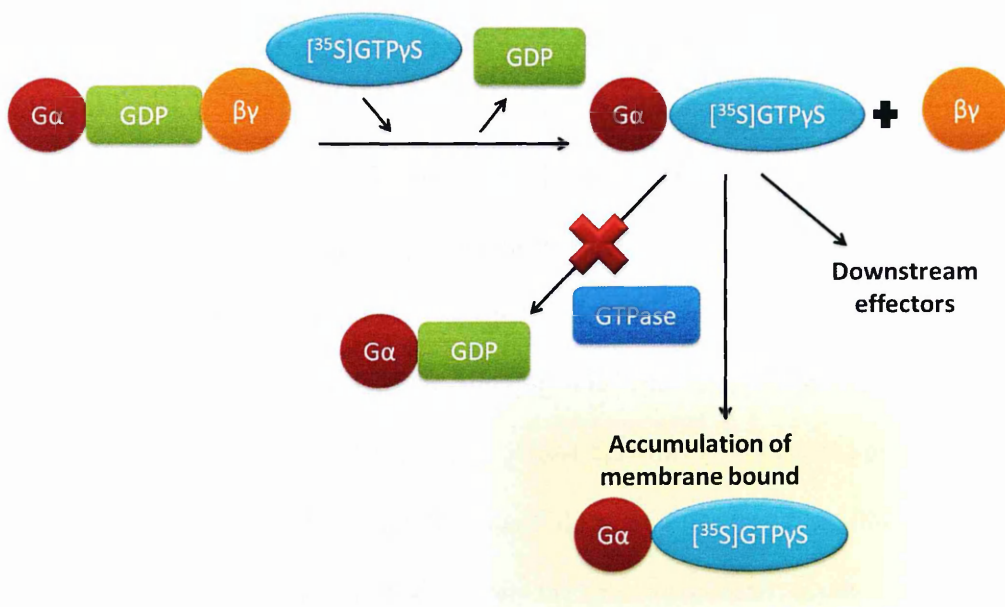


Figure 4.6. Schematic diagram for the principle of $[^{35}\text{S}]\text{GTP}\gamma\text{S}$ binding assay. $[^{35}\text{S}]\text{GTP}\gamma\text{S}$ replaces the endogenous GTP and binds to the Gα subunit. As $[^{35}\text{S}]\text{GTP}\gamma\text{S}$ cannot be hydrolysed by the GTPase of the Gα subunit, heterotrimeric reformation step cannot occur, resulting in the accumulation of $[^{35}\text{S}]\text{GTP}\gamma\text{S}$ -labelled Gα subunit. Taken that, activity of ligand binding to GPCR can be measured by quantifying $[^{35}\text{S}]$ -labelled $\text{GTP}\gamma\text{S}$ in the sample. *Figure adapted from (Harrison and Traynor, 2003).*



ii. Preparation of cell samples for [³⁵S] GTPγS Binding Assay

Two CaCo2_CNR1KD clones with shRNA cassette ID TI363209 were cultured in T150 culture flask and grown into fully differentiated cell monolayer. Cells were rinsed with PBS, scraped with a cell scraper and transferred into a 50mL falcon tube. The sample was centrifuged at 10,000rpm for 5minutes to obtain a cell pellet, which was then stored at -20°C for later use.

iii. Experimental Procedures

[³⁵S]GTPγS binding assays were performed using previously prepared cell pellet (5μg protein per well). Cells were treated with 0.1% vehicle, 30μM of unlabelled GTPγS or ACEA in assay buffer (50mM Tris-HCL, 50mM Tris-base, 5mM MgCl₂, 1mM EDTA, 100mM NaCl, 1mM dithiothreitol, 50mM HEPES and 0.1% fatty acid free BSA) supplemented with 20μM GDP and 0.1nM [³⁵S]GTPγS to a total assay volume of 500μL (Table 4.2.). This was followed by the incubation step at 30°C for 60 minutes. Binding was initiated with the addition of [³⁵S]GTPγS. Non-specific binding was measured by using 30μM of unlabelled GTPγS. Binding was terminated by the addition of ice cold GTPγS wash buffer (50mM Tris-HCL, 50mM Tris-Base, 0.1% BSA) and rapid vacuum filtration by using a 24-well sampling manifold and GF/B glass-fibre filters that has been soaked for at least 24 hours at 4°C in the GTPγS wash buffer. Each reaction well was washed around 6 times with GTPγS wash buffer. The filters were oven dried for 60 minutes and placed in 5mL scintillation vials with 4mL scintillation fluid (Ultima Gold). Radioactivity was quantified by using liquid scintillation spectrometry. Specific binding was defined as the difference between the binding in the presence and absence of 30μM GTPγS and varied between 70-90% of the total binding.

Table 4.2. Plate set up for [³⁵S]GTPγS binding assay.

Well	Assay buffer (μL)	50μL	50μL cell sample	50μL [³⁵ S]GTPγS
A1-2	350	30μM GTPγS		
A3-4	350	0.1% Vehicle		
A5-6	350	1nM ACEA		
A7-8	350	10nM ACEA		
A9-A10	350	100nM ACEA		
A11-12	350	1000nM ACEA		
B1-2	350	10000nM ACEA		
B3-4	350	1nM ACEA		
B5-6	350	10nM ACEA		
B7-8	350	100nM ACEA		
B9-10	350	1000nM ACEA		
B11-12	350	10000nM ACEA		

iv. ACEA-induced functional consequences on GPCR activation in CNR1 knockdown CaCo2 cells.

[³⁵S]GTPγS Binding with ACEA

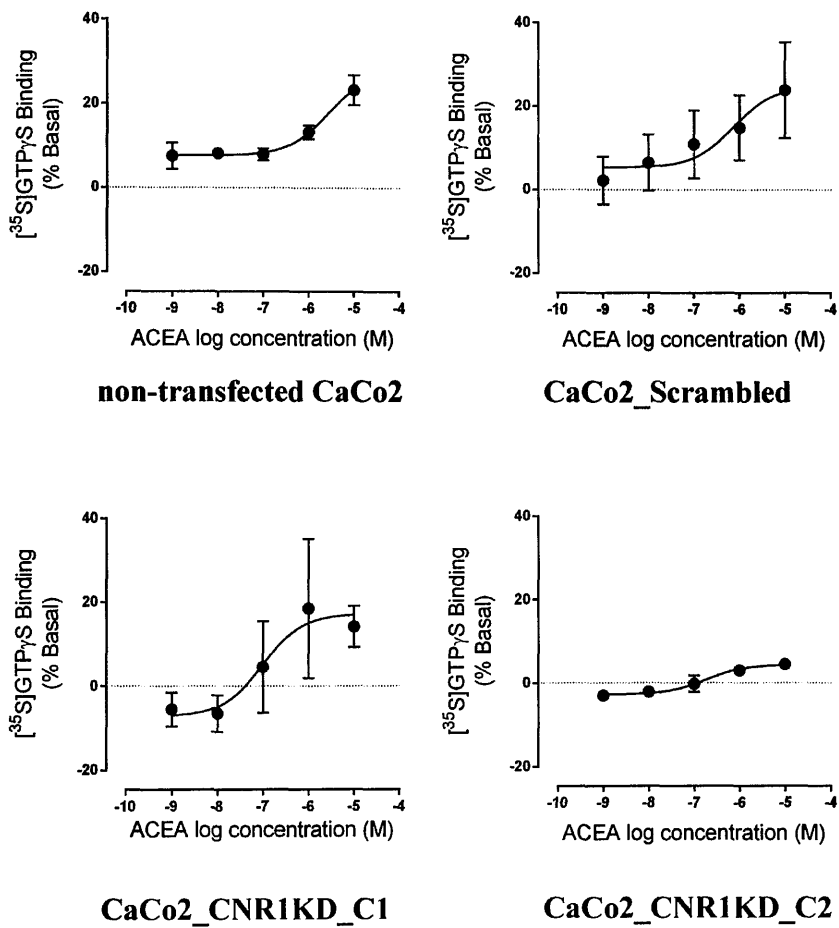


Figure 4.7. [³⁵S]GTPγS binding activity in response to ACEA treatment in CNR1 knockdown CaCo2 cells (CaCo2_CNR1KD). Both non-transfected CaCo2 cells and cells transfected with shRNA cassette with non-effective (scrambled) sequence (CaCo2-Scrambled) were treated as the negative controls for the CNR1KD cells. Overall, two different clones of CaCo2_CNR1KD with shRNA cassette ID TI363209 were tested in the assay. Data represents percentage of [³⁵S]GTPγS binding activity ± S.E.M (n=5).

**C1 corresponded to sample in Figure 4.4/A/Lane3; C2 corresponded to sample in Figure 4.4/A/Lane4.0*

Arachidonyl-2-chloroethylamide (ACEA), a cannabinoid agonist for CNR1, was applied as a binding ligand for the [^{35}S]GTP γ S binding assay in both wild type and CNR1KD CaCo2 cells (Hillard et al., 1999). CNR1 is classified under G-coupled protein receptor (GPCR) superfamily, where CNR1 couples and activates the G_i/G_o subunits in G-proteins (Glass and Northup, 1999). Application of ACEA as the binding ligand in the [^{35}S]GTP γ S binding assay will provide an indication towards the level of activated CNR1 present in the cell system.

Result showed that both non-transfected and “scrambled” CaCo2 cells induced an approximate 25% increase in [^{35}S]GTP γ S binding activity in response to 10^{-5}M of ACEA treatment (Figure 4.7). With the use of ACEA, a high affinity CNR1 agonist, one would expect to achieve a higher percentage of ACEA-induced [^{35}S]GTP γ S binding activity in wild type CaCo2 cells. Nevertheless, here, ACEA only managed to induce an approximate 25% increase in the [^{35}S]GTP γ S binding activity. Such relatively low binding activity may relate to the basal amount of functional CNR1 present in the wild type CaCo2 cells. It is worth noting that most of the [^{35}S]GTP γ S binding assays were performed on cells which have been manipulated to stably expressed CNR1 gene (Hillard et al., 1999). Therefore, it is fairly reasonable to obtain a relatively low percentage of ACEA-induced receptor binding in the non-transfected CaCo2 cells. Thus, the result obtained from [^{35}S]GTP γ S binding assay for non-transfected CaCo2 cells is still reliable to be used as the negative control for the CaCo2_CNR1KD cells.

There were two different clones of CaCo2_CNR1KD cells being tested in the assay. The first clone of CaCo2_CNR1KD cells (CaCo2_CNR1KD_C1) showed an approximate 17% increase in [^{35}S]GTP γ S binding activity. Conversely, for the second clone of CaCo2_CNR1KD cells (CaCo2_CNR1KD_2), insignificant [^{35}S]GTP γ S binding

activity was observed in response to the ACEA treatment (Figure 4.7). By comparing to the percentage of [³⁵S]GTPγS binding activity obtained in both non-transfected and “scrambled” CaCo2 cells, CNR1 gene was successfully knocked down by approximately 70% in CaCo2-CNR1KD_C2 cells.

4.5 Discussion

As stated previously, CNR1 is reported to be associated with cannabinoid-induced beneficial effects in the gut and the role of CNR1 in cannabinoid-induced effect is suggested to be functionally dependent (Capasso et al., 2008; Izzo and Sharkey, 2010; Vaccani et al., 2005; Wright et al., 2005). Taken that, it is interesting to generate CNR1-knockdown CaCo2 cells to further explore the functional consequence of CNR1 in cannabinoids-induced effect during autophagy process.

In this project, shRNA system was selected to generate the CNR1-knockdown CaCo2 cells in this project. Such system was chosen against the conventional siRNA system. The advantage of selecting shRNA over siRNA is that shRNA can induce a stable integration of CNR1-shRNA sequence into the cell genome, which allows the long term knockdown of CNR1 gene. siRNA, on the other hand, is introduced into the cytoplasm of the host cells, therefore will only be able to induce a transient CNR1 knockdown in CaCo2 cells (Moore et al., 2010; Sandy et al., 2005). As the knockdown of a gene can effectively change the fundamental DNA in the cells, it is useful to generate a stable cell line to study the corresponded consequences from the knockdown of CNR1 gene in the host cell.

Regarding the culture characteristics of the CNR1 knockdown CaCo2 cells, it was noticed that adherence of CaCo2 cells was affected by the knockdown of CNR1 gene in the cell system. In normal non-transfected wild type CaCo2 cells, cells can be grown and maintained in the culture medium up to 21 days. However, for the CNR1KD cells, it was surprisingly difficult to maintain the culture up to 21 days as the cell monolayer would lift from the surface around day 16. This response may be a consequence of CNR1 loss in cell system. *In vivo* studies have reported that mice lacking in CNR1 exhibited an enhanced colitis compared to their wild-type

control and such effect may be associated with the increased permeability in response to the loss of CNR1 gene (Massa et al., 2004). Therefore, it could be speculated that knockdown of the CNR1 gene disrupted the cell adhesion such that changes in permeability in the CaCo2 cells.

In addition, the seeding cell density also greatly affected the growth of CNR1-knockdown CaCo2 cells. In a 12 well plate, these cells have been optimized to be seeded at approximate 4×10^4 cells per well. Seeding the knockdown cells above or below the optimized cell density will lead to a poor outcome in cell adherence. The importance in seeding the wild type CaCo2 cells at the right cell density has been addressed previously as the differentiation of CaCo2 cells only started once the cells were grown to confluence (Sambuy et al., 2005). It has been reported that the seeding density of CaCo2 cells greatly affects the monolayer structure and the associated carrier-mediated transport (Behrens and Kissel, 2003). Lower cell density may impact on the cell permeability as the cells may have encountered irregular growth along with a reduction in the intercellular contacts (Sambuy et al., 2005). Therefore, as well as the receptor loss, the transfection process may have slightly affected the growth characteristics of the CaCo2 cells, resulting in increased difficulty in reaching full maturity.

As for the process in verifying the transfection efficiency in the CNR1-knockdown CaCo2 cells, the lack of specificity in CNR1 antibody led to the difficulty in obtaining an absolute level of CNR1 protein expression in the CNR1-knockdown cells via western blotting. The problem encountered was in agreement with previous finding as the study addressed the unreliability of data obtained from CNR1 western blotting due to the lack of good commercially available CNR1 antibody in the current market (Grimsey et al., 2008). Apart from that, quantitative RT-PCR (qRT-PCR) was also performed by using the extracted RNA samples from the CNR1

knockdown cells. However, the CNR1-knockdown cells have significant low copies of CNR1 gene in the cells and this resulted in no single peak for the DNA melt curve in qRT-PCR (see appendix). As it is well-known that DNA melting curve represents the total number of product generated from the amplification of the gene of interest and based on the golden rules for qRT-PCR, it is essential to ensure that analysis was performed based on the amplification of a single product (Pfaffl, 2001). As a result, no data was obtained via qRT-PCR but the failure in obtaining a single peak in the DNA melt curve indicated a possible knockdown of CNR1 gene in the CaCo2 cells since both wild type CaCo2 cells and the CaCo2_Scrambled cells did produce a single peak in their DNA melt curve (see appendix).

To resolve the problems encountered via qRT-PCR and western blotting, another method was applied to verify the transfection efficiency in CNR1 knockdown CaCo2 cells. Considering CNR1 is classified under G-coupled protein receptor (GPCR) superfamily, [³⁵S]GTPγS binding assay was selected to verify the level of functional CNR1 in the CNR1 knockdown cells (Glass and Northup, 1999). The formal principle for this [³⁵S]GTPγS binding assay is to measure the level of G-protein activation following agonist occupation of the GPCR (Harrison and Traynor, 2003). Based on that, ACEA, an CNR1 agonist, was applied as the binding ligand for GPCR and results showed that second clone of the CaCo2-CNR1KD cells have insignificant [³⁵S]GTPγS binding activity as compared to the non-transfected CaCo2 cells and the CaCo2_Scrambled cells. Overall, result showed that a high concentration of ACEA was required to induce the ligand binding (ie. ACEA at 1 and 10 μM induced the binding activity but ACEA at 100 nM induced a low, negligible binding activity), indicating only a low level of CNR1 receptor present in the wild type CaCo2 (Figure 4.7). Therefore, this explained the [³⁵S]GTPγS binding activity of ACEA in wild type CaCo2 cells where this synthetic cannabinoid compound only managed to induce an approximate 25% increase in the binding

activity. As for the knockdown cells, the low binding activity in the CaCo2-CNR1KD cells is possible as the CNR1 gene is not being completely knocked out from the cell system; therefore it is likely to still have a relatively low copy of CNR1 gene in CaCo2-CNR1KD in the system.

Overall based on the [³⁵S]GTPγS binding assay, the CNR1 gene has been successfully knocked down by ~70%, hence indicated a CaCo2-CNR1KD cell line was successfully generated.



Chapter 5

Cannabinoid action on Autophagosome formation

Table of Contents

5.1 **Introduction..... 119**

5.2 **Aims 121**

5.3 **Cannabinoid action on autophagy induction in intestinal epithelial cells 122**

5.4 **Mechanism of Action for cannabinoid-induced LC3-II formation 127**

 5.4.1 Canonical autophagy vs Non-canonical autophagy 128

 i. Dose and time course response for 3MA 129

 ii. Cannabinoid differentially impact on canonical pathway 131

 iii. Assess cannabinoid-induced effect via confocal imaging 132

 5.4.2 Autophagosome formation vs Autophagosome degradation 134

 i. Time course for Bafilomycin-A1 135

 ii. Cannabinoids inhibit autophagosome degradation 137

 5.4.3 Association of Cannabinoid receptor (CNR)-1 138

 i. Assess CNR1 via pharmacologically-induced CNR1 inhibition 139

 ii. Assess CNR1 via CaCo2_CNR1KD cell model 140

5.5 **Discussion 141**

5.6 **Comments on methodologies used 145**

5.7 **Limitation of the *in vitro* system 149**

5.1 Introduction

Autophagy exhibits multifunctional physiological roles in the cellular process. Regulation and induction of autophagy will correspond to the outcome of the cell: survival or death. In normal colonic cells, autophagy process is required for the renewal of colonic epithelium. This is demonstrated in the lower part of the crypt in the colonic gland where autophagy occurs at high frequency to sustain proliferation of the colonic stem cell populations (Groulx et al., 2012). Induction of such cellular mechanism may also act as a key regulator of cellular fate. During nutrient or growth factor deprivation, stress-induced autophagy may initiate a catabolic process to maintain cellular homeostasis through the recycling of non-essential cellular compartments (Chang et al., 2009; Lum et al., 2005; Sakiyama et al., 2009). Additionally, autophagy has been reported to be involved in immunity and cellular defence mechanism. Such mechanism protects cytosol from microbial invasion by targeting the invading microbes to the degradation pathway (Kirkegaard et al., 2004; Levine et al., 2011; Mihalache and Simon, 2012).

Importance of autophagy regulation has been demonstrated in various pathologies, for instance, Crohn's Disease (CD) (Levine and Kroemer, 2008; Massey and Parkes, 2007). An increase in susceptibility in Crohn's Disease (CD) has been reported with polymorphism of autophagy-associated genes such as ATG16L1 and IRGM (Massey and Parkes, 2007; Parkes et al., 2007). Variation (T300A) of ATG16L1 gene in CD delivered an autophagy-associated defect to Paneth cells, which reside in the crypt of Lieberkühn within the small intestinal epithelium (Cadwell et al., 2008; Klionsky, 2009).

During intestinal inflammation, up-regulation of endocannabinoid levels and the increased expression of cannabinoid receptor will enhance the action of endocannabinoid system (Di Marzo and Izzo, 2006). This is shown by increased cannabinoid receptor (CB1)-1 expression in

the colon of the intrarectal dinitrobenzene sulphonic acid (DNBS) treated mice (Massa et al., 2004). Interestingly, cannabinoids such as Δ^9 -tetrahydrocannabinol (THC) and Cannabidiol (CBD) have been previously shown to induce autophagy in cancer cell lines (Salazar et al., 2009; Shrivastava et al., 2011). However, to date, no studies have been performed to explore the cannabinoid action in the non-cancer cell model system. Therefore, in this chapter, the roles of phyto-, synthetic-, and endo-cannabinoid in autophagy induction were investigated in human intestinal epithelial cell model.

5.2 Aims



Investigate the action of phyto-, synthetic, and endo-cannabinoids in autophagy process and possible mechanisms involved by using mature human intestinal cells, CaCo2 cell line.



Investigate the possibility that cannabinoid receptor (CN R)-1 contributes towards the cannabinoid-induced effects in autophagy process through the use of synthetic CNR1 antagonist, as well as the generated CaCo2-CNR1KD cell model.

5.3 Cannabinoid action on autophagy induction in intestinal epithelium cells

A recent study revealed that CBD exerted a cytotoxic effect on tumor cells, resulting in autophagy induction in breast cancer cells (Shrivastava et al., 2011). Interestingly, thus far, no studies have explored the association of cannabinoids in autophagy induction in the gut epithelium, considering that it has been previously reported that polymorphism of autophagy genes did contribute to an increase of susceptibility to CD and endocannabinoid levels were up-regulated during intestinal inflammation (Di Marzo and Izzo, 2006; Massey and Parkes, 2007). Hence, to study the effect of cannabinoids (ACEA, AEA, CBD) in the context of autophagy on fully differentiated CaCo2 cells, I examined autophagosome formation by monitoring the conversion of microtubule-associated protein light chain 3 (LC3) from LC3-I to LC3-II through immunoblot analysis (Kabeya et al., 2000). Modification of LC3 is the hallmark for autophagy (Cherra et al., 2010). LC3 protein was first discovered as the mammalian autophagosomal homologue of Apg8p protein in yeast. During autophagosome formation, LC3 is cleaved into LC3-I, followed by lipidation to form LC3-II. LC3-I is a cytosolic protein whereas LC3-II is a membrane bound protein (Kabeya et al., 2000; Tanida et al., 2005). LC3-II protein is localized on autophagosome, therefore accumulation of LC3-II provides an indication towards the level of autophagosome formed in the cells (Tanida et al., 2005). LC3 has three isoforms in mammalian cells, named LC3A, LC3B and LC3C. However, only LC3B correlates to the formation of autophagic vesicles, hence only antibody targeted towards LC3B isoform is used for the analysis (Barth et al., 2010). LC3-I consists of the molecular weight of approximately 16KDa and LC3-II at approximately 14KDa. Interestingly, during SDS-PAGE, despite the molecular weight of LC3-II is shown to be higher than LC3-I, LC3-II migrates faster than LC3-I and this is due to the hydrophobicity of LC3-II (Mizushima and Yoshimori, 2007; Mizushima et al., 2010).

Dose and time course responses revealed that CBD at 10 μ M induced LC3-II formation within 4 to 6h (Figure 5.1) and that this effect was dose-dependent up from 0.1 μ M to 25 μ M (Figure 5.2). However, the low dose of 0.1 μ M appeared to inhibit this effect. To further evaluate the inhibition of LC3-II formation, low dose of 0.1 μ M CBD was applied under low nutrient conditions to explore whether the low dose of CBD could still reverse the stress-induction autophagy. Result showed that CBD was able to inhibit autophagosome formation but this effect was not sustained after 8h (Figure 5.3).

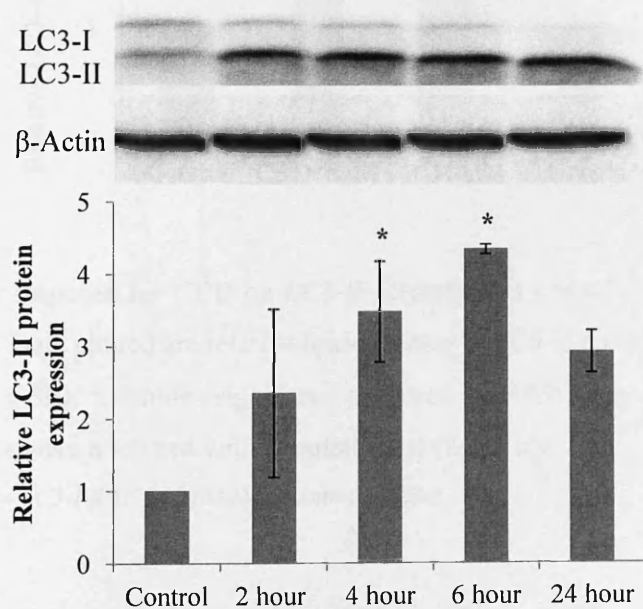


Figure 5.1. Immunoblot analysis of LC3-II in fully differentiated CaCo2 cells in response to 10 μ M cannabidiol (CBD) treatment within 24h. Data plotted are relative fold-increase in LC3-II protein expression (adjusted to β -actin, mean \pm SE). * denotes significant different (p<0.05) when compared to untreated control. (n \geq 3, data were analyzed with Dunnett t-test (2-sided)) (Molecular weight for LC3-I & II: 14&16KDa; β -Actin: 45KDa)

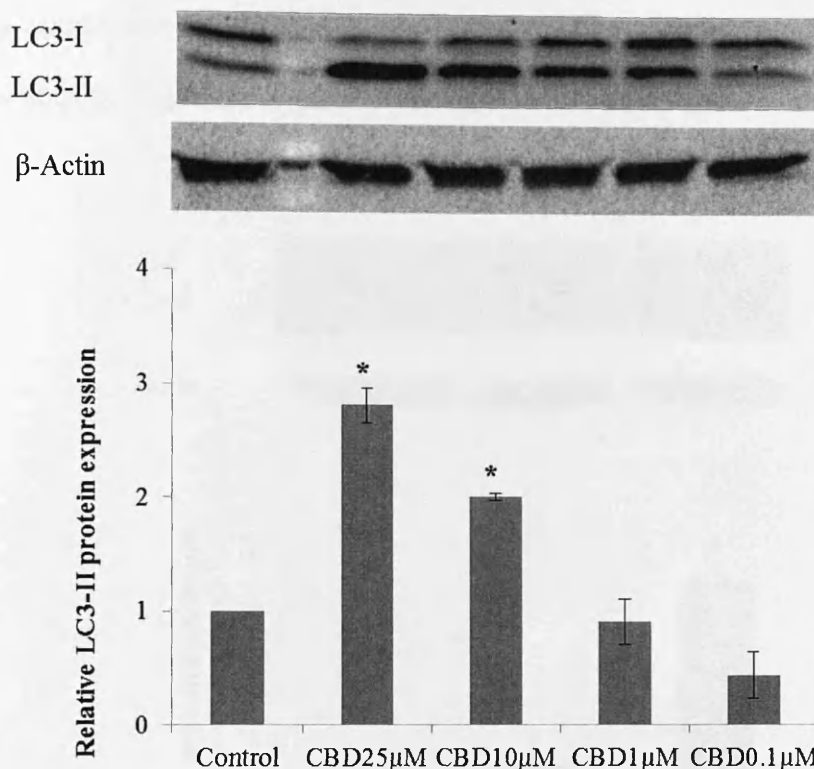


Figure 5.2. Dose response for CBD on LC3-II formation in CaCo2 cells. Cells were treated with CBD for 4h. Data plotted are relative fold-increase in LC3-II protein expression (adjusted to β -actin, mean \pm SE). * denotes significant different ($p < 0.05$) when compared to untreated control. ($n \geq 3$, data were analyzed with Dunnett t-test (2-sided)).

(Molecular weight for LC3-I & II: 14&16KDa; β -Actin: 45KDa)

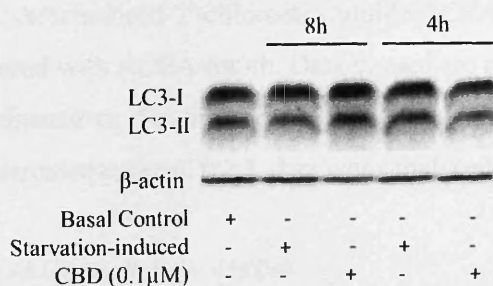


Figure 5.3. LC3-II formation for 0.1μM CBD treated starvation-induced CaCo2 cells. Cells were pre-starved with MEM supplemented with 1%(vol/vol) NEAA for 48h before adding cannabinoids for additional 4 to 8h.

(Molecular weight for LC3-I & II: 14&16KDa; β -Actin: 45KDa)

Both synthetic cannabinoid (ACEA) and endocannabinoid (AEA) significantly increased LC3-II formation within 4h time frame (Figure 5.4 and 5.5).

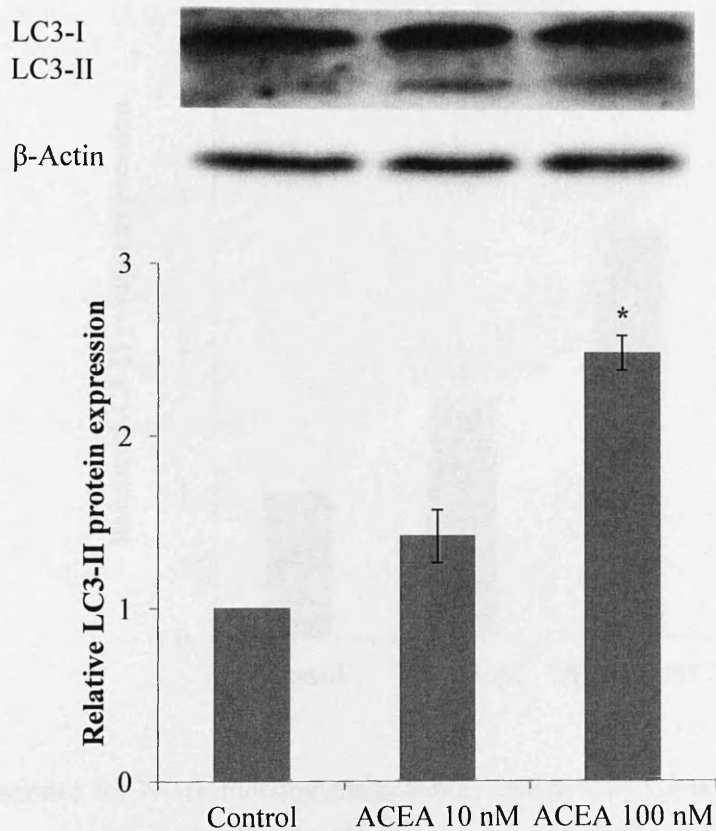


Figure 5.4. Dose response for Arachidonyl-2'-chloroethylamide(ACEA) on LC3-II formation in CaCo2 cells. Cells were treated with ACEA for 4h. Data plotted are relative fold-increase in LC3-II protein expression (adjusted to β-actin, mean ± SE). * denotes significant different ($p<0.05$) when compared to untreated control. ($n\geq 3$, data were analysed with Dunnett t-test (2-sided)).

(Molecular weight for LC3-I & II: 14&16KDa; β-Actin: 45KDa)

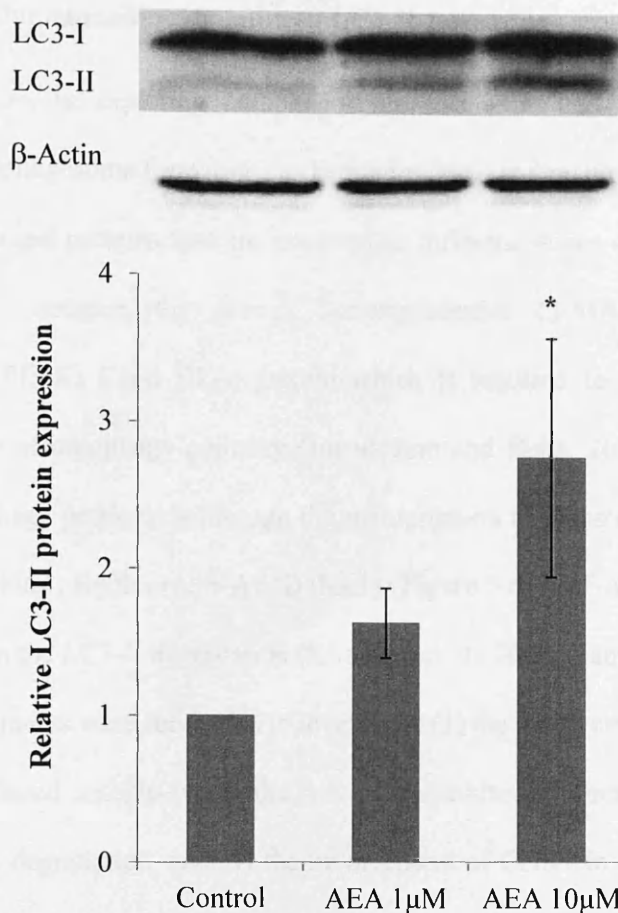


Figure 5.5. Dose response for N-arachidonylethanolamine (AEA) on LC3-II formation in CaCo2 cells. Cells were treated with AEA for 4h. Data plotted are relative fold-increase in LC3-II protein expression (adjusted to β -actin, mean \pm SE). * denotes significant different ($p < 0.05$) when compared to untreated control. ($n \geq 3$, data were analysed with Dunnett t-test (2-sided)).

(Molecular weight for LC3-I & II: 14&16KDa; β -Actin: 45KDa)

5.4 Mechanism of action for cannabinoids-induced LC3-II formation

There are various approaches in exploring autophagosome formation and the route to lysosomal degradation. Autophagosome formation can be manipulated and quantified with the use of protein inhibitor to target proteins that are involved in different stages of autophagy pathway (Figure 5.6). For instance, the use of 3-methyladenine (3-MA) to inhibit phosphoinositide 3-kinase (PI3-K) Class III, a protein which is required for phagophore formation in the early stage of autophagy pathway (Juenemann and Reits, 2012). Another frequent tool to study autophagy pathway is through the manipulation of lysosomal pH with endosomal acidification inhibitor, Bafilomycin-A1 (Baf-A1) (Figure 5.6). Baf-A1 neutralizes lysosomal pH and impacts on the LC3-II degradation (Klionsky et al., 2008; Yamamoto et al., 1998). In this section, experiments were conducted to investigate (1) the involvement of PI3K-Class III in cannabinoid-induced autophagy (2) the role of cannabinoid in autophagosome synthesis and autolysosomal degradation, and (3) the involvement of CNR1 in cannabinoid-induced autophagic process.

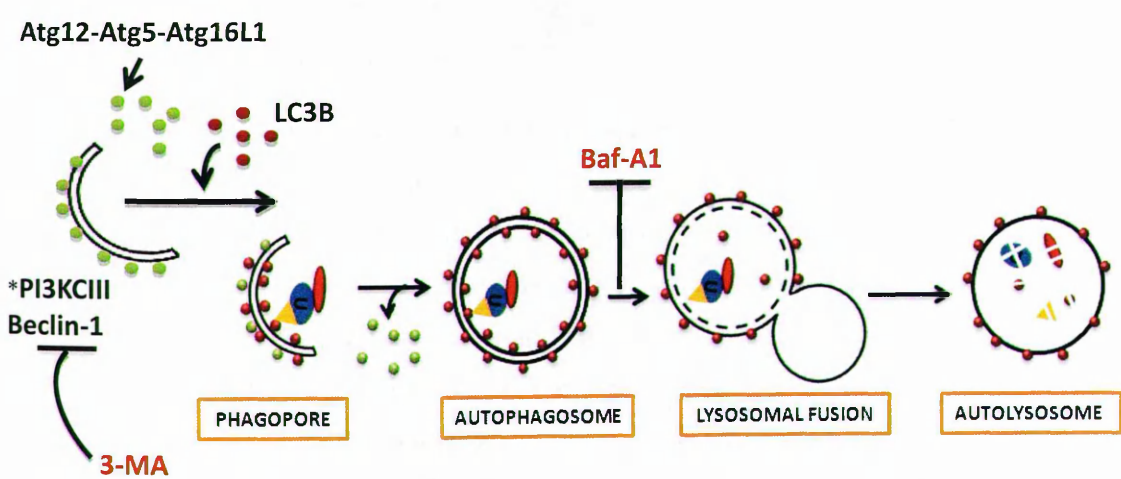


Figure 5.6. Point of inhibition for 3-methyladenine (3-MA) and bafilomycin-A1 (Baf-A1) on autophagosome formation and degradation.

5.4.1 Mechanism of Action: Canonical vs Non-canonical autophagy

PI3K-Class III has a significant role in the initiation of autophagy by recruiting autophagy-related gene (ATG) complexes to induce membrane phagophore formation (Axe et al., 2008). Involvement of PI3K-Class III in autophagy can be assessed through the use of the PI3K-Class III inhibitor, 3-methyladenine (3-MA) (Figure 5.6). Studies proposed that there are alternative routes that lead to the induction of autophagy and 3-MA can be used to determine which routes cannabinoids may engage in bringing cytoplasmic compartment towards lysosomal degradation (Figure 5.7) (Juenemann and Reits, 2012).

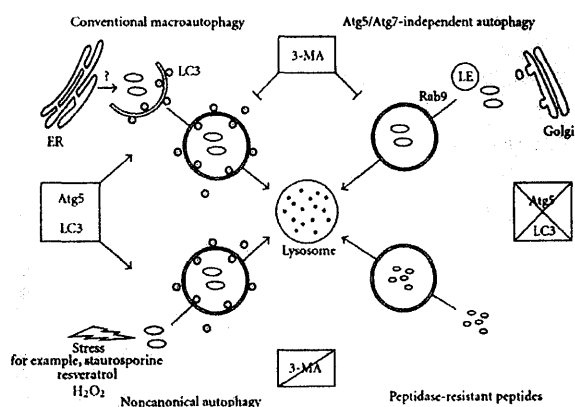


Figure 5.7. Alternative routes towards autophagy lysosomal degradation. 4 distinct autophagy pathways that lead to the formation of double membrane autophagy structures, followed by delivery of the cytoplasmic component towards lysosomal degradation. Conventional autophagy involved the recruitment of LC3 which may be origin from endoplasmic reticulum (ER) whereas Atg5/Atg7-independent autophagy pathway forms Rab9 positive double membrane autophagy structure which may be origin from Golgi and late endosome (LE). Both of these autophagy pathways are 3-MA dependent. Stress-induced non-canonical autophagy is 3-MA independent but requires Atg5 and LC3 for autophagy induction. Peptidase-resistance peptides-induced autophagy is independent to Atg5/LC3 and insensitive to 3-MA treatment.

Figure adapted from Juenemann and Reits, 2012.

i. Dose and time course response for 3-MA treatment

3-MA is an inhibitor that is widely used to inhibit autophagy as PI3K class III, the corresponded target of inhibition, is known to be required for autophagosome formation (Simonsen and Tooze, 2009). However, a recent study proposed that 3-MA established dual roles in the modulation of autophagy: inhibition or induction. 3-MA has been shown to suppress autophagy formation in nutrient-deprived condition but promote autophagy when treated in nutrient-rich condition for up to 9h. The latter effect was not the consequence effect from the inhibition of lysosomal degradation pathway but it was shown to be related to the increased autophagy flux resulted from 3-MA treatment (Wu et al., 2010). This suggested that 3-MA may act as autophagy inducer or suppressor and the response is treatment condition dependent. Therefore, to determine the exact role of 3-MA under the current experiment setting where low serum condition was applied to the treated cells, cells were treated with both high (10mM) and low (5mM) doses of 3-MA at three time frame (1h, 5h and 8h). Again, 3-MA induced effect on autophagosome formation was examined by monitoring the conversion of microtubule-associated protein light chain 3 (LC3) from LC3-I to LC3-II through immunoblot analysis (Kabeya et al., 2000).

Under the experimental setting where cells were treated with 1% serum, the low dosage (5mM) of 3-MA was insufficient to inhibit LC3-II formation. Conversely, the increased dosage of 3-MA to 10mM successfully inhibited LC3-II formation within 5h (Figure 5.8). This indicated in my experimental setting, , 3-MA at 10mM inhibited PI3K Class III, consequently led to the inhibition of autophagosome formation within 5h time frame. Therefore, 10mM of 3-MA with the total of 5h incubation period was selected to applied in the following study where experiment was conducted to explore the role of PI3K Class III in cannabinoid-induced autophagy.

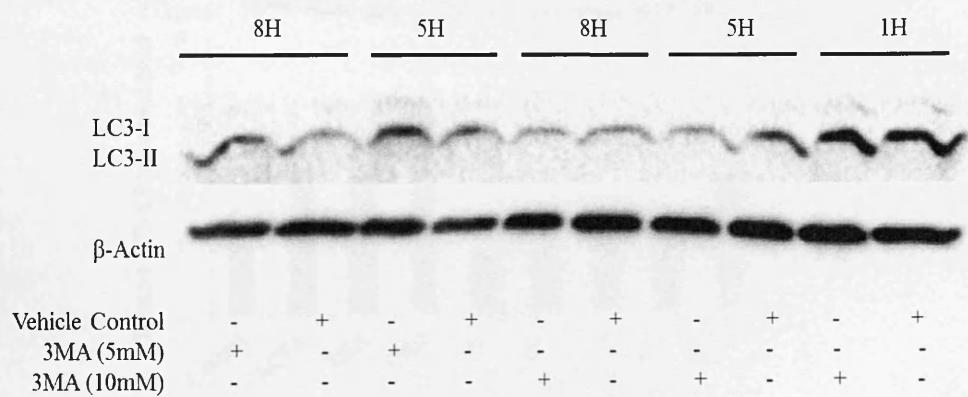


Figure 5.8. Dose response for 3-methyladenine (3-MA) on LC3-II formation in CaCo2 cells. Fully differentiated CaCo2 cells were treated with low dose (5mM) and high dose (10mM) of 3-MA treatment within 8h time frame.

(Molecular weight for LC3-I & II: 14&16KDa; β-Actin: 45KDa)

ii. Cannabinoids differentially impact on the canonical pathway

To study the involvement of PI3K-Class III in ACEA, AEA or CBD-induced LC3-II formation, cells were pre-treated with 3-MA (10mM) for 1h, followed by cannabinoid treatment for an additional 4h.

All three cannabinoids significantly reduce LC3-II formation in the presence of 3-MA (Figure 5.9).

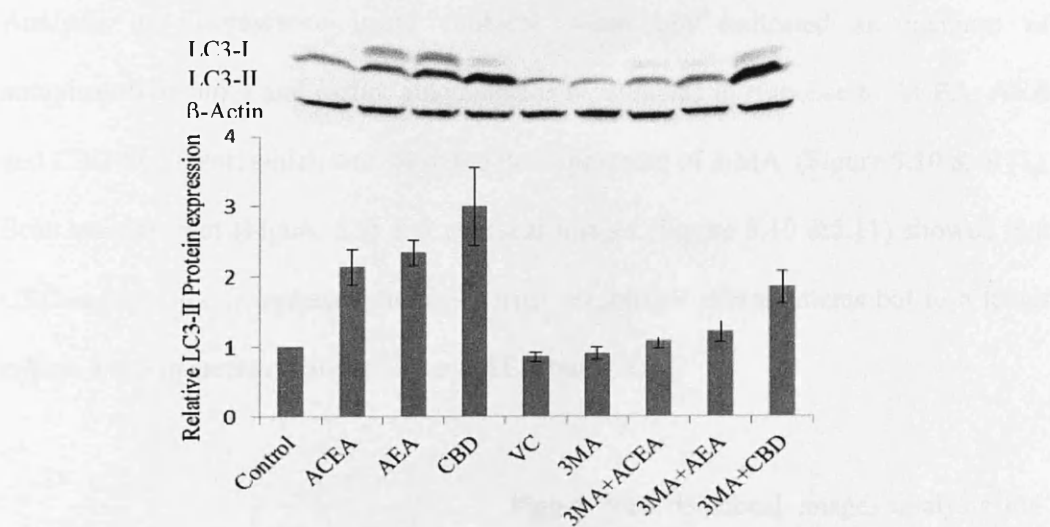


Figure 5.9. Effect of cannabinoids treatment on LC3-II formation in the presence of 3-MA. Fully differentiated CaCo2 cells were pre-treated with 3-MA (10mM) for 1h prior to addition of cannabinoids: CBD (10μM), ACEA (100nM), AEA (10μM) for additional 4h. Data plotted are relative fold-increase in LC3-II protein expression (adjusted to β-actin, mean ± SE). * denotes significant different (p<0.05) when compared to untreated control. † denotes significant different (p<0.05) when compared to paired treatment control. (n≥3, data were analysed with Tukey post hoc test).

(Molecular weight for LC3-I & II: 14&16KDa; β-Actin: 45KDa)

iii. Assess cannabinoid action via confocal imaging

Fluorescent imaging is another method to use to measure autophagy process apart from the western blotting assay, where processed LC3 can be detected. This additional method in measuring autophagy is performed to validate the findings found through LC3 western blotting. Therefore, to further verify the significance of these data, cells were stained with the Cyto-ID® green autophagy dye which served as the selective marker of autophagolysosomes and earlier autophagic compartments (Chan et al., 2012).

Analysis of fluorescence using confocal microscopy indicated an increase of autophagolysosomes and earlier autophagic compartments in response to ACEA, AEA and CBD treatment, which was inhibited in the presence of 3-MA, (Figure 5.10 & 5.11). Both western blot (Figure 5.9) and confocal images (Figure 5.10 & 5.11) showed that CBD reduced the autophagosome and earlier autophagic compartments but to a lesser extent, as compared to both ACEA and AEA treatments.

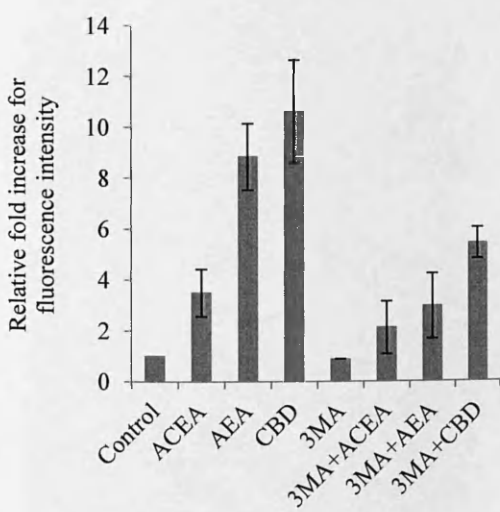


Figure 5.10. Confocal images analysis for cannabinoids and/or 3-MA treated CaCo2 cells. Bar chart showed the relative fold change of fluorescence intensity in relation to the untreated control. Data correlated to the confocal images presented in Figure 5.11. (n≥2).

(Molecular weight for LC3-I & II: 14&16KDa;
β-Actin: 45KDa)

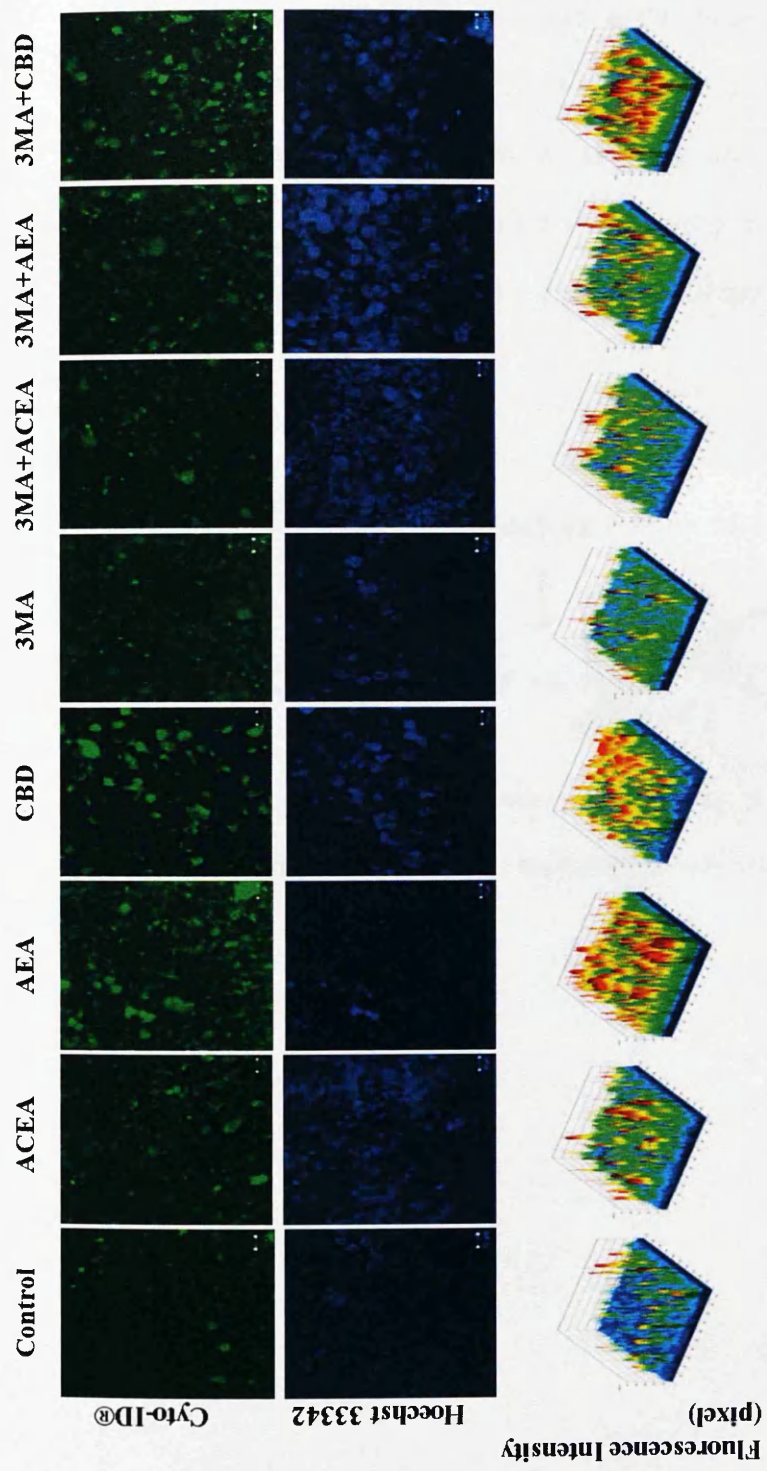


Figure 5.11. Confocal microscopy projection images of fully differentiated CaCo2 cells stained with Cyto-ID® and Hoechst 33342 dyes following cannabinoid treatments. CaCo2 cells were grown on a cover slip and cultured until they are fully differentiated before proceeding to staining procedure. Projection images obtained after combining all the Z-stack images in each treatment. Psedo3D graph is plotted with the fluorescence intensity against the amount of pixels detected from each level of intensity.

5.4.2 Autophagosome formation vs Autophagosome degradation

A snapshot of LC3-II by immunoblotting may not accurately reflect the effect the cannabinoids on autophagosome formation, as the increased LC3-II may well correlate to increased autophagic flux with a reduction in autophagosome degradation (Rubinsztein et al., 2009). Therefore, an autophagy modulator, Bafilomycin A₁ (Baf-A₁), was applied to investigate the act of cannabinoid in autophagy induction by inhibiting the formation of autolysosome, hence disrupting the lysosomal degradation pathway (Figure 5.12).

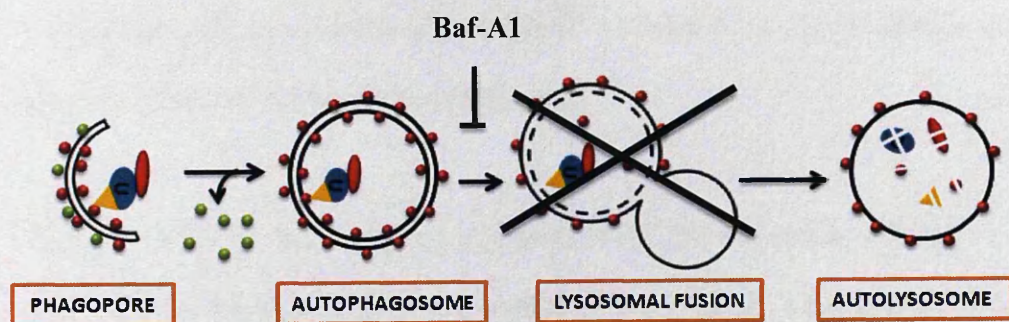


Figure 5.12. Point of inhibition for bafilomycin-A₁ (Baf-A₁) in autophagy process.

i. Time course response for Bafilomycin A1

Baf-A1 neutralizes lysosomal pH and impacts on the LC3-II degradation (Klionsky et al., 2008; Yamamoto et al., 1998). A review by Klionsky *et al.* in 2008 discussed the possible impact of Baf-A1 treatment time on LC3-II formation in treated cells as there was a controversy over the Baf-A1 data obtained from different labs (Klionsky et al., 2008). At short incubation time, Baf-A1 acts by slowing the degradation of LC3-II within the existing autophagolysosome whereas at prolonged incubation time, Baf-A1 acts by inhibiting the fusion between autophagosome and lysosome (Klionsky et al., 2008). Therefore, Baf-A1 induced effect on LC3-II formation was examined at two different time points; cells were pre-treated with Baf-A1 (100nM) for prolonged (20h) or short (1h) treatment time prior to cannabinoid treatment.

Treatment between Baf-A1 alone and Baf-A1 with CBD showed no differences at both time frames. Prolonged Baf-A1 treatment resulted in an accumulation of LC3-II formation, as compared to the shorter treatment time (Figure 5.13). However, despite the similarity in Baf-A1 induced effect at both time frames, interpretation for the outcome is different as the target of inhibition for Baf-A1 varies in according to the treatment time (as stated above). Additionally, study showed that short incubation for Baf-A1 only inhibits the lysosomal acidification but did not impact on the autophagy flux into the lysosomal compartment (Mousavi et al., 2001), suggesting that the BAF-A1-induced LC3-II increase in my treated cells may be the indirect result of the acidification defect. With that, prolonged incubation period (24h) of Baf-A1 has been selected to apply on the treated cells to investigate the corresponded effect of cannabinoid induced autophagosome in response to the blockage of lysosomal degradation pathway.

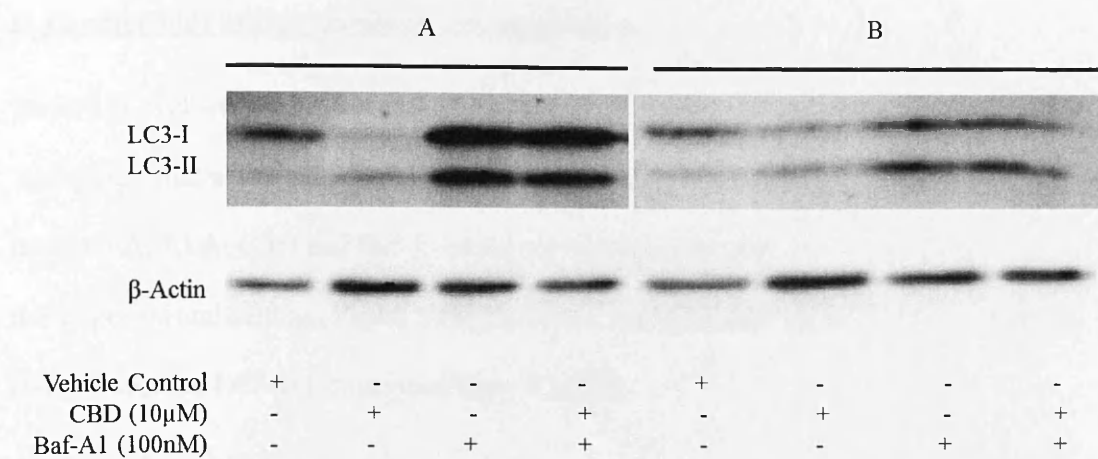


Figure 5.13. Immunoblotting showed the effect of Bafilomycin A1 (Baf-A1) on LC3-II protein expression within 24 hour time course. Fully differentiated CaCo2 cells were pre-treated with Baf-A1 (100nM) for two different time course: (A)20h (B)1h prior to CBD treatment for additional 4h.

(Molecular weight for LC3-I & II: 14&16KDa; β-Actin: 45KDa)

ii. Cannabinoids inhibit autophagosome degradation

To further evaluate the impact of ACEA, AEA and CBD on autophagosome synthesis, a ‘autophagy flux assay’ was performed by treating the cells with Baf-A1. Result showed that ACEA, AEA, CBD and Baf-A₁ alone significantly increase LC3-II formation under this experimental setting (Figure 5.14/A) but the cannabinoids did not further enhance Baf-A1-induced LC3-II formation (Figure 5.14/B).

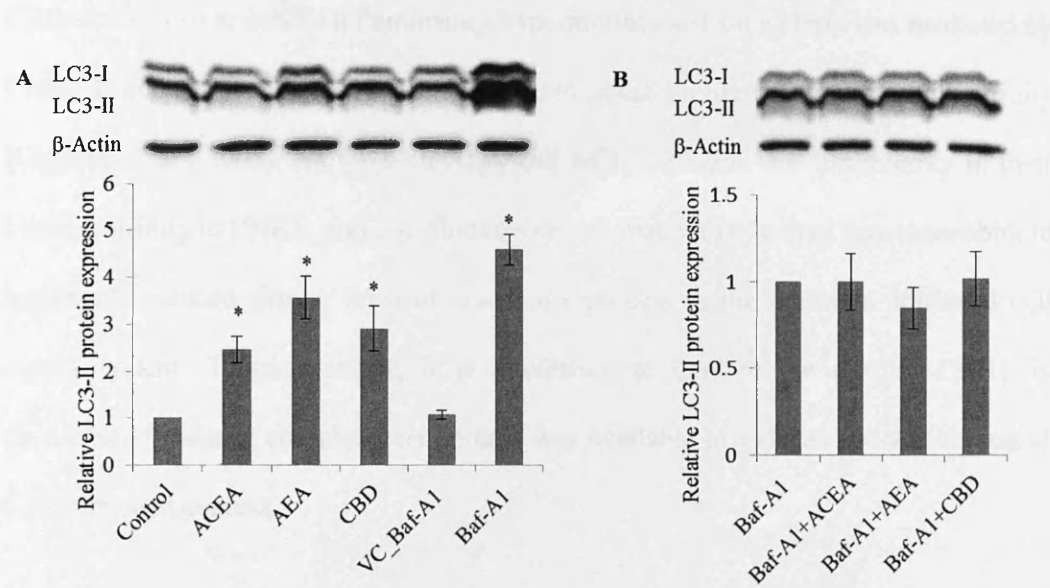


Figure 5.14. Immunoblotting showed the effect of cannabinoids treatment on LC3-II protein expression in the presence of Bafilomycin A1 (Baf-A1). Fully differentiated CaCo2 cells were pre-treated with Baf-A1 (100nM) for 20h prior to addition of cannabinoids: CBD (10μM), ACEA (100nM), AEA (10μM) for additional 4h. Due to non-linearity of enhanced chemiluminescence (ECL) with the use of Baf-A₁, Baf-A₁ data is presented in two forms: (A) overexposed and (B) normal exposure. Data plotted are relative fold-increase in LC3-II protein expression (adjusted to β-actin, mean ± SE). * denotes significant different (p<0.05) when compared to untreated control. † denotes significant different (p<0.05) when compared to paired treatment control. (n≥3, data were analysed with Tukey post hoc test).

(Molecular weight for LC3-I & II: 14&16KDa; β-Actin: 45KDa)

5.4.3 Cannabinoids differentially engage CNR1

Association of CNR1 to cannabinoid treatments have previously been reported and studies suggested that the role of CNR1 in cannabinoid-induced effect is functionally dependent. For instance, administration of CBD, a non-psychoactive phytocannabinoid, induced a concentration-dependent inhibition of the migration of glioma cells and this effect was not mediated by CNR1 (Vaccani et al., 2005). Interestingly, in other study, CBD was shown to inhibit inflammatory hypermotility and such effect was mediated by CNR1 despite the fact that CBD does not bind to cannabinoid receptors with high affinity (Capasso et al., 2008). As for both AEA and ACEA, despite the dissimilarity in their binding affinity to CNR1, previous findings demonstrated that both of these cannabinoid treatments induced similar level of autophagy process in the intestinal epithelial cell model system. Taken together, it is interesting to explore the role of CNR1 in cannabinoid-induced autophagy as no data was available to indicate the association of CNR1 in such context.

i. Assess CNR1 via pharmacologically-induced CNR1 inhibition

To determine whether ACEA, AEA and CBD-induced LC3-II formation was CNR1 mediated, CaCo2 cells were pre-treated with CNR1 antagonist, **AM251**.

Despite AM251-induced blockage of CNR1 in CaCo2 cells, CBD at 10µM was able to increase LC3-II conversion. In contrast, both ACEA and AEA required the CNR1 activation (Figure 5.15).

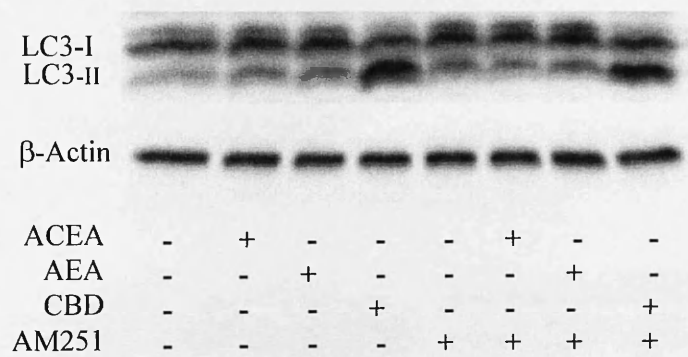


Figure 5.15. Immunoblotting showed the effect of cannabinoids treatment on LC3-II protein expression in the presence of AM251. Fully differentiated CaCo2 cells were pre-treated with AM251 (100nM) for 10min prior to cannabinoid treatments: CBD(10µM), ACEA(100nM), AEA (10µM) for additional 4h.

(Molecular weight for LC3-I & II: 14&16KDa; β-Actin: 45KDa)

ii. Assess CNR1 via CaCo2-CNR1KD cell model

As previously mentioned in chapter 4, even though the use of antagonists to the CNR1 receptor has been an important tool in the dissection of receptor-mediated signalling and function, but a novel way to study the functional consequence of CNR1 loss is by the use of CNR1 knockdown cell model system. Therefore, to further verify the role of CNR1 in cannabinoid-induced autophagy, ACEA, AEA and CBD were treated on both CaCo2-CNR1KD and CaCo2-Scrambled cells.

CBD increased LC3-II formation in both CaCo2-CNR1KD and CaCo2-Scrambled cell lines, whereas both ACEA and AEA show an increased LC3-II formation in CaCo2-Scrambled cells but not in CaCo2-CNR1KD cells (Figure 5.16)

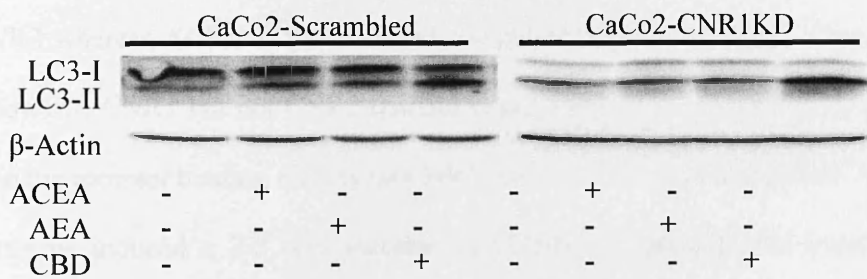


Figure 5.16. Effect of cannabinoid treatments on LC3-II protein expression in both CaCo2-Scrambled and CaCo2-CNR1KD cell lines. Cells were treated with cannabinoids: CBD(10μM), ACEA(100nM), AEA (10μM) for 4h prior to lysing.

(Molecular weight for LC3-I & II: 14&16KDa; β-Actin: 45KDa)

5.5 Discussion

The endocannabinoid, *N*-arachidonoyl-ethanolamine (Anandamide, AEA), is synthesized through the endocannabinoid system (ECS). Elevated level of AEA has been reported in the 2,4,6-trinitrobenzene sulfonic acid (TNBS)-induced inflamed mice colon samples, as well as the biopsies samples from ulcerative colitis (UC) patient (Argenio et al., 2006). Such findings suggested the role of AEA as an anti-inflammatory agent during inflammation. Here, result showed that AEA has significantly enhanced LC3-II formation in a dose-dependent manner and this may indicate that autophagy induction could be a possible mechanism mediated by AEA to limit inflammatory responses. Similarly, application of arachidonyl-2'-chloroethylamide (ACEA), the synthetic cannabinoid, also enhanced the LC3-II formation. ACEA is a synthesized analog of AEA. AEA binds and activates both cannabinoid receptor (CNR)-1 and CNR2 whereas ACEA is the modified compound of AEA to induce a greater binding affinity towards CNR1 but not CNR2 (Hillard et al., 1999). Taken together, despite the dissimilarity in the receptor binding affinity on CNR1, results demonstrated that both AEA and ACEA treatments induced a 2-3 fold increase in LC3-II formation in the intestinal epithelial cell model system, hence, suggesting the involvement of CNR1 in this context.

Apart from the endo- and synthesis cannabinoids, the phytocannabinoid, cannabidiol (CBD), also enhanced LC3-II formation and such effect was sustained up to 24 hours. CBD has been shown to be cytotoxic in a number of cell lines, in particular breast cancer cells (Shrivastava et al., 2011). CBD was shown to decrease viability of breast cancer cell line in dose dependent manner but maintained higher survival rate with normal cells (Shrivastava et al., 2011). It is important to note that fully differentiated CaCo2 cells are thought to be more like normal enterocytes and application of CBD treatment did not affect viability of fully differentiated CaCo2 cells (Macpherson, et al., 2014). Study showed induced autophagy-mediated-cell death

in breast cancer cell line whereas here, result shows that CBD induces autophagy but this does not lead to cell death. This suggests a cell type dependent effect, in which CBD has differential impact on both cancer and “normal” cells. Administration of low concentration of CBD (0.1 μ M) lead to an inhibition of LC3-II formation but this effect was transient. To date, there is no data showing the exact dose of cannabinoid delivered to the GI tract and absorbed by the gastrointestinal cells after CBD administration. Consequently, the finding of CBD induced-autophagy to be dose dependent could be an important finding for the therapeutic use in disease with disordered autophagy, for instance, CD.

Activation of PI3K Class III is required for the recruitment of ATG protein complex, leading to the induction and expanding of phagophore membrane (Lindmo and Stenmark, 2006). PI3K Class III activation is obligatory for the occurrence of the canonical formation of autophagosomes (Juenemann and Reits, 2012). Here, results showed that by blocking PI3KCIII activation, ACEA and AEA-induced effects were inhibited but not the CBD-induced autophagy effect, which was only partially inhibited. This suggests that CBD may, in part, induce the non-canonical autophagy pathway as opposed to ACEA and AEA. Genome-wide association studies (GWAS) revealed single nucleotide polymorphisms (SNPs) in ATG16L1 gene in CD patients (Prescott et al., 2007). ATG16L1 localized ATG5/12/16L1 protein complex to the isolation membrane, followed by the formation of autophagosome double membrane vesicle (Fujita et al., 2008; Henderson and Stevens, 2012). PI3KCIII activity is required for the recruitment of ATG16L1 protein complex (Nishimura et al., 2013), suggesting that CBD may still be able to induce autophagy process when ATG16L1 autophagy gene is impaired in the system and therefore, promoting the therapeutic potential of CBD in treating CD.

Another methodology to study the role of cannabinoids in autophagic process is through the use of the lysosomal inhibitor, Baf-A1. With prolonged Baf-A1 treatment, Baf-A1 alone induces a significant increase in the LC3-II formation, as the result from an accumulation of LC3-II, corresponding to the blocking of the autophagolysosomal degradation step. Cannabinoids do not further enhance or inhibit the Baf-A1 induced accumulation of LC3-II, which suggests that the cannabinoid effect on autophagy may be related to reduce autophagosome degradation as opposed to increased autophagosome synthesis. In fact, since cannabinoids induced 2-3 fold increases in LC3-II formation and Baf-A1 induced 4-5 fold increases, it is perhaps not surprising that no further enhancement of Baf-A1 effect is observed. The sensitivity of the method does not allow us to confirm or refute that cannabinoids induce autophagosome synthesis, but rather indicates an inhibitory role in late autophagy.

As stated previously, despite both ACEA and AEA exert different binding affinities on CNR1 receptor, both cannabinoids were able to induce LC3-II to the same extent, I am interested to explore the role of CNR1 in this context. AEA binds and activates both cannabinoid receptors CNR1 and CNR2. Additionally, AEA is also found to be a ligand for the vanilloid receptor, TRPV1 receptor as AEA shares a structural similarity with capsaicin, an exogenous TRPV1 receptor activator (Melck et al., 1999). In contrast, ACEA, the synthetic modified compound of AEA, only induces a greater binding affinity towards CNR1 (Hillard et al., 1999). Interestingly, despite both ACEA and AEA displayed different binding affinity on CNR1, these cannabinoid-induced effects were shown to be CNR1 mediated. Unlike other G-coupled protein receptor (GPCRs), CNR1 can be intracellularly activated by endogenous cannabinoids (Rozenfeld, 2011). Remarkably, study showed localization of CNR1 at lysosomal compartments (Rozenfeld and Devi, 2008). Intracellular injection of AEA activated functional CNR1 and the subsequent mobilization of intracellular calcium concentration was reduced by

the administration of Baf-A1 (Brailoiu et al., 2011). The results illustrated the involvement of CNR1 in lysosomal degradation. Taken together, data obtained supports the ACEA and AEA-induced effect on late degradation. In contrast to ACEA and AEA-induced effects, CBD-induced effect was not mediated by CNR1. Δ^9 -THC has previously been shown to induce autophagy in human astrocytoma cells and that study showed that the Δ^9 -THC-induced effect was CNR1 mediated (Salazar et al., 2009). Despite both studies being performed in different cell lines, these results suggest that Δ^9 -THC and CBD may act through distinct mechanisms during autophagy.

5.6 Comments on methodologies used

In this study, autophagosome formation was monitored by measuring the conversion of LC3 from LC3-I to LC3-II through immunoblot analysis (Kabeya et al., 2000). LC3 is the hallmark for autophagy and LC3-probed western blotting has been one of the most reliable techniques to Assess autophagy formation. As LC3-I and LC3-II are both involved in autophagy induction; it has been a controversy over the application of the most appropriate methodology to analyse the LC3 probed immunoblot: either the ratio of LC3-II /LC3-I or the ratio of LC3-II/ a house keeping gene (Mizushima and Yoshimori, 2007). The latter was applied in this study as the anti-LC3 antibody has a higher sensitivity of detection towards LC3-I, as compared to LC3-II. Therefore, it may not be appropriate to analyse the data by measuring the ratio of LC3-II/LC3-I. Also, it should be noted that endogenous LC3-II is degraded by lysosomal hydrolases after the formation of autolysosome (Tanida et al., 2005). Therefore, the relative fold change of LC3-II conversion may not represent the true level of cannabinoid induced LC3-II formation in the cell system as some of the cannabinoid induced LC3-II formation may have already been degraded during cannabinoid treatment. In order to resolve this problem, autophagy inhibitors such as 3-MA and Baf-A1 were applied to cannabinoids treated cells. These inhibitors disrupt different stages of autophagy process, thus providing a clearer picture on cannabinoid action on autophagy induction.

Despite the specificity of the use of anti-LC3 antibody, as well as the sensitivity provided via western blotting, such technique is very delicate and prone to errors, consequently leads to a false positive finding and increases the difficulty in replicating and analyzing the results obtained. The limitation of performing such technique has been clearly demonstrated through the experiment where experiments were conducted to investigate cannabinoid-induced autophagy effects in response to Baf-A1 treatment (section 3.4.2). Baf-A1 induced an

extraordinary increase in LC3-II formation in the treated cells, resulting in the difficulty to compare the LC3-II protein expression between the non-treated and Baf-A1 treated samples on the same blot with the same exposure intensity. The problem encountered was in agreement with previous finding as the study addressed the difficulty in analysing the Baf-A1 treated cells in LC3-II probed immunoblot due to the non-linearity of the enhanced chemiluminescence substrates, which have been applied during blot developing (Rubinsztein et al., 2009). Hence, in this study, cells treated with or without Baf-A1 were all loaded in a single SDS-PAGE but analysed under two different exposure intensities to ensure that the increased LC3-II expression is not resulting from the accumulation of chemiluminescence signal on the sample (Figure 5.14).

Apart from western blotting, fluorescent imaging has also been performed to measure cannabinoid induced autophagy process. Confocal microscopy was used to image fully differentiated CaCo2 cells which have been stained with Cyto-ID® Green autophagy dye. The use of confocal microscopy provided the opportunity to detect cannabinoid-induced effect on the treated cell from three dimensional visualization imaging. There are four autophagy associated dyes available in the market: the monodansylcadaverine dye (MDC), the Acridine Orange dye, the LysoTracker® Red dye from Life Technologies and finally, the Cyto-ID® Green autophagy dye from Enzo Life Science. MDC fluorescent dye was first selected as the lysomotrophic dye to be tested in this study (see appendix). MDC was applied to label the autophagic vacuoles in cannabinoid treated cells (Biederbick et al., 1995). However, the use of MDC generated a high background signal with weak fluorescent signal, resulting in the need to increase the laser power during imaging, which consequently damaged the treated cells. Therefore, it was decided that the MDC may not be an appropriate autophagy dye to be used in this study. Next to MDC dye, Cyto-ID® Green autophagy dye was selected as the fluorescent

maker to label autolysosomes and earlier autophagic compartments in cannabinoids-treated cells (Manual, 2011). The difference between Cyto-ID® Green autophagy dye and the Acridine Orange dye, as well as the LysoTracker® Red dye is the former weakly stains lysosomes whereas the latter primarily detect only lysosome (Manual, 2011). With that, Cyto-ID® Green autophagy dye was selected to apply on the treated cells as the detection of lysosome does not necessary correlated to the occurrence of autophagic process. Also, it is informative to detect the earlier autophagic compartments, as well as the autolysosome in the treated cells as autophagy is a sequential process and by staining both of these compartments will provided a clear picture of the total cannabinoid induced autophagic activity in the cells.

As previously stated, differentiated CaCo2 cells were stained with Cyto-ID® Green autophagy dye for confocal imaging. It is noteworthy that CaCo2 cells which were used for imaging have not been cultured up to 17 days, the length of cell growth which has been applied to all previous experiments. It is noted that cells cultured to 17 days were no longer formed a single monolayer of cell, in fact, cells have grown to overlap the first monolayer of cells, resulting in the difficulty to focus on the cells during confocal imaging. Therefore, by compromising to such issue, the length of cell growth for the treated cells has been reduced to 10 days. Previous study showed that the CaCo2 cells reached a growth plateau after day 10. The extended culture days up to day 17 would form a regular tight junction network but an irregular and fairly complete tight junction network has already been developed at day 2 (Rothen-Rutishauser et al., 2000). Hence, even by reducing the culture period for the treated cells in order to compromise the issue encountered during confocal imaging, the results generated from confocal imaging are reliable for further analysis.

Additionally, despite that the developed cell model system is more physiologically relevant to the gut epithelium; the use of non-synchronized treated cells did increase the difficulty in replicating the experiments. As previously stated in chapter 3, the rational for not synchronizing the cell cycles back to G₀ position was thought that such act would interfere with the physiological setting of the GI tract as not all the epithelial cells in GI tract were in the G₀ position. Despite that it was time consuming to generate statistical significance data for the experiments, all the findings generated from the experimental setting were definitely more physiological relevant and this increases the possibility for the findings to be translated into clinical development.

5.7 Limitations of the *in vitro* system

As previously stated, CaCo2 cells are currently the best characterised gut epithelial monolayer system available for *in vitro* study, as they exhibit display similar characteristics to enterocytes residing in human small intestinal epithelium (Bailey et al., 1996). In this study, CaCo2 cells were grown and cultured on a flat culture dish for 17 days prior to treatments. The 2-dimensional (2D) CaCo2 culture model approach was employed in this study because I wanted to explore the molecular basis for proposed beneficial cannabinoids effects on the autophagy process, and a 2D culture model was sufficient to provide reliable data. Such 2D culture models have been commonly used in studies to explore cellular homeostasis in the intestinal epithelium (Wang et al., 2000; Ruemmele et al., 2003; Lenaerts et al., 2005) and they are known to be more cost efficient, as compared to the filtered-grown CaCo2 cells on a trans-well insert (3D CaCo2 culture model). However, there are limitations with the use of such a 2D culture model, and this needs to be implicated in the data interpretation. The 2D culture model may lack physiological relevance as it fails to capture the 3D microenvironment present on the intestinal villi, which may affect the correlation between drug-induced effects *in vitro* and *in vivo*. Furthermore, a recent study showed that CaCo2 cells, which are grown on the 3D scaffolds, display a variation in their cell differentiation where cells are more polarized and columnar at the top and less differentiated near the villous base (Yu et al., 2012), suggesting different culture approaches may result in cell phenotype variation. As I have previously demonstrated in *Chapter 3* that there was a variation in the cells' response towards exogenous stimulations in different growth stages (proliferating, confluent, and differentiated) in my 2D CaCo2 cell model, this finding suggests that the culture approach may affect the cell response towards cannabinoid treatments, which subsequently impacts on the cannabinoids-induced-effects on the autophagic process.

Aside from the use of the 2D CaCo2 culture model, the culturing condition may also affect the significant findings in this study. In this project, cells were cultured under atmospheric conditions (oxygen range ~21%), because, not only does this method provide an easy access to the cultured cells, which greatly benefits the cell maintenance process, but it also eliminates further complications involved during data interpretation. However, this range of oxygen level (~21%) is known to be physiologically irrelevant as compared to the hypoxia condition found in human colon. A recent study showed that CaCo2 cells which are cultured in a hypoxia condition (5%) are more sensitive towards cannabinoid treatment and that there is an increase in oxygen reactive species (ROS) in intact mitochondria in cannabinoid-treated cells (Macpherson et al., 2014). ROS are small, high reactive molecules which are known to serve as signalling molecules in a variety of cellular processes, including growth, differentiation, as well as autophagy (Scherz-Shouval and Elazar, 2007; 2011; Sumandea and Steinberg, 2011). Accumulation of ROS, which results from induced cellular oxidative stress, leads to the onset of the autophagic process (Scherz-Shouval and Elazar, 2007), suggesting a possible impact of ROS on the cannabinoid-induced autophagy process if the experiments are performed under hypoxia conditions. Despite this, my findings are important preliminary data, which can be used to study the cannabinoid-induced autophagy effect under hypoxia conditions and the possible role of ROS in this context.

Chapter 6

Autophagy mediates cannabinoid induced SOCS3 reduction

Table of Contents

6.1 Introduction.....153

6.2 Aims154

6.3 Cannabinoid action on SOCS3 expression in intestinal epithelial cells155

6.4 Mechanism of action for cannabinoid-induced SOCS3 reduction160

6.4.1 Involvement of JAK-STAT3 signaling pathway in SOCS3 reduction162

6.4.1 i. Cannabinoid-induced p-STAT3 (Ser727) protein expression163

6.4.1 ii. Cannabinoid-induced p-STAT3 (Ser727) protein expression in autophagy inhibitor treated cells165

6.4.2 Involvement of ubiquitin-proteasome proteolytic pathway in SOCS3 protein reduction167

6.4.3 Involvement of autophagy process in SOCS3 protein reduction170

6.5 Possible correlation of CNR1 receptor in cannabinoid-induced SOCS3 reduction173

6.6 Discussion175

Abstract

Introduction

Aims

Materials and Methods

Results

Discussion

Conclusion

References

Appendix

Index

6.1 Introduction

SOCS3 acts as an inducible negative feedback regulator in cytokine-induced signaling (Dalpke et al., 2008). Binding of cytokines triggers the activation of JAK kinases. This leads to the phosphorylation of tyrosine residue on JAK kinases and recruitment of STAT3 via the phosphotyrosine-binding SH2 domain. Activated STAT3 will form STAT3 dimers with other phosphorylated STAT3 residue and translocated into cell nucleus. Subsequently, accumulation of activated STAT3 dimers will initiate the transcription of SOCS3 and other target genes (Bjorbaek et al., 1999). Activation of SOCS3 will limit transcription factor activation and its translocation in response to the stimulation from inflammatory cytokines (Rigby et al., 2007). The SOCS3 protein consists of a SH2 domain, a KIR domain and a SOCS-box located at the C-terminus of the protein (Dalpke et al., 2008). SH2 domain is responsible for the binding of phosphorylated tyrosine whilst SOCS box is mainly responsible for the recruitment of ubiquitin-transferase system, a mechanism which involves in the post translational degradation of the proteins (Yoshimura et al., 2005).

It has been reported that SOCS3 is up-regulated in both animal and human intestinal inflammation (Suzuki et al., 2001). SOCS3 (both mRNA and protein) was shown to be up-regulated in colon samples from UC and CD patients compared with healthy controls. SOCS3 also limits proliferation of epithelial cells in the damaged crypt, but contrary to in vitro investigations, up-regulation of SOCS3 in inflamed intestine, does not appear to sufficiently limit STAT3 and NF-KB inflammatory pathways (Rigby et al., 2007). Contrary to several publications showing that SOCS3 expression is silenced in many cancers (He et al., 2003; Rigby et al., 2007). Caco2 cells express high levels of SOCS3 compared with other cell lines (Rigby, personal communication). Therefore the contrasting role of SOCS3 in cancer and inflammation is highlighted in my model. Thus, I wish to explore the possible action of

cannabinoids on SOCS3 protein expression as a mediator of CBD therapeutic potential

6.2 Aims



To investigate the action of phyto-, synthetic, and endoannabinoids on SOCS3 protein expression using the CaCo2 cell line.



To determine whether the actions of CBD on SOCS3 are mediated through the cannabinoid receptor (CNR)-1.

6.3 Cannabinoid action on SOCS3 expression in intestinal epithelial cells

Cannabinoids are known to exert significant anti-inflammatory properties in various experimental models (Cluny et al., 2012; Kozela et al., 2010b; Ribeiro et al., 2012). Cannabinoids reduce lipopolysaccharide-induced STAT3 phosphorylation (Kozela et al., 2010a), but it is not clear how CBD mediates effects on this anti-inflammatory pathway. To date, there is no current study looking into the association of SOCS3 in autophagic process. Therefore, it is interesting to explore the role of SOCS3 as a novel inflammatory mediator in relation to cannabinoid-induced autophagic process in the gut epithelial cell model. My previous experiments demonstrated that 4h cannabinoid treatment appeared to be the optimal time for LC3-II formation in my model. Therefore, experiments were conducted to investigate cannabinoid-induced SOCS3 protein expression levels at the same time point. These sets of experiments provide the first insight into the impact of cannabinoids on SOCS3 protein expression in my CaCo2 cell model system.

To investigate the effects of CBD on SOCS3 protein expression in my model, a time course experiment was performed. The result showed that CBD-treatment induced the biggest reduction in SOCS3 protein expression at 4h (Figure 6.1), the same time frame that I observed the biggest induction of LC3-II. The SOCS3 protein was expressed in an oscillatory manner (i.e. not at a stable level) over a 24h period as expected (Yoshiura et al., 2007).

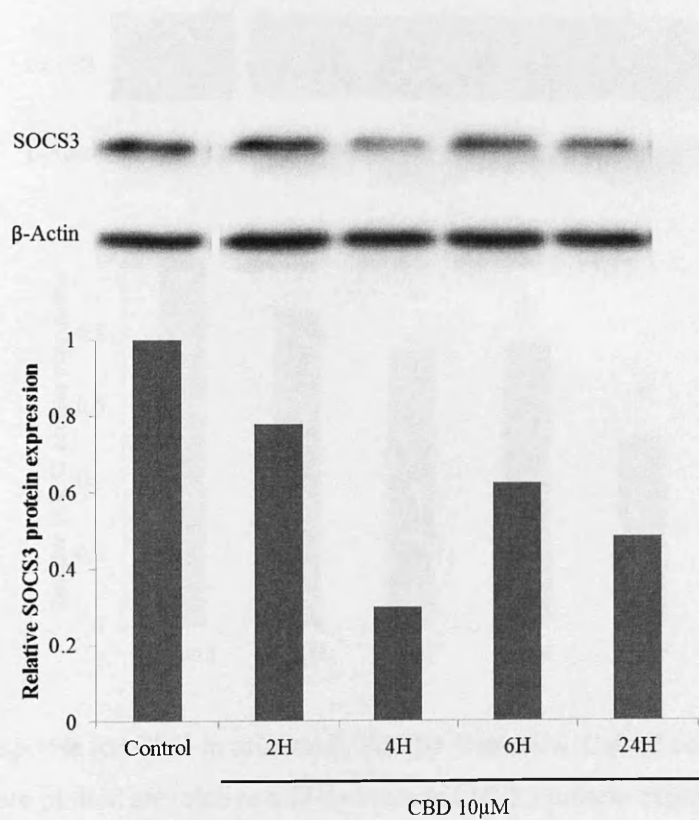


Figure 6.1. Immunoblot analysis of SOCS3 in fully differentiated CaCo2 cells in response to 10μM cannabidiol (CBD) treatment within 24h. Data plotted are relative fold-increase in SOCS3 protein expression (n=1).
(Molecular weight for SOCS3: 27KDa; β-Actin: 45KDa)

I then performed a dose-response experiment to explore whether CBD-reduced SOCS3 protein expression was dose dependant. Dose response revealed that CBD reduced SOCS3 protein expression within 4h and this effect was dose-dependent up from 1µM to the highest concentration tested (25µM) (Figure 6.2).

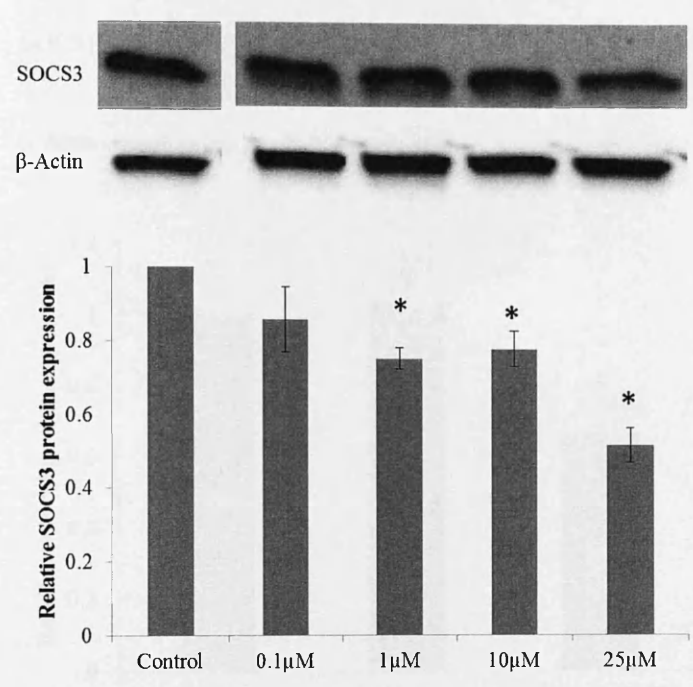


Figure 6.2. Dose response for CBD in relation to SOCS3 formation. CaCo2 cells were treated with CBD for 4h. Data plotted are relative fold-increase in SOCS3 protein expression (adjusted to β-actin, mean ± SE). * denotes significant different (p<0.05) when compared to untreated control. (n≥3, data were analyzed with Dunnett t-test (2-sided)).

(Molecular weight for SOCS3: 27KDa; β-Actin: 45KDa)

ACEA and AEA dose-response experiment was conducted to investigate the effects of these cannabinoids on SOCS3 protein expression. Result showed that both ACEA and AEA reduced SOCS3 protein expression within 4h at 100nM and 10μM, respectively (Figure 6.3 and 6.4).

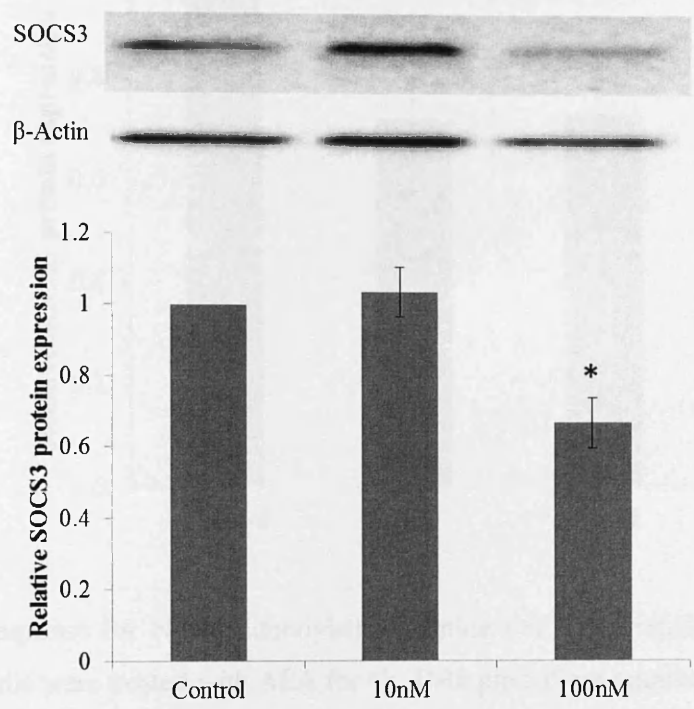


Figure 6.3. Dose response for ACEA in relation to SOCS3 formation. CaCo2 cells were treated with ACEA for 4h. Data plotted are relative fold-increase in SOCS3 protein expression (adjusted to β-actin, mean ± SE). * denotes significant different ($p<0.05$) when compared to untreated control. ($n\geq 3$, data were analyzed with Dunnett t-test (2-sided)).
(Molecular weight for SOCS3: 27KDa; β-Actin: 45KDa)

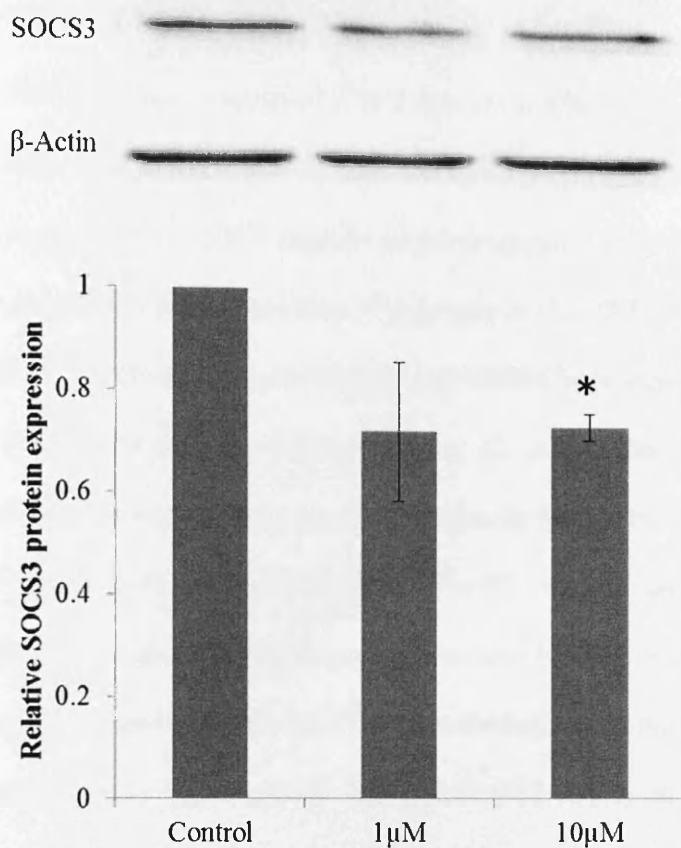


Figure 6.4. Dose response for N-arachidonylethanolamine (AEA) in relation to SOCS3 formation. CaCo2 cells were treated with AEA for 4h. Data plotted are relative fold-increase in SOCS3 protein expression (adjusted to β -actin, mean \pm SE). * denotes significant different ($p < 0.05$) when compared to untreated control. ($n \geq 3$, data were analysed with Dunnett t-test (2-sided)).

(Molecular weight for SOCS3: 27KDa; β -Actin: 45KDa)

6.4 Mechanism of action for cannabinoid-induced SOCS3 reduction

As previously stated, SOCS3 protein consists of a SH2 domain, a KIR domain and a SOCS-box (Dalpke et al., 2008). Each domain of SOCS protein mediates different interaction and functions. One of the ways in which SOCS regulate protein expression is through the SOCS box, a conserved domain located at the C-terminal (Piessevaux et al., 2008). This region was shown to interact with the E3 ubiquitin ligase complex and studies have suggested that such interaction provides SOCS with protein stability (Haan et al., 2003; Zhang et al., 1999). Additionally, SOCS box is also involved in protein degradation by linking the targeted protein towards proteasomal machinery (Piessevaux et al., 2008). The SH2 domain, on the other hand, is important for the binding of phosphorylated tyrosine residues (Crocker et al., 2008). This domain may have a role in competing for the STAT protein binding site as mutation of Val34 and Leu41 in the domain region consequently affected SOCS3 ability to inhibit STAT activation (Sasaki et al., 1999). Furthermore, the SH2 domain also possesses a PEST motif, which is involved in SOCS3 protein degradation. However, there is a controversy over the mechanism of action for such outcome and study has proposed that the PEST motif may be modulated through the proteasomal-degradation pathway (Babon et al., 2006; García-Alai et al., 2006; Rechsteiner and Rogers, 1996). Taken together, these findings suggested that there is more than one route to drive the turnover of SOCS3 protein. Therefore, experiments were conducted to investigate the cannabinoid-induced SOCS3 protein reduction in relation to: (1) JAK-STAT3 signalling pathway (2) ubiquitin-proteasome proteolytic pathway and (3) autophagy process (Figure 6.5).

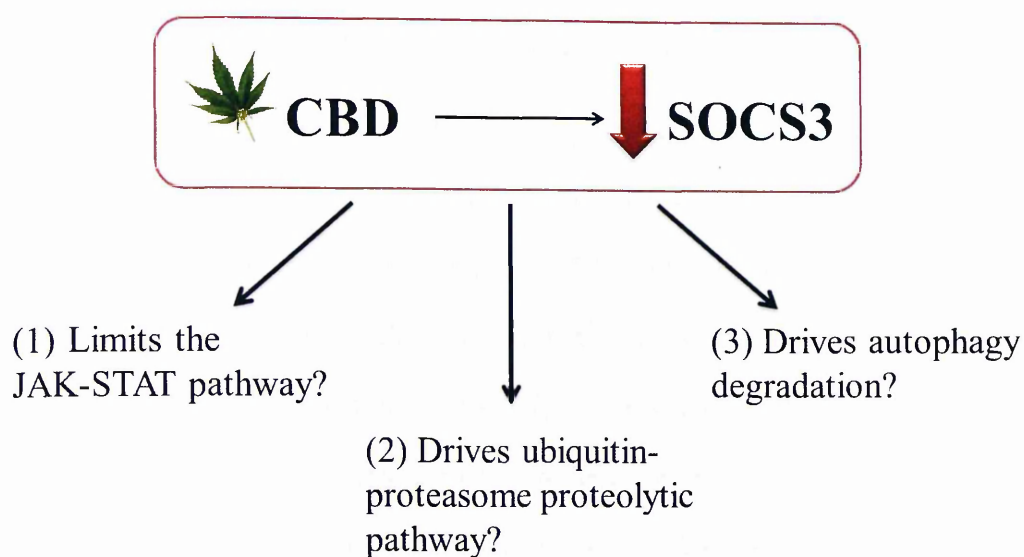


Figure 6.5. Possible mechanism of action that is responsible for Cannabidiol (CBD) or cannabinoids induced SOCS3 reduction.

6.4.1 Involvement of the JAK-STAT3 signalling pathway in SOCS3 protein reduction

SOCS protein acts as the negative feedback inhibitor of the JAK-STAT pathway. The binding of cytokines to the associated receptor initiates a conformational change on the receptor itself, resulting in the auto-phosphorylation of the tyrosine residues on Janus kinases (JAK). Consequently, the activated JAK kinases will recruit signal transducer and activator of transcription factors (STAT). The activated STAT3 will form STAT3 dimers with other phosphorylated STAT3 residue and the accumulation of activated STAT dimers in cell nucleus will eventually initiate the transcription of SOCS3 gene (Dalpke et al., 2008; Piessevaux et al., 2008). SOCS3 is capable in binding to JAK2 and STAT3, resulting in the initiation of feedback inhibition loop for STAT3 signaling pathway (Figure 6.6) (Babon et al., 2012). Taken together, it is comprehensive to speculate that cannabinoid treatment may increase the phosphorylation of STAT3, which consequently leads to the SOCS3 reduction due to SOCS3 induced negative feedback inhibition loop on the STAT3 protein.

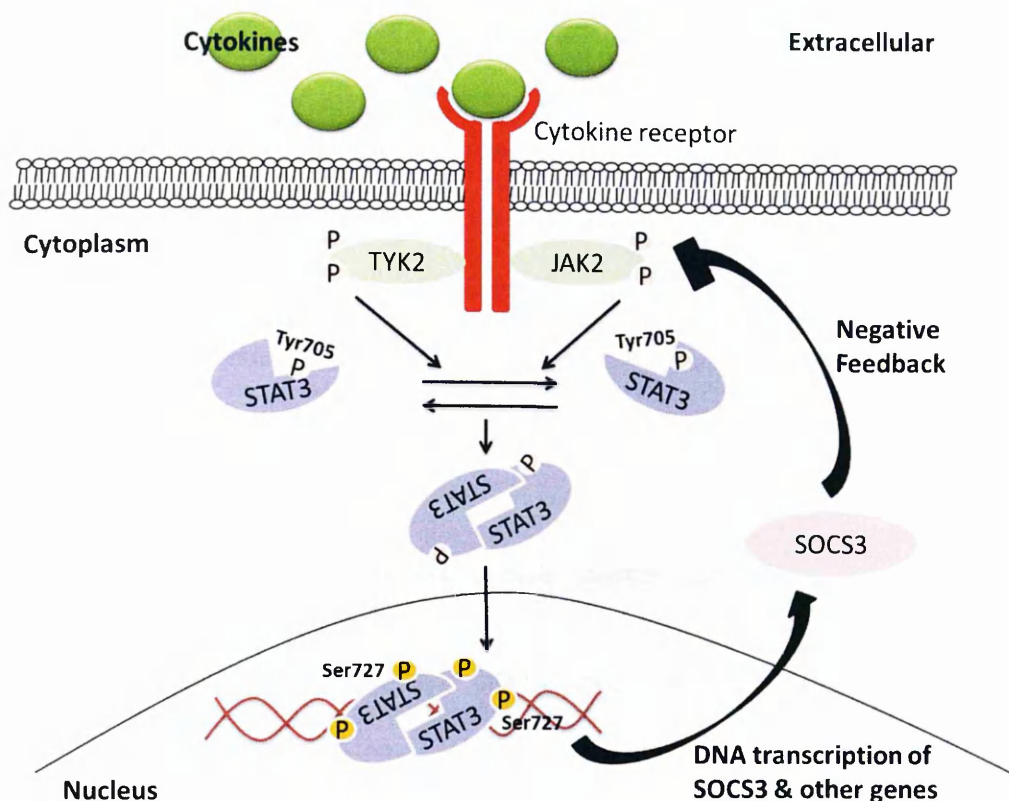


Figure 6.6. Schematic diagram shows the JAK-STAT signaling pathway and the negative feedback inhibition of SOCS3. Phosphorylation of STAT3 at Tyr705 induced the JAK-STAT pathway whereas the phosphorylation of STAT3 at Ser727 induced the DNA transcription of SOCS3 and other genes.

i. Cannabinoids induced p-STAT3(Ser727) protein expression

The activated JAK kinases phosphorylate the tyrosine residue (Tyr705) on STAT protein and this initiates STAT dimerization, which will translocate into the nucleus, leading to the binding of STAT to DNA and initiating the transcription of several genes, such as SOCS3 (Figure 6.6). Phosphorylation of the serine residue (Ser727) residues at the – COOH terminus of the transactivation domain of STAT3 protein is required for STAT3 mediated transcriptional activation (Wen and Darnell, 1997). The removal of the C-terminal domain in STAT3 resulted in the generation of transcriptionally inactive proteins (Decker and Kovarik, 2000). Therefore, cannabinoid-induced effect on the

serine residue (Ser727) of p-STAT3 protein was investigated in treated cells.

CBD was the only cannabinoid increased the phosphorylation of STAT3(Ser727) in treated cells (Figure 6.7), suggesting that CBD treatment increased the DNA transcription of SOCS3. Also, based on the negative impact of ACEA and AEA on p-STAT3 regulation, the cannabinoid-induced SOCS3 effect may be mediated through a non CNR1 associated signaling pathway.

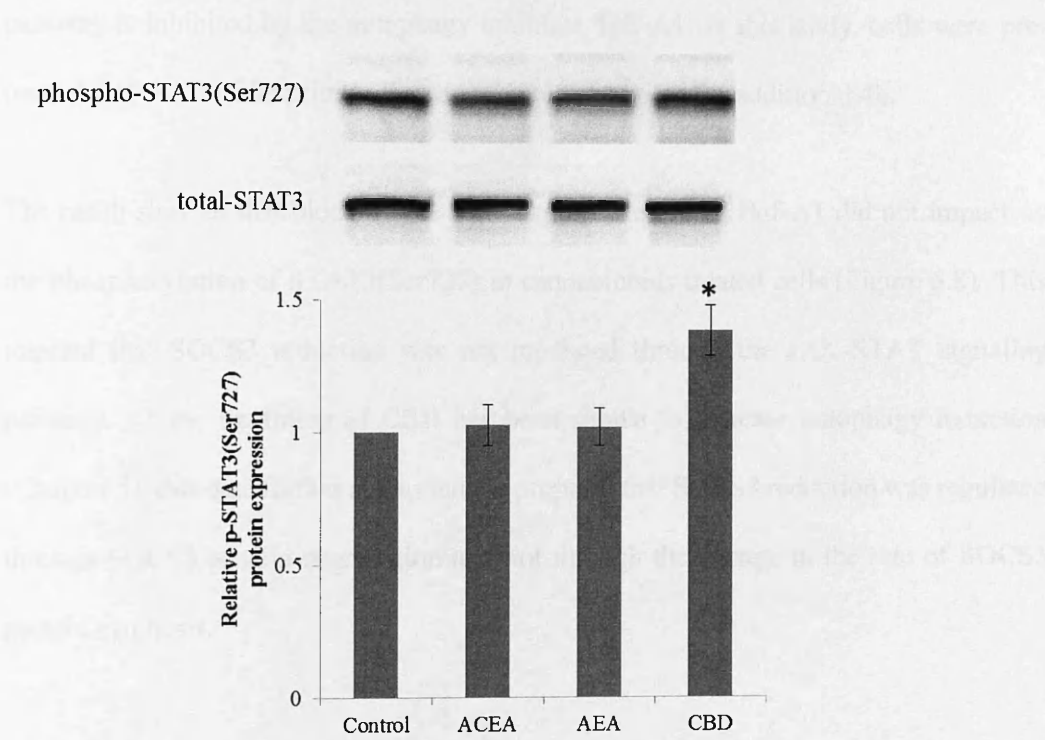


Figure 6.7. Cannabinoid induced phospho-STAT3(Ser727) protein expression. CaCo2 cells were treated with cannabinoids for 4h. Data plotted are relative fold-increase in p-STAT3 protein expression (adjusted to total-STAT3, mean \pm SE). * denotes significant different ($p < 0.05$) when compared to untreated control. (n=4, data were analysed with Dunnnett t-test (2-sided)).

(Molecular weight for p-STAT3: 91KDa; t-STAT3: 79KDa)

ii. Cannabinoid-induced p-STAT3(Ser727) protein expression in autophagy inhibitor treated cells

Based on previous findings, cannabinoids increased the autophagic induction (chapter 5) but reduced SOCS3 protein expression in treated cells. Also, CBD, but not ACEA and AEA, has been shown to increase the phosphorylation of p-STAT3 (Ser727) in treated cells. Therefore, it is interesting to further explore cannabinoid-induced effects on p-STAT3 expression under the circumstances where the autophagolysosomal degradation pathway is inhibited by the autophagy inhibitor, Baf-A1. In this study, cells were pre-treated Baf-A1 for 20h prior to the cannabinoid treatment for additional 4h.

The result showed that blocking the autophagy process with Baf-A1 did not impact on the phosphorylation of STAT3(Ser727) in cannabinoids treated cells (Figure 6.8). This implied that SOCS3 reduction was not mediated through the JAK-STAT signaling pathway. As the treatment of CBD has been shown to increase autophagy induction (Chapter 5), this data further supported the proposal that SOCS3 reduction was regulated through SOCS3 protein degradation and not through the change in the rate of SOCS3 protein synthesis.



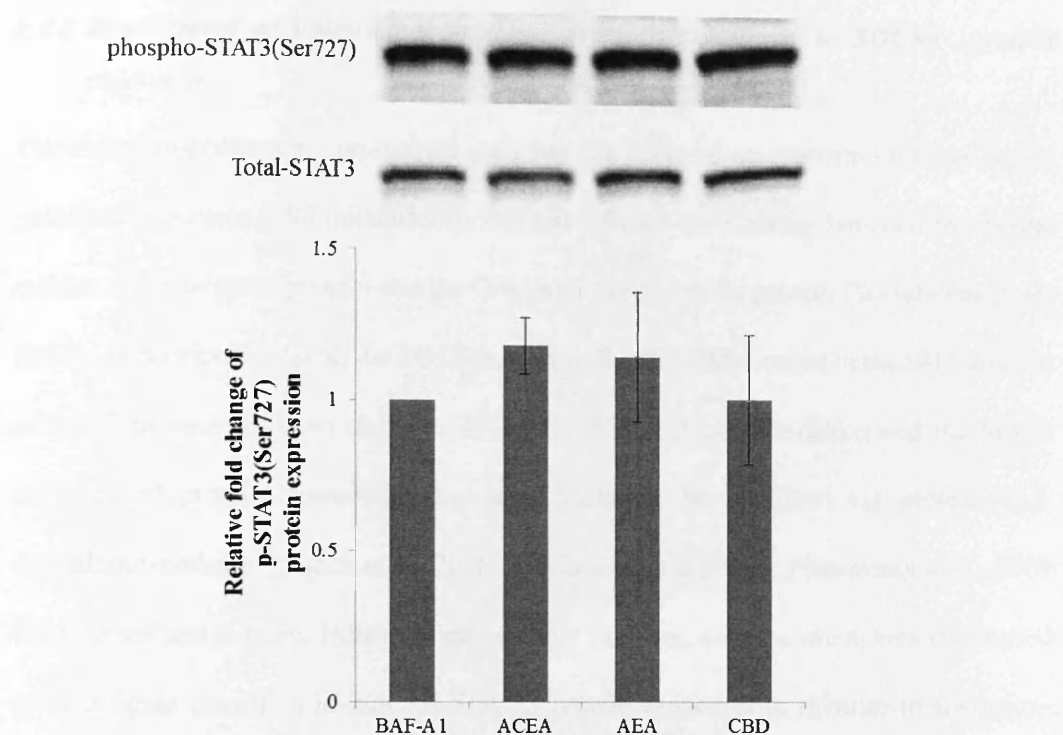


Figure 6.8. Cannabinoid induced phospho-STAT3(Ser727) protein expression in the presence of Bafilomycin-A1 (Baf-A1). CaCo2 cells were treated with cannabinoids for 4h. Data plotted are relative fold-increase in p-STAT3 protein expression normalized against Baf-A1 treatment (adjusted to total-STAT3, mean \pm SD; n=2).

(Molecular weight for p-STAT3: 91KDa; t-STAT3: 79KDa)

6.4.2 Involvement of ubiquitin-proteasome proteolytic pathway in SOCS3 protein reduction

The ubiquitin-proteasome proteolytic pathway is a common mechanism involved in the protein degradation. Ubiquitylation is formed through the binding between the lysine residue at the targeted protein and the C-terminus of ubiquitin protein (Welchman et al., 2005). As previously stated, the SOCS box, as well as the PEST motif in the SH2 domain of SOCS protein has been shown to be involved in protein degradation and the SOCS box-induced protein degradation has been shown to be mediated via proteasomal-degradation pathway (Babon et al., 2006; García-Alai et al., 2006; Piessevaux et al., 2008; Rechsteiner and Rogers, 1996). Based on these findings, an experiment was conducted to investigate cannabinoid-induced SOCS3 protein reduction in relation to ubiquitin-proteasome proteolytic pathway. The SOCS3 protein was immunoprecipitated from CBD-treated cells and analysed by immunoblotting with the Ubiquitin-1 specific antibody. The molecular weight for Ubiquitin-1 protein is 8.5KDa and together with the molecular weight of SOCS3 protein of 27KDa, the expected molecular weight for the protein complex is around 35.5KDa.

A time-course experiment was conducted on CBD treated CaCo2 cells. SOCS3 protein was immunoprecipitated from CBD-treated cells and analysed by immunoblotting with Ubiquitin-1 specific antibody. The rational for performing such experiment was to determine the protein expression of Ubiquitin-1 which would have bound to the SOCS3 protein in the CBD treated cells and to explore whether ubiquitin-1 was correlated to the reduction of SOCS3 protein in CBD treated cells. In this study, CBD was the only cannabinoid to be used as the treating compound and this was due to the promising finding obtained in previous chapter (Chapter 5) where my results suggested that CBD may have a therapeutic potential in disease with impaired autophagy. Therefore, it is

interesting to explore the mechanism of action involved in CBD-induced SOCS3 protein reduction in the treated cells.

The formation of polyubiquitylation involves the binding of a number of ubiquitin proteins to a single lysine residue on the targeted protein, resulting in the formation of a single chain of ubiquitin protein (Welchman et al., 2005). This explained the presence of a collection of ubiquitin-1 proteins at the molecular weight between 200KDa to 100KDa (Figure 6.9). Result showed that the Ubiquitin-1 protein expression was correlated to the reduction of SOCS3 protein in response to CBD treatment (Figure 6.9). However, because the reduction in ubiquitin is likely to be due to the reduction in SOCS3 available (i.e. less immunoprecipitated) I cannot conclusively state that ubiquitin is targeting SOCS3 for proteasomal degradation from this experiment.

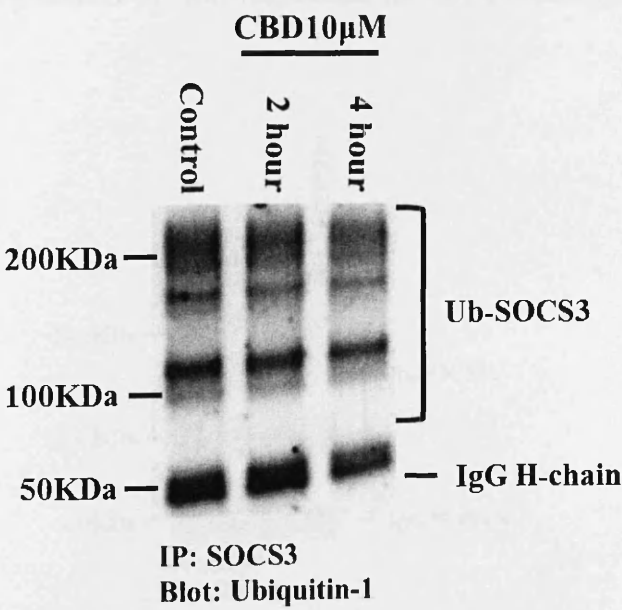


Figure 6.9. Ubiquitin-1 interacted with SOCS3 protein in CBD treated CaCo2 cells. Cells were treated with 10μM CBD for 2h and 4h respectively. SOCS3 protein was immunoprecipitated from CBD-treated cells and analysed by immunoblotting with Ubiquitin-1 specific antibody; (n=1).

As the previous experiment suggested that there was a correlation between ubiquitin-1 to the reduction of SOCS3 protein expression, an experiment was conducted to further explore the association of ubiquitin-mediated degradation pathway in SOCS3 reduction. A cell permeable proteasome inhibitor, MG132 (Guo and Peng, 2013), was applied to CBD-treated cells to inhibit ubiquitin-conjugated protein from degradation. CaCo2 cells were pre-treated with MG132 for 2h, prior to CBD treatment for additional 4 hour.

The result showed that CBD, as well as MG132, reduced ubiquitin-1 protein expression in treated cells (Figure 6.10). Interestingly, blockage of the ubiquitin-conjugated SOCS3 protein from degrading did not affect the ubiquitin-1 protein expression level in CBD treated cells (Figure 6.10). Even though this experiment has only been performed once but the result provided an indication that the ubiquitin-proteasome proteolytic pathway may not be the degradation pathway responsible for SOCS3 reduction in CBD treated cells.

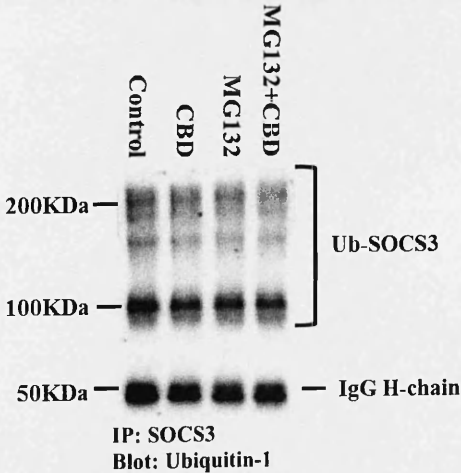


Figure 6.10. Effect of MG132 treatment on ubiquitin-1 co-precipitated SOCS3 protein in CBD treated CaCo2 cells. Cells were pre-treated with 15µM MG132 for 2h prior to 10µM CBD treatment for additional 4h. SOCS3 protein was immunoprecipitated from CBD-treated cells and analysed by immunoblotting with Ubiquitin-1 specific antibody, (n=1).

6.4.3 Involvement of autophagy process in SOCS3 protein reduction

As previous experiments indicated that neither the JAK-STAT pathway nor the ubiquitin-proteasome proteolytic pathway were responsible for cannabinoid-induced effect on SOCS3 protein reduction in treated cells, the involvement of autophagy mediated lysosomal degradation pathway was investigated in this context.

To investigate whether the autophagy degradation pathway was responsible for cannabinoid-induced SOCS3 protein reduction, cells were treated with autophagy inhibitors: 3-MA and Baf-A1. 3-MA inhibits autophagy process by targeting on the phagophore formation whereas Baf-A1 inhibits autophagy process by targeting on the autophagolysosomal formation (Klionsky et al., 2008; Simonsen and Tooze, 2009).

The results showed that by blocking the early stage of autophagy with 3-MA reversed AEA and CBD induced SOCS3 protein reduction (Figure 6.11) whereas blocking the late stage of autophagy with Baf-A1 reversed only the ACEA-induced effect (Figure 6.12).

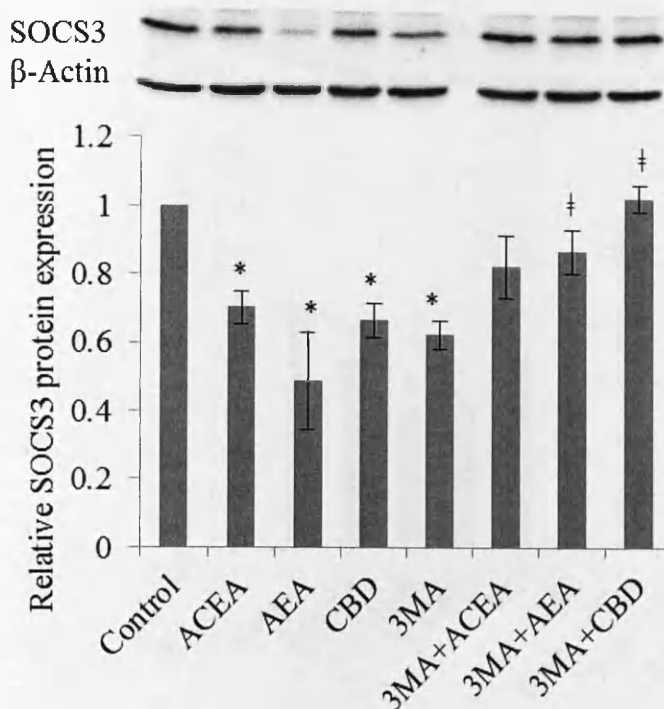


Figure 6.11. Immunoblotting showed the effect of cannabinoids treatment on SOCS3 protein expression in the presence of 3-MA. Fully differentiated CaCo2 cells were pre-treated with 3-MA (10mM) for 1h prior to addition of cannabinoids: CBD (10 μ M), ACEA (100nM), and AEA (10 μ M) for additional 4h. Data plotted are relative fold-increase in SOCS3 protein expression (adjusted to β -actin, mean \pm SE).

* denotes significant different ($p < 0.05$) when compared to untreated control.

† denotes significant different ($p < 0.05$) when compared to paired treatment control.

($n \geq 3$, data were analysed with Tukey post hoc test).

(Molecular weight for SOCS3: 27KDa; β -Actin: 45KDa)

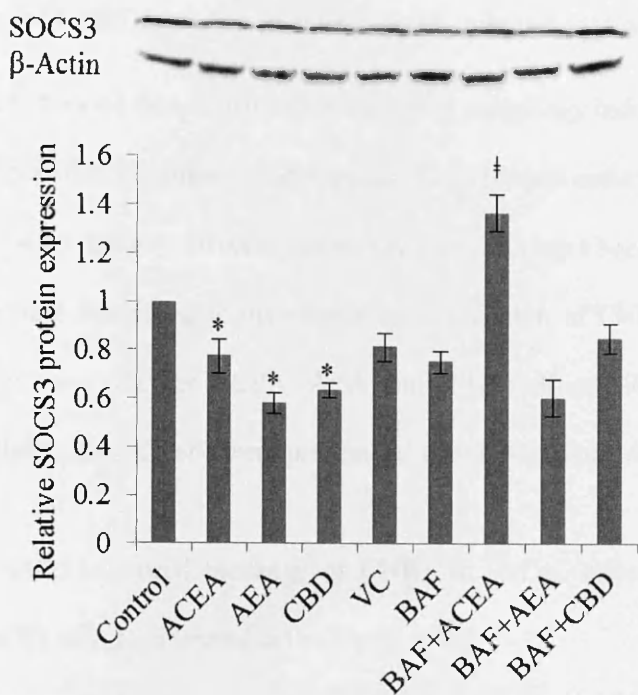


Figure 6.12. Immunoblotting showed the effect of cannabinoids treatment on SOCS3 protein expression in the presence of Baf-A1. Fully differentiated CaCo2 cells were pre-treated with Baf-A1 (100nM) for 20h prior to addition of cannabinoids: CBD (10μM), ACEA (100nM), and AEA (10μM) for additional 4h. Data plotted are relative fold-increase in SOCS3 protein expression (adjusted to β-actin, mean ± SE). * denotes significant different ($p<0.05$) when compared to untreated control. † denotes significant different ($p<0.05$) when compared to paired treatment control. ($n\geq 3$, data were analysed with Tukey post hoc test).

(Molecular weight for SOCS3: 27KDa; β-Actin: 45KDa)

6.5 Possible correlation of CNR1 receptor in cannabinoid-induced SOCS3 reduction

Thus far, experiments have revealed that cannabinoids increased autophagy induction and the autophagy process was responsible for cannabinoid-induced SOCS protein reduction in treated cells. Also, the ACEA and AEA-induced effect in autophagy induction have been shown to be CNR1 mediated; it is therefore interesting to investigate the association of CNR1 in SOCS3 protein reduction. To determine whether ACEA, AEA and CBD-induced SOCS3 protein reduction was CNR1 mediated, CaCo2 cells were pre-treated with CNR1 antagonist, **AM251**.

The result showed that AM251-induced blockage of CNR1 in CaCo2 cells may reverse cannabinoids-induced SOCS3 effects in treated cells (Figure 6.13).

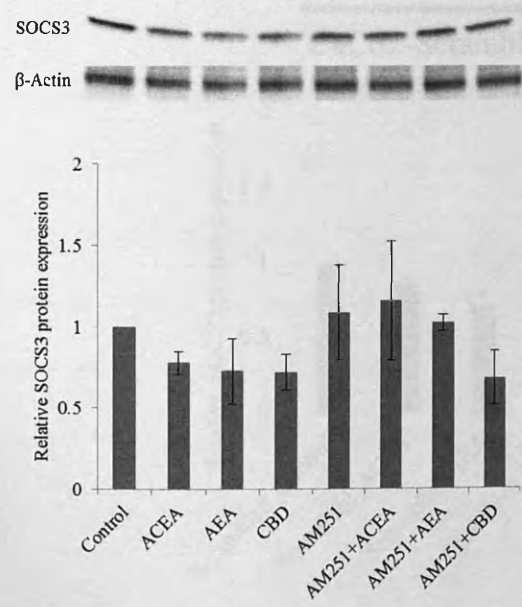


Figure 6.13. Immunoblotting showed the effect of cannabinoids treatment on SOCS3 protein expression in the presence of AM251. Fully differentiated CaCo2 cells were pre-treated with AM251 (100nM) for 10min prior to addition of cannabinoids: CBD (10μM), ACEA (100nM), AEA (10μM) for additional 4h. Data plotted are relative fold-increase in SOCS3 protein expression (adjusted to β-actin, mean ± SD, n=2).

(Molecular weight for SOCS3: 27KDa; β-Actin: 45KDa)

As previously mentioned in chapter 5, even though the use of antagonists to the CNR1 receptor has been an important tool in the dissection of receptor-mediated signalling and function, but a novel way to study the functional consequence of CNR1 loss is by the use of CNR1 knockdown cell model system. Therefore, to further verify the role of CNR1 in cannabinoid-

induced SOCS3 protein reduction, ACEA, AEA and CBD were treated on both CaCo2-CNR1KD and CaCo2-Scrambled cells.

The result showed that cannabinoid reduced SOCS3 protein expression in treated CaCo2-Scrambled cells. However, by knocking down the CNR1 gene in CaCo2 cells, the cannabinoid-induced effects on SOCS3 protein were reversed (Figure 6.14). This finding is in agreement with a previous experiment where cannabinoid-induced effect on SOCS3 protein was disrupted in CNR1 antagonist treated CaCo2 cells (Figure 6.13).

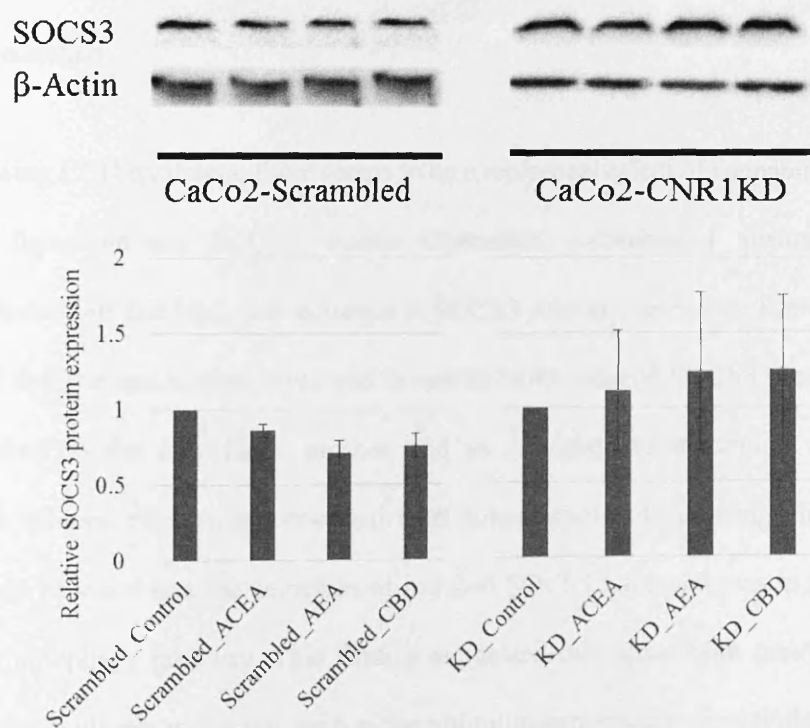


Figure 6.14. Effect of cannabinoid treatments on SOCS3 protein expression in both CaCo2-Scrambled and CaCo2-CNR1KD cell lines. Cells were treated with cannabinoids: CBD (10 μ M), ACEA (100nM), and AEA (10 μ M) for 4h prior to lysing. Data plotted are relative fold-increase in SOCS3 protein expression (adjusted to β -actin, mean \pm SD, n=2).

(Molecular weight for SOCS3: 27KDa; β -Actin: 45KDa)

6.6 Discussion

The phyto-, synthetic and endo-cannabinoids reduced SOCS3 protein expression within 4h. This finding supported a previous study where CBD reduced SOCS3 mRNA in microglial cells (Juknat et al., 2013). Results demonstrated that CBD induced SOCS3 reduction was dose dependent. Interestingly, despite ACEA being a 'high potency' analog of AEA, ACEA (Hillard et al., 1999) requires a 'high' concentration to induce a reduction of SOCS3 protein. The reduction in SOCS3 protein may be due to either increased protein degradation, or reduced protein synthesis. Caco2 cells express high levels of SOCS3 at both the protein and mRNA level (Chapter 3 and Rigby, personal communication), therefore I investigated the mechanism of SOCS3 reduction.

At 4h following CBD treatment, there seems to be a reciprocal effect of cannabinoid action on autophagic formation and SOCS3 protein expression. Cannabinoid treatment increases autophagic induction, but leads to a reduction in SOCS3 protein expression. Therefore, it could be assumed that the mechanisms involved in cannabinoid-induced SOCS3 protein reduction may be linked to the autophagic process and so I wished to determine whether such cannabinoid-induced effect was associated with enhancement of autophagy induction. My overall results revealed that the cannabinoid-induced SOCS3 reduction was in fact regulated through the autophagy pathway. This finding suggested that apart from previously known SOCS protein regulatory pathways, such as the ubiquitin-proteasome proteolytic pathway and the JAK-STAT pathway, autophagy induction may be a new mechanism in regulating the SOCS proteins (Babon et al., 2012; Babon et al., 2006; Welchman et al., 2005).

Additionally, my result also showed that ubiquitin-1 protein expression was shown to be correlated to the reduction of SOCS3 protein in response to CBD treatment but the ubiquitinated-

SOCS3 protein did not go through degradation via the ubiquitin-proteasome proteolytic pathway. As previously stated, the SOCS box in SOCS3 consists of a binding site for E3 ubiquitin ligase complex and such complex is required to facilitate the conjugation of ubiquitin to the lysine residue of the targeting protein, therefore explained the binding of ubiquitin-1 to the SOCS3 protein (Kuang et al., 2013; Piessevaux et al., 2008). This finding was in agreement with previous study which demonstrated the ubiquitylation in SOCS3 (Sasaki et al., 2003).

Chapter 7

Conclusion & Future Work

These studies demonstrated cannabinoid action in autophagy regulation in a human intestinal epithelial cell model system. The key findings of cannabinoid actions are summarized in Figure 7.1.

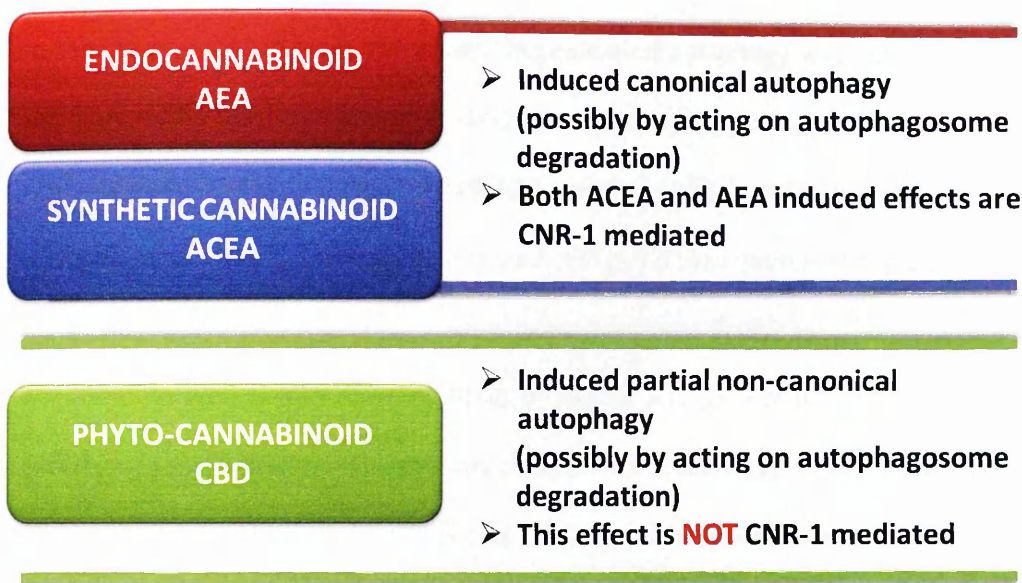


Figure 7.1. Cannabinoid action in autophagy process demonstrated in human intestinal epithelial cell model.

A recent review published by Juenemann and Reits highlighted other alternative autophagy pathways which do not require the involvement of autophagy key players (Atg5 or lipidation of LC3 or PI3K-Class III/Beclin-1) to induce lysosomal degradation (Juenemann and Reits, 2012), suggesting that autophagy can still be induced despite the absence or impairment of these autophagy key players in the regulatory system. I was particularly interested in the LC3 lipidation dependent canonical/non-canonical route of autophagy regulation (Juenemann and Reits, 2012) as my results demonstrated the formation of LC3-II in cannabinoid treated cells, suggesting that LC3-I lipidation process was required for autophagy induction. Recent studies revealed the induction of non-canonical autophagy by therapeutic potential drugs such as Resveratrol (breast cancer) and Dizocilpine/MK801 (neuronal disease) (Grishchuk et al., 2011;

Juenemann and Reits, 2012; Scarlatti et al., 2008), suggesting that CBD, which has been a potential therapeutic target for various disease (cardiovascular disease, diabetes, Huntington's disease), may also act on the non-canonical autophagy pathway.

In this study, CBD induced autophagy, but canonical autophagy was only part of the signal; therefore, CBD may also induce a non-canonical autophagy as opposed to ACEA and AEA. Genome-wide association studies (GWAS) revealed SNPs in ATG16L1 gene in CD patients (Prescott et al., 2007). ATG16L1 localized ATG5/12/16L1 protein complex to the isolation membrane, followed by the formation of autophagosome double membrane vesicle (Fujita et al., 2008; Henderson and Stevens, 2012). PI3KCIII activity is required for the recruitment of ATG16L1 protein complex (Nishimura et al., 2013). Therefore, the finding of CBD to induce a non-canonical autophagy suggests that CBD may have potential therapeutic application in CD where autophagy is compromised (Figure 7.2).

Despite AEA and ACEA binding and activating CNR1 with different binding affinities (Hillard et al., 1999), both ACEA and AEA induced effects were shown to be CNR1 mediated. Unlike other G-coupled protein receptor (GPCRs), CNR1 can be intracellularly activated by endogenous cannabinoids (Rozenfeld, 2011). My findings that CBD have effects on autophagy are perhaps not that surprising because of localization of CNR1 at lysosomal compartments (Rozenfeld and Devi, 2008). Intracellular injection of AEA activated functional CNR1 and the subsequent mobilization of intracellular calcium concentration was reduced by the administration of Baf-A1 (Brailoiu et al., 2011). The results illustrated the involvement of CNR1 in lysosomal degradation. Taken together, data obtained supports the ACEA and AEA-induced effect on late degradation. In contrast to previous findings, the CBD-induced effect in my studies was not mediated by CNR1. Δ^9 -THC has previously been shown to induce

autophagy in human astrocytoma cells and that study showed that the Δ^9 -THC-induced effect was CNR1 mediated (Salazar et al., 2009). Despite both studies being performed in different cell lines, these results may suggest that Δ^9 -THC and CBD may act through distinct mechanisms during autophagy.

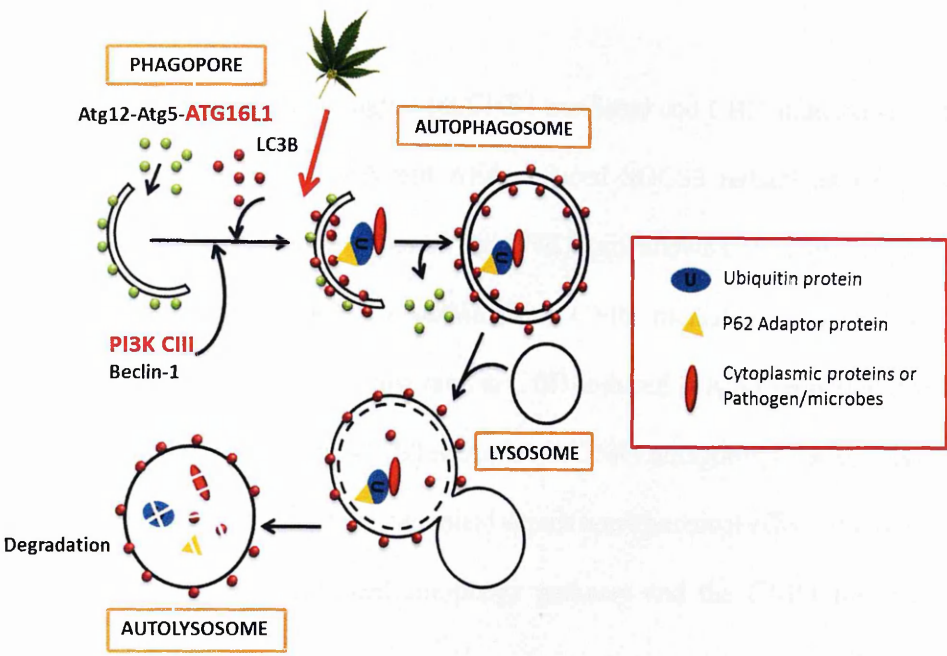


Figure 7.2. Schematic diagram showed the therapeutic potential of CBD for Crohn’s Disease (CD). CBD may induce a partially non-canonical autophagy (PI3K-Class III independent), suggesting that CBD is still capable in enhancing autophagy process when functional ATG16L1 is absence in the cell system. With that, CBD increased autophagy may be used as the tool for microbial/pathogen clearance in CD.

Cannabinoids reduce lipopolysaccharide-induced STAT3 phosphorylation suggesting a role in regulating microbial-induced inflammatory pathways (Kozela et al., 2010a). SOCS3 is also up-regulated in chronic intestinal inflammation (UC and CD) (Li et al., 2010). In my model, all three cannabinoids were able to reduce endogenous SOCS3 protein, therefore may represent anti-inflammatory therapeutic potential. Reduction of SOCS3 in an inflammatory setting may

allow intestinal homeostasis to be restored. CBD also reduced SOCS3 mRNA in microglial cells (Juknat et al., 2013), suggesting that this effect may not be intestinal specific. My findings showed SOCS3 reduction was not mediated through reduced STAT3 phosphorylation, nor ubiquitin-proteasome proteolytic pathway but, suggest that SOCS3 reduction was in fact, mediated through the autophagy degradation pathway.

ACEA and AEA induced autophagy were CNR1 mediated and CBD-induced autophagy was not CNR1 mediated, Both ACEA and AEA induced SOCS3 reductions were completely inhibited in both CNR1 antagonist treated and CNR1 knockdown CaCo2 cells, suggesting that ACEA and AEA induced SOCS3 reductions were CNR1 mediated. Interestingly, for CBD, there may be additional pathways involved in CBD-induced SOCS3 reduction because there was still a modest CBD induced SOCS3 reduction in CNR1 antagonist treated cells, suggesting that this could be reminiscent of the canonical versus non-canonical effect of CBD (ie. there is some dependence on the canonical autophagy pathway and the CNR1 the non-canonical pathway).

SOCS3 is expressed in an oscillatory manner in non-transformed cells (Yoshiura et al., 2007). Unusually, for a cancer cell line, basal SOCS3 levels are consistently high in CaCo2 cells and my finding that cannabinoids reduce SOCS3 may indicate that they act to increase autophagic degradation of SOCS3 protein, representing a possible mechanism by which cyclic protein expression could be regulated. Furthermore, elevated intestinal SOCS3 in UC and CD (Li et al., 2010) could be due to compromised autophagosomal degradation of the protein.

As I have shown previously that all cannabinoids increased autophagy and addressed that CBD may have therapeutic potential in CD, it is interesting to explore CBD-induced effect in

autophagy process under inflammatory setting. The use of CBD as a potential therapeutic drug for IBD may be through aid of pathogen clearance in CD. Preliminary experiments showed the impact of CBD treatment in IL-1 β -induced inflammatory setting (see appendix). IL-1 β was selected as the pro-inflammatory cytokine to induce inflammation in my model system as IL-1 β production was shown to be increased in inflamed gut mucosa in IBD patients (Reimund et al., 1996; Reinecker et al., 1993). My data showed that IL-1 β increased LC3-II formation in treated cells. CBD at 10 μ M further enhanced LC3-II formation in IL-1 β treated CaCo2 cells, as compared to CBD and IL-1 β treatment alone. This experiment has only been repeated twice and more replicates will be required to conclude the statistical significance of this piece of data. Based on the results in Chapter 3 (system analysis), I have shown that the IL-1 β -induced effect on LC3-II protein was serum dependent, supported by a previous study showing that IL-1 β -induced autophagy in rat annulus fibrosis cells was serum dependent (Shen et al., 2011), suggesting that CBD exerts anti-inflammatory effects in intestinal epithelial cells. Additionally, in agreement with a recent study demonstrating that autophagy regulates IL-1 β production in macrophages by targeting pro- IL-1 β for lysosomal degradation (Harris et al., 2011). Use of live microbes in my model system will offer us further verification of the possible role of CBD in ‘opportunistic-pathogen’ clearance.

Additionally, in correlation to recent studies which have revealed the role of ubiquitylation in autophagy regulation (Ohsumi, 2001; Kirkin et al., 2009; Behrends and Fulda, 2012), my study showed that the ubiquitin-1 protein expression was correlated to the reduction of SOCS3 protein in response to CBD treatment, but the ubiquitinated-SOCS3 protein did not go through degradation via the ubiquitin-proteasome proteolytic pathway. Based on previous findings, a range of E3 ubiquitin ligases were discovered to be involved in autophagy regulation. For example, the TRIM13 E3 ligase of p62 adaptor protein and the c-Cbl E3 ligase that regulates

the interaction between Src homology and LC3B protein (Kuang et al., 2013). These E3 ligases have been shown to regulate the degradation and stability of the autophagy-related proteins, as well as facilitate the regulation of recruited adaptor protein (Kuang et al., 2013). p62 has been shown to interact with LC3 protein, as this adaptor protein comprises an LC3-interacting region (LIR), which facilitates the formation of p62-LC3 complex (Kirkin et al., 2009). Nonetheless, the p62 adaptor protein has also been found to interact with ubiquitin (Long et al., 2008). Based on these findings, it is rational to suggest a mechanism for autophagy-induced SOCS3 reduction. It is possible that SOCS3 is ubiquitylated via its internal E3 ligase complex, resulting in the recruitment and binding of p62 adaptor protein. p62 bound ubiquitylated SOCS3 protein complex will then be recognised by LC3 at the phagophore. This would lead to SOCS3 protein being targeted to the autophagolysosomal degradation pathway. Taken together, this suggests an interaction between LC3, p62 and ubiquitin protein. However, further experiments will be required to validate this hypothesis. This can possibly be done through the generation of p62 knockdown CaCo2 cells to determine the expression of SOCS3 under the loss of p62 adaptor proteins.

In the whole, the research presented in this thesis supports an important role for autophagy in homeostatic regulation of cyclic proteins. Furthermore, it also describes a novel role for cannabinoids in the intestinal tract that could have therapeutic implications in the treatment of CBD.

Chapter 8

Appendix

1. The first part of the chapter discusses the importance of understanding the context of the data being analyzed. It emphasizes that without a clear understanding of the context, any statistical analysis would be meaningless. The author provides several examples to illustrate this point, such as analyzing test scores without knowing the difficulty of the test or the number of students who took it.

2. The second part of the chapter introduces the concept of the normal distribution, which is a fundamental concept in statistics. It explains how the normal distribution is used to model many natural phenomena and how it can be used to make predictions about the future. The author also discusses the Central Limit Theorem, which states that the distribution of sample means will approach a normal distribution as the sample size increases.

3. The third part of the chapter discusses the importance of hypothesis testing, which is a statistical method used to test a claim about a population parameter. It explains how to set up a hypothesis test, how to calculate the test statistic, and how to interpret the results. The author also discusses the concept of the p-value, which is a measure of the strength of the evidence against the null hypothesis.

4. The fourth part of the chapter discusses the importance of confidence intervals, which are a range of values that are likely to contain the true value of a population parameter. It explains how to calculate a confidence interval and how to interpret the results. The author also discusses the concept of the margin of error, which is a measure of the uncertainty in the estimate.

5. The fifth part of the chapter discusses the importance of regression analysis, which is a statistical method used to model the relationship between two variables. It explains how to fit a regression line to a set of data and how to use the regression line to make predictions. The author also discusses the concept of the coefficient of determination, which is a measure of the proportion of the variance in the dependent variable that is explained by the independent variable.

Table of Contents

Stock solution recipes 186

Product sheet for HuSH shRNA Plasmid, pRS 187

Quantitative Real time PCR (qRT-PCR) generated DNA melting curves for
CNR1 receptor in both CaCo2_CNR1KD and CaCo2_Scrambled cells. 188

The use of Dansylcadaverine (MDC) dye in treated cells 189

Preliminary data for CBD action in autophagy process under inflammatory setting 190

I. Stock solution recipes

Following are the recipes for stock solutions that were required for western blotting:

- RIPA Lysis Buffer
150mM of NaCl
1% of IGEPAL CA-630
0.5% of Sodium Deoxycholate
0.1% of SDS
50mM of Tris
**Buffer to be adjusted to pH 8*
- Tris-Glycine SDS running buffer
For making up 10X buffer, add:
250mM of Tris
1.92M of glycine
1% of SDS
- TBS (10x)
For making up the buffer into 1L, add:
24.2g of Tris Base
87.6g of NaCl
**Buffer to be adjusted to pH 7.5*
- Stripping buffer
2mL of 10% SDS
6.75mL of water
1.25mL of 0.5M Tris HCL (pH 6.8)
80uL of 2ME

II. Product sheet for HuSH shRNA Plasmid, pRS



HuSH shRNA Plasmid, pRS

pRS shRNA Cloning Plasmid
Catalog # TR20003

Product Description:

- Plasmid vector for cloning shRNA expression cassettes
- Designed for long term gene silencing studies
- Ampicillin (100ug/ml) and Puromycin resistance markers for easy selection of transformed or transfected cells
- U6 polymerase III promoter for shRNA expression
- MMLV LTR sequences for packaging into retroviral particles
- EcoRI and HindIII sites convenient for shuttling existing HuSH cassettes

Content: Each vial contains 5 ug of dried and purified plasmid DNA.

Storage and Stability: The plasmid is stable for at least 1 yr at -20°C from the date of shipment.

Guarantee: This product is guaranteed for the correct sequences and listed functions.

Related Products: Specific HuSH constructs are available at OriGene covering the full human, mouse and rat genomes.

Quality Control Assays

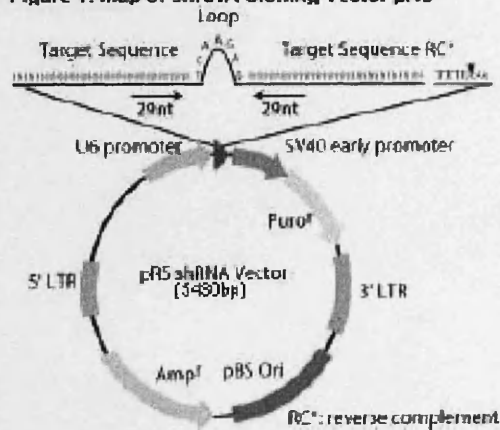
DNA Quantitation: The concentration of the purified plasmid was determined at OD₂₆₀ by a UV spectrometer.

DNA Sequence Analysis: The final purified plasmid was sequenced to confirm its identity.

Functional Analysis:

1. Cloning: the pRS plasmid was digested with BamHI and HindIII and the digested fragment isolated. Multiple shRNA expression cassettes were cloned into this plasmid.
2. Inhibition of target gene: shRNA constructs cloned into pRS were verified for inhibition of target genes.
3. Stable cell lines: pRS was verified to generate stable cell lines using direct transfection.

Figure 1: Map of shRNA Cloning Vector pRS



Terms of Use

By opening the use the product, the purchaser agrees not to distribute, resell, modify for resale or use to manufacture commercial products without prior written approval from OriGene Technologies, Inc. If you do not agree with these conditions, please return product to OriGene for a full refund.

III. Quantitative Real Time PCR (qRT-PCR) generated DNA melting curves for CNR1 receptor in both CaCo2_CNR1KD and CaCo2_Scrambled cells.

Quantitative RT-PCR was performed by using extracted RNA samples from the CNR1 knockdown cells. A single peak of CNR1 melting curve was obtained in both wild type and CaCo2_Scrambled cells but not in CaCo2_CNR1KD cells (Figure 8.1), suggesting that CaCo2_CNR1KD cells have significant low copies of CNR1 gene in the cells and this resulted in no single peak for the DNA melt curve in qRT-PCR.

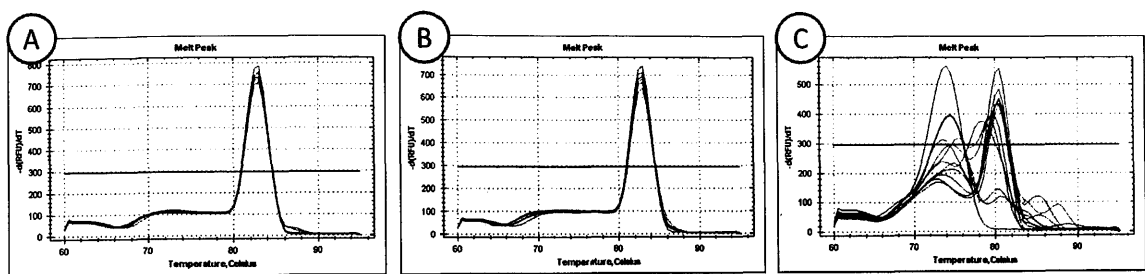


Figure 8.1. DNA melt curve for Cannabinoid receptor(CNR)-1 in (A)wild type CaCo2 cells; (B)CaCo2_Scrambled cells; and (C)CaCo2_CNR1KD cells.

IV. The use of Dansylcadaverine (MDC) dye in treated cells

MDC was the first autophagy dye to be optimized in this project. MDC was applied to label the autophagic vacuoles in cannabinoid treated cells (Biederbick et al., 1995). However, the use of MDC generated a high background signal with weak fluorescent signal (Figure 8.2), resulting in the need to increase the laser power during imaging, which consequently damaged the treated cells. Therefore, it was decided that the MDC may not be an appropriate autophagy dye to be used in this study.

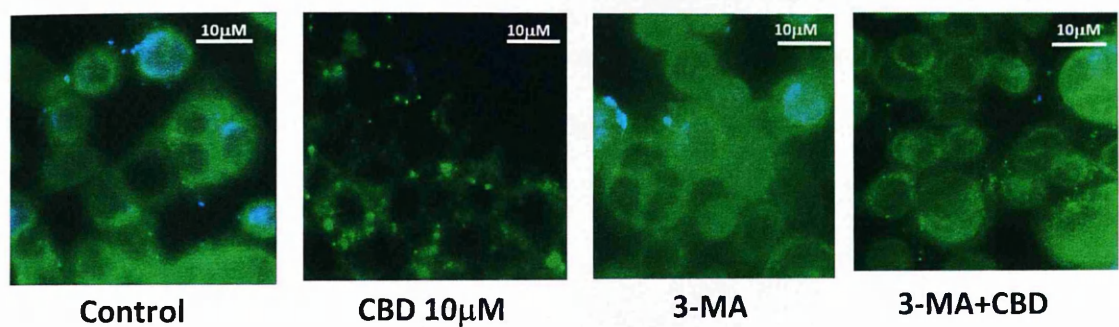


Figure 8.2. Fluorescence images with the use of dansylcadaverine (MDC) dye in treated CaCo2 cells.

V. Preliminary data for CBD action in autophagy process under inflammatory setting

IL-1 β , a pro-inflammatory cytokines, is released by immune cells to the site of injury during inflammation (Harris et al., 2011). Also, IL-1 β production was increased in inflamed gut mucosa in IBD patients (Reimund et al., 1996; Reinecker et al., 1993). Therefore, IL-1 β was selected as the pro-inflammatory cytokine to induce inflammation in my model system.

The preliminary data showed that both CBD and IL-1 β treatments increased LC3-II formation and CBD may further enhance IL-1 β -induced LC3-II formation in treated cells (Figure 8.4), suggesting that CBD exerts anti-inflammatory effects in intestinal epithelial cells. However, experiment will need to be repeated in order to confirm the statistical significance of this data.

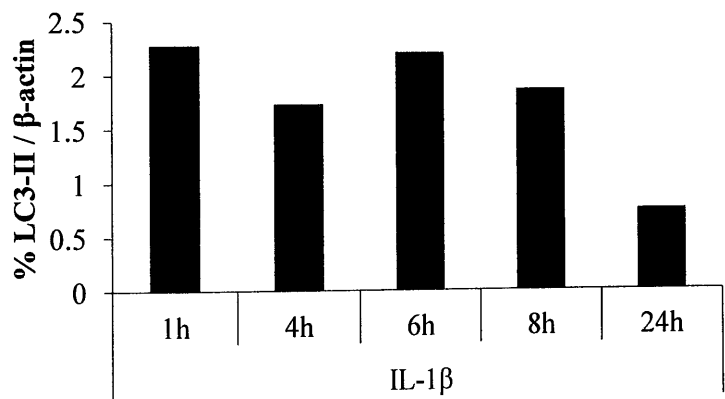


Figure 8.3. Dose response curve for IL-1 β treatment. Immunoblot analysis of LC3-II in fully differentiated CaCo2 cells in response to IL-1 β (10ng/mL) treatment within 24h. Data plotted are relative fold-increase in LC3-II protein expression (adjusted to β -actin; n=1).

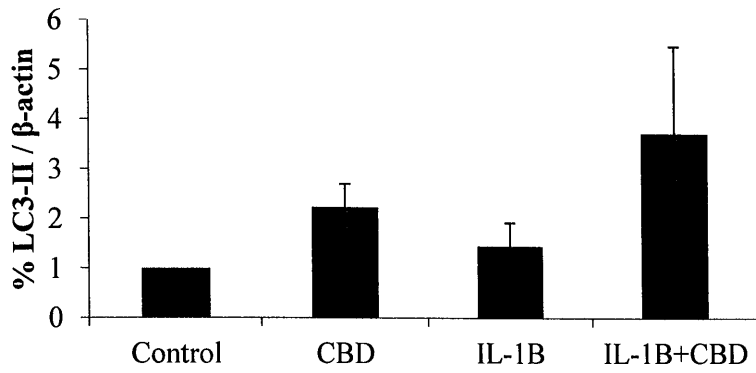


Figure 8.4. Cannabidiol (CBD)-induced LC3-II protein expression in IL-1 β -induced inflammatory setting. CaCo2 cells were pre-treated with IL-1 β for 1h prior to CBD treatment for additional 4h. Data plotted are relative fold-increase in LC3-II protein expression (adjusted to β -actin, mean \pm SD; n=2)

Chapter 9

References

- Abraham, C., and J. H. Cho, 2009, Inflammatory bowel disease: *New England Journal of Medicine*, v. 361, p. 2066-78.
- Akira, S., S. Uematsu, and O. Takeuchi, 2006, Pathogen recognition and innate immunity: *Cell*, v. 124, p. 783-801.
- Alexander, W. S., R. Starr, J. E. Fenner, C. L. Scott, E. Handman, N. S. Sprigg, J. E. Corbin, A. L. Cornish, R. Darwiche, C. M. Owczarek, T. W. H. Kay, N. A. Nicola, P. J. Hertzog, D. Metcalf, and D. J. Hilton, 1999, SOCS1 is a critical inhibitor of interferon- γ signaling and prevents the potentially fatal neonatal actions of this cytokine: *Cell*, v. 98, p. 597-608.
- Alhamoruni, A., A. C. Lee, K. L. Wright, M. Larvin, and S. E. Sullivan, 2010, Pharmacological effects of cannabinoids on the Caco-2 cell culture model of intestinal permeability: *The Journal of Pharmacology and Experimental Therapeutics*, v. 335, p. 92.
- Alhouayek, M., and G. G. Muccioli, 2012, The endocannabinoid system in inflammatory bowel diseases: from pathophysiology to therapeutic opportunity: *Trends in Molecular Medicine*, v. 18, p. 615-625.
- Antonio Waldo, Z., 2008, Cannabidiol: from an inactive cannabinoid to a drug with wide spectrum of action Canabidiol: de um canabinóide inativo a uma droga com amplo espectro de ação: *Revista Brasileira de Psiquiatria*, v. 30, p. 271.
- Axe, E. L., S. A. Walker, M. Manifava, P. Chandra, H. L. Roderick, A. Habermann, G. Griffiths, and N. T. Ktistakis, 2008, Autophagosome formation from membrane compartments enriched in phosphatidylinositol 3-phosphate and dynamically connected to the endoplasmic reticulum: *The Journal of Cell Biology*, v. 182, p. 685-701.
- Azzam, M. E., and I. D. Algranati, 1973, Mechanism of puromycin action: fate of ribosomes after release of nascent protein chains from polysomes: *Proceedings of the National Academy of Sciences of the United States of America*, v. 70, p. 3866-3869.
- Babon, Jeffrey J., Nadia J. Kershaw, James M. Murphy, Leila N. Varghese, A. Laktyushin, Samuel N. Young, Isabelle S. Lucet, Raymond S. Norton, and Nicos A. Nicola, 2012, Suppression of cytokine signaling by SOCS3: Characterization of the mode of inhibition and the basis of its specificity: *Immunity*, v. 36, p. 239-250.
- Babon, J. J., E. J. McManus, S. Yao, D. P. DeSouza, L. A. Mielke, N. S. Sprigg, T. A. Willson, D. J. Hilton, N. A. Nicola, M. Baca, S. E. Nicholson, and R. S. Norton, 2006, The Structure of SOCS3 reveals the basis of the extended SH2 domain function and identifies an unstructured insertion that regulates stability: *Molecular Cell*, v. 22, p. 205-216.
- Bailey, C. A., P. Bryla, and A. W. Malick, 1996, The use of the intestinal epithelial cell culture model, Caco-2, in pharmaceutical development: *Advanced Drug Delivery Reviews*, v. 22, p. 85-103.
- Barclay, J. L., S. T. Anderson, M. J. Waters, and J. D. Curlew, 2009, SOCS3 as a tumor suppressor in breast cancer cells and its regulation by PRL: *International Journal of Cancer*, v. 124, p. 1756-1766.
- Barth, S., D. Glick, and K. F. Macleod, 2010, Autophagy: assays and artifacts: *Journal Of Pathology*, v. 221(2), p. 117-124.
- Beck Sickinger, A. G., and K. Mörl, 2006, Posttranslational Modification of Proteins. Expanding natures inventory. By Christopher T. Walsh: *Angewandte Chemie International Edition*, v. 45, p. 1020-1020.
- Behrends, C., and S. Fulda, 2012, Receptor proteins in selective autophagy: *International Journal of Cell Biology*, v. 2012, p. 673290.

- Behrens, I., and T. Kissel, 2003, Do cell culture conditions influence the carrier- mediated transport of peptides in Caco- 2 cell monolayers?: *European Journal of Pharmaceutical Sciences*, v. 19, p. 433-442.
- Biagi, E., M. Candela, S. Turrone, P. Garagnani, C. Franceschi, and P. Brigidi, 2012, Ageing and gut microbes: Perspectives for health maintenance and longevity: *Pharmacological Research*, v. 69, p. 11-20.
- Biederbick, A., H. F. Kern, and H. P. Elsasser, 1995, Monodansylcadaverine (MDC) is a specific in vivo marker for autophagic vacuoles: *European Journal of Cell Biology*, v. 66, p. 3-14.
- Bisogno, T., 2008, Endogenous cannabinoids: structure and metabolism: *Journal of Neuroendocrinology*, v. 20, p. 1-9.
- Bisogno, T., L. Hanus, L. De Petrocellis, S. Tchilibon, D. E. Ponde, I. Brandi, A. S. Moriello, J. B. Davis, R. Mechoulam, and V. Di Marzo, 2001, Molecular targets for cannabidiol and its synthetic analogues: effect on vanilloid VR1 receptors and on the cellular uptake and enzymatic hydrolysis of anandamide: *British Journal of Pharmacology*, v. 134, p. 845-52.
- Bjorbaek, C., K. El-Haschimi, J. D. Frantz, and J. S. Flier, 1999, The role of SOCS-3 in leptin signaling and leptin resistance: *The Journal of Biological Chemistry*, v. 274, p. 30059-65.
- Blaut, M., and T. Clavel, 2007, Metabolic diversity of the intestinal microbiota: Implications for health and disease: *The Journal of Nutrition*, v. 137, p. 751S.
- Bosier, B., G. G. Muccioli, E. Hermans, and D. M. Lambert, 2010, Functionally selective cannabinoid receptor signalling: Therapeutic implications and opportunities: *Biochemical Pharmacology*, v. 80, p. 1-12.
- Brailoiu, G. C., T. I. Oprea, P. W. Zhao, M. E. Abood, and E. Brailoiu, 2011, Intracellular Cannabinoid Type 1 (CB1) Receptors Are Activated by Anandamide: *The Journal of Biological Chemistry*, v. 286, p. 29166-29174.
- Cadwell, K., J. Y. Liu, S. L. Brown, H. Miyoshi, J. Loh, J. K. Lennerz, C. Kishi, W. Kc, J. A. Carrero, S. Hunt, C. D. Stone, E. M. Brunt, R. J. Xavier, B. P. Sleckman, E. Li, N. Mizushima, T. S. Stappenbeck, and H. W. Virgin, 2008, A key role for autophagy and the autophagy gene Atg16L1 in mouse and human intestinal Paneth cells: *Nature*, v. 456, p. 259-U62.
- Capasso, R., F. Borrelli, G. Aviello, B. Romano, C. Scalisi, F. Capasso, and A. A. Izzo, 2008, Cannabidiol, extracted from *Cannabis sativa*, selectively inhibits inflammatory hypermotility in mice: *British Journal of Pharmacology*, v. 154, p. 1001-1008.
- Chan, L. L., D. Shen, A. R. Wilkinson, W. Patton, N. Lai, E. Chan, D. Kuksin, B. Lin, and J. Qiu, 2012, A novel image-based cytometry method for autophagy detection in living cells: *Autophagy*, v. 8, p. 1371-82.
- Chang, Y. Y., G. Juhasz, P. Goraksha-Hicks, A. M. Arsham, D. R. Mallin, L. K. Muller, and T. P. Neufeld, 2009, Nutrient-dependent regulation of autophagy through the target of rapamycin pathway: *Biochemical Society Transactions*, v. 37, p. 232-236.
- Chassaing, B., and A. Darfeuille-Michaud, 2011, The commensal microbiota and enteropathogens in the pathogenesis of inflammatory bowel diseases: *Gastroenterology*, v. 140, p. 1720-1728.e3.
- Cherra, S. J., S. M. Kulich, G. Uechi, M. Balasubramani, J. Mountzouris, B. W. Day, and C. T. Chu, 2010, Regulation of the autophagy protein LC3 by phosphorylation: *The Journal of Cell Biology*, v. 190, p. 533-539.

- Cluny, N. L., R. A. Reimer, and K. A. Sharkey, 2012, Cannabinoid signalling regulates inflammation and energy balance: The importance of the brain– gut axis: *Brain Behavior and Immunity*, v. 26, p. 691-698.
- Comes, F., A. Matrone, P. Lastella, B. Nico, F. C. Susca, R. Bagnulo, G. Ingravallo, S. Modica, G. Lo Sasso, A. Moschetta, G. Guanti, and C. Simone, 2007, A novel cell type- specific role of p38-alpha in the control of autophagy and cell death in colorectal cancer cells: *Cell Death and Differentiation*, v. 14, p. 693.
- Console-Bram, L., J. Marcu, and M. E. Abood, 2012, Cannabinoid receptors: nomenclature and pharmacological principles: *Progress in Neuropsychopharmacology and Biological Psychiatry*, v. 38, p. 4-15.
- Coombes, J. L., and F. Powrie, 2008, Dendritic cells in intestinal immune regulation: *Nature Reviews. Immunology*, v. 8, p. 435.
- Cooney, R., J. Baker, O. Brain, B. Danis, T. Pichulik, P. Allan, D. J. P. Ferguson, B. J. Campbell, D. Jewell, and A. Simmons, 2010, NOD2 stimulation induces autophagy in dendritic cells influencing bacterial handling and antigen presentation: *Nature Medicine*, v. 16, p. 90.
- Croker, B. A., H. Kiu, and S. E. Nicholson, 2008, SOCS regulation of the JAK/ STAT signalling pathway: *Seminars in Cell and Developmental Biology*, v. 19, p. 414-422.
- Croker, B. A., D. L. Krebs, J. G. Zhang, S. Wormald, T. A. Willson, E. G. Stanley, L. Robb, C. J. Greenhalgh, I. Forster, B. E. Clausen, N. A. Nicola, D. Metcalf, D. J. Hilton, A. W. Roberts, and W. S. Alexander, 2003, SOCS3 negatively regulates IL- 6 signaling in vivo: *Nature Immunology*, v. 4, p. 540-545.
- Dalpke, A., K. Heeg, H. Bartz, and A. Baetz, 2008, Regulation of innate immunity by suppressor of cytokine signaling (SOCS) proteins: *Immunobiology*, v. 213, p. 225-35.
- Decker, T., and P. Kovarik, 2000, Serine phosphorylation of STATs: *Oncogene*, v. 19, p. 2628.
- Demuth, D. G., and A. Molleman, 2006, Cannabinoid signalling: *Life Sciences*, v. 78, p. 549-563.
- Deplancke, B., and H. R. Gaskins, 2001, Microbial modulation of innate defense: goblet cells and the intestinal mucus layer: *The American Journal of Clinical Nutrition*, v. 73, p. 1131S-1141S.
- Deretic, V., and B. Levine, 2009, Autophagy, Immunity, and Microbial Adaptations: *Cell Host and Microbe*, v. 5, p. 527-549.
- Deter, R. L., P. Baudhuin, and C. de Duve, 1967, Participation of lysosomes in cellular autophagy induced in rat liver by glucagon: *The Journal of Cell Biology*, v. 35, p. 11-16.
- Devane, W. A., L. Hanuš, A. Breuer, R. G. Pertwee, L. A. Stevenson, G. Griffin, D. Gibson, A. Mandelbaum, A. Etinger, and R. Mechoulam, 1992, Isolation and structure of a brain constituent that binds to the cannabinoid receptor: *Science*, v. 258, p. 1946-1949.
- Di Marzo, V., 2006, A brief history of cannabinoid and endocannabinoid pharmacology as inspired by the work of British scientists: *Trends in Pharmacological Sciences*, v. 27, p. 134-140.
- Di Marzo, V., and A. A. Izzo, 2006, Endocannabinoid overactivity and intestinal inflammation: *Gut*, v. 55, p. 1373-1376.
- Diaz-Troya, S., M. E. Perez-Perez, F. J. Florencio, and J. L. Crespo, 2008, The role of TOR in autophagy regulation from yeast to plants and mammals: *Autophagy*, v. 4, p. 851-65.
- Didierlaurent, A., M. Simonet, and J. C. Sirard, 2005, Innate and acquired plasticity of the intestinal immune system: *Cellular and Molecular Life Sciences*, v. 62, p. 1285.

- Donadelli, M., I. Dando, T. Zaniboni, C. Costanzo, E. D. Pozza, M. T. Scupoli, A. Scarpa, S. Zappavigna, M. Marra, A. Abbruzzese, M. Bifulco, M. Caraglia, and M. Palmieri, 2011, Gemcitabine/ cannabinoid combination triggers autophagy in pancreatic cancer cells through a ROS- mediated mechanism: *Cell Death & Disease*, v. 2, p.152.
- Fegley, D., S. Kathuria, R. Mercier, C. Li, A. Goutopoulos, A. Makriyannis, and D. Piomelli, 2004, Anandamide transport is independent of fatty-acid amide hydrolase activity and is blocked by the hydrolysis-resistant inhibitor AM1172: *Proceedings of the National Academy of Science of the United States of America*, v. 101, p. 8756-8761.
- Ferruzza, S., C. Rossi, M. L. Scarino, and Y. Sambuy, 2012, A protocol for differentiation of human intestinal Caco-2 cells in asymmetric serum-containing medium: *Toxicology in Vitro*, v. 26, p. 1252-1255.
- Flint, H. J., 2012, The impact of nutrition on the human microbiome: *Nutrition Reviews*, v. 70, p. 10-13.
- Frank, D. N., A. L. St. Amand, R. A. Feldman, E. C. Boedeker, N. Harpaz, and N. R. Pace, 2007, Molecular-phylogenetic characterization of microbial community imbalances in human inflammatory bowel diseases: *Proceedings of the National Academy of Sciences of the United States of America*, v. 104, p. 13780-13785.
- Frazier, T. H., J. K. DiBaise, and C. J. McClain, 2011, Gut microbiota, Intestinal permeability, Obesity-induced inflammation, and Liver injury: *Journal of Parenteral and Enteral Nutrition*, v. 35, p. 14-20.
- Fujita, N., T. Itoh, H. Omori, M. Fukuda, T. Noda, and T. Yoshimori, 2008, The Atg16L complex specifies the site of LC3 lipidation for membrane biogenesis in autophagy: *Molecular Biology of the Cell*, v. 19, p. 2092-2100.
- Fukata, M., K. S. Michelsen, R. Eri, L. S. Thomas, B. Hu, K. Lukasek, C. C. Nast, J. Lechago, R. Xu, Y. Naiki, A. Soliman, M. Arditi, and M. T. Abreu, 2005, Toll-like receptor-4 is required for intestinal response to epithelial injury and limiting bacterial translocation in a murine model of acute colitis: *American Journal of Physiology. Gastrointestinal and Liver Physiology*, v. 288, p. 1055.
- Galluzzi, L., O. Kepp, and G. Kroemer, 2011, Autophagy and innate immunity ally against bacterial invasion: *The EMBO Journal*, v. 30, p. 3213.
- García-Alai, M. M., M. Gallo, M. Salame, D. E. Wetzler, A. A. McBride, M. Paci, D. O. Cicero, and G. de Prat-Gay, 2006, Molecular Basis for Phosphorylation- Dependent, PEST-Mediated Protein Turnover: *Structure*, v. 14, p. 309-319.
- Gee, M. I., M. G. Grace, R. H. Wensel, R. W. Sherbaniuk, and A. B. Thomson, 1985, Nutritional status of gastroenterology outpatients: comparison of inflammatory bowel disease with functional disorders: *Journal of the American Dietetic Association*, v. 85, p. 1591-9.
- Ghosh, S., A. Preet, J. E. Groopman, and R. K. Ganju, 2006, Cannabinoid receptor CB2 modulates the CXCL12/CXCR4-mediated chemotaxis of T lymphocytes: *Molecular Immunology*, v. 43, p. 2169.
- Glass, M., and J. K. Northup, 1999, Agonist selective regulation of G proteins by cannabinoid CB(1) and CB(2) receptors: *Molecular Pharmacology*, v. 56, p. 1362.
- Glick, D., S. Barth, and K. F. Macleod, 2010, Autophagy: cellular and molecular mechanisms: *The Journal of Pathology*, v. 221, p. 3-12.
- Grimsey, N. L., C. E. Goodfellow, E. L. Scotter, M. J. Dowie, M. Glass, and E. S. Graham, 2008, Specific detection of CB1 receptors; cannabinoid CB1 receptor antibodies are not all created equal: *Journal of Neuroscience Methods*, v. 171, p. 78.

- Grishchuk, Y., V. Ginet, A. C. Truttmann, P. G. Clarke, and J. Puyal, 2011, Beclin 1-independent autophagy contributes to apoptosis in cortical neurons: *Autophagy*, v. 7, p. 1115-31.
- Groulx, J. F., T. Khalfaoui, Y. D. Benoit, G. Bernatchez, J. C. Carrier, N. Basora, and J. F. Beaulieu, 2012, Autophagy is active in normal colon mucosa: *Autophagy*, v. 8, p. 893-902.
- Guo, N., and Z. Peng, 2013, MG132, a proteasome inhibitor, induces apoptosis in tumor cells: *Asia Pacific Journal of Clinical Oncology*, v. 9, p. 6-11.
- Guzmán, M., 2003, Cannabinoids: potential anticancer agents: *Nature Reviews. Cancer*, v. 3, p. 745.
- Haan, S., P. Ferguson, U. Sommer, M. Hiremath, D. W. McVicar, P. C. Heinrich, J. A. Johnston, and N. A. Cacalano, 2003, Tyrosine phosphorylation disrupts elongin interaction and accelerates SOCS3 degradation: *The Journal of Biological Chemistry*, v. 278, p. 31972.
- Hardy, M. P., A. F. McGettrick, and L. A. J. Neill, 2004, Transcriptional regulation of the human TRIF (TIR domain-containing adaptor protein inducing interferon beta) gene: *The Biochemical Journal*, v. 380, p. 83.
- Harris, J., M. Hartman, C. Roche, S. G. Zeng, A. Shea, F. A. Sharp, E. M. Lambe, E. M. Creagh, D. T. Golenbock, J. Tschopp, H. Kornfeld, K. A. Fitzgerald, and E. C. Lavelle, 2011, Autophagy controls IL-1 β secretion by targeting pro-IL-1 β for degradation: *The Journal of Biological Chemistry*, v. 286, p. 9587.
- Harrison, C., and J. R. Traynor, 2003, The [35S] GTP γ S binding assay: approaches and applications in pharmacology: *Life Sciences*, v. 74, p. 489-508.
- Hausmann, M., K. Leucht, C. Ploner, S. Kiessling, A. Villunger, H. Becker, C. Hofmann, W. Falk, M. Krebs, S. Kellermeier, M. Fried, J. Scholmerich, F. Obermeier, and G. Rogler, 2011, BCL-2 modifying factor (BMF) is a central regulator of anoikis in human intestinal epithelial cells: *The Journal of Biological Chemistry*, v. 286, p. 26533-40.
- Hayeshi, R., C. Hilgendorf, P. Artursson, P. Augustijns, B. Brodin, P. Dehertogh, K. Fisher, L. Fossati, E. Hovenkamp, T. Korjamo, C. Masungi, N. Maubon, R. Mols, A. Müllertz, J. Mönkkönen, C. O'Driscoll, H. M. Oppers-Tiemissen, E. G. E. Ragnarsson, M. Rooseboom, and A.-L. Ungell, 2008, Comparison of drug transporter gene expression and functionality in Caco-2 cells from 10 different laboratories: *European Journal of Pharmaceutical Sciences*, v. 35, p. 383-396.
- He, B., L. You, K. Uematsu, K. Zang, Z. Xu, A. Y. Lee, J. F. Costello, F. McCormick, and D. M. Jablons, 2003, SOCS-3 is frequently silenced by hypermethylation and suppresses cell growth in human lung cancer: *Proceedings of the National Academy of Sciences of the United States of America*, v. 100, p. 14133-14138.
- Henderson, P., and C. Stevens, 2012, The role of autophagy in Crohn's Disease: *Cells*, v. 1, p. 492-519.
- Herkenham, M., A. B. Lynn, M. R. Johnson, L. S. Melvin, B. R. de Costa, and K. C. Rice, 1991, Characterization and localization of cannabinoid receptors in rat brain: a quantitative in vitro autoradiographic study: *The Journal of Neuroscience: The Official Journal of the Society for Neuroscience*, v. 11, p. 563.
- Hidalgo, I. J., T. J. Raub, and R. T. Borchardt, 1989, Characterization of the human colon carcinoma cell line (Caco-2) as a model system for intestinal epithelial permeability: *Gastroenterology*, v. 96, p. 736-49.
- Hilgers, A., R. Conradi, and P. Burton, 1990, Caco-2 cell monolayers as a model for drug transport across the intestinal mucosa: *An Official Journal of The American Association of Pharmaceutical Scientists*, v. 7, p. 902-910.

- Hillard, C. J., S. Manna, M. J. Greenberg, R. DiCamelli, R. A. Ross, L. A. Stevenson, V. Murphy, R. G. Pertwee, and W. B. Campbell, 1999, Synthesis and characterization of potent and selective agonists of the neuronal cannabinoid receptor (CB1): *Journal of Pharmacology and Experimental Therapeutics*, v. 289, p. 1427-33.
- Homer, C. R., A. L. Richmond, N. A. Rebert, J. P. Achkar, and C. McDonald, 2010, ATG16L1 and NOD2 interact in an autophagy-dependent antibacterial pathway implicated in Crohn's Disease pathogenesis: *Gastroenterology*, v. 139, p. 1630-1641.e2.
- Hooper, L. V., T. Midtvedt, and J. I. Gordon, 2002, How host- microbial interactions shape the nutrient environment of the mammalian intestine: *Annual Review of Nutrition*, v. 22, p. 283.
- Hooper, L. V., M. H. Wong, A. Thelin, L. Hansson, P. G. Falk, and J. I. Gordon, 2001, Molecular analysis of commensal host-microbial relationships in the intestine: *Science*, v. 291, p. 881-884.
- Hughes, J., T. W. Smith, H. W. Kosterlitz, L. A. Fothergill, B. A. Morgan, and H. R. Morris, 1975, Identification of two related pentapeptides from the brain with potent opiate agonist activity: *Nature*, v. 258, p. 577-80.
- Hugot, J. P., M. Chamaillard, H. Zouali, S. Lesage, J. P. C'zard, J. Belaiche, S. Almer, C. Tysk, A. Morain, M. Gassull, V. Binder, Y. Finkel, A. Cortot, R. Modigliani, P. Laurent-Puig, C. Gower-Rousseau, J. Macry, J. F. Comombel, M. Sahbatou, and G. Thomas, 2001, Association of NOD2 leucine- rich repeat variants with susceptibility to Crohn's disease: *Nature*, v. 411, p. 599-603.
- Ikonomou, G., V. Kostourou, S. Shirasawa, T. Sasazuki, M. Samiotaki, and G. Panayotou, 2012, Interplay between oncogenic K-Ras and wild-type H-Ras in Caco2 cell transformation: *Journal of Proteomics*, v. 75, p. 5356-69.
- Izzo, A. A., F. Borrelli, R. Capasso, V. Di Marzo, and R. Mechoulam, 2009, Non-psychoactive plant cannabinoids: new therapeutic opportunities from an ancient herb: *Trends in Pharmacological Sciences*, v. 30, p. 515-527.
- Izzo, A. A., F. Fezza, R. Capasso, T. Bisogno, L. Pinto, T. Iuvone, G. Esposito, N. Mascolo, V. Di Marzo, and F. Capasso, 2001, Cannabinoid CB1-receptor mediated regulation of gastrointestinal motility in mice in a model of intestinal inflammation: *British Journal of Pharmacology*, v. 134, p. 563-570.
- Izzo, A. A., and K. A. Sharkey, 2010, Cannabinoids and the gut: New developments and emerging concepts: *Pharmacology & Therapeutics*, v. 126, p. 21-38.
- Jacobsson, S. O. P., E. Rongard, M. Stridh, G. Tiger, and C. J. Fowler, 2000, Serum-dependent effects of tamoxifen and cannabinoids upon C6 glioma cell viability: *Biochemical Pharmacology*, v. 60, p. 1807-1813.
- Juenemann, K., and E. A. Reits, 2012, Alternative macroautophagic pathways: *International Journal of Cell Biology*, v. 2012, p. 189794.
- Juknat, A., M. Pietr, E. Kozela, N. Rimmerman, R. Levy, F. Y. Gao, G. Coppola, D. Geschwind, and Z. Vogel, 2013, Microarray and pathway analysis reveal distinct mechanisms underlying cannabinoid-mediated modulation of LPS-induced activation of BV-2 microglial cells: *PLOS One*, v. 8, p. 17.
- Jung, C. H., S.-H. Ro, J. Cao, N. M. Otto, and D.-H. Kim, 2010, mTOR regulation of autophagy: *FEBS Letters*, v. 584, p. 1287-1295.
- Kabeya, Y., N. Mizushima, T. Ueno, A. Yamamoto, T. Kirisako, T. Noda, E. Kominami, Y. Ohsumi, and T. Yoshimori, 2000, LC3, a mammalian homologue of yeast Apg8p, is localized in autophagosome membranes after processing: *EMBO Journal*, v. 19, p. 5720-5728.

- Kamada, Y., T. Funakoshi, T. Shintani, K. Nagano, M. Ohsumi, and Y. Ohsumi, 2000, TOR-mediated induction of autophagy via an Apg1 protein kinase complex: The Journal of Cell Biology, v. 150, p. 1507-1513.
- Kershaw, N. J., J. M. Murphy, N. P. D. Liao, L. N. Varghese, A. Laktyushin, E. L. Whitlock, I. S. Lucet, N. A. Nicola, and J. J. Babon, 2013, SOCS3 binds specific receptor-JAK complexes to control cytokine signaling by direct kinase inhibition: Nature Structural and Molecular Biology, v. 20, p. 469-476.
- Kersse, K., M. J. M. Bertrand, M. Lamkanfi, and P. Vandenabeele, 2011, NOD-like receptors and the innate immune system: Coping with danger, damage and death: Cytokine and Growth Factor Reviews, v. 22, p. 257-276.
- Kirkegaard, K., M. P. Taylor, and W. T. Jackson, 2004, Cellular autophagy: Surrender, avoidance and subversion by microorganisms: Nature Reviews Microbiology, v. 2, p. 301-314.
- Kirkin, V., D. G. McEwan, I. Novak, and I. Dikic, 2009, A role for ubiquitin in selective autophagy: Molecular Cell, v. 34, p. 259-269.
- Klein, T. W., 2005, Cannabinoid-based drugs as anti-inflammatory therapeutics: Nature Reviews. Immunology, v. 5, p. 400.
- Klionsky, D. J., 2009, Crohn's Disease, Autophagy, and the Paneth Cell: New England Journal of Medicine, v. 360, p. 1785-1786.
- Klionsky, D. J., Z. Elazar, P. O. Seglen, and D. C. Rubinsztein, 2008, Does bafilomycin A(1) block the fusion of autophagosomes with lysosomes?: Autophagy, v. 4, p. 849-850.
- Klionsky, D. J., and S. D. Emr, 2000, Autophagy as a regulated pathway of cellular degradation: Science, v. 290, p. 1717-1721.
- Knights, D., K. G. Lassen, and R. J. Xavier, 2013, Advances in inflammatory bowel disease pathogenesis: Linking host genetics and the microbiome: Gut, v. 62, p. 1505-1510.
- Komatsu, M., S. Waguri, T. Chiba, S. Murata, J.-i. Iwata, I. Tanida, T. Ueno, M. Koike, Y. Uchiyama, E. Kominami, and K. Tanaka, 2006, Loss of autophagy in the central nervous system causes neurodegeneration in mice: Nature, v. 441, p. 880.
- Komatsu, M., S. Waguri, T. Ueno, J. Iwata, S. Murata, I. Tanida, J. Ezaki, N. Mizushima, Y. Ohsumi, Y. Uchiyama, E. Kominami, K. Tanaka, and T. Chiba, 2005, Impairment of starvation-induced and constitutive autophagy in Atg7-deficient mice: The Journal of Cell Biology, v. 169, p. 425-434.
- Kozela, E., M. Pietr, A. Juknat, N. Rimmerman, R. Levy, and Z. Vogel, 2010, Cannabinoids Delta(9)-tetrahydrocannabinol and Cannabidiol differentially inhibit the lipopolysaccharide-activated NF-kappa B and interferon-beta/STAT proinflammatory pathways in BV-2 microglial cells: The Journal of Biological Chemistry, v. 285, p. 1616-1626.
- Kuang, E., J. Qi, and Z. e. Ronai, 2013, Emerging roles of E3 ubiquitin ligases in autophagy: Trends in Biochemical Sciences, v. 28, p. 453-460.
- Kuballa, P., A. Huett, J. D. Rioux, M. J. Daly, R. J. Xavier, and N. Gay, 2008, Impaired autophagy of an intracellular pathogen induced by a Crohn's Disease associated ATG16L1 variant: PLOS ONE, v. 3, p. 3391.
- Kufe, D. W., 2009, Mucins in cancer: function, prognosis and therapy: Nature Reviews. Cancer, v. 9, p. 874-885.
- Kuma, A., and N. Mizushima, 2010, Physiological role of autophagy as an intracellular recycling system: With an emphasis on nutrient metabolism: Seminars in Cell and Developmental Biology, v. 21, p. 683-690.

- Kunzelmann, K., and B. McMorran, 2004, First encounter: how pathogens compromise epithelial transport: *Physiology* (Bethesda, Md.), v. 19, p. 240-244.
- Lee, J., J. H. Mo, K. Katakura, I. Alkalay, A. N. Rucker, Y. T. Liu, H. K. Lee, C. Shen, G. Cojocaru, S. Shenouda, M. Kagnoff, L. Eckmann, Y. Ben-Neriah, and E. Raz, 2006, Maintenance of colonic homeostasis by distinctive apical TLR9 signalling in intestinal epithelial cells: *Nature Cell Biology*, v. 8, p. 1327-1336.
- Lenaerts, K., E. Mariman, F. Bouwman, and J. Renes, 2005, Differentiation stage-dependent preferred uptake of basolateral (systemic) glutamine into Caco-2 cells results in its accumulation in proteins with a role in cell-cell interaction: *FEBS Journal*, v. 272, p. 3350-3364.
- Levine, B., and V. Deretic, 2007, Unveiling the roles of autophagy in innate and adaptive immunity: *Nature Reviews. Immunology*, v. 7, p. 767.
- Levine, B., and G. Kroemer, 2008, Autophagy in the pathogenesis of disease: *Cell*, v. 132, p. 27-42.
- Levine, B., N. Mizushima, and H. W. Virgin, 2011, Autophagy in immunity and inflammation: *Nature*, v. 469, p. 323-335.
- Li, Y., C. de Haar, M. Chen, J. Deuring, M. M. Gerrits, R. Smits, B. Xia, E. J. Kuipers, and C. J. van der Woude, 2010, Disease-related expression of the IL6/STAT3/SOCS3 signalling pathway in ulcerative colitis and ulcerative colitis-related carcinogenesis: *Gut*, v. 59, p. 227-35.
- Li, Y., J. Deuring, M. P. Peppelenbosch, E. J. Kuipers, C. de Haar, and C. J. van der Woude, 2012, IL-6-induced DNMT1 activity mediates SOCS3 promoter hypermethylation in ulcerative colitis-related colorectal cancer: *Carcinogenesis*, v. 33, p. 1889-96.
- Ligresti, A., T. Bisogno, I. Matias, L. De Petrocellis, M. G. Cascio, V. Cosenza, G. D'argenio, G. Scaglione, M. Bifulco, I. Sorrentini, and V. Di Marzo, 2003, Possible endocannabinoid control of colorectal cancer growth: *Gastroenterology*, v. 125, p. 677-687.
- Lindmo, K., and H. Stenmark, 2006, Regulation of membrane traffic by phosphoinositide 3-kinases: *Journal of Cell Science*, v. 119, p. 605-614.
- Long, J., T. R. A. Gallagher, J. R. Cavey, P. W. Sheppard, S. H. Ralston, R. Layfield, and M. S. Searle, 2008, Ubiquitin recognition by the ubiquitin-associated domain of p62 involves a novel conformational switch: *The Journal of Biological Chemistry*, v. 283, p. 5427-5440.
- Looijer-van Langen, M. A., and L. A. Dieleman, 2009, Prebiotics in chronic intestinal inflammation: *Inflammatory Bowel Disease*, v. 15, p. 454-62.
- Luchicchi, A., and M. Pistis, 2012, Anandamide and 2-arachidonoylglycerol: Pharmacological properties, functional features, and emerging specificities of the two major endocannabinoids: *Molecular Neurobiology*, v. 46, p. 374-392.
- Lum, J. J., D. E. Bauer, M. Kong, M. H. Harris, C. Li, T. Lindsten, and C. B. Thompson, 2005, Growth factor regulation of autophagy and cell survival in the absence of apoptosis: *Cell*, v. 120, p. 237-248.
- Macpherson, T., J. A. Armstrong, D. N. Criddle, and K. L. Wright, 2014, Physiological intestinal oxygen modulates the Caco-2 cell model and increases sensitivity to the phytocannabinoid cannabidiol: *In Vitro Cell & Development Biology-Animal*, v. 50, p. 417-426.
- Mao, Y., S. Nobaek, B. Kasravi, D. Adawi, U. Stenram, G. Molin, and B. Jeppsson, 1996, The effects of *Lactobacillus* strains and oat fiber on methotrexate-induced enterocolitis in rats: *Gastroenterology*, v. 111, p. 334-344.

- Massa, F., G. Marsicano, H. Hermann, A. Cannich, K. Monory, B. F. Cravatt, G. L. Ferri, A. Sibaev, M. Storr, and B. Lutz, 2004, The endogenous cannabinoid system protects against colonic inflammation: *Journal of Clinical Investigation*, v. 113, p. 1202-1209.
- Massey, D. C. O., and M. Parkes, 2007, Genome-wide association scanning highlights two autophagy genes, ATG16L1 and IRGM, as being significantly associated with Crohn's disease: *Autophagy*, v. 3, p. 649-651.
- Matsumoto, H., R. H. Erickson, J. R. Gum, M. Yoshioka, E. Gum, and Y. S. Kim, 1990, Biosynthesis of alkaline phosphatase during differentiation of the human colon cancer cell line Caco-2: *Gastroenterology*, v. 98, p. 1199-207.
- Mehran, M., E. Seidman, R. Marchand, C. Gurbindo, and E. Levy, 1995, Tumor necrosis factor- α inhibits lipid and lipoprotein transport by Caco-2 cells: *American Journal of Physiology-Gastrointestinal and Liver Physiology*, v. 269, p. 953-960.
- Melck, D., T. Bisogno, L. De Petrocellis, H.-h. Chuang, D. Julius, M. Bifulco, and V. Di Marzo, 1999, Unsaturated long-chain N-Acyl-vanillyl-amides (N-AVAMs): Vanilloid receptor ligands that inhibit Anandamide-facilitated transport and bind to CB1 cannabinoid receptors: *Biochemical and Biophysical Research Communications*, v. 262, p. 275-284.
- Mihalache, C. C., and H. U. Simon, 2012, Autophagy regulation in macrophages and neutrophils: *Experimental Cell Research*, v. 318, p. 1187-1192.
- Mizushima, N., 2007, Autophagy: process and function: *Genes & Development*, v. 21, p. 2861.
- Mizushima, N., B. Levine, A. M. Cuervo, and D. J. Klionsky, 2008, Autophagy fights disease through cellular self-digestion: *Nature*, v. 451, p. 1069.
- Mizushima, N., A. Yamamoto, M. Hatano, Y. Kobayashi, Y. Kabeya, K. Suzuki, T. Tokuhi, Y. Ohsumi, and T. Yoshimori, 2001, Dissection of autophagosome formation using Apg5-deficient mouse embryonic stem cells: *Journal of Cell Biology*, v. 152, p. 657-667.
- Mizushima, N., and T. Yoshimori, 2007, How to interpret LC3 immunoblotting: *Autophagy*, v. 3, p. 542-5.
- Mizushima, N., T. Yoshimori, and B. Levine, 2010, Methods in mammalian autophagy research: *Cell*, v. 140, p. 313-326.
- Moore, C. B., E. H. Guthrie, M. T. Huang, and D. J. Taxman, 2010, Short hairpin RNA (shRNA): design, delivery, and assessment of gene knockdown: *Methods in Molecular Biology*, v. 629, p. 141-58.
- Moreau, K., and D. C. Rubinshtein, 2012, The plasma membrane as a control center for autophagy: *Autophagy*, v. 8, p. 861-3.
- Mousavi, S. A., R. Kjekens, T. O. Berg, P. O. Seglen, T. Berg, and A. Brech, 2001, Effects of inhibitors of the vacuolar proton pump on hepatic heterophagy and autophagy: *Biochimica Biophysica Acta*, v. 1510, p. 243-57.
- Mudter, J., and M. F. Neurath, 2007, IL-6 signaling in inflammatory bowel disease: pathophysiological role and clinical relevance: *Inflammatory Bowel Disease*, v. 13, p. 1016-23.
- Nakatogawa, H., K. Suzuki, Y. Kamada, and Y. Ohsumi, 2009, Dynamics and diversity in autophagy mechanisms: lessons from yeast: *Nature Reviews. Molecular Cell Biology*, v. 10, p. 458.
- Nishimura, T., T. Kaizuka, K. Cadwell, M. H. Sahani, T. Saitoh, S. Akira, H. W. Virgin, and N. Mizushima, 2013, FIP200 regulates targeting of Atg16L1 to the isolation membrane: *EMBO Reports*, v. 14, p. 284-291.
- Ohsumi, Y., 2001, Molecular dissection of autophagy: two ubiquitin-like systems: *Nature Reviews. Molecular Cell Biology*, v. 2, p. 211.

- Okamoto, Y., J. Morishita, K. Tsuboi, T. Tonai, and N. Ueda, 2004, Molecular characterization of a phospholipase D generating Anandamide and its congeners: *The Journal of Biological Chemistry*, v. 279, p. 5298-5305.
- Onodera, J., and Y. Ohsumi, 2005, Autophagy is required for maintenance of amino acid levels and protein synthesis under nitrogen starvation: *The Journal of Biological Chemistry*, v. 280, p. 31582.
- Parkes, M., J. C. Barrett, N. J. Prescott, M. Tremelling, C. A. Anderson, S. A. Fisher, R. G. Roberts, E. R. Nimmo, F. R. Cummings, D. Soars, H. Drummond, C. W. Lees, S. A. Khawaja, R. Bagnall, D. A. Burke, C. E. Todhunter, T. Ahmad, C. M. Onnie, W. McArdle, D. Strachan, G. Bethel, C. Bryan, C. M. Lewis, P. Deloukas, A. Forbes, J. Sanderson, D. P. Jewell, J. Satsangi, J. C. Mansfield, L. Cardon, C. G. Mathew, and C. Wellcome Trust Case Control, 2007, Sequence variants in the autophagy gene IRGM and multiple other replicating loci contribute to Crohn's disease susceptibility: *Nature Genetics*, v. 39, p. 830-832.
- Patel, K. K., and T. S. Stappenbeck, 2013, Autophagy and intestinal homeostasis: *Annual Review of Physiology*, v. 75, p. 241-262.
- Pattingre, S., A. Tassa, X. Qu, R. Garuti, X. H. Liang, N. Mizushima, M. Packer, M. D. Schneider, and B. Levine, 2005, Bcl-2 antiapoptotic proteins inhibit Beclin 1-dependent autophagy: *Cell*, v. 122, p. 927-39.
- Peterson, D. A., D. N. Frank, N. R. Pace, and J. I. Gordon, 2008, Metagenomic approaches for defining the pathogenesis of inflammatory bowel diseases: *Cell Host & Microbe*, v. 3, p. 417-427.
- Petersson, J., O. Schreiber, G. C. Hansson, S. J. Gendler, A. Velcich, J. O. Lundberg, S. Roos, L. Holm, and M. Phillipson, 2011, Importance and regulation of the colonic mucus barrier in a mouse model of colitis: *American Journal of Physiology. Gastrointestinal and Liver Physiology*, v. 300, p. 327.
- Petrilli, V., S. Papin, and J. Tschopp, 2005, The inflammasome: *Current Biology*, v. 15, p. 581.
- Pfaffl, M. W., 2001, A new mathematical model for relative quantification in real-time RT-PCR: *Nucleic Acids Research*, v. 29, p. 45.
- Philpott, D. J., M. T. Sorbara, S. J. Robertson, K. Croitoru, and S. E. Girardin, 2013, NOD proteins: regulators of inflammation in health and disease: *Nature Reviews Immunology*, v. 14, p. 9-23.
- Piessevaux, J., D. Lavens, F. Peelman, and J. Tavernier, 2008, The many faces of the SOCS box: *Cytokine and Growth Factor Reviews*, v. 19, p. 371-381.
- Piomelli, D., 2003, The molecular logic of endocannabinoid signalling: *Nature reviews. Neuroscience*, v. 4, p. 873.
- Portella, G., C. Laezza, P. Laccetti, L. De Petrocellis, V. Di Marzo, and M. Bifulco, 2003, Inhibitory effects of cannabinoid CB1 receptor stimulation on tumor growth and metastatic spreading: actions on signals involved in angiogenesis and metastasis: *FASEB Journal, Official Publication of The Federation of American Societies for Experimental Biology*, v. 17, p. 1771.
- Prescott, N. J., S. A. Fisher, A. Franke, J. Hampe, C. M. Onnie, D. Soars, R. Bagnall, M. M. Mirza, J. Sanderson, A. Forbes, J. C. Mansfield, C. M. Lewis, S. Schreiber, and C. G. Mathew, 2007, A nonsynonymous SNP in ATG16L1 predisposes to ileal Crohn's disease and is independent of CARD15 and 1BD5: *Gastroenterology*, v. 132, p. 1665-1671.
- Radtke, F., and H. Clevers, 2005, Self-renewal and cancer of the gut: Two sides of a coin: *Science*, v. 307, p. 1904-1909.

- Rautava, S., and W. Walker, 2007, Commensal bacteria and epithelial cross talk in the developing intestine: *Current Gastroenterology Reports*, v. 9, p. 385-392.
- Rechsteiner, M., and S. W. Rogers, 1996, PEST sequences and regulation by proteolysis: *Trends in Biochemical Sciences*, v. 21, p. 267-271.
- Reimund, J. M., C. Wittersheim, S. Dumont, C. D. Muller, J. S. Kenney, R. Baumann, P. Poindron, and B. Duclos, 1996, Increased production of tumour necrosis factor-alpha interleukin-1 beta, and interleukin-6 by morphologically normal intestinal biopsies from patients with Crohn's disease: *Gut*, v. 39, p. 684-9.
- Reinecker, H. C., M. Steffen, T. Witthoeft, I. Pflueger, S. Schreiber, R. P. MacDermott, and A. Raedler, 1993, Enhanced secretion of tumour necrosis factor-alpha, IL-6, and IL-1 beta by isolated lamina propria mononuclear cells from patients with ulcerative colitis and Crohn's disease: *Clinical & Experimental Immunology*, v. 94, p. 174-81.
- Ribeiro, A., V. Ferraz-de-Paula, M. L. Pinheiro, L. B. Vitoretti, D. P. Mariano-Souza, W. M. Quinteiro-Filho, A. T. Akamine, V. I. Almeida, J. Quevedo, F. Dal-Pizzol, J. E. Hallak, A. W. Zuardi, J. A. Crippa, and J. Palermo-Neto, 2012, Cannabidiol, a non-psychotropic plant-derived cannabinoid, decreases inflammation in a murine model of acute lung injury: Role for the adenosine A2A receptor: *European Journal of Pharmacology*, v. 678, p. 78-85.
- Rigby, R. J., J. G. Simmons, C. J. Greenhalgh, W. S. Alexander, and P. K. Lund, 2007, Suppressor of cytokine signaling 3 (SOCS3) limits damage-induced crypt hyper-proliferation and inflammation-associated tumorigenesis in the colon: *Oncogene*, v. 26, p. 4833-4841.
- Rossi, S., V. De Chiara, A. Musella, L. Sacchetti, C. Cantarella, M. Castelli, F. Cavasinni, C. Motta, V. Studer, G. Bernardi, B. F. Cravatt, M. Maccarrone, A. Usiello, and D. Centonze, 2010, Preservation of striatal cannabinoid CB1 receptor function correlates with the antianxiety effects of fatty acid amide hydrolase inhibition: *Molecular Pharmacology*, v. 78, p. 260.
- Rothen-Rutishauser, B., A. Braun, M. Günthert, and H. Wunderli-Allenspach, 2000, Formation of Multilayers in the Caco- 2 Cell Culture Model: A Confocal Laser Scanning Microscopy Study: *An Official Journal of the American Association of Pharmaceutical Scientists*, v. 17, p. 460-465.
- Rozenfeld, R., 2011, Type I cannabinoid receptor trafficking: All roads lead to lysosome: *Traffic*, v. 12, p. 12-18.
- Rozenfeld, R., and L. A. Devi, 2008, Regulation of CB1 cannabinoid receptor trafficking by the adaptor protein AP-3: *FASEB Journal*, v. 22, p. 2311-2322.
- Rubinsztein, D. C., A. M. Cuervo, B. Ravikumar, S. Sarkar, V. Korolchuk, S. Kaushik, and D. J. Klionsky, 2009, In search of an "autophagomometer": *Autophagy*, v. 5, p. 585-589.
- Ruemmele, F. M., S. Schwartz, E. G. Seidman, S. Dionne, E. Levy, and M. J. Lentze, 2003, Butyrate induced caco- 2 cell apoptosis is mediated via the mitochondrial pathway: *Gut*, v. 52, p. 94.
- Saitoh, T., N. Fujita, M. H. Jang, S. Uematsu, B.-G. Yang, T. Satoh, H. Omori, T. Noda, N. Yamamoto, M. Komatsu, K. Tanaka, T. Kawai, T. Tsujimura, O. Takeuchi, T. Yoshimori, and S. Akira, 2008, Loss of the autophagy protein Atg16L1 enhances endotoxin-induced IL- 1beta production: *Nature*, v. 456, p. 264.
- Sakiyama, T., M. W. Musch, M. J. Ropeleski, H. Tsubouchi, and E. B. Chang, 2009, Glutamine Increases autophagy under basal and stressed conditions in intestinal epithelial cells: *Gastroenterology*, v. 136, p. 924-932.

- Salazar, M., A. Carracedo, I. J. Salanueva, S. Hernandez-Tiedra, M. Lorente, A. Egia, P. Vazquez, C. Blazquez, S. Torres, S. Garcia, J. Nowak, G. M. Fimia, M. Piacentini, F. Cecconi, P. P. Pandolfi, L. Gonzalez-Feria, J. L. Iovanna, M. Guzman, P. Boya, and G. Velasco, 2009, Cannabinoid action induces autophagy-mediated cell death through stimulation of ER stress in human glioma cells: *Journal of Clinical Investigation*, v. 119, p. 1359-1372.
- Sambuy, Y., I. Angelis, G. Ranaldi, M. Scarino, L. Stammati, A. Zucco, and F. Zucco, 2005, The Caco-2 cell line as a model of the intestinal barrier: influence of cell and culture-related factors on Caco-2 cell functional characteristics: *Cell Biology and Toxicology*, v. 21, p. 1-26.
- Sandy, P., A. Ventura, and T. Jacks, 2005, Mammalian RNAi: a practical guide: *Biotechniques*, v. 39, p. 215-24.
- Sasaki, A., K. Inagaki-Ohara, T. Yoshida, A. Yamanaka, M. Sasaki, H. Yasukawa, A. E. Koromilas, and A. Yoshimura, 2003, The N-terminal truncated isoform of SOCS3 translated from an alternative initiation AUG codon under stress conditions is stable due to the lack of a major ubiquitination site, Lys-6: *The Journal of Biological Chemistry*, v. 278, p. 2432.
- Sasaki, A., H. Yasukawa, A. Suzuki, S. Kamizono, T. Syoda, I. Kinjyo, M. Sasaki, J. A. Johnston, and A. Yoshimura, 1999, Cytokine-inducible SH2 protein-3 (CIS3/SOCS3) inhibits Janus tyrosine kinase by binding through the N-terminal kinase inhibitory region as well as SH2 domain: *Genes To Cells: Devoted to Molecular & Cellular Mechanisms*, v. 4, p. 339.
- Scarlatti, F., R. Maffei, I. Beau, P. Codogno, and R. Ghidoni, 2008, Role of non-canonical Beclin 1-independent autophagy in cell death induced by resveratrol in human breast cancer cells: *Cell Death & Differentiation*, v. 15, p. 1318-29.
- Scherz-Shouval, R., and Z. Elazar, 2007, ROS, mitochondria and the regulation of autophagy: *Trends in Cell Biology*, v. 17, p. 422-427.
- Scherz-Shouval, R., and Z. Elazar, 2011, Regulation of autophagy by ROS: physiology and pathology: *Trends in Biochemical Sciences*, v. 36, p. 30-38.
- Scott, R. C., O. Schuldiner, and T. P. Neufeld, 2004, Role and regulation of starvation-induced autophagy in the drosophila fat body: *Developmental Cell*, v. 7, p. 167-178.
- Sharma, R., U. Schumacher, V. Ronaasen, and M. Coates, 1995, Rat intestinal mucosal responses to a microbial flora and different diets: *Gut*, v. 36, p. 209.
- Shen, C., J. Yan, L.-S. Jiang, and L.-Y. Dai, 2011, Autophagy in rat annulus fibrosus cells: evidence and possible implications: *Arthritis Research & Therapy*, v. 13, p. 132.
- Shrivastava, A., P. M. Kuzontkoski, J. E. Groopman, and A. Prasad, 2011, Cannabidiol induces programmed cell death in breast cancer cells by coordinating the cross-talk between apoptosis and autophagy: *Molecular Cancer Therapeutics*, v. 10, p. 1161-1172.
- Simonsen, A., and S. A. Tooze, 2009, Coordination of membrane events during autophagy by multiple class III PI3-kinase complexes: *The Journal of Cell Biology*, v. 186, p. 773-82.
- Singh, R., and Ana M. Cuervo, 2011, Autophagy in the cellular energetic balance: *Cell Metabolism*, v. 13, p. 495-504.
- Siolas, D., C. Lerner, J. Burchard, W. Ge, P. S. Linsley, P. J. Paddison, G. J. Hannon, and M. A. Cleary, 2005, Synthetic shRNAs as potent RNAi triggers: *Nature Biotechnology*, v. 23, p. 227.
- Sirard, J. c., M. Bayardo, and A. Didierlaurent, 2006, Pathogen- specific TLR signaling in mucosa: Mutual contribution of microbial TLR agonists and virulence factors: *European Journal of Immunology*, v. 36, p. 260-263.
- Sliva, K., and B. S. Schnierle, 2010, Selective gene silencing by viral delivery of short hairpin RNA: *Virology Journal*, v. 7, p. 248.

- Sokol, H., B. Pigneur, L. Watterlot, O. Lakhdari, L. G. Bermúdez-Humarán, J.-J. Gratadoux, S. Blugeon, C. Bridonneau, J.-P. Furet, G. Corthier, C. Grangette, N. Vasquez, P. Pochart, G. Trugnan, G. Thomas, H. M. Blottière, J. Doré, P. Marteau, P. Seksik, and P. Langella, 2008, *Faecalibacterium prausnitzii* Is an anti-inflammatory commensal bacterium identified by gut microbiota analysis of Crohn Disease patient: Proceedings of the National Academy of Sciences of the United States of America, v. 105, p. 16731-16736.
- Stappenbeck, T. S., 2010, The role of autophagy in Paneth cell differentiation and secretion: *Mucosal Immunology*, v. 3, p. 8.
- Stierum, R., M. Gaspari, Y. Dommels, T. Ouatas, H. Pluk, S. Jespersen, J. Vogels, K. Verhoeckx, J. Groten, and B. v. Ommen, 2003, Proteome analysis reveals novel proteins associated with proliferation and differentiation of the colorectal cancer cell line Caco-2: *BBA-Proteins and Proteomics*, v. 1650, p. 73-91.
- Sugiura, T., S. Kondo, A. Sukagawa, S. Nakane, A. Shinoda, K. Itoh, A. Yamashita, and K. Waku, 1995, 2- Arachidonoylglycerol: A possible endogenous cannabinoid receptor ligand in brain: *Biochemical and Biophysical Research Communications*, v. 215, p. 89.
- Sumandea, M. P., and S. F. Steinberg, 2011, Redox signaling and cardiac sarcomeres: *The Journal of Biological Chemistry*, v. 286, p. 9921.
- Sun, H., E. C. Chow, S. Liu, Y. Du, and K. S. Pang, 2008, The Caco-2 cell monolayer: Usefulness and limitations: *Expert Opinion on Drug Metabolism & Toxicology*, v. 4, p. 395-411.
- Suzuki, A., T. Hanada, K. Mitsuyama, T. Yoshida, S. Kamizono, T. Hoshino, M. Kubo, A. Yamashita, M. Okabe, K. Takeda, S. Akira, S. Matsumoto, A. Toyonaga, M. Sata, and A. Yoshimura, 2001, CIS3/SOCS3/SSI3 plays a negative regulatory role in STAT3 activation and intestinal inflammation: *Journal of Experimental Medicine*, v. 193, p. 471-481.
- Swidsinski, A., J. Weber, V. Loening-Baucke, L. P. Hale, and H. Lochs, 2005, Spatial organization and composition of the mucosal flora in patients with Inflammatory Bowel Disease: *Journal of Clinical Microbiology*, v. 43, p. 3380.
- Szymanska, H., 2007, Genetically engineered mice: Mouse models for cancer research: *Postępy Higieny i Medycyny Doświadczalnej (Online)*, v. 61, p. 639-45.
- Tanida, I., N. Minematsu-Ikeguchi, T. Ueno, and E. Kominami, 2005, Lysosomal turnover, but not a cellular level, of endogenous LC3 is a marker for autophagy: *Autophagy*, v. 1, p. 84-91.
- Ueda, N., Y. Okamoto, and J. Morishita, 2005, N-acylphosphatidylethanolamine-hydrolyzing phospholipase D: A novel enzyme of the β -lactamase fold family releasing anandamide and other N-acylethanolamines: *Life Sciences*, v. 77, p. 1750-1758.
- Vaccani, A., P. Massi, A. Colombo, T. Rubino, and D. Parolaro, 2005, Cannabidiol inhibits human glioma cell migration through a cannabinoid receptor-independent mechanism: *British Journal of Pharmacology*, v. 144, p. 1032-1036.
- Van Der Stelt, M., and V. Di Marzo, 2004, Endovanilloids. Putative endogenous ligands of transient receptor potential vanilloid 1 channels: *European journal of Biochemistry*, v. 271, p. 1827.
- Van Sickle, M. D., M. Duncan, P. J. Kingsley, A. Mouihate, P. Urbani, K. Mackie, N. Stella, A. Makriyannis, D. Piomelli, J. S. Davison, L. J. Marnett, V. Di Marzo, Q. J. Pittman, K. D. Patel, and K. A. Sharkey, 2005, Identification and functional characterization of brainstem cannabinoid CB2 receptors: *Science*, v. 310, p. 329-332.
- von Muhlinen, N., T. Thurston, G. Ryzhakov, S. Bloor, and F. Randow, 2010, NDP52, a novel autophagy receptor for ubiquitin-decorated cytosolic bacteria: *Autophagy*, v. 6, p. 288-9.

- Wang, J., R. Liu, M. Hawkins, N. Barzilai, and L. Rossetti, 1998, A nutrient-sensing pathway regulates leptin gene expression in muscle and fat: *Nature*, v. 393, p. 684.
- Wang, T. G., Y. Gotoh, M. H. Jennings, C. A. Rhoads, and T. Y. Aw, 2000, Lipid hydroperoxide-induced apoptosis in human colonic CaCo-2 cells is associated with an early loss of cellular redox balance: *FASEB journal*, v. 14, p. 1567.
- Watanabe, I., and S. Okada, 1967, Stationary phase of cultured mammalian cells (L5178Y): *The Journal of Cell Biology*, v. 35, p. 285.
- Watanabe, K., Y. Kayano, T. Matsunaga, I. Yamamoto, and H. Yoshimura, 1996, Inhibition of anandamide amidase activity in mouse brain microsomes by cannabinoids: *Biological & Pharmaceutical Bulletin*, v. 19, p. 1109-11.
- Welchman, R. L., C. Gordon, and R. J. Mayer, 2005, Ubiquitin and ubiquitin-like proteins as multifunctional signals: *Nature reviews. Molecular Cell Biology*, v. 6, p. 599.
- Wen, Z., and J. E. Darnell, 1997, Mapping of Stat3 serine phosphorylation to a single residue (727) and evidence that serine phosphorylation has no influence on DNA binding of Stat1 and Stat3: *Nucleic Acids Research*, v. 25, p. 2062.
- Wilson, T. H., 1962, *Intestinal absorption*: Philadelphia, Philadelphia: Saunders.
- Wright, K., N. Rooney, M. Feeney, J. Tate, D. Robertson, M. Welham, and S. Ward, 2005, Differential expression of cannabinoid receptors in the human colon: Cannabinoids promote epithelial wound healing: *Gastroenterology*, v. 129, p. 437-453.
- Wu, Y. T., H. L. Tan, G. Shui, C. Bauvy, Q. Huang, M. R. Wenk, C. N. Ong, P. Codogno, and H. M. Shen, 2010, Dual role of 3-methyladenine in modulation of autophagy via different temporal patterns of inhibition on class I and III phosphoinositide 3-kinase: *The Journal of Biological Chemistry*, v. 285, p. 10850-61.
- Xie, C.-M., W. Y. Chan, S. Yu, J. Zhao, and C. H. K. Cheng, 2011, Bufalin induces autophagy-mediated cell death in human colon cancer cells through reactive oxygen species generation and JNK activation: *Free Radical Biology and Medicine*, v. 51, p. 1365-1375.
- Yamamoto, A., Y. Tagawa, T. Yoshimori, Y. Moriyama, R. Masaki, and Y. Tashiro, 1998, Bafilomycin A(1) prevents maturation of autophagic vacuoles by inhibiting fusion between autophagosomes and lysosomes in rat hepatoma cell line, H-4-II-E cells: *Cell Structure and Function*, v. 23, p. 33-42.
- Yasukawa, H., M. Ohishi, H. Mori, M. Murakami, T. Chinen, D. Aki, T. Hanada, K. Takeda, S. Akira, M. Hoshijima, T. Hirano, K. R. Chien, and A. Yoshimura, 2003, IL- 6 induces an anti-inflammatory response in the absence of SOCS3 in macrophages: *Nature Immunology*, v. 4, p. 551.
- Yoshimori, T., 2004, Autophagy: a regulated bulk degradation process inside cells: *Biochemical and Biophysical Research Communications*, v. 313, p. 453-458.
- Yoshimura, A., T. Naka, and M. Kubo, 2007, SOCS proteins, cytokine signalling and immune regulation: *Nature Reviews. Immunology*, v. 7, p. 454.
- Yoshimura, A., H. Nishinakamura, Y. Matsumura, and T. Hanada, 2005, Negative regulation of cytokine signaling and immune responses by SOCS proteins: *Arthritis Research & Therapy*, v. 7, p. 100-10.
- Yoshiura, S., T. Ohtsuka, Y. Takenaka, H. Nagahara, K. Yoshikawa, and R. Kageyama, 2007, Ultradian oscillations of Stat, Smad, and Hes1 expression in response to serum: *Proceedings of the National Academy of Sciences of the United States of America*, v. 104, p. 11292-7.

- Yu, J., S. Peng, D. Luo, and J. C. March, 2012, In vitro 3D human small intestinal villous model for drug permeability determination: *Biotechnology and Bioengineering*, v. 109, p. 2173-2178.
- Zhang, J.-G., A. Farley, S. E. Nicholson, T. A. Willson, L. M. Zugaro, R. J. Simpson, R. L. Moritz, D. Cary, R. Richardson, G. Hausmann, B. J. Kile, W. S. Alexander, D. Metcalf, D. J. Hilton, N. A. Nicola, and M. Baca, 1999, The conserved SOCS box motif in suppressors of cytokine signaling binds to Elongins B and C and may couple bound proteins to proteasomal degradation: *Proceedings of the National Academy of Sciences of the United States of America*, v. 96, p. 2071-2076.
- Zhang, X., and W. T. Godbey, 2006, Viral vectors for gene delivery in tissue engineering: *Advanced Drug Delivery Reviews*, v. 58, p. 515-534.
- Zuardi, A. w., J. a. s. Crippa, J. e. c. Hallak, F. a. Moreira, and F. s. Guimarães, 2006, Cannabidiol, a Cannabis sativa constituent, as an antipsychotic drug: *Brazilian Journal of Medical and Biological Research*, v. 39, p. 421.